Chemistry Dissertations   Department of Chemistry

Spring 4-27-2011

On the Biochemistry, Mechanism and Physiological Role of Fungal Nitronate Monooxygenase

Kevin Francis
Georgia State University

Follow this and additional works at: https://scholarworks.gsu.edu/chemistry_diss

Part of the Chemistry Commons

ON THE BIOCHEMISTRY, MECHANISM AND PHYSIOLOGICAL ROLE OF FUNGAL

NITRONATE MONOOXYGENASE

by

KEVIN FRANCIS

Under the Direction of Giovanni Gadda

ABSTRACT

Nitronate monooxygenase (E.C. 1.13.11.16), formerly known as 2-nitropropane dioxygenase (EC 1.13.11.32), is a flavin dependent enzyme that catalyzes the oxidation of nitronates to their corresponding carbonyl compounds and nitrite. Despite the fact that the enzyme was first isolated from *Neurospora crassa* 60 years ago, the biochemical and physiological properties of nitronate monooxygenase have remained largely elusive. This dissertation will present the work that established both the catalytic mechanism and physiological role of the fungal enzyme.

The biological and biochemical properties of propionate-3-nitronate, the recently discovered physiological substrate for nitronate monooxygenase, will be extensively reviewed. The nitronate is produced by a variety of variety leguminous plants and fungi and is a potent and irreversible inhibitor of succinate dehydrogenase. Nitronate monooxygenase allows *N. crassa* to

overcome the toxicity of propionate-3-nitronate as demonstrated by *in vivo* studies of the yeast, which showed that the wild-type can grow in the presence of the toxin whereas a knock out mutant that lacks the gene encoding for the enzyme could not.

In addition to establishing the physiological role of nitronate monooxygenase, the work presented here demonstrates that the catalytic mechanism of the enzyme involves the formation of an anionic flavosemiquinone intermediate. This intermediate is stabilized by the protonated form of an active site histidine residue (His-196) that acts as an electrostatic catalyst for the reaction as demonstrated by pH studies of the reductive half reaction of the enzyme. Histidine 196 also serves as the catalytic base for the reaction of the enzyme with nitroethane as substrate as revealed through mutagenesis studies in which the residue was replaced with an asparagine.

The kinetic implications of branching of reaction intermediates in enzymatic catalysis are also demonstrated through studies of the kinetic isotope effects of nitronate monooxygenase with $1,1-[^2H_2]$-nitroethane as substrate. Finally the use of competitive inhibitors as a probe of enzyme structure will be presented through a study of the inhibition of nitronate monooxygenase with mono-valent inorganic ions. The dissertation will close with unpublished work on the enzyme and concluding remarks concerning the biochemistry and physiology of nitronate monooxygenase.

INDEX WORDS: Nitronate monooxygenase, 2-Nitropropane dioxygenase, Kinetic isotope and pH effects, Flavin semiquinone, Nitroalkanes, 3-Nitropropionate, Propionate-3-nitronate

ON THE BIOCHEMISTRY, MECHANISM AND PHYSIOLOGICAL ROLE OF FUNGAL

NITRONATE MONOOXYGENASE

by

KEVIN FRANCIS

A Dissertation Submitted in Partial Fulfillment of the Requirements for the Degree of

Doctor of Philosophy

in the College of Arts and Sciences

Georgia State University

2011

ON THE BIOCHEMISTRY, MECHANISM AND PHYSIOLOGICAL ROLE OF FUNGAL

NITRONATE MONOOXYGENASE

by

KEVIN FRANCIS

Committee Chair: Giovanni Gadda

Committee: Dabney White Dixon

Aimin Liu

Binghe Wang

Electronic Version Approved:

Office of Graduate Studies

College of Arts and Sciences

Georgia State University

May 2011

DEDICATION

This dissertation is lovingly dedicated to Mary Arliss Quinlan Couey who was tragically

killed by a drunk driver on March 31, 2009. You are forever missed by many.

ACKNOWLEDGEMENTS

I would like to thank my advisor, Dr. Giovanni Gadda for his continued support and advice throughout my PhD career. In addition, I would also like to thank my committee members and all lab mates past and present. It could not have been done without you all.

TABLE OF CONTENTS

LIST OF TABLES

LIST OF FIGURES

LIST OF SCHEMES

1   CHAPTER I

GENERAL INTRODUCTION: NITRONATE MONOOXYGENASE AND OXIDATION OF NITRONATES BY FLAVIN DEPENDANT ENZYMES

1.1   Abstract

Nitronate monooxygenase (E.C. 1.13.11.16), formerly known as 2-nitropropane dioxygenase (EC 1.13.11.32) is a flavin mononucleotide-dependent (FMN) enzyme that catalyzes the oxidative denitrification of alkyl nitronates to their corresponding carbonyl compounds and nitrite. The enzyme has been isolated from *Neurospora crassa* and *Williopsis saturnus* var Mrakii and the biochemical and mechanistic features have been studied in great detail as outlined in both a recent review article (*1*) and in this dissertation. The present chapter outlines the isolation and initial characterization of the fungal enzymes and provides an account of the more recent studies that lead to the proper classification of the enzyme as a nitronate monooxygenase. A brief description of the catalytic mechanism of nitronate monooxygenase is then provided and put into a broader context of nitroalkane and alkyl nitronate oxidation by flavin dependent enzymes through a detail review of the literature on this subject. Finally, an overview of the specific goals of the research project described in the dissertation will be presented along with an overview of the studies carried out to achieve the research objectives.

1.2   Isolation and Initial Characterization of Nitronate Monooxygenase as a 2-Nitropropane Oxidizing Enzyme

The first report of nitroalkane oxidation by *Neurospora crassa* came from Little in 1951, who demonstrated that extracts of the fungus grown in nitrate medium oxidized nitroethane to produce acetylaldhyde and nitrite (*2*). The enzyme was classified as an oxidase and was suggested to be involved inorganic nitrogen assimilation, although it was also concluded that the

physiological substrate and role of the enzyme could not be definitively determined due to the limited number of nitro compounds and mutant strains tested in the study (*2*). Nitroalkane oxidation in *Williopsis saturnus* was later identified in 1975 through a survey of ~70 fungal and bacterial strains grown in the presence of 0.5% nitroethane as a sole nitrogen source (*3*). Cultures of *W. saturnus* were able to grow rapidly in the presence of nitroethane and nitrite accumulation was observed in the culture medium (*3*), suggesting that the enzyme involved in nitroalkane oxidation might be similar to the one isolated from *N. crassa*. Extracts were prepared from *W. saturnus* and of a limited number of nitroalkane substrates tested, 2-nitropropane was found to show the highest activity (*3*).

$$H_3C{-}\underset{\underset{\underset{{}^-O}{\overset{\|}{}}N^+}{|}}{\overset{\overset{\color{red}H}{|}}{C}}{-}CH_3 \quad \xrightleftharpoons[\color{red}H^+]{pK_a = 8.4} \quad \underset{\underset{{}^-O\quad O^-}{N^+}}{\overset{H_3C\quad CH_3}{C}} \quad \longleftrightarrow \quad H_3C{-}\overset{-}{\underset{\underset{{}^-O\quad O}{N^+}}{C}}{-}CH_3$$

2-nitropropane   propyl-2-nitronate
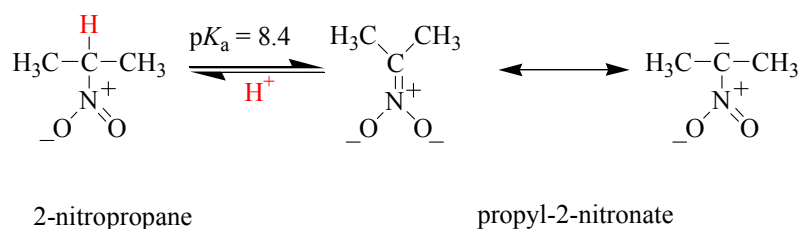
Scheme 1.1 Ionization of 2-nitropropane (left) to yield propyl-2-nitronate (right).

Additional studies of the purified enzymes from *N. crassa* and *W. saturnus* lead the authors to propose that the nitroalkane oxidizing enzyme most effectively oxidizes 2-nitropropane as compared with primary nitroalkanes as substrate (*5, 6*). End point assays are undesirable when studying nitroalkane oxidizing enzymes both because of the traditional complications arising from deviations from the requirements of the Michaelis-Menten model of enzyme kinetics (*7*) and because of the known ionization of nitroalkanes at physiological pH values (Scheme 1.1) (*4, 8*). Enzymatic activity was monitored after 5 min of incubation by measuring the nitrite liberated from the nitroalkane substrates tested (*5, 6*). During the time course of the assay equilibrium between the neutral and anionic forms of the nitroalkane would have been approached, thus preventing an unambiguous conclusion as to which ionic form of the

compound is utilized by the enzyme as substrate. Further, complications arise in the interpretation of the substrate specificity of the nitroalkane oxidizing enzymes determined with end-point assays given the known reactivity of 2-nitropropane with superoxide anion that was established by Fridovich after the initial studies of the *W. saturnus* enzyme was conducted (*9*). The known reactivity of 2-nitropropane with superoxide anion and that many flavin dependent enzymes such as glucose oxidase (*10*) and propionate-3-nitronate oxidase (*11*) release the free radical during turnover with nitroalkanes lead to additional studies of the fungal enzymes, in which the enzymatic activity assays were carried out in the presence of superoxide dismutase. As described in Chapter 3 and in published report on the *W. saturnus* enzyme (*49*) running activity assays in the presence of superoxide dismutase scavenges any superoxide anion that is produced and released during turnover of the enzyme with 2-nitropropane and thereby abates any non-enzymatic component of the observed reaction rates. The results with both the *N. crassa* and *W. saturnus* enzymes showed a significantly lower rate of oxygen consumption with 2-nitropropane as substrate when superoxide dismutase was included in the reaction mixture, which demonstrates that the majority of the activity observed is due to a free radical oxidation that is initiated and propagated by the superoxide anion.

$$O_2 + 2e\text{-} + 2H\text{+} + X \xrightarrow{\text{monooxygenase}} H_2O + XO$$

$$O_2 + X \xrightarrow{\text{dioxygenase}} XO_2$$

$$O_2 + 2e\text{-} + 2H\text{+} \xrightarrow{\text{oxidase}} H_2O_2$$
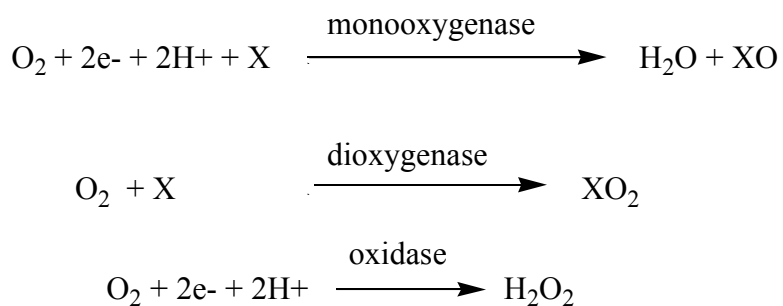
Scheme 1.2 Stoichiometries for the reduction of molecular oxygen catalyzed by flavoprotein, monooxygenases, dioxygenases and oxidases.
Both the electrons and protons required to reduce molecular oxygen are provided by the reduced flavin-containing enzyme, which are not shown for clarity.

The classification of flavin dependent enzymes as monooxygenases, dioxygenases, or oxidases depends on the fate of molecular oxygen after flavin oxidation occurs during turnover (12). Dioxygenases incorporate both the oxygen atoms of dioxygen into the organic product of the reaction, whereas monooxygenases incorporate only one, and oxidases none (Scheme 1.2). Flavin dependent oxidases are further distinguished from the oxygenases in that hydrogen peroxide forms from the reduction of molecular oxygen in the former, but not the latter (12). The original proposal by Little that the *N. crassa* nitroalkane oxidizing enzyme is an oxidase was tested by monitoring for hydrogen peroxide formation during turnover of the enzyme with 2-nitropropane (6). Hydrogen peroxide was not detected with the purified enzymes from either *N. crassa* or *W. saturnus* either through fluorometric detection methods (5, 6) or coupling the enzymatic assays with catalase (13, 14). Thus, the enzyme is not an oxidase, but rather is an oxygenase.

1.3 Classification of the Fungal Enzyme as Nitronate Monooxygenase

The cloning, expression and development of rapid purification procedures for the nitroalkane oxidizing enzymes from *N. crassa* (*13*) and *W. saturnus* (*14*) by Gadda *et al*. allowed for a more detailed characterization of the substrate specificity and mechanistic properties of the enzyme. Initial rates were measured using a variety of nitroalkanes in either their fully protonated or deprotonated forms to establish the substrate specificity. Assays were carried out in either the absence or presence of superoxide dismutase to scavenge any superoxide anion that might be present that would initiate the non-enzymatic component of the reaction. As outlined in Chapters 3 and 7, the results demonstrated that while 2-nitropropane as well as primary nitroalkanes ranging from two to six carbon atoms is substrates for the *N. crassa* enzyme,

significantly higher activity was observed with primary alkyl nitronates. No activity was observed with 2-nitropropane or primary nitroalkanes as substrate for the *W. saturnus* enzyme, but significant rates of oxygen consumption were observed with primary alkyl nitronates (*14*).

As described in Chapters 3 through 6, studies of the *N. crassa* enzyme are consistent with the monooxygenase mechanism of Scheme 3. After binding the nitroalkane (step 1), catalysis is initiated with the histidine-196 catalyzed deprotonation of the α-carbon to yield ethylnitronate (*15*) (step 2). Alternatively, ethylnitronate can bind directly to the enzyme, as has been shown to be the case with the *W. saturnus* enzyme (*14*). The enzyme-bound nitronate is then either oxidized through the transfer of a single electron to the flavin cofactor of the nitronate monooxygenase to generate an anionic flavosemiquinone (*13*) and a radical substrate intermediate (step 4) or is released from the enzyme as a non-oxidative product (step 3) (*15, 16*). Molecular oxygen then reacts with the flavosemiquinone to oxidize the flavin (step 5) and generate superoxide (*13, 17*). Superoxide then reacts with the substrate-derived radical to generate a peroxynitroalkyl intermediate (step 6) which is then likely released from the enzyme where it undergoes a non-enzymatic reaction to generate the carbonyl product of the reaction (step 7).

The detailed mechanistic studies carried out over the past 10 years on the nitroalkane oxidizing enzymes from *N. crassa* and *W. saturnus* have lead to the reclassification of the biocatalysts from 2-nitropropane dioxygenases to nitronate monooxygenases by the International Union of Biochemistry and Molecular Biology. As will be outlined in Chapter 8, primary alkyl nitronates are likely not the true physiological substrates for the enzyme. Recent *in vivo* and *in vitro* studies of the enzymes have demonstrated that the nitronate monooxygenase is involved in the detoxification of the plant metabolite, propionate-3-nitronate.
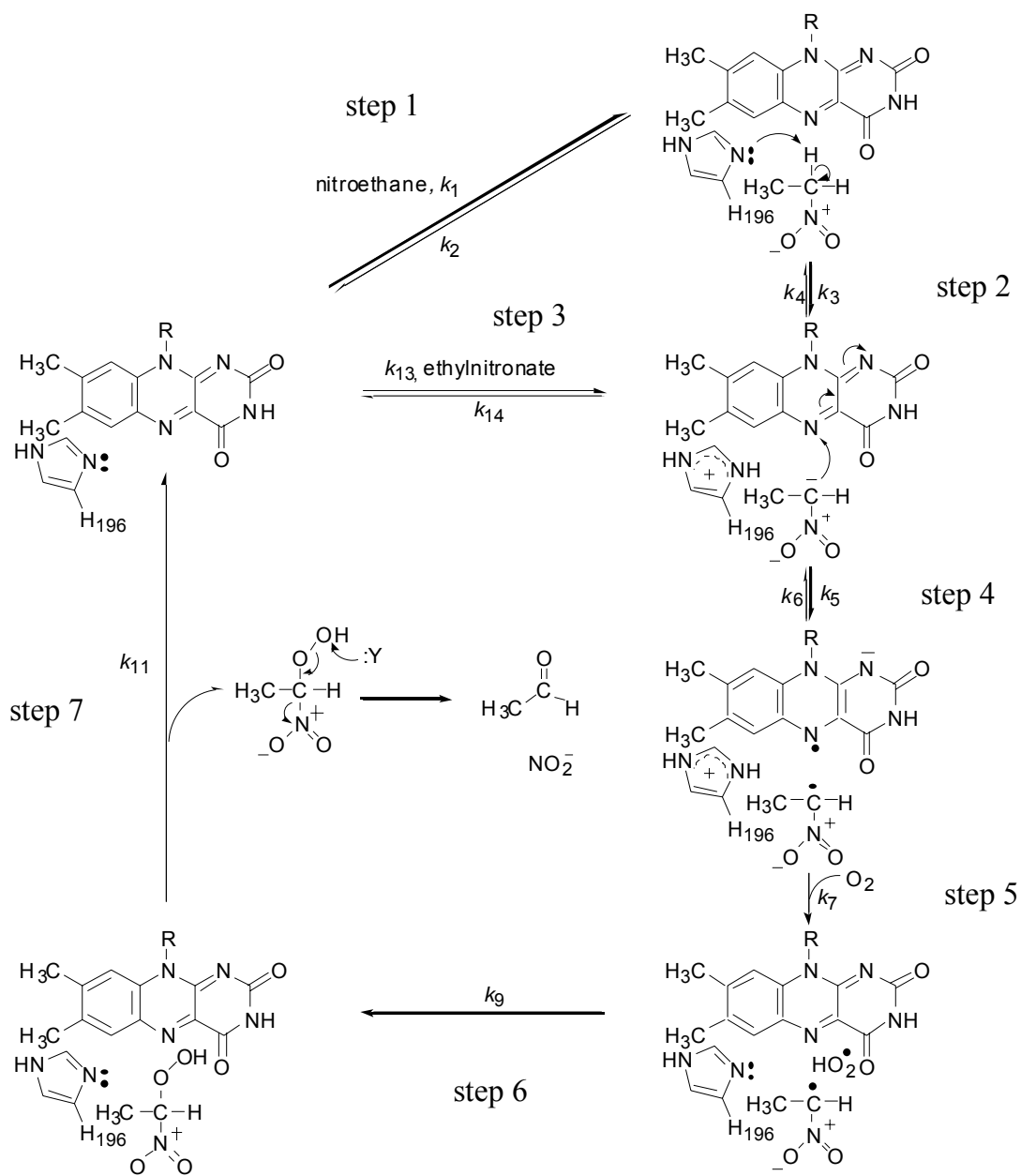
Scheme 1.3 The catalytic mechanism of *N. crassa* nitronate monooxygenase with nitroethane as substrate.

1.4   General Mechanisms of Flavin Dependent Nitroalkane Oxidizing Enzymes

The studies establishing the catalytic mechanism of nitronate monooxygenase described in this dissertation add to a long list of studies on nitroalkane oxidation by flavin dependant enzymes. Nitroalkanes have historically been used as mechanistic probes of flavin dependent enzymes, since many have been shown to be either alternate substrates or mechanism based inhibitors (*10, 11, 18-26*). Flavin dependent enzymes that catalyze the oxidation of nitroalkanes in a non-physiological reaction include D-amino acid oxidase (*24, 25*) and glucose oxidase (*10*). Nitro compounds that irreversibly inhibit flavin dependent enzymes include the natural toxin propionate-3-nitronate, which is a potent inhibitor of mitochondrial succinate dehydrogenase (*18, 21, 27*), along with 1-chloro-1-nitroethane and dibromonitromethane which inactivate D-amino acid oxidase (*19*) and glucose oxidase (*24*), respectively. In addition the mechanism of the flavin dependant enzymes nitroalkane oxidase (*28-36*) and propionate-3-nitronate oxidase (*11, 37*), whose physiological role is ascribed to the oxidation of nitro alkyl compounds have been elucidated.

Table 1.1 Nitroalkane Oxidation by Flavin Dependent Enzymes

source	enzyme	mechanism	references
N. crassa	nitronate monooxygenase	scheme 3	(*13, 15, 33*)
W. saturnus	nitronate monooxygenase	scheme 3	(*14*)
P. aeuroginosa	propionate-3-nitronate monooxygenase	scheme 3	chapter 10
F. oxysporum	nitroalkane oxidase	scheme 4	(*34, 35*)
hog kidney	D-amino acid oxidase	scheme 4	(*25*)
P. atrovenetum	propionate-3-nitronate oxidase	scheme 5	(*11*)
H. comosa	propionate-3-nitronate oxidase	scheme 5	(*37*)
A. niger	glucose oxidase	scheme 5	(*10*)

As summarized in Table 1.1, three general mechanisms of nitroalkane oxidation by flavin dependent enzymes have been established. These include the mechanisms involving the formation of a covalent flavin N(5) adduct, an anionic flavosemiquinone intermediate and

oxidation through a non-enzymatic free radical chain reaction initiated by the enzyme. The mechanism involving a flavosemiquinone is described above. The mechanism involving a covalent flavin N(5) will be described using nitroalkane oxidase as a model adduct and the initiation of a free radical chain reaction will be described using propionate-3-nitronate oxidase as a model.

The mechanism involving a covalent flavin-N(5) adduct with a nitronate intermediate formed during catalytic turnover has been most extensively studied with nitroalkane oxidase (*28-35, 38-45*), but also has been proposed for the reaction of D-amino acid oxidase with nitroethane as substrate (*25*). The oxidation of nitroethane by nitroalkane oxidase is initiated by a proton abstraction between the nitroalkane and aspartate 402 in the *F. oxysporum* enzyme as established by crystallographic and mutagenesis studies (*31, 32, 46*). The resulting ethylnitronate intermediate then forms a covalent flavin N(5) adduct with the FAD cofactor of the enzyme as evident from trapping experiments with cyanide and a crystal structure of the N5-(2-nitrobutyl)-1,5-dihydro-FAD

Scheme 1.4 Nitroalkane oxidation by *F. oxysporum* nitroalkane oxidase.

(*29*). Flavin reduction is followed by expulsion of nitrite to generate a cationic imine that undergoes a nucleophilic attack to ultimately generate the aldehyde product of the reaction (*34*).

The catalytic mechanism of propionate-3-nitronate oxidase from *P. atrovenetum* (*11*) is shown in Scheme 1.5. The catalytic mechanism of the fungal enzyme is also proposed for the glucose oxidase catalyzed oxidation of nitroethane (*10*). Both enzymes act exclusively on the nitronate
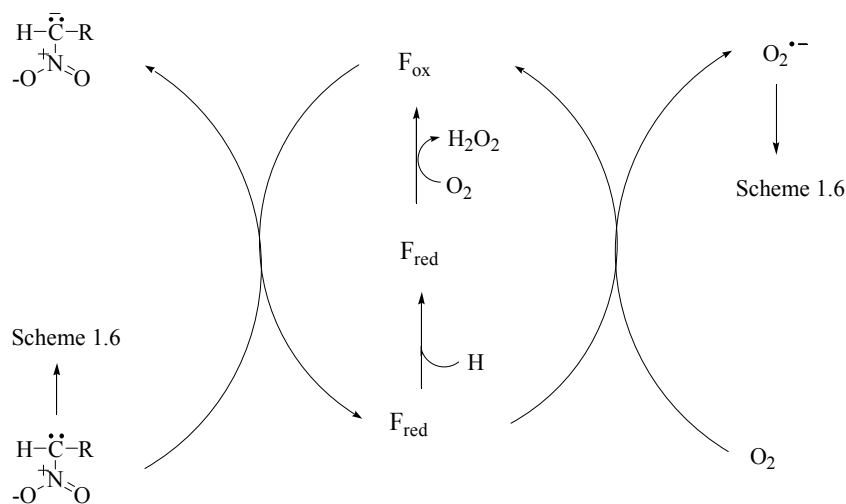
Scheme 1.5 Nitroalkane oxidation by propionate-3-nitronate oxidase.
F_{ox} – oxidized flavin; F_{sq} = flavin semiquinone; F_{red} = reduced flavin.

form of nitroalkanes where catalysis is initiated by the transfer of a single electron to the flavin cofactors to generate a nitronate radical that is released from the enzyme to initiate a non-enzymatic free radical chain reaction upon reacting with molecular oxygen. Molecular oxygen is then partially reduced by the flavosemiquinone form of the enzyme and is released to the solvent where it undergoes a similar free radical reaction.

The non-enzymatic reaction between superoxide anion and alkyl nitronates was studied in detail by Fridovich *et al.* and is shown in Scheme 1.6. Hydrolysis of the nitronate radical expels nitrite and generates a hydroxyl radical intermediate, which propagates the reaction through a single electron reduction of molecular oxygen to regenerate superoxide anion. The termination of the reaction occurs once two superoxide anions react to generate hydrogen peroxide and O_2.

ionization

$$R\text{--}\overset{\overset{\displaystyle H}{|}}{\underset{\underset{\displaystyle NO_2}{|}}{C}}\text{--}R \longrightarrow R\text{--}\overset{\overset{\displaystyle \cdot\cdot}{}}{\underset{\underset{\displaystyle NO_2}{|}}{C}}{}^{-}\text{--}R$$

initiation

$$R\text{--}\overset{\overset{\displaystyle \cdot\cdot}{}}{\underset{\underset{\displaystyle NO_2}{|}}{C}}{}^{-}\text{--}R + O_2^{\bullet-} + 2H^+ \longrightarrow R\text{--}\overset{\overset{\displaystyle \bullet}{}}{\underset{\underset{\displaystyle NO_2}{|}}{C}}\text{--}R + H_2O_2$$

hydrolysis

$$R\text{--}\overset{\overset{\displaystyle \bullet}{}}{\underset{\underset{\displaystyle NO_2}{|}}{C}}\text{--}R + OH^- \longrightarrow R\text{--}\overset{\overset{\displaystyle \bullet}{}}{\underset{\underset{\displaystyle OH}{|}}{C}}\text{--}R + NO_2^-$$

propagation

$$R\text{--}\overset{\overset{\displaystyle \bullet}{}}{\underset{\underset{\displaystyle OH}{|}}{C}}\text{--}R + O_2 \longrightarrow R\text{--}\overset{\overset{}{}}{\underset{\underset{\displaystyle O}{||}}{C}}\text{--}R + H^+ + O_2^{\bullet-}$$

termination

$$O_2^{\bullet-} + O_2^{\bullet-} + H^+ \longrightarrow H_2O_2 + O_2$$

Scheme 1.6 The free radical chain reaction between superoxide anion and alkyl nitronates.

1.5   Specific Goals Addressed in the Dissertation

The majority of the studies described in this dissertation were aimed at an understanding of the biochemical and mechanistic properties of the nitroalkane oxidizing enzyme from *N. crassa* that was first introduced by Little in 1951 (*2*). As outlined in this chapter, the exact nature of the reaction catalyzed by the enzyme and the role it plays in the survival of the fungus has eluded scientists for the past 60 years. Experiments establishing the physiological role of nitronate monooxygenase were carried out during the last chapter of the author's doctoral research. Since this was the question that was constantly asked during presentations of the work described in subsequent chapters, a detailed review of the biology and biochemistry of propionate-3-nitronate will first be presented in Chapter 2.

An initial goal of the doctoral research described in the dissertation was to elucidate the catalytic mechanism of the nitroalkane oxidizing enzyme from *N. crassa.* Chapters 3 and 4 will present the details establishing that the once classified 2-nitropropane dioxygenase is actually a

nitronate monooxygenase. In addition, these chapters will describe the first reports of an experimentally detectable anionic flavosemiquinone intermediate in oxidative catalysis by flavoenzymes that have since been used by other investigators in the field to understand the catalytic nature of other flavin dependent enzymes. The kinetic consequences arising from the branching of reaction intermediates were discovered while investigating the catalytic mechanism of the enzyme and are described in Chapters 5 and 6. These studies illustrate an important consideration that must be applied when studying the physical nature of enzymatic catalysis as pointed out in recent articles on this subject**.**

Another goal of the doctoral research was to gain an understanding of the structural and biochemical properties of fungal nitronate monooxygenase. Chapter 7 presents a study of the structural features of the enzyme that allows it to bind nitro-compounds for subsequent oxidation. This was achieved through the use of competitive inhibitors and demonstrates ways in which the structural determinants to enzymatic catalysis can be inferred in the absence of a 3D crystallographic structure.

Establishing the physiological role of fungal nitronate monooxygenase was another goal of the doctoral research. Chapter 8 provides a report on unpublished results that establish the physiological substrate for the enzyme and provide insights into the role of nitronate oxidation in nature. Chapter 9 describes studies carried out in collaboration with Dr. Jim spain at the Georgia Institute of Technology, which expands on the findings of Chapter 8 and suggest that a recently discovered propionate-3-nitronate oxidizing enzyme from *P. aeuroginosa (47)*. Finally, a general conclusion concerning the lessons learned from the study of nitronate monooxygenase will be presented in Chapter 11.

1.6 References

1. Gadda, G., and Francis, K. (2009) Nitronate monooxygenase, a model for anionic flavin semiquinone intermediates in oxidative catalysis, *Arch. Biochem. Biophys*. *493*, 53-61.

2. Little, H. N. (1951) Oxidation of nitroethane by extracts from *Neurospora*, *J. Biol. Chem. 193*, 347-358.

3. Kido, T., Yamamoto, T., and Soda, K. (1975) Microbial assimilation of alkyl nitro compounds and formation of nitrite, *Arch. Microbiol. 106*, 165-169.

4. Baer, H. H., and Urbas, L., (Eds.) (1970) in *The Chemistry of the Nitro and Nitroso Groups Part 2*, Interscience, New York.

5. Kido, T., and Soda, K. (1978) Properties of 2-nitropropane dioxygenase of *Hansenula mrakii*. Formation and participation of superoxide, *J. Biol. Chem. 253*, 226-232.

6. Gorlatova, N., Tchorzewski, M., Kurihara, T., Soda, K., and Esaki, N. (1998) Purification, characterization, and mechanism of a flavin mononucleotide-dependent 2-nitropropane dioxygenase from *Neurospora crassa*, *Appl. Environ. Microbiol. 64*, 1029-1033.

7. Allison, R. D., and Purich, D. L. (1979) Practical considerations in the design of initial velocity enzyme rate assays, *Methods. Enzymol. 63*, 3-22.

8. Watt, C. I. F. (2010) Primary kinetic hydrogen isotope effects in deprotonations of carbon acids, *J. Phys. Org. Chem*. (2010), 561-571.

9. Kuo, C. F., and Fridovich, I. (1986) Free-radical chain oxidation of 2-nitropropane initiated and propagated by superoxide, *Biochem. J. 237*, 505-510.

10. Porter, D. J., and Bright, H. J. (1977) Mechanism of oxidation of nitroethane by glucose oxidase, *J. Biol. Chem. 252*, 4361-4370.

11. Porter, D. J., and Bright, H. J. (1987) Propionate-3-nitronate oxidase from *Penicillium atrovenetum* is a flavoprotein which initiates the autoxidation of its substrate by O$_2$, *J. Biol. Chem. 262*, 14428-14434.

12. Massey, V. (1994) Activation of molecular oxygen by flavins and flavoproteins, *J. Biol. Chem. 269*, 22459-22462.

13. Francis, K., Russell, B., and Gadda, G. (2005) Involvement of a flavosemiquinone in the enzymatic oxidation of nitroalkanes catalyzed by 2-nitropropane dioxygenase, *J. Biol. Chem. 280*, 5195-5204.

14. Mijatovic, S., and Gadda, G. (2008) Oxidation of alkyl nitronates catalyzed by 2-nitropropane dioxygenase from *Hansenula mrakii*, *Arch. Biochem. Biophys. 473*, 61-68.

15. Francis, K., and Gadda, G. (2008) The nonoxidative conversion of nitroethane to ethylnitronate in *Neurospora crassa* 2-nitropropane dioxygenase is catalyzed by histidine 196, *Biochemistry 47*, 9136-9144.

16. Francis, K., and Gadda, G. (2009) Inflated kinetic isotope effects in the branched mechanism of N. crassa 2-nitropropane dioxygenase, *Biochemistry 48*, 2403-2410.

17. Francis, K., and Gadda, G. (2006) Probing the chemical steps of nitroalkane oxidation catalyzed by 2-nitropropane dioxygenase with solvent viscosity, pH, and substrate kinetic isotope effects, *Biochemistry 45*, 13889-13898.

18. Alston, T. A., Mela, L., and Bright, H. J. (1977) 3-Nitropropionate, the toxic substance of *Indigofera*, is a suicide inactivator of succinate dehydrogenase, *Proc. Natl. Acad. Sci. U. S. A. 74*, 3767-3771.

19. Alston, T. A., Porter, D. J., and Bright, H. J. (1983) Suicide inactivation of D-amino acid oxidase by 1-chloro-1-nitroethane, *J. Biol. Chem. 258*, 1136-1141.

20. Alston, T. A., Seitz, S. P., Porter, D. J., and Bright, H. J. (1980) Inhibition of succinate dehydrogenase by nitroacetate and by the toxic antibiotic nitraminoacetate, *Biochem. Biophys. Res. Commun. 97*, 294-300.

21. Coles, C. J., Edmondson, D. E., and Singer, T. P. (1979) Inactivation of succinate dehydrogenase by 3-nitropropionate, *J. Biol. Chem. 254*, 5161-5167.

22. Porter, D. J., and Bright, H. J. (1985) The Bioorganic Chemistry of the Nitro Alkyl Group, *Bioorg. Chem. 13*, 375-403.

23. Porter, D. J., Voet, J. G., and Bright, H. J. (1972) Nitroalkanes as reductive substrates for flavoprotein oxidases, *Z. Naturforsch B. 27*, 1052-1053.

24. Porter, D. J., Voet, J. G., and Bright, H. J. (1972) Nitromethane. A novel substrate for D-amino acid oxidase, *J. Biol. Chem. 247*, 1951-1953.

25. Porter, D. J., Voet, J. G., and Bright, H. J. (1973) Direct evidence for carbanions and covalent N 5 -flavin-carbanion adducts as catalytic intermediates in the oxidation of nitroethane by D-amino acid oxidase, *J Biol Chem 248*, 4400-4416.

26. Porter, D. J., Voet, J. G., and Bright, H. J. (2000) Active site generation of a protonically unstable suicide substrate from a stable precursor: glucose oxidase and dibromonitromethane, *Biochemistry 39*, 11808-11817.

27. Huang, L. S., Sun, G., Cobessi, D., Wang, A. C., Shen, J. T., Tung, E. Y., Anderson, V. E., and Berry, E. A. (2006) 3-nitropropionic acid is a suicide inhibitor of mitochondrial respiration that, upon oxidation by complex II, forms a covalent adduct with a catalytic base arginine in the active site of the enzyme, *J. Biol. Chem. 281*, 5965-5972.

28. Fitzpatrick, P. F., Bozinovski, D. M., Heroux, A., Shaw, P. G., Valley, M. P., and Orville, A. M. (2007) Mechanistic and structural analyses of the roles of Arg409 and Asp402 in the reaction of the flavoprotein nitroalkane oxidase, *Biochemistry 46*, 13800-13808.

29. Valley, M. P., Tichy, S. E., and Fitzpatrick, P. F. (2005) Establishing the kinetic competency of the cationic imine intermediate in nitroalkane oxidase, *J. Am. Chem. Soc. 127*, 2062-2066.

30. Fitzpatrick, P. F., Orville, A. M., Nagpal, A., and Valley, M. P. (2005) Nitroalkane oxidase, a carbanion-forming flavoprotein homologous to acyl-CoA dehydrogenase, *Arch. Biochem. Biophys. 433*, 157-165.

31. Valley, M. P., and Fitzpatrick, P. F. (2003) Inactivation of nitroalkane oxidase upon mutation of the active site base and rescue with a deprotonated substrate, *J. Am. Chem. Soc. 125*, 8738-8739.

32. Valley, M. P., and Fitzpatrick, P. F. (2003) Reductive half-reaction of nitroalkane oxidase: effect of mutation of the active site aspartate to glutamate, *Biochemistry 42*, 5850-5856.

33. Gadda, G., Choe, D. Y., and Fitzpatrick, P. F. (2000) Use of pH and kinetic isotope effects to dissect the effects of substrate size on binding and catalysis by nitroalkane oxidase, *Arch. Biochem. Biophys. 382*, 138-144.

34. Gadda, G., and Fitzpatrick, P. F. (2000) Mechanism of nitroalkane oxidase: 2. pH and kinetic isotope effects, *Biochemistry 39*, 1406-1410.

35. Gadda, G., and Fitzpatrick, P. F. (2000) Iso-mechanism of nitroalkane oxidase: 1. Inhibition studies and activation by imidazole, *Biochemistry 39*, 1400-1405.

36.   Heasley, C. J., and Fitzpatrick, P. F. (1996) Kinetic mechanism and substrate specificity of nitroalkane oxidase, *Biochem. Biophys. Res. Commun. 225*, 6-10.

37.   Hipkin, C. R., Salem, M. A., Simpson, D., and Wainwright, S. J. (1999) 3-nitropropionic acid oxidase from horseshoe vetch (Hippocrepis comosa): a novel plant enzyme, *Biochem. J. 340 (Pt 2)*, 491-495.

38.   Gadda, G., Banerjee, A., Dangott, L. J., and Fitzpatrick, P. F. (2000) Identification of a cysteine residue in the active site of nitroalkane oxidase by modification with N-ethylmaleimide, *J. Biol. Chem. 275*, 31891-31895.

39.   Gadda, G., Banerjee, A., and Fitzpatrick, P. F. (2000) Identification of an essential tyrosine residue in nitroalkane oxidase by modification with tetranitromethane, *Biochemistry 39*, 1162-1168.

40.   Gadda, G., Banerjee, A., Fleming, G. S., and Fitzpatrick, P. F. (2001) Evidence for an essential arginine in the flavoprotein nitroalkane oxidase, *J. Enzyme Inhib. 16*, 157-163.

41.   Gadda, G., Dangott, L. J., Johnson, W. H., Jr., Whitman, C. P., and Fitzpatrick, P. F. (1999) Characterization of 2-oxo-3-pentynoate as an active-site-directed inactivator of flavoprotein oxidases: identification of active-site peptides in tryptophan 2-monooxygenase, *Biochemistry 38*, 5822-5828.

42.   Gadda, G., Edmondson, R. D., Russell, D. H., and Fitzpatrick, P. F. (1997) Identification of the naturally occurring flavin of nitroalkane oxidase from *Fusarium oxysporum* as a 5-nitrobutyl-FAD and conversion of the enzyme to the active FAD-containing form, *J. Biol. Chem. 272*, 5563-5570.

43. Gadda, G., and Fitzpatrick, P. F. (1998) Biochemical and physical characterization of the active FAD-containing form of nitroalkane oxidase from *Fusarium oxysporum*, *Biochemistry 37*, 6154-6164.

44. Gadda, G., and Fitzpatrick, P. F. (1999) Substrate specificity of a nitroalkane-oxidizing enzyme, *Arch. Biochem. Biophys. 363*, 309-313.

45. Valley, M. P., and Fitzpatrick, P. F. (2004) Comparison of enzymatic and non-enzymatic nitroethane anion formation: thermodynamics and contribution of tunneling, *J. Am. Chem. Soc. 126*, 6244-6245.

46. Nagpal, A., Valley, M. P., Fitzpatrick, P. F., and Orville, A. M. (2006) Crystal structures of nitroalkane oxidase: insights into the reaction mechanism from a covalent complex of the flavoenzyme trapped during turnover, *Biochemistry 45*, 1138-1150.

47. Nishino, S.F., Shin, K.A., Payne, R.B. and Spain, J.C. Growth of bcteria on 3-nitropropionic acid as a sole source of carbon, nitrogen, and energy, *Appl. Environ. Microbiol.*76, 3590-3598.

2   CHAPTER II

THE BIOLOGY AND BIOCHEMISTRY OF 3-NITROPROPIONATE: A POTENT INHIBITOR OF SUCCINATE DEHYDROGENASE

2.1   Abstract

3-Nitropropionate is a highly toxic nitro compound that is widely distributed in fungi and leguminous plants. The toxicity of the nitro compound arises from its conjugate base, propionate-3-nitronate, that upon ingestion irreversibly inhibits the mitochondrial enzyme succinate dehydrogenase leading to a variety of neurological disorders and, at sufficiently high concentrations, death. 3-Nitropropionate poisoning results in striatal degeneration that gives rise to symptoms resembling those of Huntington's disease. Thus, the compound has been extensively used in model studies of the Huntington's disease and numerous reviews have been written on this subject. This review outlines the biological distribution, synthesis and function of 3-nitropropionate in plants and fungi as well as the biochemical basis for its toxicity. In addition the biochemical and mechanistic properties of several 3-nitropropionate oxidizing enzymes are discussed and their physiological roles in the detoxification and utilization of the compound as a growth substrate are described. The review closes by raising several open questions concerning the production and role of 3-nitropropionate in the environment.

2.2   Introduction

3-Nitropropionate is a highly toxic nitro compound that has been isolated from several leguminous plants and fungal species (*2, 4-8*). The first report of the toxin was in 1920, when it was isolated from the bark *Hiptage mandoblota* and identified as hiptagenic acid (*6*). A detailed chemical analysis of the toxin from *Hiptage* was later carried out in 1949, where the structure of the nitro compound was determined to be that of 3-nitropropionate (Scheme 1) (*5*). The

discovery of 3-nitropropionate almost a century ago represents the first isolation of an organic nitro compound in nature (*11, 12*). As summarized in recent review articles (*13, 14*), well over 200 naturally occurring nitro compounds have now been isolated and the biosynthesis, geological distribution and physiological functions of many are well understood. This article outlines the current knowledge concerning the biological and chemical properties of 3-nitropropionate along with the mechanistic properties of the enzymes that are known to act on the compound.

The review will start with a description of the physical properties of the toxin and will continue into the biological distribution and synthesis of the 3-nitropropionate. A detailed overview of the biochemical basis for the toxicity of 3-nitropropionate will be provided along with a description of the physiological effects of poisoning in humans and in domestic livestock. Finally, the biochemical and mechanistic properties of a number of enzymes that serve as nature's defense against the compound by oxidizing 3-nitropropionate to a less toxic semialdehyde will be outlined. The review will close by raising open questions regarding the biology and biochemistry of 3-nitropropionate.

2.3 Chemical Properties of 3-Nitropropionate
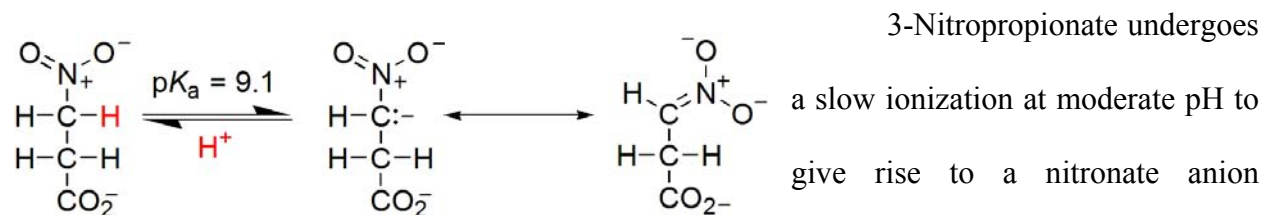
Scheme 2.1 Ionization of 3-nitropropionate (right) to yield propionate-3-nitronate (left).

3-Nitropropionate undergoes a slow ionization at moderate pH to give rise to a nitronate anion (Scheme 2.1). The ionization of the CH bond of 3-nitroproprionate is unusual given the large pK_a values for alkyl groups, which prevents CH bond cleavage at moderate pH values. The physical-chemical nature of this ionization has been extensively

studied in nitroalkanes and is commonly referred to as the principle of nonperfect synchronization (*18*). Ionization of the α-carbon results in a delocalization of electrons on the nitro group of the nitro alkyl compound, which makes the equilibrium thermodynamically favored. Thus, pK_a values of nitro alkyl compounds are quite low and range from 5 to 10 (*19*), or in the case of 3-nitropropionate, 9.1 (*2*). The the intrinsic barrier for the ionization is high, though which makes the deprotonation of the nitrolaknae a slow process ionization of nitroalkyl compounds is a slow process (*18*). The second-order rate constants for the ionization of nitroalkyl compounds range from 2 to 6 M^{-1} s^{-1} for the deprotonation of the α-carbon and 15 to 75 $M^{-1}s^{-1}$ for the protonation of the nitronate (*19*). The slow rates of ionization allow for the biological and chemical properties of 3-nitropropionate to be evaluated using either the fully protonated or the conjugate base form of the toxin that is easily prepared by incubating the toxin in potassium hydroxide. Some physical properties of 3-nitropropionate are listed in Table 2.1.

Table 2.1 Physical Properties of 3-Nitropropionate

molecular weight	119.08 g/mol
pK_a (carboxylate)[a]	3.8
pK_a (α-carbon)[a]	9.1
melting point[a]	64-65 ^{o}C
λ_{max}[b]	204 nm
ε_{230}[b]	8,400 $M^{-1}cm^{-1}$

[a]From (*2*). [b]From (*5*).

2.4 Biological Occurrence and Function of 3-Nitropropionate

As illustrated in Table 2.2, 3-nitropropionate has been found in a vast array of plants and fungal species since its original isolation in 1920 (*2, 4, 5, 9, 11, 16*). 3-Nitropropionate is a potent and irreversible inhibitor of mitochondrial succinate dehydrogenase (see below), so it most likely produced as a means of defense by the organism against herbivores. 3-Nitropropionate is found as an ester in the glycoside hiptakin in the bark of *Hiptage (12, 14)*. The

Table 2.2 Biological Occurrence of 3-Nitropropionate

Fungal Species	Plant Species	Plant Species (continued)
Arthrinium aureum[a]	*Astragalus* sp[h]	*Lotus angustissimus*[g]
Arthrinium phaeospermum[a]	*Astragalus falcatus*[g]	*Lotus uliginosus*[h]
Arthrinium sacchari[a]	*Cirsium avense*[g]	*Securigeva oriontalis*[h]
Arthrinium sereaeusis[a]	*Coronilla varia*[h]	*Securigeva parviflora*[h]
Arthrinium terminalis[a]	*Coronilla viminalis*[h]	*Securigeva securidaca*[h]
Astragalus miser[b]	*Corynocarpus laevisatus*[h]	*Securigeva varian*[h]
Aspergillus flavus[b]	*Hippocrepis balearica*[h]	*Scorpiurus muricatus*[h]
Aspergillus oryzae[c]	*Hippocrepis comosa*[h]	*Scorpiurus vermicutatus*[h]
Aspergillus wentii[b]	*Hippocrepis emerus*[h]	*Viola ordarata*[h]
Penicillium atroventum[d]	*Hippocrepis unisiliquosa*[h]	
Pestalotia palmorum[e]	*Hiptage mandoblota*[h]	
Phomopsis sp[f]	*Indigofera spicata*[h]	
Septorive cirsii[g]	*Indigofera endecaphylla*[h]	

[a]from (*3*); [a]from (*5*); [c]from (*10*); [d]from(*4*); [e]from (*15*); [f]from(*16*); [g]from (*17*), [h]from (*11*); [d]from (*9*).

a) 3-nitropropanoyl ester

b) 3-nitropropanoyl ester of 4-hydroxybutanate

c) 3-nitropropanoyl glycoside

d) isoxazolinone derivative

e) 5-oxotetrahydrofuran-3-acetate derivative
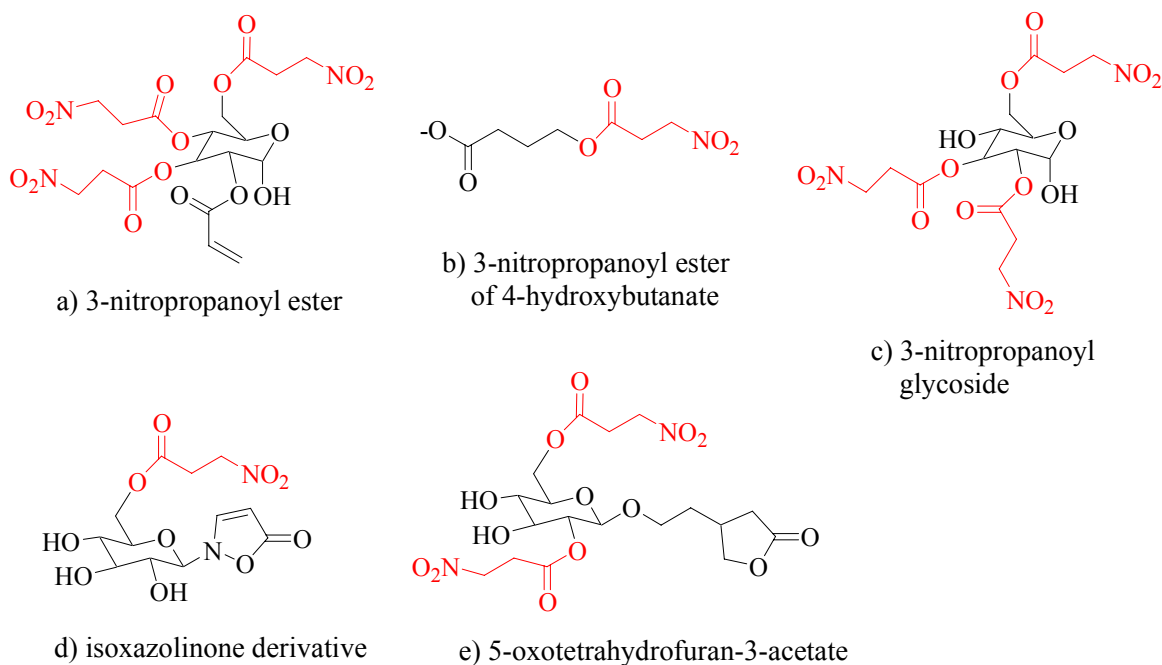
Figure 2.1 Examples of natural products contacting 3-nitropropionate moieties.

ester of 3-nitropropionate has also been found in the glycoside karakin in the berries of *Corynocarpus* (*12*). The toxin has also been isolated from 3-nitropropanoyl acryloyl esters in *Indigofera* sp. (*14*), esters of 4-hydroxybutanate in *Hippocrepis comosa* (*14*), and esters containing 5-oxotetrahydrofuran-3-acetic acid or isoxazolinone derivatives in *Astragalus (14)*.

Free forms of 3-nitropropionate are found in the fungi *Arthrinium* sp., *Aspergillus flavus*, *Aspergillus oryzae* and *Penicillium atroventum* (*2, 4, 11*). The structures of selected natural products containing the 3-nitropropionate moiety are given in Figure 2.1. For a more extensive list the reader is referred to (*14*).

In plants, 3-nitropropionate is thought to serve as both an anti-herbivory strategy and as a mechanism for nitrogen fixation in certain legumes. The role of 3-nitropropionate in protection against herbivores is supported both by its known toxicity to ruminant animals (*10, 15-17*) and its location in the plant (*9*). In horseshoe vetch, 3-nitropropionate accumulates in all parts of the shoots, but is not detected in the roots of the plant. The concentration of the nitro-compound can exceed 7% of the total amount of soluble nitrogen in the shoot (*9*). The large concentrations of 3-nitropropionate and the occurrence of the toxin only in the parts of the plants that are exposed to herbivores, strongly imply that the compound serves as a means of defense. Upon ingestion of the glycosides of 3-nitropropionate, the toxin is readily hydrolyzed by bacterial enzymes in the gut of ruminant animals to give a free form of the nitro compound (*11*). 3-Nitropropionate then irreversibly inhibits succinate dehydrogenase (*2, 18, 19*), a key enzyme in the Kreb's cycle that leads to energy production in the grazing animal. This leads to a variety of neurological disorders and, at sufficiently high concentrations, death. The role of the toxin in fungi is not fully established although it may serve a similar protective strategy as in plants.

In addition to providing the plant a means of defense, 3-nitropropionate also plays a role in the terrestrial nitrogen cycle as it is an intermediate in the nitrification process in many legumes (*9*). The role of 3-nitropropionate in the nitrification process was realized after an extensive survey that revealed each plant found to produce the nitro compound also contains a 3-nitropropionate oxidase activity (*9*). 3-Nitropropionate oxidase catalyzes the oxidation of the

nitro compound to yield nitrite and nitrate, in addition to malonic semialdehyde and hydrogen peroxide as illustrated in Scheme 2.2. The oxidation of 3-nitropropionate by enzymes in the leaves of these plants generate oxidized inorganic nitrogen that can that is then be released to the soil after senescence to replenish the nitrogen in the soil.

2.5   Biosynthesis of 3-Nitropropionate

3-nitropropionate   malonic semialdehyde
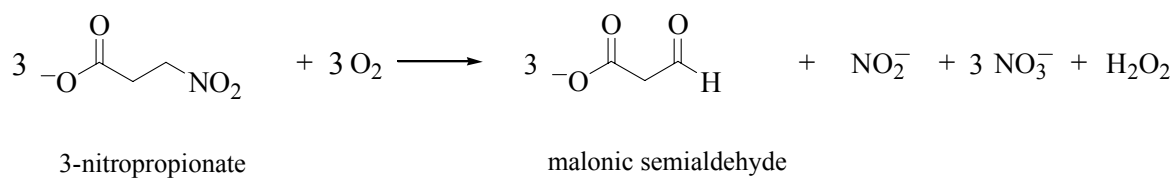
Scheme 2.2 3-Nitropropionate oxidation by legumes.

The biosynthesis of 3-nitropropionate occurs through different metabolic pathways in plants compared to fungi. 3-Nitropropionate production was first studied in *Penicillium atroventum*, where it was found that efficient incorporation of ^{14}C arose when the fungus was fed isotopically labeled aspartate (*15*). In creeping indigo *(Indigofera spicata)*, however, no heavy isotope incorporation was observed with aspartate, but maximal ^{14}C incorporation into 3-nitropropionate was observed when the plant was fed either labeled malonate or malonyl monohydroxamate (*1*). The labeled carbon atoms were incorporated into the C1 and C2 positions of 3-nitropropionate in the fungus and plant, respectively, as outlined below.

The biosynthetic pathway for 3-nitropropionate production in *P. atrovenetum* is shown in Scheme 2.3. The conversion of aspartate to 3-nitropropionate occurs through both an oxidation of the amino group and a decarboxylation at position C1 of aspartate. The amino group is first oxidized to give N-hydroxyaspartate by glutamate dehydrogenase (step a) (*26-28*). This reaction
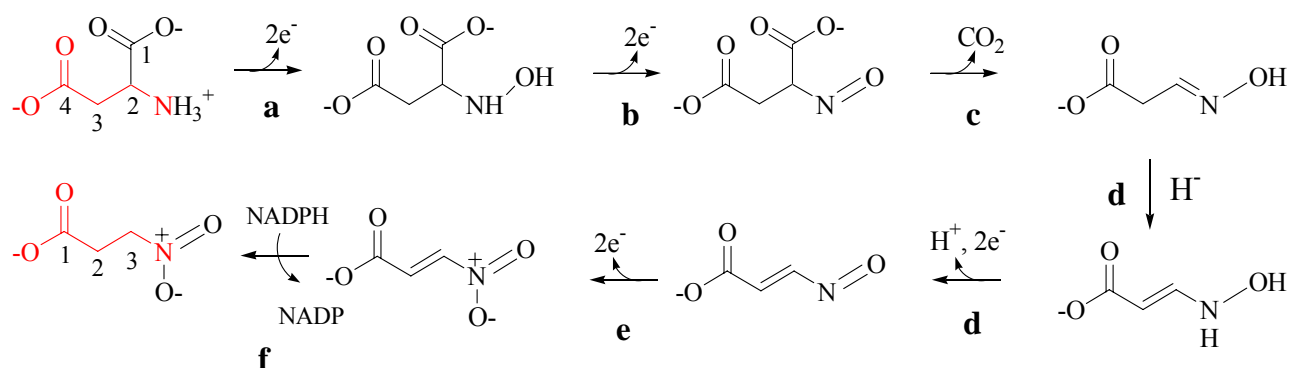
Scheme 2.3 Biosynthesis of 3-nitropropionate in *P. atrovenetum*.
a) gluatamte dehydrogenase; b and c) glutamate-oxaloacetate transaminase; d) presumably non-enzymatic; e) peroxidase; f) unidentified dehydrogenase.

is followed by a further oxidation of the N-hydroxy group (step b) and a decarboxylation reaction (step c) (*26-28*), which are both catalyzed by glutamate-oxaloacetate transaminase to yield a highly reactive oximine intermediate. Tautomerization of the oximine, presumably in a non-enzymatic reaction (step d), gives a nitroso compound that undergoes a peroxidase dependent oxidation to yield 3-nitroacrylate (step e). The C2-C3 double bond of 3-nitroacrylate is then reduced by a NADPH-dependent dehydrogenase (step f) (*28*) to generate 3-nitropropionate.

The biosynthetic pathway for the production of 3-nitropropionate in *Indigofera* is less understood, but a probable pathway is outlined in Scheme 2.4. No incorporation of ^{14}C was found in 3-nitropropionate when *Indigofera* was fed labeled aspartate, which indicates that the plant utilizes a different biosynthetic pathway than *Penicillium*. Maximal incorporation of ^{14}C was found when plants were given either malonate or malonylmonohydroxamate. Malonate is proposed to be converted first to malonyl CoA by thiokinase (step a). Malonyl CoA is then aminated (step b) and hydroxylated (step c) to give malonylmonohydroxamate. While no direct evidence for the conversion of malonyl CoA to the hydroxamate is available, ^{14}C incorporation into 3-nitropropionate was also observed when plants were fed labeled malonyl monohydroxamate, which suggests that it is an intermediate in 3-nitropropionate metabolism by

the plant. A reduction of this intermediate (steps d) would then produce a nitroso compound that undergoes a two step oxidation (steps e and f) to yield 3-nitropropionate. While the enzymes involved in the pathway have yet to be identified, the proposed pathway is supported by studies of malonate metabolism in photosynthetic bacteria and plants (1).
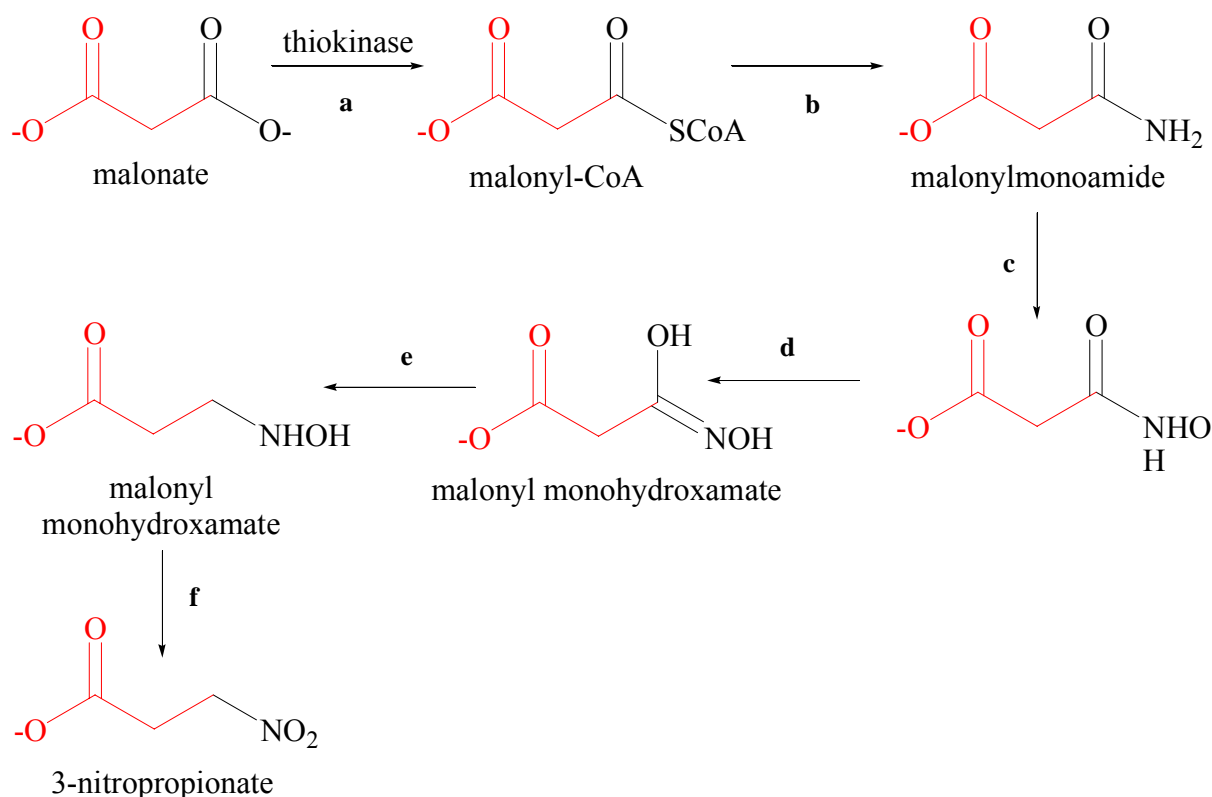
Scheme 2.4 3-Nitropropionate production in *Indigofera* (*1*).

2.6 Biochemical Basis for 3-Nitropropionate Toxicity
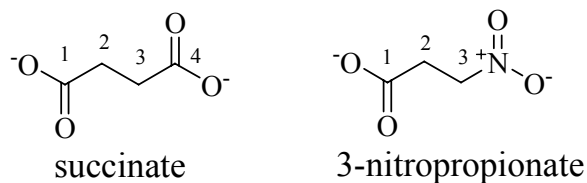
Figure 2.2 Chemical structures of succinate (left) and 3-nitropropionate (right).

Following the identification of 3-nitropropionate as the primary toxic component of *Indigofera* (*1*), Alston *et al.* tested the nitro compound as an inhibitor of succinate dehydrogenase (*2*). The mitochondrial enzyme catalyzes the oxidation of succinate to fumarate during the Krebs cycle and is the second

complex that shuttles electrons into the respiratory chain for oxidative phosphorylation (*4*). The nitronate form of the 3-nitropropionate was predicted to be a potent inhibitor of succinate dehydrogenase since it is an isoelectronic analogue of the physiological substrate for the enzyme (Figure 2) and because of the known reactivity of flavin dependent enzymes with nitronates (*5-7*).

No inhibition of succinate dehydrogenase was observed when mitochondria were mixed with 3-nitropropionate. However, when mitochondria were mixed with propionate-3-nitronate, inhibition of the succinate dehydrogenase was observed. Addition of propionate-3-nitronate to mitochondria incubated in the presence of succinate caused the concentration of oxygen to decrease in an exponential fashion to a non-zero value. Further addition of mitochondria resulted in a similar decrease in oxygen, which demonstrated that the lack of complete oxygen consumption was due to an irreversible inactivation of succinate dehydrogenase and not a reversible inhibition of the product of propionate-3-nitronate oxidation. Further evidence for an irreversible inhibition of succinate dehydrogenase was provided by washing mitochondria that had been inactivated by propionate-3-nitronate with a mannitol/sucrose solution to see if activity with succinate could be rescued. Washing the mitochondria did not restore activity, which is in contrast to the activity regained when the organelle is incubated with the reversible succinate dehydrogenase inhibitor malonate. Taken together these results established that the toxicity of the 3-nitropropionate arises from an irreversible inactivation of succinate dehydrogenase by its conjugate base propionate-3-nitronate.
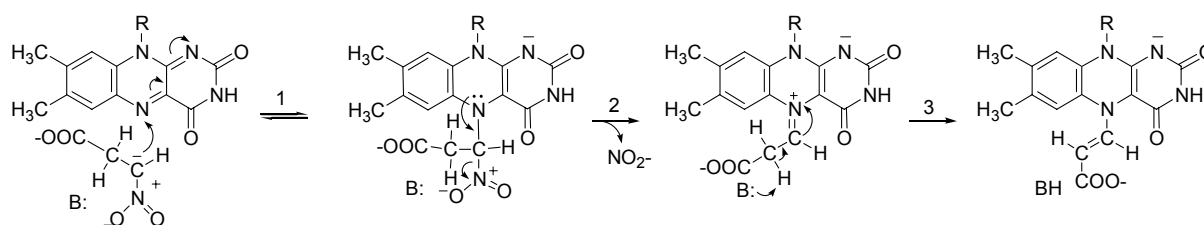
Scheme 2.5 Proposed mechanism of Alston *et al.* (*3*) for the inactivation of succinate dehydrogenase by propionate-3-nitronate.

The mechanism of inactivation of succinate dehydrogenase by propionate-3-nitronate was proposed to involve the formation of an irreversible covalent adduct between the nitronate inhibitor and the N(5) position of the flavin cofactor of the enzyme (Scheme 2.5) (*3*). The structural similarity between propionate-3-nitronate and succinate would make it likely that the toxin binds in the active site of the enzyme and is accessible to the flavin cofactor. After binding, propionate-3-nitronate would form a covalent bond between the α-carbon of the nitronate and the N(5) position of the flavin, which would readily eliminate nitrite to form a flavin N(5)-iminium intermediate (Scheme 2.5). The formation of a nitronate-flavin adduct is supported by previous studies of D-amino acid oxidase with ethylnitronate as substrate (*31*). A proton abstraction from the C(2) position of propionate-3-nitronate (Scheme 2.5) would then result in a stable flavin N(5) enamine adduct that would render the enzyme completely inactive.

The proposed mechanism for succinate dehydrogenase inactivation by propionate-3-nitronate was later tested by Coles *et al.* using purified enzyme from beef heart mitochondria (*23*). While the results obtained confirmed that the nitronate is an irreversible inhibitor of the metabolic enzyme, they were inconsistent with the formation of a flavin adduct. A covalent adduct between the nitronate inhibitor and the flavin cofactor of the enzyme would result in a bleaching of the absorbance at 450 nm of the oxidized flavin. However, inactivation of succinate dehydrogenase with propionate-3-nitronate did not result in a significant bleaching of the flavin spectrum, but rather resulted in spectral changes resembling those observed when incubating the enzyme with the irreversible inhibitor oxaloacetate (*23*). Mild proteolysis of inactivated succinate dehydrogenase, even under anaerobic conditions, reversed the spectral changes observed upon incubation of the enzyme with the nitronate (*23*), which further argued against the formation of an irreversible flavin adduct.
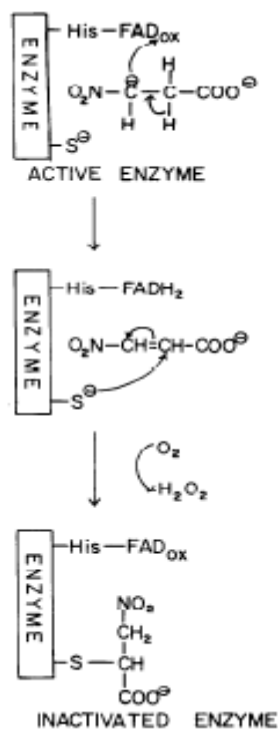
Figure 2.3 Postulated mechanism for the inactivation of succinate dehydrogenase by 3-nitropropionate. Taken from (23).

The evidence ruling out an irreversible modification of the flavin cofactor of succinate dehydrogenase as the culprit for inactivation lead to an alternative hypothesis that inhibition arises through a covalent modification of a cysteine thiol group in the active site of the enzyme (Figure 2.3). Previous studies of the enzyme demonstrated that the binding of succinate, malonate or oxaloacetate prevents modification of succinate dehydrogenase by the thiol alkylating agent *N*-ethylmaleimide. From these results it was proposed that an active site cysteine interacts with succinate to keep it bound in the active site for subsequent oxidation. Propionate-3-nitronate inactivation prevented the alkylation of a cysteine located on the 70,000 Da subunit of the enzyme by *N*-ethyl[^{14}C]malimidie. Prior treatment of succinate dehydrogenase with the irreversible inhibitor oxaloacetate prevented propionate-3-nitronate inactivation, which further suggests that the nitronate reacts with a key thiol group of the enzyme. Finally, oxidation of propionate-3-nitronate by succinate dehydrogenase would result in the formation of 3-nitroacrylate, which readily reacts with thiols (*32*). 3-Nitroacrylate was therefore tested as an irreversible inhibitor of succinate dehydrogenase where it was found to irreversibly inactivate the enzyme at significantly higher rates than propionate-3-nitronate. The mechanism of succinate dehydrogenase inactivation was therefore proposed to involve an activation of the nitronate through an oxidation reaction with the flavin cofactor of the enzyme to generate 3-nitroacylate, which would then irreversibly alkylate a key cysteine residue

in the active site (Figure 2.3). Alkylation of the active site cysteine would prevent the binding of

succinate and would therefore prevent catalysis.
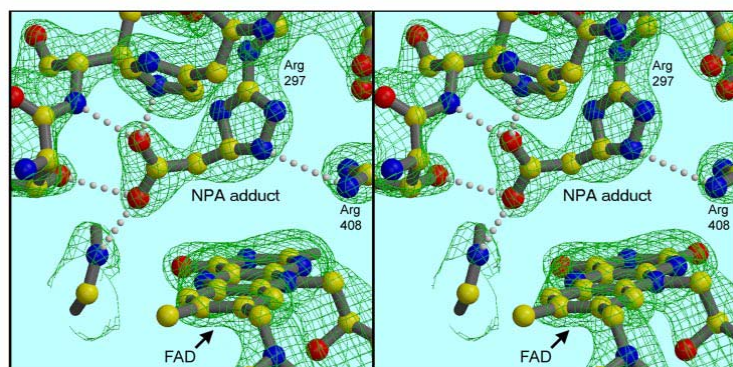
Figure 2.4 The dicarboxylate site in the 3-NPtreated enzyme.
The density attributed to the ligand has shrunk and moved away from the flavin toward Arg297 and His253. It can be modeled by assuming two atoms from the backbone of 3-NP (C-3 and N) fuse with the guanidino group to form a five-membered ring, with loss of the two nitro oxygens. The carboxylate at the other end fits into the clearly forked density branching off the ring. $2F$o - Fc map contoured at 1.7 σ. Figure taken from (24).

The advent of protein crystallography allowed for a third possible mechanism for succinate dehydrogenase inhibition by propionate-3-nitronate to be proposed.

Huang *et al.* solved the three dimensional structures of succinate dehydrogenase from chicken for the unbound enzyme, the enzyme in complex with oxaloacetate and the propionate-3-nitronate inactivated

form (*24*). The cysteine residue that was proposed by to be modified by propionate-3-nitronate

was observed to be ~8 Å from the active site making it an unlikely candidate for modification by

the toxin. In addition, the FAD cofactor of inactivated enzyme did not show covalent

modifications, which further suggests that inactivation does not occur through a flavin N(5)

adduct (Figure 2.4). Rather, the structure of the inactivated enzyme showed that an arginine

residue at position 296 was modified by propionate-3-nitronate. While the crystal structure of

inactivated succinate dehydrogenase allowed for the unambiguous determination that arginine

296 was the residue modified by propionate-3-nitronate, the resolution was not high enough to

deduce the exact chemical structure of the adduct. The oxaloacetate structure shows that arginine

296 would be in the correct location to act as a base for the proton abstraction at the C2 position

of succinate. Furthermore, the residue is conserved among the succinate:quinine oxidoreductase and fumarate reductase family of enzymes and has been shown through both structural and mutagenesis studies to serve as an acid/base catalyst (*24*). Thus, the inactivation of succinate dehydrogenase by propionate-3-nitronate likely occurs through the modification of the catalytic base for the reaction in a mechanism that is still not fully established.

2.7   Physiological Effects of 3-Nitropropionate Poisoning

Cases of 3-nitropropionate poisoning have been widely documented in both domestic livestock and humans. In North America, the worst impact of 3-nitropropionate poisoning has been revealed in the agricultural industry, particularly in the western parts of the United States and Canada and in the northern regions of Mexico (*11, 20, 33-36*). Clinical signs of intoxication in cattle include poor coordination of the limbs, foaming of the mouth and nose and respiratory distress (*11*). Lethal doses of the toxin will result in a rapid death of the animal, which could occur just a few hours after ingestion of 3-nitropropionate (*11*). The causative agent of the majority of 3-nitropropionate poisoning in livestock is the shrub *Astragalus* sp. (*20, 37, 38*), which thrives in pastures after periods of drought or overgrazing. During these periods, the effects of 3-nitropropionate poisoning can be severe as evident by one outbreak in New Mexico, which resulted in a 3% mortality and a 20% morbidity rate in cattle and sheep grazing in affected pastures (*35*). Cases of human 3-nitropropionate poisoning have been largely limited to the Northern regions of China (*39, 40*). These outbreaks have been linked to the ingestion of moldy sugarcane, which spoiled during the transport and storage of the crop from the southern regions of the country (*22, 41*). From 1972 until 1989, at least 884 cases of sugar cane poisoning were reported and of those ~10% were fatal (*11*). Children are more susceptible to fatalities, but

persistent dystonia can occur among both the young and old after 3-nitropropionate intoxication (*11, 41*).

The neurotoxicity of 3-nitropropionate has been well established in animal models (*33, 42-45*). The toxin preferentially targets the striatum resulting in mitochondrial damage and cell death. The toxin targets complex II in the mitochondria of the striatum by irreversibly inhibiting succinate dehydrogenase, but the pathological effects are revealed even with partial production of ATP (*42*). The earliest pathological effects of 3-nitropropionate poisoning observed in rats are a loss of the mitochondrial membrane potential (*42*). This leads to a relocation of cytochrome c and triggers the production of several apoptogenic factors such as capase-9, Smac/Diablo and calpain (*42*). 3-Nitropropionate poisoning also results in the production of superoxide and hydroxyl radicals along with nitric oxide (*42*). While the mechanism for activation of reactive oxygen species is not fully understood, their production clearly leads in oxidative damage in striatal cells and contributes to the neurotoxicity of 3-nitropropionate.

2.8 3-Nitropropionate Oxidizing Enzymes

Enzymes that catalyze the oxidative denitrification of 3-nitropropionate or propionate-3-nitronate have been isolated in plants, fungi and more recently in bacteria (Table 2.3). Each enzyme contains a single non-covalently bound flavin mononucleotide cofactor per monomer and is devoid of metal (*5, 46-50*). With the exception of *H. comosa* 3-nitropropionic acid oxidase, which can only use the protonated form of the toxin, each enzyme is more or only active with propionate-3-nitronate as substrate than
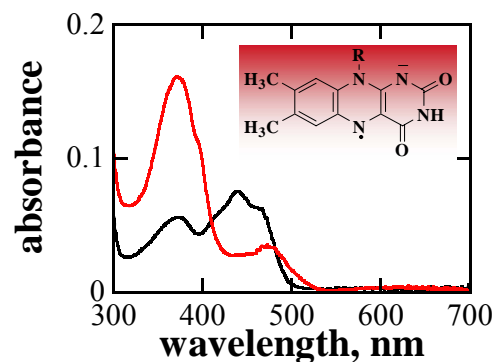
Figure 2.5 Formation of an anionic flavosemiquinone upon anaerobic mixing of *N. crassa* nitronate monooxygenase with substrate.

with the with the protonated form of the toxin (*5, 46-50*). The substrate specificity of each enzyme is listed in Table 2.3. The catalytic mechanism of substrate oxidation occurs through the unusual formation of an anionic flavosemiquinone (Figure 2.5) intermediate as best characterized with the *N. crassa* enzyme, but also applies to enzymes from *W. saturnus* and *P. aeuroginosa* (*5, 46, 47, 49, 50*). The monooxygenase enzymes catalyze the oxidation of the substrate without the release of radical intermediates (*49-51*), whereas the oxidases release reactive intermediates to oxidize nitronates in both an enzymatic and non-enzymatic fashion (*5, 48*).

Table 2.3 3-Nitropropionate and Propionate-3-Nitronate Oxidizing Enzymes

enzyme	source	substrate[f]	mechanism
nitronate monooxygenase[a]	*Neurospora crassa*	P3N or 3NPA	Scheme 6
nitronate monooxygenase[b]	*Williopsis saturnus*	3NPA	Scheme 6
propionate-3-nitronate monnoxygenase[c]	*Pseudomonas aeuroginosa*	P3N	Scheme 6
propionate-3-nitronate oxidase[d]	*Penicillium atrovenetum*	P3N	Scheme 7
3-nitropropionic acid oxidase[e]	*Hippocrepis comosa*	3NPA	Scheme 7

[a] from (*52*); [b] from (*49*); [c] from (*50*) [d] from (*5*) [e] from (*48*) [f] P3N = propionate-3-nitronate, 3NPA = 3-nitropropionate.

The monooxygenase mechanism is shown in Scheme 2.6 as established with the *N. crassa* enzyme with nitroethane or ethylnitronate as substrate (*1, 2, 7, 8*). After binding nitroethane, catalysis is initiated the base-catalyzed deprotonation of the α-carbon to yield ethylnitronate. Alternatively, free ethylnitronate can directly bind to the enzyme as in the case of the *W. saturnus* and *P. aeuroginosa* enzymes. The enzyme-bound nitronate is then oxidized through the transfer of a single electron transfer to the flavin cofactor of the monooxygenase to generate an anionic flavosemiquinone and radical substrate intermediate. Molecular oxygen then reacts with the flavosemiquinone complex to oxidize the flavin and generate superoxide. Superoxide then reacts with the substrate-derived radical to generate a peroxynitroalkyl intermediate which is then likely released from the enzyme where it undergoes a non-enzymatic reaction   to   generate   the   carbonyl   product   of   the   reaction.

Scheme 2.6 The monooxygenation of 3-nitropropionate by flavin dependent enzymes.

The numbering of the histidine residue corresponds to *N. crassa* nitronate monooxygenase.
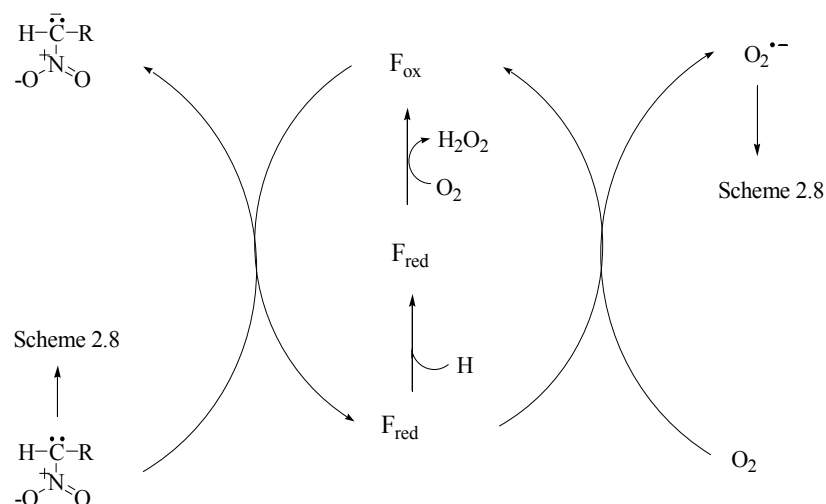
Scheme 2.7 Oxidation of propionate-3-nitronate by flavin dependent oxidases. The mechanism was adapted from (*6*).

The oxidase mechanism of propionate-3-nitronate oxidation is shown in Scheme 2.7 as established in the *P. atrovenetum* (*6*) enzyme and through the studies of Fridovich for the non-enzymatic component of the reaction (*9*). The nitronate transfers a single electron to the flavin cofactor in a similar manner to that in the monooxygenase, but the resulting nitroalkyl radical is released where it undergoes a non-enzymatic oxidation to malonic semialdehyde (*6*). The flavosemiquinone undergoes a slow reduction to give the fully reduced hydroquinone form of the cofactor, which is then rapidly oxidized by molecular oxygen to regenerate the enzyme. Superoxide anion is released during the cycle, which reacts with propionate-3-nitronate in solution to non-enzymatically generate malonic semialdehyde. The non-enzymatic reaction of superoxide anion with propionate-3-nitronate is illustrated in Scheme 2.8. The nitronate is formed through either the enzymatic or non-enzymatic ionization of 3-nitropropionate and reacts with superoxide anion to generate hydrogen peroxide and a nitroalkyl radical. Alternatively, in the propionate-3-nitronate oxidases the nitronate radical is simply released from the enzyme to initiate the free-radical reaction. Hydrolysis of the nitroalkyl radical expels nitrite and generates a hydroxy-containing radical intermediate, which propagates the reaction through a single electron reduction of molecular

oxygen to regenerate superoxide anion. The termination of the reaction occurs once two superoxide anions react to generate hydrogen peroxide and O_2.

$$R-\underset{\underset{NO_2}{|}}{\overset{\overset{H}{|}}{C}}-R \longrightarrow R-\underset{\underset{NO_2}{|}}{\overset{..}{C}}-R \qquad \text{ionization}$$

$$R-\underset{\underset{NO_2}{|}}{\overset{..}{C}}-R + O_2^{\bullet -} + 2H^+ \longrightarrow R-\underset{\underset{NO_2}{|}}{\overset{\bullet}{C}}-R + H_2O_2 \qquad \text{initiation}$$

$$R-\underset{\underset{NO_2}{|}}{\overset{\bullet}{C}}-R + OH^- \longrightarrow R-\underset{\underset{OH}{|}}{\overset{\bullet}{C}}-R + NO_2^- \qquad \text{hydrolysis}$$

$$R-\underset{\underset{OH}{|}}{\overset{\bullet}{C}}-R + O_2 \longrightarrow R-\underset{\underset{O}{||}}{C}-R + H^+ + O_2^{\bullet -} \qquad \text{propagation}$$

$$O_2^{\bullet -} + O_2^{\bullet -} + H^+ \longrightarrow H_2O_2 + O_2 \qquad \text{termination}$$

Scheme 2.8 Non-enzymatic free radical oxidation of propionate-3-nitronate.
The mechanism was adapted from (*9*).

2.9 Physiological Role of 3-Nitropropionate Oxidizing Enzymes

The major role of 3-nitropropionate oxidation in plants, fungi and bacteria is likely to protect the organism against the toxicity of the compound. Plants express 3-nitropropionate oxidase as a means of self-protection against the toxin they produce and as an alternate means of nitrification as outlined above (*9*). The self-protection of 3-nitropropionate oxidation in plants is evident from a survey conducted by Hipkin *et al.* of over 500 species of legumes, which found that 3-nitropropionate oxidase activity is found only in species that also produce the toxin (*9*). In bacteria, 3-nitropropionate oxidation serves both as both a means of protection against the environmental occurrence of the toxin and to allow the cell to utilize the compound as a sole source of carbon, nitrogen and energy (*50*). The role of propionate-3-nitronate oxidation in yeast

has recently been shown to be similar to that in bacteria as evident from studies on *Neurospora crassa* and *Williopsis saturnus* strains that express nitronate monooxygenase (see Chapter 8).

3-Nitropropionate oxidation by bacteria is best understood in the case of *Pseudomonas* sp. JS189, *Cupriavidus* sp. JS190 and *Burkholderia phytofirmans* PsJN. Isolated bacteria were grown on media containing up to 2 mM of the toxin as the sole source of nitrogen, carbon and energy and propionate-3-nitrate oxidizing enzymes were isolated in each strain (*50*). The enzymes were found to transform the toxin into malonic semialdehyde, nitrite, nitrate and hydrogen peroxide (*50*). A malonic semialdehyde oxidative decarboxylating activity was also detected, allowing for a metabolic pathway for 3-nitropropionate metabolism to be proposed. Propionate-3-nitronate, which is derived from 3-nitropropionate either non-enzymatically or through an unidentified enzymatic activity, is converted to malonic semialdehyde by the flavin dependent monooxygenase isolated in that study. Malonic semialdehyde is then converted to acetyl CoA by an inducible oxidative decarboxylase and then enters central metabolic pathways.

The role of propionate-3-nitronate oxidation in bacteria has only been rigorously established in *Pseudomonas* sp. JS189, and *Cupriavidus* sp. JS190, although putative nitronate monooxygenases have been found in a wide range of prokaryotes. The widespread occurrence of 3-nitropropionate in nature and the fact that over 2,100 nucleotide sequences are known that encode for probable 3-nitropropionate oxidizing enzymes suggest that the enzyme may serve a general role in protection of prokaryotes from the toxin. Current studies are underway to test this hypothesis.

2.10 References

1. Candish, E., La Croix, L. J., and Unran, A. M. (1969) The Biosynthesis of 3-Nitropropionic Acid in Creeping Indigo (*Indigofera spicata*), *Biochemistry 8*, 182-186.

2. Bush, M. T., Touster, O., and Brockman, J. E. (1951) The production of beta-nitropropionic acid by a strain of *Aspergillus flavus*, *J. Biol. Chem. 188*, 685-693.

3. Alston, T. A., Mela, L., and Bright, H. J. (1977) 3-Nitropropionate, the toxic substance of *Indigofera*, is a suicide inactivator of succinate dehydrogenase, *Proc. Natl. Acad. Sci. U. S. A. 74*, 3767-3771.

4. Ding-Ling Wei, S.-C. C., Shu-Chien Lin, Ming-Luen Doong, and Shung-Chang Jong. (1994) Production of 3-Nitropropionic acid by *Arthrinium* Species, *Curr. Microbiol. 28*, 1-5.

5. Porter, D. J., and Bright, H. J. (1987) Propionate-3-nitronate oxidase from *Penicillium atrovenetum* is a flavoprotein which initiates the autoxidation of its substrate by O_2, *J. Biol. Chem. 262*, 14428-14434.

6. Carter, C. L., and Mc, C. W. (1949) Hiptagenic acid identified as beta-nitropropionic acid, *Nature 164*, 575.

7. Gorter, K. (1920) *L'Hiptagine, Glucoside Nouveau Retire De L'Hiptage Madablota Gaertin*, Vol. 2, Archipel Brukkerij, Builenzora, Indonesia.

8. Morris, M. P., Pagan, C., and Warmke, H. E. (1954) Hiptagenic Acid, a Toxic Component of *Indigofera endecaphylla*, *Science 119*, 322-323.

9. Hipkin, C. R., Simpson, D. J., Wainwright, S. J., and Salem, M. A. (2004) Nitrification by plants that also fix nitrogen, *Nature 430*, 98-101.

10. Orth, R. (1977) Mycotoxins of *Apergillus oryzae* for Use in the Food Industry as Starters and Enzyme Producing Molds, *Ann. Nutr. Alim. 31*, 617-624.

11. Hamilton, B. F., Gould, D. H., and Gustine, D. L. (1999) History of 3-Nitropropionic acid, In *Mitrochrondrial Inhibitors and Neurodegenerative Disorders* (Sanberg, P. R., Nishino, H., and Borlongan, C. V., Eds.), Humana Press, Totowa, NJ.

12. Alston, T. A., Porter, D. J., and Bright, H. J. (1985) The Bioorganic Chemistry of the Nitroalkyl Group, *Bioorg. Chem. 13*, 375-403.

13. Ju, K. S., and Parales, R. E. (2010) Nitroaromatic compounds, from synthesis to biodegradation, *Microbiol. Mol. Biol. Rev. 74*, 250-272.

14. Perry, R., Nishino, S. F., and Spain, J. C. (2010) Naturally-occurring nitro compounds, *Nat. Prod. Rep*. doi:10.1039/C0NP00024H

15. Porter, D. J., and Bright, H. J. (1985) The Bioorganic Chemistry of the Nitro Alkyl Group, *Bioorg. Chem. 13*, 375-403.

16. Chomcheon, P., Wiyakrutta, S., Sriubolmas, N., Ngamrojanavanich, N., Isarangkul, D., and Kittakoop, P. (2005) 3-Nitropropionic acid (3-NPA), a potent antimycobacterial agent from endophytic fungi: is 3-NPA in some plants produced by endophytes?, *J. Nat. Products 68*, 1103-1105.

17. Strange, R. N. (2007) Phytotoxins Produced by Microbial Plant Pathogens, *Natural Prot. Rep. 24*, 127-144.

18. Bernasconi, C. F. (1987) Intrinsic barriers of reactions and the principle of nonperfect synchronization, *Acc. Chem. Res. 20*, 301-308.

19. Nielsen, A. T. (1969) Nitronic acids and esters, In *The Chemistry of the nitro and nitroso groups* (Feuer, H., Ed.), pp 349-486, Interscience Publishers, New York.

20. James, L. F., Hartley, W. J., and Van Kampen, K. R. (1981) Syndromes of astragalus poisoning in livestock, *J. Am. Vet. Med. Assoc. 178*, 146-150.

21. James, L. F., Hartley, W. J., Williams, M. C., and Van Kampen, K. R. (1980) Field and experimental studies in cattle and sheep poisoned by nitro-bearing Astragalus or their toxins, *Am. J. Vet. Res. 41*, 377-382.

22. Ludolph, A. C., He, F., Spencer, P. S., Hammerstad, J., and Sabri, M. (1991) 3-Nitropropionic acid-exogenous animal neurotoxin and possible human striatal toxin, *Can. J. Neurol. Sci. 18*, 492-498.

23. Coles, C. J., Edmondson, D. E., and Singer, T. P. (1979) Inactivation of succinate dehydrogenase by 3-nitropropionate, *J. Biol. Chem. 254*, 5161-5167.

24. Huang, L. S., Sun, G., Cobessi, D., Wang, A. C., Shen, J. T., Tung, E. Y., Anderson, V. E., and Berry, E. A. (2006) 3-nitropropionic acid is a suicide inhibitor of mitochondrial respiration that, upon oxidation by complex II, forms a covalent adduct with a catalytic base arginine in the active site of the enzyme, *J. Biol. Chem. 281*, 5965-5972.

25. Matsuo, M., Kirkland, D. F., and Underhill, E. W. (1972) 1-Nitro-2-phenylethane, a Possible Intermediate in the Biosynthesis of Benzylglucosinolate, *Phytochemistry 11*, 697-701.

26. Hylin, J. W., and Matusumoto, H. (1960) The biosynthesis of 3-nitropropanoic acid by *Penicillium atrovenetum*. *Arch. Biochem. Biophys. 93*, 542-545.

27. Shaw, P. D., and McCloskey, J. A. (1967) Biosynthesis of Nitro Compounds. II. Studies on Potential Precursors for the Nitro Group of β-Nitropropionic Acid, *Biochemsitry 6*, 2247-2253.

28. Shaw, P. D. (1967) Biosynthesis of Nitro Compounds. III. The Enzymatic Reduction of β-Nitroacrylic Acid to β-Nitropropionic Acid, *Biochemistry 6*, 2253-2260.

29. Porter, D. J., Voet, J. G., and Bright, H. J. (1972) Nitroalkanes as reductive substrates for flavoprotein oxidases, *Z. Naturforsch B. 27*, 1052-1053.

30. Porter, D. J., Voet, J. G., and Bright, H. J. (1972) Nitromethane. A novel substrate for D-amino acid oxidase, *J. Biol. Chem. 247*, 1951-1953.

31. Porter, D. J., Voet, J. G., and Bright, H. J. (1973) Direct evidence for carbanions and covalent N 5-flavin-carbanion adducts as catalytic intermediates in the oxidation of nitroethane by D-amino acid oxidase, *J. Biol. Chem. 248*, 4400-4416.

32. Baer, H. H., and Urbas, L., (Eds.) (1970) *The Chemistry of the Nitro and Nitroso Groups Part 2*, Interscience, New York.

33. Al Mutairy, A., Al Kadasah, S., Elfaki, I., Arshaduddin, M., Malik, D., Al Moutaery, K., and Tariq, M. Trolox ameliorates 3-nitropropionic acid-induced neurotoxicity in rats, *Neurotox. Teratol. 32*, 226-233.

34. Mathews, F. P. (1940) Poisioning in sheep and goats by sacahuiste (*Nolina texana*) buds and blooms, *J. Am. Vet. Med. Assoc. 97*, 125-134.

35. Williams, M. C., James, L. F., and Bond, B. O. (1979) Emory milkvetch (*Astragalus emoryanus* var *emoryanus*) poisoning in chicks, sheep, and cattle, *Am. J. Vet. Res. 40*, 403-406.

36. Williams, M. C., van Kampen, K. R., and Norris, F. A. (1969) Timber milkvetch poisoning in chickens, rabbits, and cattle, *Am. J. Vet. Res. 30*, 2185-2190.

37. Tarazona, J. V., and Sanz, F. (1987) Aliphatic nitro compounds in *Astragalus lusitanicus* Lam, *Vet. Hum. Toxicol. 29*, 437-439.

38. Williams, M. C. (1994) Impact of poisionous weeds on livestock and humans in North America, *Rev. Weed. Sci. 6*, 1-27.

39. Burdock, G. A., Carabin, I. G., and Soni, M. G. (2001) Safety assessment of b-nitropropionic acid: a monograph in support of an acceptable daily intake in humans, *Food Chem. 75*, 1-27.

40. Ming, L. (1995) Moldy sugarcane poisoning-a case report with a brief review, *J. Toxicol. Clin. Toxicol. 33*, 363-367.

41. Liu, X., Luo, X., and Hu, W. (1992) Studies on the epidemiology and etiology of moldy sugar can poisioning in China, *Biomed. Enviro. Sci.*, 161-177.

42. Brouillet, E., Jacquard, C., Bizat, N., and Blum, D. (2005) 3-Nitropropionic acid: a mitochondrial toxin to uncover physiopathological mechanisms underlying striatal degeneration in Huntington's disease, *J. Neurochem. 95*, 1521-1540.

43. He, F., Zhang, S., Qian, F., and Zhang, C. (1995) Delayed dystonia with striatal CT lucencies induced by a mycotoxin (3-nitropropionic acid), *Neurology 45*, 2178-2183.

44. Kumar, P., and Kumar, A. (2009) Protective effects of epigallocatechin gallate following 3-nitropropionic acid-induced brain damage: possible nitric oxide mechanisms, *Psychopharmacology* (Berl) *207*, 257-270.

45. Tsang, T. M., Haselden, J. N., and Holmes, E. (2009) Metabonomic characterization of the 3-nitropropionic acid rat model of Huntington's disease, *Neurochem. Res. 34*, 1261-1271.

46. Francis, K., Russell, B., and Gadda, G. (2005) Involvement of a flavosemiquinone in the enzymatic oxidation of nitroalkanes catalyzed by 2-nitropropane dioxygenase, *J. Biol. Chem. 280*, 5195-5204.

47. Gadda, G., and Francis, K. (2009) Nitronate monooxygenase, a model for anionic flavin semiquinone intermediates in oxidative catalysis, *Arch. Biochem. Biophys. 493*, 53-61.

48. Hipkin, C. R., Salem, M. A., Simpson, D., and Wainwright, S. J. (1999) 3-Nitropropionic acid oxidase from horseshoe vetch (*Hippocrepis comosa*): a novel plant enzyme, *Biochem. J. 340 (Pt 2)*, 491-495.

49. Mijatovic, S., and Gadda, G. (2008) Oxidation of alkyl nitronates catalyzed by 2-nitropropane dioxygenase from *Hansenula mrakii*, *Arch. Biochem. Biophys. 473*, 61-68.

50. Nishino, S. F., Shin, K. A., Payne, R. B., and Spain, J. C. (2010) Growth of bacteria on 3-nitropropionic acid as a sole source of carbon, nitrogen, and energy, *Appl. Environ. Microbiol. 76*, 3590-3598.

51. Francis, K., and Gadda, G. (2006) Probing the chemical steps of nitroalkane oxidation catalyzed by 2-nitropropane dioxygenase with solvent viscosity, pH, and substrate kinetic isotope effects, *Biochemistry 45*, 13889-13898.

52. Francis, K., and Gadda, G. (2008) The nonoxidative conversion of nitroethane to ethylnitronate in *Neurospora crassa* 2-nitropropane dioxygenase is catalyzed by histidine 196, *Biochemistry 47*, 9136-9144.

53. Kuo, C. F., and Fridovich, I. (1986) Free-radical chain oxidation of 2-nitropropane initiated and propagated by superoxide, *Biochem. J. 237*, 505-510.

3   CHAPTER III

INVOLVEMENT OF A FLAVOSEMIQUINONE IN THE ENZYMATIC OXIDATION

OF NITROALKANES CATALYZED BY 2-NITROPROPANE DIOXYGENASE

3.1   Summary

2-Nitropropane dioxygenase (E.C. 1.13.11.32) catalyzes the oxidation of nitroalkanes into their corresponding carbonyl compounds and nitrite. In this study, the *ncd*-2 gene encoding for the enzyme in *Neurospora crassa* was cloned, expressed in *Escherichia coli* strain BL21(DE3), and the resulting enzyme was purified. Size-exclusion chromatography, heat denaturation and mass spectroscopic analyses showed that 2-nitropropane dioxygenase is a homodimer of 80,000 dalton, containing a mol of non-covalently bound FMN per mol of subunit, and is devoid of iron. With neutral nitroalkanes and anionic nitronates other then propyl-1- and propyl-2-nitronate, for which a non-enzymatic free radical reaction involving superoxide was established using superoxide dismutase, substrate oxidation occurs within the enzyme active site. The enzyme was more specific for nitronates than nitroalkanes, as suggested by the second order rate constant k_{cat}/K_m determined with 2-nitropropane and primary nitroalkanes with alkyl chain lengths between 2 and 6 carbons. The steady state kinetic mechanism with 2-nitropropane, nitroethane, nitrobutane, and nitrohexane, in either the neutral or anionic form, was determined to be sequential, consistent with oxygen reacting with a reduced form of enzyme before release of the carbonyl product. Enzyme monitored turnover with ethylnitronate as substrate indicated that the catalytically relevant reduced form of enzyme is an anionic flavin semiquinone, whose

formation requires the substrate, but not molecular oxygen, as suggested by anaerobic substrate reduction with nitroethane or ethylnitronate. Substrate deuterium kinetic isotope effects with 1,2-[^{2}H$_4$]-nitroethane and 1,1,2-[^{2}H$_3$]-ethylnitronate at pH 8 yielded normal and inverse effects on the k_{cat}/K_m value, respectively, and were negligible on the k_{cat} value. The k_{cat}/K_m and k_{cat} pH profiles with anionic nitronates showed the requirement of an acid, whereas those for neutral nitroalkanes were consistent with the involvement of both an acid and a catalytic base in catalysis. The kinetic data reported herein are consistent with an oxidase-style catalytic mechanism for 2-nitropropane dioxygenase, in which the flavin-mediated oxidation of the substrate and the subsequent oxidation of the enzyme-bound flavin occur in two independent steps, and with the participation of a flavosemiquinone in catalysis. A chemical mechanism for the oxidation of both anionic nitronates and neutral nitroalkanes catalyzed by 2-nitropropane dioxygenase is discussed.

3.2   Introduction

2-Nitropropane dioxygenase (E.C. 1.13.11.32) from *Neurospora crassa* is a flavin dependent enzyme, which catalyzes the oxidative denitrification of nitroalkanes to their corresponding carbonyl compounds and nitrite. The enzyme was first characterized by Little in 1951 as an oxidase (1), but was later classified as a dioxygenase based on the observation that the oxygen atom of the organic product formed upon oxidation of propyl-2-nitronate originates from molecular oxygen and not from water (2). To date, 2-nitropropane dioxygenase has been isolated from *N. crassa* (1) and *Hansenula mrakii* (3). While the two enzymes have similar molecular weights of about 40,000, they differ in their prosthetic group content in that FMN and FAD are found in the *N. crassa* and *H. mrakii* enzymes, respectively (2,4).

45

$R_1-\underset{\underset{\underset{O}{N^+}}{|}}{\overset{\overset{H}{|}}{C}}-R_2 \quad \xrightleftharpoons[H^+]{pK_a = 7.7\text{-}10.2} \quad R_1-\underset{\underset{N^+}{|}}{\overset{\overset{-}{C}}{}}-R_2$
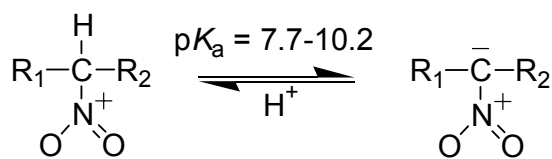
R_1, -H or alkyl group
R_2, -H or -CH$_3$

Scheme 3.1 Ionization of nitroalkanes (right) to alkylnitronates (left).

A study on the enzymatic oxidation of nitroalkanes by 2-nitropropane dioxygenase is of considerable interest for both applied and fundamental reasons. Due to the low pK_a values for deprotonation of the α-carbon (Scheme 1) (5), nitroalkanes are widely used in industry as they provide a quick and effective method of synthesizing common reagents (6-8), however many are anticipated to be toxic and some have been demonstrated to be carcinogenic (9-15). 2-Nitropropane, for example, has been shown to cause the formation of both 8-hydroxy- and 8-amino-guanine in the DNA and RNA of liver cells in Sprague-Dawley rats (16). The enzymatic oxidation of nitroalkanes into less toxic species can therefore be exploited for use in bioremediation. The oxidation of nitroalkanes has been observed to occur physiologically in *N. crassa* (1), *H. mrakii* (17) and *Fusarium oxysporum* (18), however the implications of the reaction in biological systems are not yet fully understood. Consequently, a characterization of the biochemical and mechanistic properties of 2-nitropropane dioxygenase might shed light into the role of nitroalkane oxidation by living organisms. From a mechanistic standpoint, 2-nitropropane dioxygenase is unique in that it can effectively utilize both the neutral (nitroalkane) and anionic (nitronate) forms of the nitroalkane substrate (2). In contrast, the numerous reported studies on the enzymatic oxidation of nitroalkanes catalyzed by flavin-dependent enzymes have only characterized the reaction using a single form of substrate (19-21). Therefore, 2-nitropropane dioxygenase offers the unique opportunity for a direct comparison of the enzyme-catalyzed oxidation of nitroalkanes in their neutral and anionic forms. To date, due to the limited amount of enzyme that can be obtained in a pure form upon extraction from the natural sources,

minimal biochemical, structural or mechanistic information is available on 2-nitropropane dioxygenase.

In this study, the *ncd*-2 gene encoding for 2-nitropropane dioxygenase was cloned into the expression vector pET20b(+), expressed in *E. coli* strain BL21(DE3) cells and the resultant enzyme was characterized in its kinetic and biochemical properties. The data presented herein indicate that the enzymatic oxidation of neutral nitroalkanes and anionic nitronates catalyzed by 2-nitropropane dioxygenase occurs through an oxidase-style catalytic mechanism in which the flavin-mediated oxidation of the substrate and the subsequent oxidation of the enzyme-bound flavin occur in two independent steps. Evidence is presented that the enzyme-catalyzed oxidation of the nitroalkane substrate involves the unusual formation of an anionic flavin semiquinone species as a catalytic intermediate.

3.3   Experimental Procedures

Materials. The plasmid pUCncd containing the *ncd*-2 gene encoding for 2-nitropropane dioxygenase in *Neurosporra crassa* was a generous gift from Drs. Nobuyoshi Esaki and Tatsuo Kurihara, Kyoto University, Japan. *Pfu* DNA polymerase was from Stratagene. Restriction endonucleases *Nde*I and *Eco*RI, T4 DNA ligase and calf intestinal alkaline phosphatase were from Promega. DNase I and the Rapid DNA Ligation kit were from Roche Biomedicals. Luria-Bertani agar and broth, ampicillin, FMN, phenylmethysulfonylfluoride (PMSF), superoxide dismutase, lysozyme and nitroalkanes were from Sigma-Aldrich. Ammonium sulfate and $MgCl_2$ were from ICN Biomedicals. EDTA was from Fisher Scientific. The plasmid vector pET20b(+) was from Novagen. Primers and products deriving from primer extension amplification were purified using mini-kits from Qiagen. *Escherichia coli* strain BL21(DE3) (Novagen) was used for protein expression and strain XL1-Blue (Stratagene) was used during cloning procedures.

Both strains were stored at –80 $^{\circ}$C as 7% dimethyl sulfoxide suspensions. The Hi-Prep 16/10 Octyl Fast Flow column and the DEAE-Sepharose used in packing the DEAE column were from Amersham Pharmacia Biotech. All other reagents were of the highest purity commercially available.

Instruments. DNA sequencing was carried out using an Applied Biosystems Big Dye kit on an Applied Biosystems model ABI 377 DNA sequencer at the DNA Core Facility of the Biology Department of Georgia State University. Oligonucleotides were custom synthesized on an Applied Biosystems model 380B DNA Synthesizer by the Gene Technology Laboratory of the Biology Department of Texas A&M University, College Station. UV-visible absorbance spectra were recorded using an Agilent Technologies diode-array spectrophotometer Model HP 8453, equipped with a thermostated water bath. Fluorescence emission spectra were recorded with a Shimadzu Spectrofluorometer Model RF-5301 PC, thermostated at 15 $^{\circ}$C. MALDI-TOF spectra were recorded using an ABI Voyager DE-pro mass spectrophotometer. Stopped-flow experiments were carried out using a Hi-Tech SF-61 Double Mixing Stopped Flow System.

Cloning of ncd-2 into pET20b(+). Plasmid pUCncd containing the *ncd*-2 gene for 2-nitropropane dioxygenase was used directly to transform *E. coli* strain XL1-Blue competent cells, using the heat shock method of Inoue et *al.* (22), and the pUCncd plasmid was isolated through a QIAquick Spin miniprep kit, according to the manufacturer's instructions. The extracted pUCncd plasmid was used as a DNA template for primer extension amplification of the *ncd*-2 gene, using oligonucleotide sense and antisense primers containing *Nde*I and *Eco*RI restriction endonuclease sites designed to anneal to the 5' and 3' ends of the gene, respectively. The engineered *Nde*I (CGAGTA<u>CATATG</u>ACTTCCCAGGCCACAGC) and *Eco*RI (TCACC<u>GAATTC</u>TACACGCGGCACCCCTTAGGC) restriction sites (underlined) were

designed to facilitate directional cloning into the corresponding sites in pET20b(+). The *ncd*-2 gene was ligated into pET20b(+) to construct plasmid pET/2NPDnc using a Rapid DNA Ligation kit (Roche) and the ligation mixture was used directly to transform *E. coli* strain XL1-Blue competent cells. The correct construct was sequenced in both directions using oligonucleotide primers designed to bind to the DNA regions of pET flanking the inserted gene and was used to transform *E. coli* strain BL21(DE3) competent cells for protein expression.

Purification of 2-Nitropropane Dioxygenase. E. coli strain BL21(DE3) cells harboring plasmid pET/2NPDnc were used to inoculate 5 x 1.25 liters of Luria-Bertani broth containing 50 μg/ml ampicillin and the cultures were incubated for ~15 h at 30 °C. The temperature was then lowered to 22 °C and IPTG was added at a final concentration of 0.1 mM. After 17 h, cells were harvested by centrifugation and were resuspended with four volumes of 1 mM EDTA, 100 mM NaCl, 0.1 mM PMSF, 0.2 mg/ml lysozyme, 5 μg/ml DNase I and 10 mM $MgCl_2$, in 50 mM Tris-Cl at pH 8, before sonication and collection of the cell-free extract by centrifugation at 12,000 *g* for 25 min. After 70% ammonium sulfate saturation and centrifugation, the resultant pellet was dialyzed against 5 mM potassium phosphate, pH 7.4, and was loaded onto a DEAE Fast Flow column (4 x 30 cm) connected to an Åkta*prime* Amersham Biotech system equilibrated with the same buffer. The column was eluted with a linear gradient from 0 to 80 mM ammonium sulfate developed over 2 L at a flow rate of 4 mL/min. Catalytically active fractions, typically eluting at ~35 mM ammonium sulfate, were pooled and adjusted to a final concentration of 1.5 M ammonium sulfate before loading directly onto a Hi-Prep 16/10 Octyl Fast Flow column (3.5 x 20 cm) equilibrated with 1.5 M ammonium sulfate in 50 mM potassium phosphate, pH 7.4. Protein elution was carried out with a linear gradient from 1.5 to 0 M ammonium sulfate over 200 ml at a flow rate of 2 mL/min. Fractions of the highest purity were pooled, dialyzed against

50 mM potassium phosphate, pH 7.4, and stored at $-20\ ^{\circ}$C until use. The purified enzyme was found to be stable upon storage under these conditions for at least 6 months.

Biochemical Methods. The concentration of 2-nitropropane dioxygenase was determined with the method of Bradford (23), using the Bio-Rad protein assay kit with bovine serum albumin as standard. The molecular weight of the enzyme under non-denaturing conditions was determined by size exclusion chromatography through a Sephacryl S-400 column (1 x 50 cm) connected to an Åkta*prime* Amersham Pharmacia Biotech system equilibrated with 300 mM KCl in 20 mM potassium phosphate, pH 7, at a flow rate of 0.5 ml/min. The following proteins were used as standards: horse heart cytochrome c [12,400], bovine serum albumin [66,000], yeast alcohol dehydrogenase [150,000], sweet potato β-amylase [200,000] and horse spleen apoferritin [443,000]. For denaturation experiments aimed at the determination of flavin to protein stoichiometry, ~40 μM of 2-nitropropane dioxygenase was incubated at 100 $^{\circ}$C for 30 min, followed by removal of precipitated protein by centrifugation. The flavin content per monomer of enzyme was calculated from the ratio of the concentration of flavin released from the enzyme, using an ε_{455nm} value of 12,500 $M^{-1}cm^{-1}$ (24), to the concentration of protein determined by the Bradford assay. Identification of the flavin cofactor of 2-nitropropane dioxygenase was determined through MALDI-TOF mass spectrometry in the negative ion mode using a 50:50 methanol:acetonitrile matrix. Samples were prepared by denaturing the enzyme with 10% trichloroacetic acid, followed by centrifugation and collection of the supernant. Determination of the iron content of 2-nitropropane dioxygenase was carried out by inductively coupled plasma mass spectroscopic analysis at the Chemical Analysis Facility of the University of Georgia.

Spectral Studies. The molar extinction coefficient of the flavin cofactor was determined by following the change in UV-visible absorbance at 444 nm of the enzyme at pH 8, before and

after incubation at 100 $^{\circ}$C for 30 min and centrifugation to remove precipitated protein. Reduced flavin was obtained through anaerobic photoreduction of the enzyme in the presence of 15 mM EDTA using a 100-watt light bulb. The anionic semiquinone of 2-nitropropane dioxygenase was prepared through anaerobic reduction of the enzyme with 0.78 mM ethylnitronate or nitroethane at 15 $^{\circ}$C. Samples were made anaerobic by repeated cycles of vacuuming and flushing with ultra-pure argon in an anaerobic cuvette equipped with two side arms. The organic substrate was loaded into one side arm and was mixed with enzyme after the cuvette was devoid of oxygen.

Enzyme Kinetics. Enzymatic activity was measured with the method of initial rates (25) in air saturated 50 mM Tris-Cl, pH 8, by monitoring the rate of oxygen consumption with a computer interfaced Oxy-32 oxygen monitoring system (Hansatech Instrument Ltd.) thermostated at 30 $^{\circ}$C. Enzyme concentration was expressed per enzyme bound FMN content, using the experimentally determined ε_{444nm} value of 11,850 $M^{-1}cm^{-1}$. Stock solutions of nitroalkane substrates were prepared in 100% ethanol; the final concentration of ethanol in each assay mixture was kept constant at 1% to minimize possible effects on enzymatic activity. Alkyl nitronates were prepared as described above, except that the nitroalkane solution was allowed to react for 24 h at room temperature, with a 1.2 molar excess of KOH. Enzymatic assays were initiated by the addition of substrate, in order to minimize changes in the ionization state of the nitroalkane[1]. When both the organic substrate and oxygen were varied, the assay mixtures were equilibrated with the appropriate O_2/N_2 gas mixture by bubbling the gas for at least 10 min, before the reaction was started with the addition of the enzyme and the organic substrate. When

[1] The second order rate constants for deprotonation of the nitroalkanes used in the present study have values comprised between 5 and 6 $M^{-1}s^{-1}$ (48), ensuring that in assays initiated with fully protonated nitroalkanes a negligible amount of anionic substrate is present during the time required to determine initial rates (typically ~30 s). Similarly, the second-order rate constants for protonation of alkyl nitronates have values in the 15 to 75 $M^{-1}s^{-1}$ range (5), ensuring a negligible amount of neutral substrate in assays initiated with fully unprotonated alkyl nitronates.

the pH was varied, 50 mM sodium phosphate was used as a buffer between pH 6 and 9.5. Deuterium substrate kinetic isotope effects were determined using 1,2-[^{2}H$_4$]-nitroethane or 1,2,2-[^{2}H$_3$]-ethylnitronate as substrate in air-saturated 50 mM potassium phosphate, pH 8. Activity assays were carried out by alternating substrate isoptomers. The presence of superoxide during turnover of the enzyme with different nitroalkane substrates was monitored by measuring the rate of oxygen consumption at a fixed concentration of substrate, in either the presence or absence of 125 units of superoxide dismutase, in air saturated 50 mM Tris-Cl, pH 8 at 30 ^{o}C. Production of hydrogen peroxide during turnover was monitored by measuring the rate of oxygen consumption at a fixed concentration of substrate, in either the presence or absence of 75 units of catalase.

Stopped-Flow Analysis of 2-Nitropropane Dioxygenase in Turnover. 2-Nitropropane dioxygenase was mixed with ethylnitronate at a final concentration of 5 mM in 50 mM potassium phosphate and 1% ethanol, pH 7.4, in a stopped-flow spectrophotometer thermostated at 15 ^{o}C. Traces were recorded for 60 s, while following the reaction at 370 and 445 nm. Spectra of the enzyme in turnover with substrate were obtained by following absorbance changes at a single wavelength between 300-600 nm at 10 nm intervals and plotting the absorbance versus wavelength for any given time.

Data Analysis. Data were fit with KaleidaGraph software (Adelbeck Software, Reading, PA) or Enzfitter software (Biosoft, Cambridge, UK). Kinetic parameters determined in atmospheric oxygen were obtained by fitting the data to the Michaelis-Menten equation for one substrate. When initial rates of reaction were determined by varying the concentrations of both the nitroalkane substrate and oxygen, the data were fit to equations 1 and 2, which describe a sequential and ping-pong steady state kinetic mechanism, respectively. K_a and K_b represent the

Michaelis constants for the nitroalkane substrate (A) and oxygen (B), respectively and k_{cat} is the turnover number of the enzyme (e). The pH dependence of the steady state kinetic parameters was determined by fitting initial rate data obtained at varying concentrations of organic substrate to equations 3 and 4, which describe a bell shaped curve with a slope of +1 at low pH and a slope of −1 at high pH, and a curve with a slope of −1 and a plateau region at low pH, respectively. C is the pH independent value of the kinetic parameter of interest. Substrate deuterium kinetic isotope effects were determined by fitting the data to equation 5, which describes isotope effects on k_{cat} and k_{cat}/K_m. F_i is the atom fraction of deuterium label in the substrate and E_{cat} and $E_{kcat/K}$ are the isotope effects minus one on k_{cat} and k_{cat}/K_m, receptively.

$$\frac{v}{e} = \frac{k_{cat}AB}{K_aB + K_bA + AB + K_{ia}K_b} \tag{1}$$

$$\frac{v}{e} = \frac{k_{cat}AB}{K_aB + K_bA + AB} \tag{2}$$

$$\log Y = \log\left(\frac{C}{1 + \dfrac{10^{-pH}}{10^{-pKa1}} + \dfrac{10^{-pKa2}}{10^{-pH}}} \right) \tag{3}$$

$$\log Y = \log\left(\frac{C}{1 + \dfrac{10^{-pKa2}}{10^{-pH}}} \right) \tag{4}$$

$$\frac{v}{e} = \frac{k_{cat}A}{K_m(1 + F_i \times E_{kcat/K}) + A(1 + F_i \times E_{kcat})} \tag{5}$$

3.4 Results
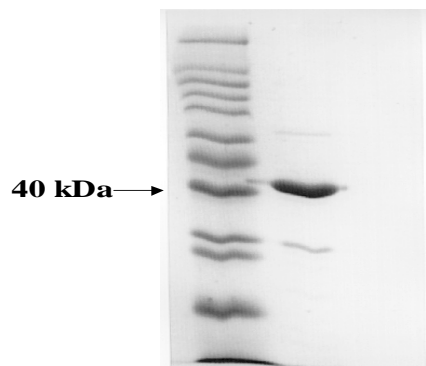
Figure 3.1 Purification of 2-nitropropane dioxygenase. Lane 1, marker proteins; lane 2, enzyme as purified.

Expression and Purification of 2-Nitropropane Dioxygenase. One of the most critical impediments for a detailed biochemical and mechanistic investigation of 2-nitropropane dioxygenase to date has been a lack of an efficient and rapid method for the obtainment of large amounts of purified enzyme. Indeed, an earlier study reported that 2 mg of purified enzyme could be obtained in five chromatographic steps from a 100 L liquid culture of *Neurospora crassa* cells (2). In the present study, the previously identified *ncd*-2 gene encoding for 2-nitropropane dioxygenase form *N. crassa* was PCR-cloned in the expression vector pET20b(+). After the successful construction of the resulting pET/2NPDnc plasmid was confirmed by nucleotide sequence analysis, 2-nitropropane dioxygenase was expressed in large amounts (~15% of the total protein content) in *Escherichia coli* strain BL21(DE3) upon incubation with 0.1 mM IPTG for 17 h at 21 $^{\circ}$C. 2-Nitropropane dioxygenase was then purified to high levels, as judged by SDS-PAGE analysis (Figure 1), with two chromatographic steps onto DEAE-Sepharose and Octyl-Sepharose columns. As shown in Table 1 for a representative purification of the enzyme, 34 mg of recombinant 2-nitropropane dioxygenase could be obtained from 6.25 L of bacterial cell culture, corresponding to a ~300-fold increase in the amount of purified enzyme per liter of culture as compared to the procedure employing *N. crassa* cells (2).

Table 3.1 Purification of Recombinant 2-Nitropropane Dioxygenase

step	total protein, mg	total activity[b], μmol O_2 min^{-1}	specific activity, μmol O_2 min^{-1}mg^{-1}
Cell-free extract	1,000	13,600	13
70% $(NH_4)_2SO_4$ saturation	730	12,000	16
DEAE-Sepharose FF	100	4,900	49
Octyl-Sepharose FF	34	2,800	80

[a]Starting from 51 g of wet cell paste; [b]Enzyme activity was determined with 10 mM ethylnitronate in air-saturated 50 mM Tris-Cl, pH 8, and 25 °C.

Biochemical Characterization of 2-Nitropropane Dioxygenase. In agreement with the predicted molecular weight of 39,916.1 calculated from the amino acid composition of the enzyme (GenBank accession # XP_323268), a molecular weight of 40,000 was determined under
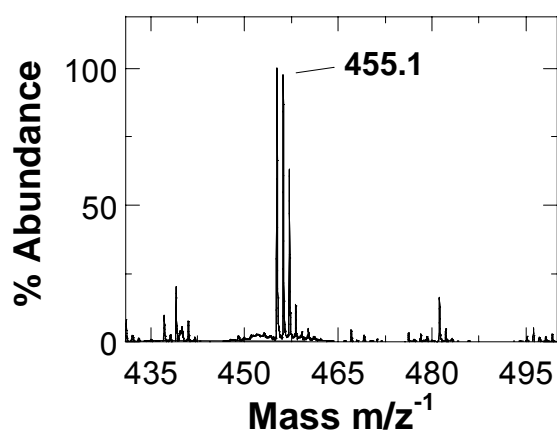
Figure 3.2 MALDI-TOF mass spectrometric analysis of the flavin cofactor of 2-nitropropane dioxygenase.
The spectrum was recorded in negative ion mode with a 50:50 methanol: acetonitrile matrix using a sample prepared by treating the enzyme with trichloroacetic acid, centrifugation and collection of the supernant.

denaturing conditions from an SDS-PAGE analysis of the purified enzyme (Figure 1). Size exclusion chromatography under non-denaturing conditions of 2-nitropropane dioxygenase, at a concentration of 45 μM, yielded a single peak with an apparent molecular weight of 80,000 (data not shown), consistent with a dimeric oligomerization state for the enzyme in solution. The non-covalently bound flavin cofactor of 2-nitropropane dioxygenase was determined to be FMN, based on the peak with an m/z^- value of 455.1 seen in the MALDI-TOF

spectrum of the flavin released upon denaturation of the enzyme followed by centrifugation to remove the precipitated protein (Figure 2). A stoichiometry of 0.84 ± 0.23 FMN per monomer of enzyme could be calculated from the ratio of the concentration of flavin released after heat

treatment of the enzyme to the concentration of enzyme determined by the Bradford assay. An

iron content of 0.02 per monomer of enzyme was determined by inductively coupled plasma

mass spectroscopic analysis of the purified enzyme, consistent with negligible iron content in 2-nitropropane dioxygenase (data not shown). These data indicate that recombinant 2-nitropropane dioxygenase expressed in the heterologous bacterial system has the same oligomerization state and flavin content[2] of the native enzyme extracted from *N. crassa* (2).
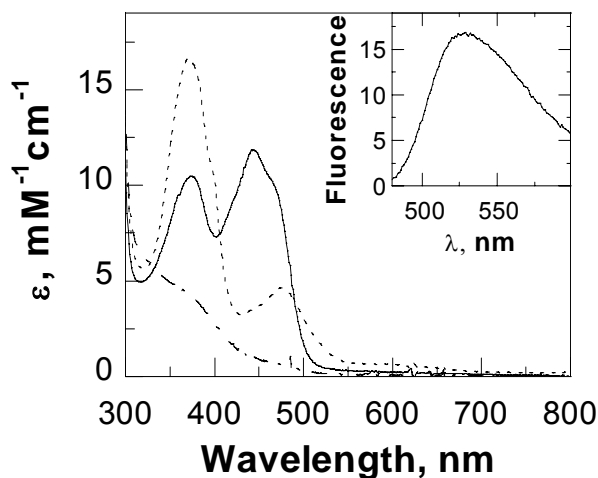
Figure 3.3 UV-visible absorbance spectra of recombinant 2-nitropropane dioxygenase. *Solid curve*, UV-visible absorbance spectrum of 2-nitropropane dioxygenase as purified recorded in 50 mM potassium phosphate pH 7.4; *dotted curve*, spectrum of the enzyme-bound anionic flavin semiquinone obtained by anaerobic mixing of the oxidized enzyme with 750 µM ethylnitronate; *dashed curve*, spectrum of the enzyme-bound flavin hydroquinone obtained upon photoreduction of 2-nitropropane dioxygenase in the presence of 15 mM EDTA. *Inset*, flavin fluorescence emission spectrum of 2-nitropropane dioxygenase (λ_{ex} at 444 nm).

Spectral Characterization of 2-Nitropropane Dioxygenase. 2-Nitropropane dioxygenase showed maxima at 375 and 444 nm (Figure 3) in its UV-visible absorbance spectrum, as expected for a flavin dependant enzyme with the bound flavin in the oxidized state (26). An extinction coefficient of 11,850 $M^{-1}cm^{-1}$ (λ_{444} at pH 8) was determined for the

enzyme-bound FMN from the ratio of the absorbance of bound to free FMN extracted by heat

[2] Earlier studies identified the prosthetic group of *N. crassa* 2-nitropropane dioxygenase as FMN, based on reverse-phase HPLC analysis of the flavin extracted by heat treatment of the enzyme (2). In that same study, it was reported that the quantitative analysis revealed the presence of two mol of flavin per mol of subunit, although the experimental procedure used in the determination was not reported. In this respect, other flavoenzymes with molecular mass of ~40 kDa, such as rat kidney L-α-hydroxy acid oxidase (49), L-lactate 2-monooxygenase (50) and Old Yellow Enzyme (51), all contain one mol of FMN per mol of monomer of enzyme, making the originally reported stoichiometry of 2 FMN per monomer of 2-nitropropane dioxygenase very unlikely.

treatment of the enzyme. The flavin fluorescence emission at 530 nm (with λ_{ex} at 444 nm) of the enzyme was weak, with about 4% the intensity of an equimolar solution of free FMN. Photoreduction of 2-nitropropane dioxygenase in the absence of an active site ligand resulted in the direct reduction of the enzyme-bound flavin to the hydroquinone form with no stabilization of flavosemiquinone intermediates, as indicated by the bleaching of the peak centered at 444 nm and the isosbestic point at 333 nm (Figure 4). The UV-visible absorbance spectrum of the reduced enzyme showed an unresolved peak in the 350 nm region of the near-UV spectrum (Figure 4), suggesting that the anionic species of the flavohydroquinone is stabilized in the enzyme active site (27).

Figure 3.4 Photoreduction of 2-nitropropane dioxygenase
2-Nitropropane dioxygenase was irraditiated with a 100-watt light bulb in the presence of 15 mM EDTA in 50 mM potassium phosphate, pH 7.4. Spectra of a 2-nitropropane dioxygenase were recorded after different intervals of irradiation. Only selected spectra are presented: *curve 1*, spectrum of 2-nitropropane dioxygenase as purified at a concentration of 29 μM; curve 18, same sample after 23 min of irradiation. *Inset*: absorbance changes at 444 nm as a function of irradiation time.

Effect of Superoxide Dismutase on the Enzymatic Activity of 2-Nitropropane Dioxygenase. As pointed out in an elegant study by Kuo and Fridovich, the oxidation of propyl-2-nitronate to acetone and nitrite can be catalyzed via a non-enzymatic free radical chain reaction that is initiated and propagated by superoxide (28). Since it has been amply demonstrated that flavin-dependant enzymes in the hydroquinone state transiently produce superoxide upon reacting with molecular oxygen (29-31), there exists the possibility that the oxidation of nitroalkanes catalyzed by 2-nitropropane dioxygenase might involve a non-enzymatic free radical mechanism that is initiated and propagated by the

enzymatic formation and release of superoxide. If this were the case, one would expect the rate of oxygen consumption to decrease significantly when the enzymatic activity of 2-nitropropane dioxygenase is measured in the presence of superoxide dismutase, since the superoxide would be converted to oxygen and hydrogen peroxide. Consequently, the effect of superoxide dismutase on the reaction catalyzed by 2-nitropropane dioxygenase with several nitroalkanes as substrate was determined. As shown in Table 2, with all the substrate tested except propyl-1- and propyl-2-nitronate, the rate of oxygen consumption did not change when superoxide dismutase was present in the reaction.

Table 3.2 Effect of Superoxide Dismutase and Catalase on Enzymatic Activity of 2-Nitropropane Dioxygenase

substrate	control	+ superoxide dismutase	+ catalase
		rate, $s^{-1 b}$	
nitroalkanes			
2-nitropropane, 20 mM	0.82 ± 0.07	0.78 ± 0.04	0.73 ± 0.03
nitroethane, 10 mM	3.5 ± 0.1	3.6 ± 0.2	3.6 ± 0.1
nitropropane, 40 mM	8.3 ± 0.1	8.3 ± 0.2	8.3 ± 0.1
nitrobutane, 28 mM	3.6 ± 0.2	3.6 ± 0.3	3.6 ± 0.1
nitropentane, 10 mM	3.0 ± 0.3	2.9 ± 0.1	3.1 ± 0.1
nitrohexane, 10 mM	1.3 ± 0.1	1.3 ± 0.1	1.3 ± 0.1
alkyl nitronates			
propyl-2-nitronate, 20 mM	29 ± 1	14 ± 1	29 ± 1
ethylnitronate, 10 mM	40 ± 3	38 ± 1	38 ± 1
propyl-1-nitronate, 25 mM	42 ± 1	27 ± 1	27 ± 1
butyl-1-nitronate, 28 mM	42 ± 1	43 ± 1	42 ± 1
pentyl-1-nitronate, 29 mM	35 ± 1	36 ± 1	35 ± 2
hexyl-1-nitronate, 30 mM	21 ± 1	21 ± 1	21 ± 1

[a]Enzyme activity was measured in the absence or presence of 125 units of superoxide dismutase or 75 catalase in air-saturated 50 mM Tris-Cl, at pH 8.0 and 30 ^{o}C. [b]Kinetic data are the average of two independent measurements.

mixture, consistent with the oxidation of the nitroalkane substrates catalyzed by 2-nitropropane dioxygenase occurring at the enzyme active site and not involving a free radical chain reaction. With propyl-1- and propyl-2-nitronate as substrate for the enzyme, the enzymatic activity in the presence of superoxide dismutase decreased by 65 and 50%, respectively, suggesting that the oxidation of these nitronates catalyzed by 2-nitropropane dioxygenase has a significant non-enzymatic component.

Steady State Kinetic Mechanism. The steady state kinetic mechanism of 2-nitropropane dioxygenase with a number of substrates in either the neutral or anionic form was determined by varying the concentration of both the organic substrate and oxygen at pH 8 and 30 $^{\circ}$C. As shown in Figure 5 for the case of butyl-1-nitronate, with all the substrates tested double reciprocal plots of the initial rate of oxygen consumption as a function of substrate concentration yielded converging lines, consistent with oxygen reacting with an enzyme species reversibly connected to the enzyme species that binds the organic substrate. Consistent with the observed kinetic pattern, the initial rate data with all substrates were fit best to equation 1, which describes a sequential steady state kinetic mechanism. The kinetic parameters determined with nitroethane, nitrobutane, nitrohexane and 2-nitropropane both in the neutral and anionic forms are summarized in Table 3.
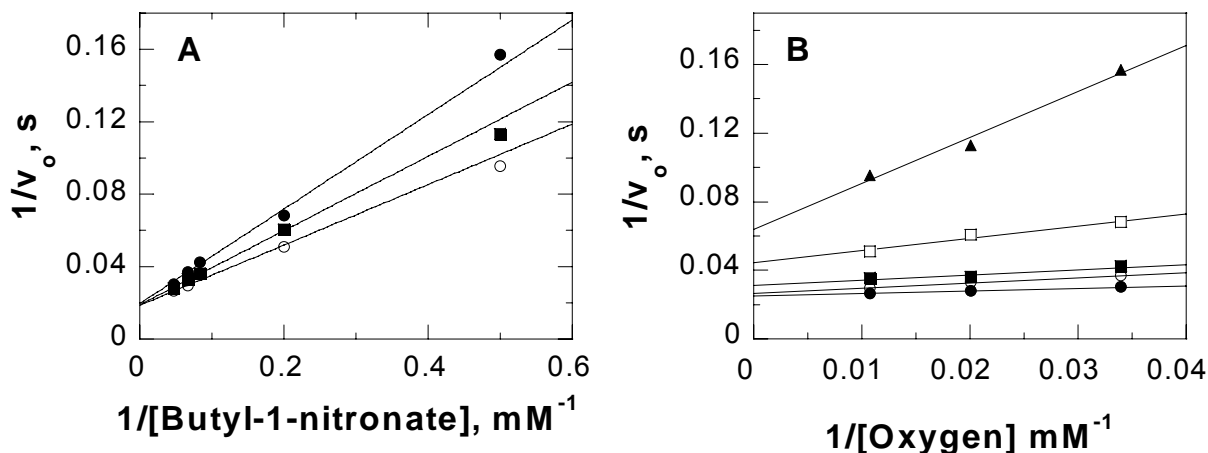
Figure 3.5 Double reciprocal plot of the reaction catalyzed by 2-nitropropane dioxygenase with butyl-1-nitronate as substrate.

Enzyme activity was measured at varying concentrations of both butyl-1-nitronate and oxygen in 50 mM Tris-Cl, pH 8 and 30 °C. *Panel A*, $1/v_o$ as a function of inverse butyl-1-nitronate concentration determined at oxygen concentrations of: (■) 29.5 μM, (o) 49.9 μM; and (●) 93.2 μM. *Panel B*, $1/v_o$ as a function of inverse O_2 concentration determined at several fixed concentrations of butyl-1-nitronate: (▲) 2.0 μM, (□) 5.0 μM, (■) 12.0 μM, (o) 15.0 μM, and (●) 21.1 μM. The lines are fits of the data to equation 1.

Substrate Specificity. Since K_{O2} values of 5 μM or below were determined with primary nitroalkanes and nitronates, initial rates measured with these substrates at atmospheric oxygen would be expected to provide fairly good estimates of the true k_{cat} and k_{cat}/K_m values measured at saturating oxygen[3]. Consequently, the investigation of the enzyme specificity for substrates with different alkyl chain length was carried out by measuring initial rates of reaction with primary nitroalkanes and nitronates in air-saturated buffer. As shown in Table 4, both k_{cat} and k_{cat}/K_m values were not significantly affected by the length of the substrate alkyl chain irrespective of whether the neutral or the anionic nitroalkane was the substrate for the enzyme. In contratst,

---

[3] In air-saturated buffer at 30 °C the concentration of oxygen in solution is 230 μM, i.e., ~50-fold the K_{O2} values determined with primary nitroalkanes, ensuring that the enzyme is at least ~98% saturated with oxygen with these substrates. Consequently, both the apparent k_{cat} and k_{cat}/K_m values determined at atmospheric oxygen with primary nitroalkanes approximate well the values that would be measured by varying the concentration of both organic substrate and oxygen. As expected based on this analysis, the k_{cat} and k_{cat}/K_m determined with the neutral and anionic forms of nitroethane, nitrobutane, and nitrohexane at atmospheric oxygen (Table 4) were similar to those determined by varying the concentration of oxygen (Table 3).

Table 3.3 Steady State Kinetic Parameters for 2-Nitropropane Dioxygenase at pH 8

substrate	k_{cat}, s^{-1}	$K_a{}^b$, mM	k_{cat}/K_m, $M^{-1}s^{-1}$	$K_{O2}{}^b$, μM	k_{cat}/K_{O2}, $\mu M^{-1}s^{-1}$	K_{ia}, mM	R^2
			nitroalkanes				
nitroethane	11 ± 1	19 ± 1	560 ± 10	4.9 ± 0.2	2.2 ± 0.1	11 ± 1	0.998
nitrobutane	5.9 ± 0.1	15 ± 1	400 ± 1	≤ 2	12 ± 1	190 ± 1	0.981
nitrohexane	1.7 ± 0.1	0.8 ± 0.1	$2,100 \pm 50$	2.4 ± 0.1	0.7 ± 0.1	30 ± 1	0.971
2-nitropropane	4.0 ± 0.1	16 ± 1	250 ± 1	≤ 2	6.4 ± 0.1	420 ± 2	0.997
			alkyl nitronates				
ethylnitronate	57 ± 1	3.4 ± 0.1	$16,900 \pm 30$	2.4 ± 0.1	24 ± 1	19 ± 1	0.998
butyl-1-nitronate	56 ± 1	6.5 ± 0.1	$8,600 \pm 30$	2.6 ± 0.1	21 ± 1	86 ± 1	0.997
hexyl-1-nitronate	21 ± 1	1.2 ± 0.1	$17,900 \pm 800$	2.1 ± 0.1	10 ± 1	8 ± 1	0.992
propyl-2-nitronate[c]	15 ± 1	4.9 ± 0.1	$3,100 \pm 200$	30 ± 1	0.50 ± 0.01	15 ± 1	0.963

[a]Enzyme activity was measured at varying concentrations of both organic substrate and oxygen in 50 mM Tris-Cl, pH 8 at 30 °C. Data were fit to eqs 1 and 2; with all the substrates tested the best fit was with eq 1. [b]K_a is the Michaelis constant for the organic substrate; K_{O2} is the Michaelis constant for oxygen. [c]Measured in the presence of 21 units superoxide dismutase.

the k_{cat}/K_m values determined with alkyl nitronates were between 2 and 35 times as large as the corresponding values determined with nitroalkanes, suggesting a preference of the enzyme for the anionic substrates. Similarly, the k_{cat} values with alkyl nitronates were 3 to 15 times larger than those with nitroalkanes.

Table 3.4 Substrate Specificity of 2-Nitropropane Dioxygenase at pH 8

substrate	k_{cat}, s^{-1}	K_m, mM	k_{cat}/K_m, M^{-1}s^{-1}	R^2
nitroalkanes				
nitroethane	14 ± 1	29 ± 2	480 ± 20	0.995
nitropropane	20 ± 1	24 ± 2	830 ± 60	0.998
nitrobutane	6.2 ± 0.4	17.9 ± 2.0	350 ± 50	0.992
nitropentane	4.3 ± 0.1	7.1 ± 0.4	610 ± 40	0.998
nitrohexane	1.5 ± 0.1	1.4 ± 0.1	1,100 ± 100	0.994
alkyl nitronates				
ethylnitronate	51 ± 3	3.1 ± 0.4	16,500 ± 2,300	0.986
propyl-1-nitronate[b]	60 ± 1	5.5 ± 0.4	11,400 ± 500	0.996
butyl-1-nitronate	55 ± 2	10 ± 1	5,600 ± 500	0.994
pentyl-1-nitronate	n.d.[c]	n.d.	1,200 ± 100	0.995
hexyl-1-nitronate	22 ± 1	1.4 ± 0.2	16,000 ± 1,000	0.987

[a]Enzyme activity was measured at varying concentrations of organic substrate in air-saturated 50 mM Tris-Cl, at 30 °C. [b]Measured in the presence of 500 units of superoxide dismutase. [c]n.d., not determined because saturation could not be achieved due to limited solubility of the nitroalkane substrate.
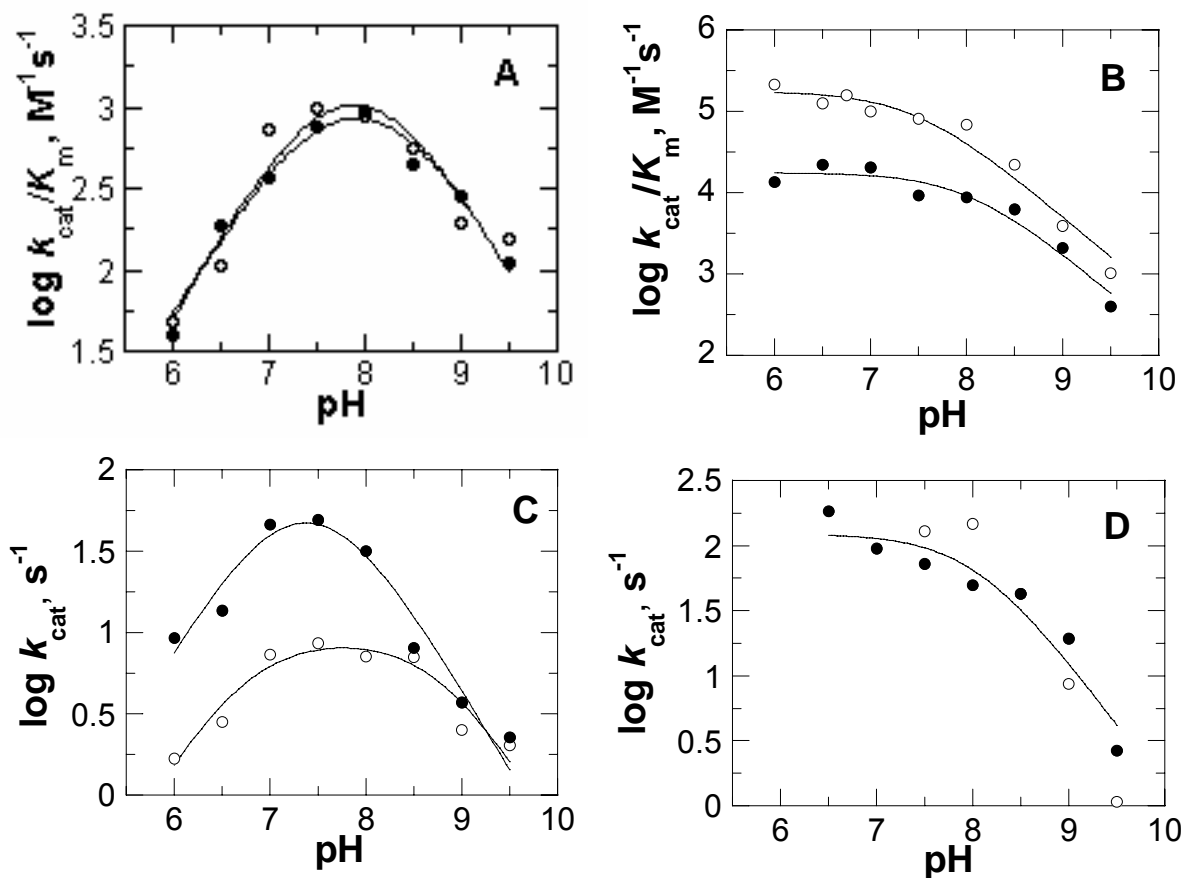
Figure 3.6 pH dependence of the k_{cat}/K_m and k_{cat} values with nitroalkanes and nitronates. Initial rates were measured in air saturated 50 mM sodium pyrophosphate at 30 °C, in the pH range from 6 to 9.5. Kinetic parameters were determined using nitroethane (o), nitrobutane (•), ethylnitronate (o), and nitrobutane (•) as substrate. Panel A, k_{cat}/K_m values with neutral nitroalkanes; panel B, k_{cat}/K_m values with anionic nitronates; panel C, k_{cat} values with neutral nitroalkanes; and panel D, k_{cat} value with anionic nitronates. The curves are fits of the data to equations 3 (for nitroalkanes) and 4 (for nitronates).

pH-Dependence of the k_{cat}/K_m and k_{cat} Values. The pH dependences of the kinetic parameters of 2-nitropropane dioxygenase with nitroethane, nitrobutane, ethylnitronate, and butyl-1-nitronate as substrate were measured in air-saturated buffer[3] in the accessible pH range. With nitroethane and nitrobutane, both the k_{cat} and k_{cat}/K_m values yielded bell-shaped pH profiles, consistent with the involvement of two ionizable groups that must be protonated and unprotonated for the oxidation of the neutral substrates (Figure 6). In contrast, with ethylnitronate and butyl-1-nitronate, the k_{cat} and k_{cat}/K_m values increased to

limiting values with decreasing pH, consistent with the requirement of a single ionizable group that must be protonated for catalysis with anionic substrates. The pK_a values determined in this study are summarized in Table 5.

Table 3.5 pH Dependence of Reaction Catalyzed by 2-Nitropropane Dioxygenase

substrate	kinetic parameter	pK_1	pK_2	eq.
nitroethane	k_{cat}/K_m	7.6 ± 0.3	8.0 ± 0.3	3
	k_{cat}	7.0 ± 0.3	7.7 ± 0.3	3
ethylnitronate	k_{cat}/K_m		7.5 ± 0.2	4
	k_{cat}		nd^b	
nitrobutane	k_{cat}/K_m	7.4 ± 0.2	8.4 ± 0.2	3
	k_{cat}	6.7 ± 0.2	8.8 ± 0.2	3
butyl-1-nitronate	k_{cat}/K_m		8.0 ± 0.1	4
	k_{cat}		7.9 ± 0.2	4

[a]Initial rates were measured at varying concentrations of organic substrate in air-saturated 50 mM sodium pyrophosphate buffer in the pH range 6-9.5 at 30° C. [b]Not determined because below pH 7 substrate saturation could not be achieved due to limited substrate solubility and high K_m values.

Substrate Deuterium Kinetic Isotope Effects. Substrate deuterium kinetic isotope effects were measured with $[1,2-{}^2H_4]$-nitroethane as substrate for 2-nitropropane dioxygenase in air-saturated buffer. A $^D(k_{cat}/K_m)$ value of 4.1 ± 0.5 was determined at pH 8, consistent with the CH bond of the neutral nitroalkane substrate being cleaved in a kinetically slow step during catalysis by 2-nitropropane dioxygenase. When $1,2,2-[{}^2H_3]$-ethyl-nitronate was used as substrate for the enzyme, an inverse $^D(k_{cat}/K_m)$ value of 0.76 ± 0.06 was determined, consistent with a change in the hybridization state of the α-carbon from sp^3 to sp^2 occurring in the oxidation of alkyl nitronates catalyzed by 2-nitropropane dioxygenase. The $^Dk_{cat}$ values were not significantly different from unity, with values of 1.3 ± 0.2 and 0.99 ± 0.09 with deuterated nitroethane and ethylnitronate, suggesting that chemical steps that are isotope sensitive are masked by some later kinetic steps, such as product release, in the catalytic pathway of 2-nitropropane dioxygenase.
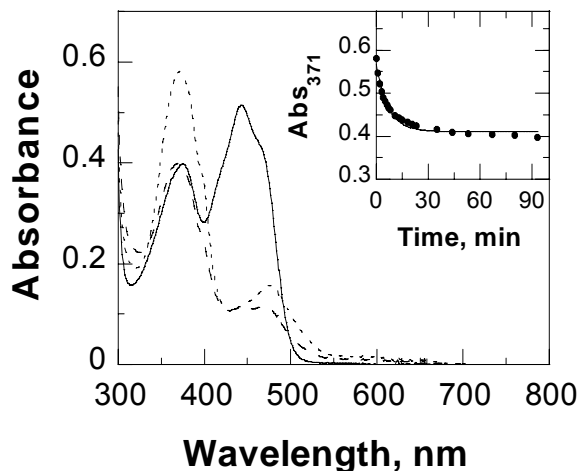
Figure 3.7 Anaerobic reduction of 2-nitropropane dioxygenase by ethylnitronate.
Solid curve, UV-visible absorbance spectrum of oxidized enzyme; *dotted curve*, the same sample ~1 min after mixing with 750 μM ethylnitronate; and *dashed curve*, the same sample 94 min after mixing. *Inset:* absorbance changes at 371 nm as a function of time. The curve is a fit of the data to
$y = 0.16e^{-0.14x} + 0.41$ $(R^2 = 0.977)$.

Anaerobic Substrate-Reduction of 2-Nitropropane Dioxygenase. The steady state kinetic data determined at varying concentrations of both organic substrate and oxygen reported in this study support a kinetic mechanism in which an enzyme species in complex with the organic ligand reacts with oxygen, but do not establish whether the enzyme-bound ligand is the nitroalkane substrate or the carbonyl product of the reaction. A ternary complex involving the carbonyl product requires the enzyme to be in a reduced form, since an oxidation-reduction reaction must have necessarily occurred between the nitroalkane and the enzyme-bound flavin prior to reaction with oxygen. If this were the case, anaerobic mixing of the oxidized enzyme with the nitroalkane substrate would result in the reduction of the enzyme-bound flavin. In contrast, no changes in the oxidation state of the enzyme-bound flavin would be expected upon mixing anaerobically the oxidized enzyme with the substrate if the ternary complex involves the nitroalkane substrate, since catalysis would occur only in the presence of oxygen. As shown in Figure 7, anaerobic mixing of the enzyme with ethylnitronate at 15 °C resulted in the rapid formation of an anionic flavin semiquinone species with peaks centered at 371 and 476 nm, consistent with oxidation of the substrate

occurring in the absence of oxygen. The enzyme-bound flavin semiquinone then slowly decayed to the hydroquinone form at a rate of 8.4 ± 0.6 s^{-1}, as determined from the decrease in absorbance at 371 nm over time. However, complete formation of the flavin hydroquinone species was not observed even after 94 min of incubation, consistent with the fully reduced form of the enzyme-bound flavin not being in the normal catalytic pathway of the enzyme. Similar results were obtained when nitroethane was used as the reductant (data not shown), indicating that the anaerobic one-electron reduction of the flavin did not depend on the ionization state of the substrate, but was a property of 2-nitropropane dioxygenase.
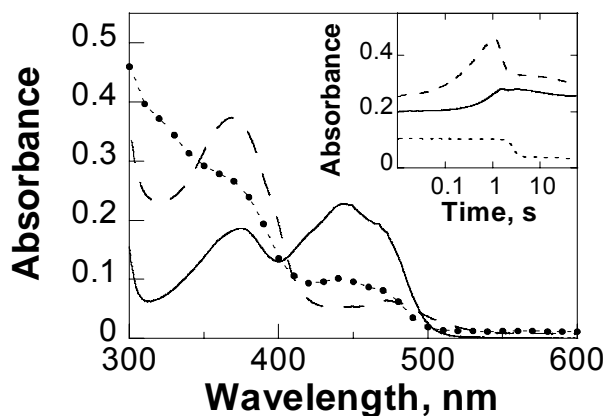
Figure 3.8 Enzyme monitored turnover with ethylnitronate as substrate.
2-Nitropropane dioxygenase was mixed aerobically with ethylnitronate at a final concentration of 5 mM in 50 mM potassium phosphate, pH 7.4 at 15 °C, and traces were recorded at 10 nm intervals between 300 and 600 nm. *Solid curve*, the absorbance spectrum of the resting enzyme in the oxidized state; *dotted curve*, absorbance spectrum of the reaction mixture 1.2 ms after mixing; and *dashed curve*, absorbance spectrum of the resting enzyme after turnover at 80 s after mixing. *Inset*, traces collected at 300 nm (*dashed curve*), 370 nm (*solid curve*), and 440 nm (*dotted curve*).

Enzyme Monitored Turnover with Ethylnitronate as Substrate. To determine whether the anionic flavin semiquinone of 2-nitropropane dioxygenase was on the direct catalytic pathway for the oxidation of the nitroalkane substrate, the enzyme was allowed to turnover in the presence of 5 mM ethylnitronate and 0.46 mM oxygen at 15 °C, and the reaction was monitored using a stopped-flow spectrophotometer. A mixture of enzyme-bound oxidized and

semiquinone flavin species was rapidly established within 1.2 ms during enzymatic turnover under the conditions used, as indicated by the relative absorbance of the traces recorded at 370 and 440 nm (Figure 8). Under these conditions, steady state enzymatic turnover persisted for ~7 s, as indicated by the lack of absorbance changes at 440 nm, after which the rapid depletion of oxygen resulted in the reduction of the enzyme-bound flavin to the flavosemiquinone form (Figure 8). A species with λ_{max} at ~300 nm was transiently formed in the UV-visible absorbance spectrum of the enzyme under turnover in the steady state phase, consistent with the formation and subsequent decay of a product of the reaction. It is likely that the transient species is acetaldehyde, the expected product of the oxidation of ethylnitronate catalyzed by 2-nitropropane dioxygenase, since it absorbs light at 300 nm and is known to rapidly convert in aqueous solution to its hydrated form, which absorbs at ~278 nm (32).

Effect of Catalase on the Enzymatic Activity of 2-Nitropropane Dioxygenase. To determine whether hydrogen peroxide is formed in the reaction catalyzed by 2-nitropropane dioxygenase, the rate of oxygen consumption during turnover of the enzyme with neutral nitroalkanes or anionic nitronates was determined in either the absence or presence of 75 units of catalase. As shown in Table 2, with the exception of propyl-1-nitronate, there was no significant effect of catalase on the initial rates of reaction when the reaction was carried out in the presence of catalase, indicating that hydrogen peroxide is not formed in the catalytic pathway of 2-nitropropane dioxygenase.

3.5   Discussion

In the present study, the *ncd*-2 gene encoding for 2-nitropropane dioxygenase from *Neurospora crassa* was ligated into pET20b(+) to construct plasmid pET/2NPDnc,

which was subsequently expressed to high yields in *Escherichia coli* strain BL21(DE3).
The use of the heterologous bacterial expression system allowed for the obtainment of
large amounts of purified enzyme with a simplified purification procedure, enabling the
characterization of the biochemical and kinetic properties of 2-nitropropane dioxygenase.
The original goal of the present study was to investigate the steady state kinetic
mechanism of 2-nitropropane dioxygenase to define a framework for future mechanistic
investigations of the enzyme aimed at a thorough understanding of the catalytic
mechanism of the enzyme. In the course of the study, evidence was collected indicating
the involvement of an anionic flavin semiquinone species in the oxidation reaction
catalyzed by 2-nitropropane dioxygenase.

Scheme 3.2 Steady state kinetic mechanism with
nitronates as substrate for 2-nitropropane
dioxygenase.

Scheme 3.3 Steady state kinetic mechanism with
nitroalkanes as substrate for 2-nitropropane
dioxygenase.

The oxidation of
nitroalkanes, in both their neutral
and anionic forms, by 2-
nitropropane dioxygenase
proceeds by an oxidase-style
mechanism in which the flavin-
mediated oxidation of the
substrate and the subsequent
oxidation of the enzyme-bound
flavin occur in two independent
steps. With nitronates as substrate

(Scheme 2), after formation of an enzyme-substrate complex the organic substrate is
oxidized through the transfer of a single electron to the enzyme-bound flavin with

formation of an anionic flavin semiquinone species (E-FMN$_{sq}$-S$^{\bullet}$). The subsequent

reaction of molecular oxygen with the E-FMN$_{sq}$-S$^{\bullet}$ complex results in the oxidation of the

enzyme-bound flavin and production of the carbonyl product of the reaction, which is

then released from the enzyme active site. With nitroalkanes as substrate (Scheme 3),

catalysis is initiated by an enzyme-catalyzed proton abstraction from the α-carbon of the

neutral substrate to yield an enzyme-bound nitronate (vide infra), which is then oxidized

following the same catalytic pathway described for the nitronate substrates. The order of

the kinetic steps involving substrate binding and product release is supported by the

kinetic data observed with nitroethane, nitrobutane, nitrohexane, and 2-nitropropane as

substrate for the enzyme, both in their anionic and neutral forms. Evidence for the

formation of an anionic flavin semiquinone in the enzyme-substrate complex before

reaction with molecular oxygen comes from the spectral investigation of the enzyme-

bound flavin upon mixing the enzyme anaerobically with either ethylnitronate or

nitroethane. The stopped-flow spectrophotometric analysis of the enzyme under turnover

clearly establishes that the formation of the flavin semiquinone occurs in the catalytic

pathway for the oxidation of the nitroalkane substrate, with the enzyme cycling between

its oxidized and one-electron reduced state. The enzyme monitored turnover data also

rule out the involvement of the flavin hydroquinone in the enzymatic oxidation of the

nitroalkane substrate, since formation of the two-electron reduced form of the enzyme-

bound flavin was observed only after complete depletion of oxygen from the reaction

mixture. Consistent with formation of the enzyme-bound flavin semiquinone requiring

the nitroalkane substrate in either its neutral or anionic form, but not molecular oxygen,

superoxide dismutase did not have any effect on the enzymatic activity expressed as rate

of oxygen consumption with nitroethane, nitropropane, nitrobutane, nitropentane, nitrohexane, 2-nitropropane, ethylnitronate, butyl-1-nitronate, pentyl-1-nitronate, and hexyl-1-nitronate. While other flavin-dependent enzymes, such as DNA photolyase (33,34) and luciferase (35,36) have been previously shown to utilize neutral flavin semiquinones in their catalytic cycles, to our knowledge 2-nitropropane dioxygenase is the first example of an enzyme operating with an oxidase-like catalytic mechanism in which an anionic flavin semiquinone has been directly observed in the catalytic pathway with physiological substrates.

Oxidation of the neutral nitroalkane substrates requires a catalytic base with pK_a of ~7.5, as suggested by the pH-profiles of the k_{cat}/K_m and k_{cat} values with nitroethane and nitrobutane, showing the requirement for an unprotonated group for catalysis. Such a catalytic base does not participate in the oxidation of the anionic substrates, as indicated by the pH-dependence studies of the k_{cat}/K_m and k_{cat} values with ethylnitronate and butyl-1-nitronate. A likely role for the catalytic base of 2-nitropropane dioxygenase is to initiate the oxidation of the neutral substrates by abstracting the proton from the substrate α-carbon to yield an enzyme-bound nitronate species of the substrate (Scheme 4). Such a chemical step is at least partially limiting the rate of the chemical processes catalyzed by 2-nitropropane dioxygenase, as suggested by the magnitude of the substrate deuterium kinetic isotope effects on the k_{cat}/K_m value determined with 1,2-[$^2H_4$]-nitroethane. A similar requirement for a catalytic base that abstracts the α-proton from the nitroalkane substrate was previously established in another nitroalkane-oxidizing enzyme, nitroalkane oxidase, where the catalytic base was identified as Asp_{402} with mutagenesis studies (37). Due to the uniqueness of the amino acid sequence of 2-nitropropane

dioxygenase, the elucidation of the identity of the catalytic base in this enzyme will have to await future structural studies.

Reaction of the enzyme-bound anionic flavin semiquinone with molecular oxygen occurs with a second order rate constant k_{cat}/K_{O2} in the range of 10^6 to 10^7 $M^{-1}s^{-1}$, in agreement with studies on the oxygen reactivity in solution showing second order rate constants of ~10^8 $M^{-1}s^{-1}$ (29). Recent *ab initio* theoretical calculations showed that most of the spin density in anionic flavin semiquinones is located either on the $N(5)$ position or the benzene moiety of the isoalloxazine ring (38,39). The $N(5)$ locus is expected to be freely accessible to oxygen, making it a good candidate for reaction with oxygen in 2-nitropropane dioxygenase via a rapid one-electron transfer that results in the oxidation of the flavin and formation of superoxide (Scheme 4). The participation of an acid with pK_a of ~8.0 in the formation of a neutral superoxide speciesis suggested by the pH-dependence of the k_{cat}/K_m and k_{cat} values with both nitroalkane and nitronate substrates, showing the involvement of a protonated group in catalysis. Such a chemistry is supported by recent mechanistic studies on glucose oxidase using viscosity, solvent and ^{18}O isotope effects, suggesting that with that enzyme at high pH the association of molecular oxygen with the reduced enzyme is accompanied by the transfer of a single electron resulting in the formation of superoxide anion at the binding step (40,41). Formation of a superoxide species in 2-nitropropane dioxygenase is supported by the effect of superoxide dismutase on the rate of oxygen consumption when propyl-nitronates are used as substrates (vide infra). As shown in Scheme 4, the superoxide species thus generated would rapidly react with the nitroalkane radical within the enzyme active site, resulting in the formation of an α-peroxynitroalkane intermediate. Consistent with the

formation of such a peroxynitroalkane species, an inverse secondary substrate deuterium kinetic isotope effect was observed on the k_{cat}/K_m value with 1,2,2-$[^2H_3]$-ethyl-nitronate as substrate, which is expected for a change in hybridization of the nitronate α-carbon from sp^2 to sp^3 (42). The final elimination of nitrite from the peroxynitroalkane to yield the carbonyl product would then likely occur through a non-enzymatic attack by a nucleophile, such as for example the nitronate. The lack of a catalase effect on the enzymatic activity of 2-nitropropane dioxygenase rules out the alternative possibility of superoxide reacting with the enzyme-bound flavin, since if that were the case a 50% decrease in the rate of oxygen consumption would have been observed with catalase due to the formation of hydrogen peroxide following the decay of the C(4a)-peroxyflavin intermediate (18,43).
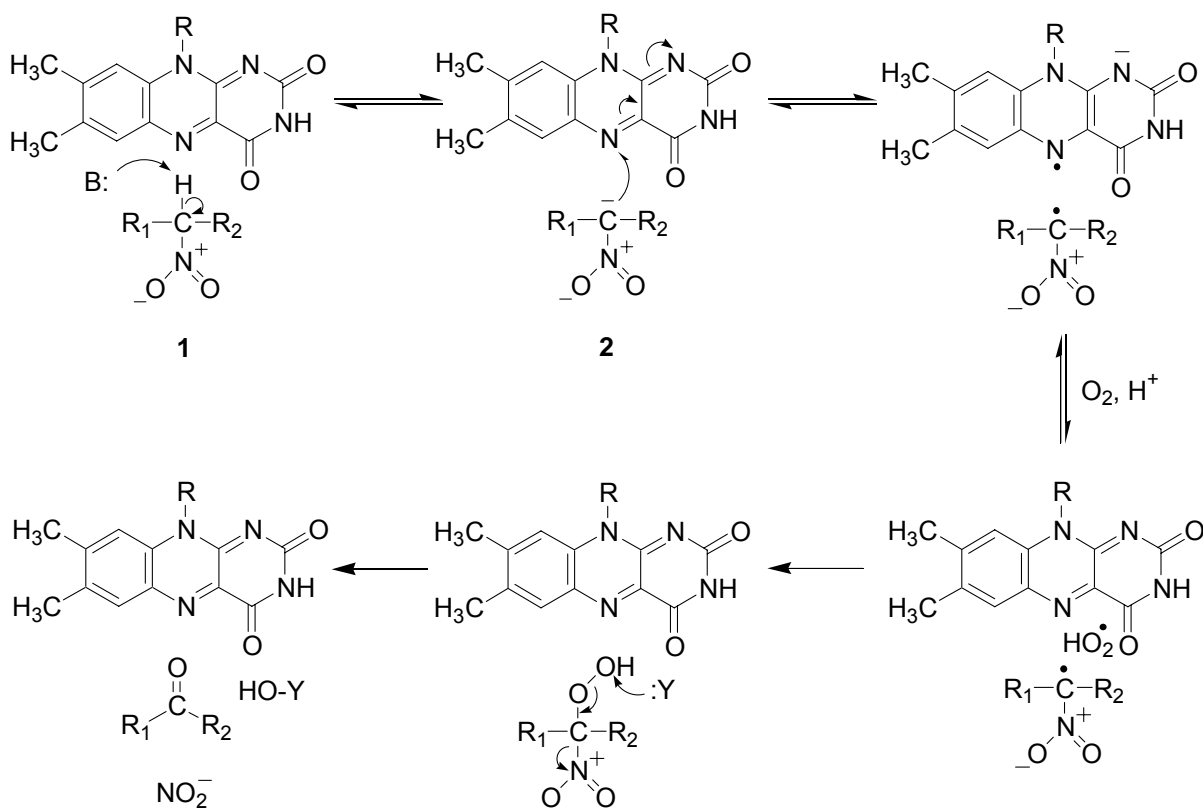
Scheme 3.2 Proposed mechanism for oxidation of nitroalkanes (from step 1) and nitronates (from step 2) catalyzed by 2-nitropropane dioxygenase.

A significant component of the oxidation of both propyl-1- and propyl-2-nitronate catalyzed by 2-nitropropane dioxygenase involves a radical chain reaction that occurs mostly off of the enzyme active site, as indicated by the effect of superoxide dismutase on the enzymatic activity with these substrates. The decreased rates of oxygen consumption observed in the presence of superoxide dismutase are readily explained with superoxide being normally produced in the catalytic pathway of 2-nitropropane dioxygenase, but being released from the active site only when the enzyme species that reacts with oxygen is in complex with propyl-1- and propyl-2-nitronate. The superoxide released in solution would initiate and propagate a non-enzymatic radical chain reaction with the propyl-nitronates, a reaction fully established and characterized in solution (28,44), leading to a significant amplification of the rate of oxygen consumption with these substrates. In the presence of the superoxide-scavenging enzyme superoxide dismutase, such a non-enzymatic oxidation of the propyl-nitronates would be abated, as experimentally observed. Enzymatic initiation of nitronate oxidation via facile free radical reactions triggered by the formation and release of superoxide anion was previously reported for glucose oxidase (21), horseradish peroxidase (45), and propionate-3-nitronate oxidase (46). With primary and secondary nitroalkanes and with alkyl nitronates other then the propyl ones, the 2-nitropropane dioxygenase oxidation reaction occurs enzymatically at the enzyme active site, as indicated by the lack of a superoxide dismutase effect on the rate of oxygen consumption. Therefore, it is likely that the non-enzymatic component of the oxidation of propyl-nitronates is due to an adventitious release of superoxide from the enzyme active site.

Earlier studies on 2-nitropropane dioxygenase showed that the enzyme is capable of oxidizing both anionic nitronates and neutral nitroalkanes (2). The more extensive kinetic analyses reported in the present study are consistent with a broad range of substrate specificity, in that the enzyme can oxidize both 2-nitropropane and a number of primary nitroalkanes in their neutral and anionic forms. The enzyme has a higher specificity for alkyl nitronates as compared to neutral substrates, as indicated by the second order rate constant k_{cat}/K_m that reflects the relative selectivity of the enzyme with different substrates. Interestingly, the specificity of the enzyme for primary nitroalkanes and nitronates is independent of the size of the substrate, since similar k_{cat}/K_m values were observed with substrates with increasing length in the alkyl chain. Furthermore, substrate size does not significantly affect the overall enzymatic rate of turnover, as shown by the similar k_{cat} values seen within the nitroalkane and nitronate series. These results are in stark contrast with those previously reported for another nitroalkane-oxidizing enzyme, namely nitroalkane oxidase, for which both the substrate specificity and the overall turnover number were shown to be significantly affected by the size of the nitroalkane substrate (47,48). With that enzyme, it was proposed that substrate binding occurs at a hydrophobic site sufficiently large to accommodate nitroalkanes with a four-carbon linear chain (47). With 2-nitropropane dioxygenase the substrate binding site is likely to be less restrictive than that of nitroalkane oxidase.

In summary, in the present study the gene coding for 2-nitropropane dioxygenase from *N. crassa* was cloned and heterogously expressed in *E. coli*. The resulting enzyme was purified to high yields and was found to be a homodimer containing a mol of tightly bound FMN per mol of subunit. With neutral nitroalkanes and anionic nitronates other

than propyl-1-nitronate and propyl-2-nitronate, substrate oxidation occurs at the enzyme active site. A steady state kinetic analysis showed that the preferred substrates for the enzyme are anionic nitronates as compared to neutral nitroalkanes, and that the enzyme has broad substrate specificity that is independent of substrate size. From a mechanistic standpoint, 2-nitropropane dioxygenase operates through an oxidase-like catalytic mechanism, in which substrate oxidation occurs prior to and independently from reaction with oxygen, via the formation of an enzyme-bound anionic flavin semiquinone. To our knowledge, this represents the first account in which an anionic flavin semiquinone has been experimentally observed in the catalytic pathway for the oxidation of organic molecules catalyzed by a flavin-dependent enzyme. The availability of large amounts of recombinant 2-nitropropane dioxygenase will be instrumental for detailed mechanistic and structural studies aimed at a better understanding of the chemical mechanism of oxidation of both neutral nitroalkanes and anionic nitronates catalyzed by 2-nitropropane dioxygenase, and of the role the anionic flavin semiquinone plays in catalysis.

3.6   Acknowledgements

75

conditions; and Dr. Siming Wang and Sarah Shealy for mass spectral analysis of the flavin cofactor of the enzyme.

3.7　References

1.　Little, H. N. (1951) Oxidation of nitroethane by extracts from *Neurospora*, *J. Biol. Chem. 193*, 347-358.

2.　Gorlatova, N., Tchorzewski, M., Kurihara, T., Soda, K., and Esaki, N. (1998) Purification, characterization, and mechanism of a flavin mononucleotide-dependent 2-nitropropane dioxygenase from *Neurospora crassa*, *Appl. Environ. Microbiol. 64*, 1029-1033.

3.　Tchorzewski, M., Kurihara, T., Esaki, N., and Soda, K. (1994) Unique primary structure of 2-nitropropane dioxygenase from *Hansenula mrakii*, *Eur. J. Biochem. 226*, 841-846.

4.　Kido, T., and Soda, K. (1978) Properties of 2-nitropropane dioxygenase of *Hansenula mrakii*. Formation and participation of superoxide, *J. Biol. Chem. 253*, 226-232.

5.　Nielsen, A. T. (1969) Nitronic acids and esters, In *The Chemistry of the nitro and nitroso groups* (Feuer, H., Ed.), pp 349-486, Interscience Publishers, New York.

6.　Ballini, R., Barboni, L., and Giarlo, G. (2003) Nitroalkanes in aqueous medium as an efficient and eco-friendly source for the one-pot synthesis of 1,4-diketones, 1,4-diols, delta-nitroalkanols, and hydroxytetrahydrofurans, *J. Org. Chem. 68*, 9173-9176.

7.　Hanessian, S., and Pham, V. (2000) Catalytic asymmetric conjugate addition of nitroalkanes to cycloalkenones, *Org. Lett. 2*, 2975-2978.

8. Matt, C., Wagner, A., and Mioskowski, C. (1997) Novel Transformation of Primary Nitroalkanes and Primary Alkyl Bromides to the Corresponding Carboxylic Acids, *J. Org. Chem. 62*, 234-235.

9. Davis, R. (1993) *Patty's Industrial Hygiene and Toxicology*, John Wiley and Sons, New York.

10. Sittig, M. (1985) *Handbook of Toxic and Hazardous Chemicals and Carcinogens*, 2 ed., Noyes Publications, Park Ridge, NJ.

11. Haas-Jobelius, M., Coulston, F., and Korte, F. (1992) Effects of short-term inhalation exposure to 1-nitropropane and 2-nitropropane on rat liver enzymes, *Ecotoxicol. Environ. Saf. 23*, 253-259.

12. Fiala, E. S., Czerniak, R., Castonguay, A., Conaway, C. C., and Rivenson, A. (1987) Assay of 1-nitropropane, 2-nitropropane, 1-azoxypropane and 2-azoxypropane for carcinogenicity by gavage in Sprague-Dawley rats, *Carcinogenesis 8*, 1947-1949.

13. Lewis, T. R., Ulrich, C. E., and Busey, W. M. (1979) Subchronic inhalation toxicity of nitromethane and 2-nitropropane, *J. Environ. Pathol. Toxicol. 2*, 233-249.

14. Dayal, R., Gescher, A., Harpur, E. S., Pratt, I., and Chipman, J. K. (1989) Comparison of the hepatotoxicity in mice and the mutagenicity of three nitroalkanes, *Fundam. Appl. Toxicol. 13*, 341-348.

15. Conaway, C. C., Nie, G., Hussain, N. S., and Fiala, E. S. (1991) Comparison of oxidative damage to rat liver DNA and RNA by primary nitroalkanes, secondary

nitroalkanes, cyclopentanone oxime, and related compounds, *Cancer Res. 51*, 3143-3147.

16. Sakano, K., Oikawa, S., Murata, M., Hiraku, Y., Kojima, N., and Kawanishi, S. (2001) Mechanism of metal-mediated DNA damage induced by metabolites of carcinogenic 2-nitropropane, *Mutat. Res. 479*, 101-111.

17. Kido, T., Soda, K., Suzuki, T., and Asada, K. (1976) A new oxygenase, 2-nitropropane dioxygenase of *Hansenula mrakii*. Enzymologic and spectrophotometric properties, *J. Biol. Chem. 251*, 6994-7000.

18. Kido, T., Hashizume, K., and Soda, K. (1978) Purification and properties of nitroalkane oxidase from *Fusarium oxysporum*, *J. Bacteriol. 133*, 53-58.

19. Porter, D. J., Voet, J. G., and Bright, H. J. (1973) Direct evidence for carbanions and covalent N 5 -flavin-carbanion adducts as catalytic intermediates in the oxidation of nitroethane by D-amino acid oxidase, *J. Biol. Chem. 248*, 4400-4416.

20. Gadda, G., and Fitzpatrick, P. F. (2000) Mechanism of nitroalkane oxidase: 2. pH and kinetic isotope effects, *Biochemistry 39*, 1406-1410.

21. Porter, D. J., and Bright, H. J. (1977) Mechanism of oxidation of nitroethane by glucose oxidase, *J. Biol. Chem. 252*, 4361-4370.

22. Inoue, H., Nojima, H., and Okayama, H. (1990) High efficiency transformation of *Escherichia coli* with plasmids, *Gene 96*, 23-28.

23. Bradford, M. M. (1976) A rapid and sensitive method for the quantitation of microgram quantities of protein utilizing the principle of protein-dye binding, *Anal. Biochem. 72*, 248-254.

24.   Whitby, L. G. (1953) A new method for preparing flavin-adenine dinucleotide, *Biochem. J. 54*, 437-442.

25.   Allison, R. D., and Purich, D. L. (1979) Practical considerations in the design of initial velocity enzyme rate assays, *Methods Enzymol. 63*, 3-22.

26.   Gadda, G., Choe, D. Y., and Fitzpatrick, P. F. (2000) Use of pH and kinetic isotope effects to dissect the effects of substrate size on binding and catalysis by nitroalkane oxidase, *Arch. Biochem. Biophys. 382*, 138-144.

27.   Urban, P., Chirat, I., and Lederer, F. (1988) Rat kidney L-2-hydroxyacid oxidase. Structural and mechanistic comparison with flavocytochrome b2 from baker's yeast, *Biochemistry 27*, 7365-7371.

28.   Giegel, D. A., Williams, C. H., Jr., and Massey, V. (1990) L-lactate 2-monooxygenase from *Mycobacterium smegmatis*. Cloning, nucleotide sequence, and primary structure homology within an enzyme family, *J. Biol. Chem. 265*, 6626-6632.

29.   Akeson, A., and Theorell, H. (1956) Molecular weight and FMN content of crystallin old yellow enzyme, *Arch. Biochem. Biophys. 65*, 439-448.

30.   Massey, V. (2000) The chemical and biological versatility of riboflavin, *Biochem. Soc. Trans. 28*, 283-296.

31.   Ghisla, S., Massey, V., Lhoste, J. M., and Mayhew, S. G. (1974) Fluorescence and optical characteristics of reduced flavines and flavoproteins, *Biochemistry 13*, 589-597.

32.   Kuo, C. F., and Fridovich, I. (1986) Free-radical chain oxidation of 2-nitropropane initiated and propagated by superoxide, *Biochem. J. 237*, 505-510.

33.   Massey, V. (1994) Activation of molecular oxygen by flavins and flavoproteins, *J. Biol. Chem. 269*, 22459-22462.

34.   Messner, K. R., and Imlay, J. A. (1999) The identification of primary sites of superoxide and hydrogen peroxide formation in the aerobic respiratory chain and sulfite reductase complex of *Escherichia coli*, *J. Biol. Chem. 274*, 10119-10128.

35.   Fridovich, I. (1970) Quantitative aspects of the production of superoxide anion radical by milk xanthine oxidase, *J. Biol. Chem. 245*, 4053-4057.

36.   Bell, R. P. a. C., J.C. (1952) The Hydrationof Acetaldehyde in Aqueous Solution, *Faraday Soc.Trans. 48*, 439-442.

37.   Jorns, M. S., Baldwin, E. T., Sancar, G. B., and Sancar, A. (1987) Action mechanism of *Escherichia coli* DNA photolyase. II. Role of the chromophores in catalysis, *J. Biol. Chem. 262*, 486-491.

38.   Sancar, G. B., Jorns, M. S., Payne, G., Fluke, D. J., Rupert, C. S., and Sancar, A. (1987) Action mechanism of *Escherichia coli* DNA photolyase. III. Photolysis of the enzyme-substrate complex and the absolute action spectrum, *J. Biol. Chem. 262*, 492-498.

39.   Eckstein, J. W., Hastings, J. W., and Ghisla, S. (1993) Mechanism of bacterial bioluminescence: 4a,5-dihydroflavin analogs as models for luciferase hydroperoxide intermediates and the effect of substituents at the 8-position of flavin on luciferase kinetics, *Biochemistry 32*, 404-411.

40.   Francisco, W. A., Abu-Soud, H. M., DelMonte, A. J., Singleton, D. A., Baldwin, T. O., and Raushel, F. M. (1998) Deuterium kinetic isotope effects and the mechanism of the bacterial luciferase reaction, *Biochemistry 37*, 2596-2606.

41. Valley, M. P., and Fitzpatrick, P. F. (2003) Inactivation of nitroalkane oxidase upon mutation of the active site base and rescue with a deprotonated substrate, *J. Am. Chem. Soc. 125*, 8738-8739.

42. Massey, V. (1994) Activation of molecular oxygen by flavins and flavoproteins, *J. Biol. Chem. 269*, 22459-22462.

43. Zheng, Y. J., and Ornstein, R. L. (1996) A Theoretical Study of the Structures of Flavin in Different Oxidation and Protonation States, *J. Am. Chem. Soc. 118*, 9402-9408.

44. Martinez, J. I., Alonso, P. J., Gomez-Moreno, C., and Medina, M. (1997) One- and two-dimensional ESEEM spectroscopy of flavoproteins, *Biochemistry 36*, 15526-15537.

45. Su, Q., and Klinman, J. P. (1999) Nature of oxygen activation in glucose oxidase from *Aspergillus niger*: the importance of electrostatic stabilization in superoxide formation, *Biochemistry 38*, 8572-8581.

46. Roth, J. P., and Klinman, J. P. (2003) Catalysis of electron transfer during activation of O_2 by the flavoprotein glucose oxidase, *Proc. Natl. Acad. Sci. U. S. A. 100*, 62-67.

47. Streitwieser A., J. R. H., Fahey R. C., and Suzuki S. (1958) Kinetic Isotope Effects in the Acetolyses of Deuterated Cyclopentyl Tosylates, *J. Am. Chem. Soc. 80*, 2326-2332.

48. Simonetta, M. P., Vanoni, M.A., Casalin, P. (1987) Purification and properties of D-amino acid oxidase, an inducible flavoenzyme from *Rhodotorula gracilis*, *Biochim. Biophys. Acta 914*, 136.

49. Bors, W., Michel, C., Dalke, C., Stettmaier, K., Saran, M., and Andrae, U. (1993) Radical intermediates during the oxidation of nitropropanes. The formation of NO_2 from 2-nitropropane, its reactivity with nucleosides, and implications for the genotoxicity of 2-nitropropane, *Chem. Res. Toxicol. 6*, 302-309.

50. Porter, D. J., and Bright, H. J. (1983) The mechanism of oxidation of nitroalkanes by horseradish peroxidase, *J. Biol. Chem. 258*, 9913-9924.

51. Porter, D. J., and Bright, H. J. (1987) Propionate-3-nitronate oxidase from *Penicillium atrovenetum* is a flavoprotein which initiates the autoxidation of its substrate by O_2, *J. Biol. Chem. 262*, 14428-14434.

52. Gadda, G., and Fitzpatrick, P. F. (1999) Substrate specificity of a nitroalkane-oxidizing enzyme, *Arch. Biochem. Biophys. 363*, 309-313.

4   CHAPTER IV

PROBING THE CHEMICAL STEPS OF NITROALKANE OXIDATION CATALYZED BY 2-NITROPROPANE DIOXYGENASE WITH SOLVENT VISCOSITY, PH, AND SUBSTRATE KINETIC ISOTOPE EFFECTS

4.1   Abstract

Among the enzymes that catalyze the oxidative denitrification of nitroalkanes to carbonyl compounds 2-nitropropane dioxygenase is the only one known to effectively utilize both the neutral and anionic (nitronate) forms of substrate. A recent study has established that the catalytic pathway is common to both types of substrates, except for the initial removal of a proton from the α-carbon of the neutral substrates [Francis, K., Russell, B., and Gadda, G. (2005) *J. Biol. Chem.* 280, 5195-5204]. In the present study, the mechanistic properties of the enzyme have been investigated with solvent viscosity, pH, and kinetic isotope effects. With nitroethane or ethylnitronate the k_{cat}/K_m and k_{cat} values were independent of solvent viscosity, consistent with substrate and product binding to the enzyme in rapid equilibrium. The abstraction of the proton from the α-carbon of neutral substrates was investigated by measuring the pH dependence of the $^D(k_{cat}/K_{NE})$ value with 1,1-$[^2H_2]$-nitroethane. The formation of the enzyme-bound flavosemiquinone formed during catalysis was examined by determining the pH dependence of the k_{cat}/K_m values with ethylnitronate and nitroethane, and of the inhibition by *m*-nitrobenzoate. Finally, α-secondary kinetic isotope effects with 1-$[^2H]$-ethylnitronate were used to propose a non-oxidative tautomerization pathway, in which

the enzyme catalyzes the interconversion of nitroalkanes between their anionic and neutral forms. The data presented suggest that enzymatic turnover of 2-nitropropane dioxygenase with neutral substrates is limited by the cleavage of the substrate CH bond at low pH, whereas that with anionic substrates is limited by the non-oxidative tautomerization of ethylnitroante to nitroethane at high pH.

4.2 Introduction
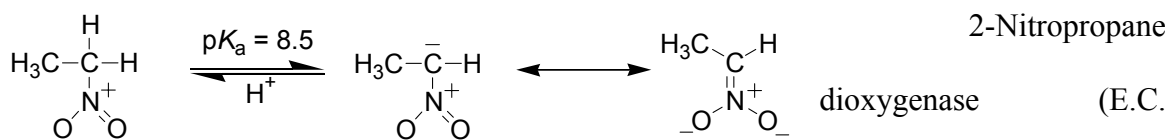
Scheme 4.1 The ionization of nitroethane (*left*) to yield ethylnitronate (*right*) in solution.

2-Nitropropane dioxygenase (E.C. 1.13.11.32) from *Neurospora crassa* is an FMN-dependent enzyme that catalyzes the oxidative denitrification of nitroalkanes to their corresponding carbonyl compounds and nitrite[1] (*1*). Among the enzymes that are known to oxidize nitroalkanes, which comprise nitroalkane oxidase, horseradish peroxidase, D-amino acid oxidase, glucose oxidase, and propionate-3-nitronate oxidase (*2-6*), 2-nitropropane dioxygenase is unique in that it can effectively utilize both the neutral and anionic nitronate forms of substrate (Scheme 1) (*7*). The study of the biochemical and mechanistic properties of 2-nitropropane dioxygenase is of considerable

---

[1] As pointed out by one of the reviewers, the mechanistic data presented in this and a previous study (*1*) suggest that 2-nitropropane dioxygenase may be a misnomer for the nitroalkane-oxidizing enzyme from *Neurospora crassa*, since the reaction mechanism is not a dioxygenase reaction and the enzyme is not most specific for 2-nitropropane (*1*). In contrast, the available evidence suggest that the enzyme, which has broad substrate specificity (*1*), catalyzes a monooxygenase reaction in which a single oxygen atom from molecular oxygen is incorporated into the organic product of the reaction, suggesting that the enzyme may be properly named as nitroalkane monooxygenase. However, as pointed out by the same reviewer, it is not even proven to be a monooxygenase, since this would require isotopic labeling experiments showing that the aldehyde oxygen atom incorporated in the product of the reaction originates from molecular oxygen, which might not be conclusive due to the expected rapid exchange of the aldehyde oxygen with solvent due to hydration-dehydration equilibrium. For these reasons, we prefer to refer to the enzyme with its official IUBMB name, 2-nitropropane dioxygenase.

interest for both applied and fundamental reasons. In industrial applications, nitroalkanes are widely used as synthetic intermediates (*8, 9*), however many are anticipated to be toxic or carcinogenic (*10-15*). The enzymatic oxidation of nitroalkanes into less toxic species can therefore be exploited in bioremediation applications. From a fundamental standpoint, 2-nitropropane dioxygenase is the only reported flavin-dependent enzyme in which a transient anionic flavosemiquinone species has been observed in catalysis (*1*). Consequently, the enzyme serves well as a model system to understand the reactivity of anionic flavosemiquinones in the enzymatic catalysis of flavoproteins.

The crystal structure of 2-nitropropane dioxygenase from *Pseudomonas aeruginosa* has been recently solved both for the free enzyme and the enzyme in complex with 2-nitropropane (*16*). A conserved histidine is located in the active site of the bacterial enzyme near the α-carbon of 2-nitropropane and has been proposed to act as the catalytic base for the oxidation of neutral nitroalkanes. In the enzyme from *N. crassa* this conserved residue is His196, which likely plays a similar role in the yeast enzyme.

The steady state kinetic mechanism of 2-nitropropane dioxygenase has been recently elucidated with both the neutral and anionic forms of nitroethane, nitrobutane, nitrohexane, and 2-nitropropane (*1*).
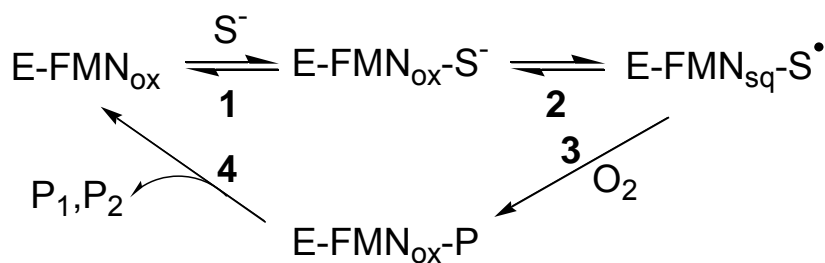
Scheme 4.2 Minimal steady-state kinetic mechanism with nitronates as substrate.
(E) Enzyme, (FMN_{ox}) oxidized flavin, (FMN_{sq}) flavin semiquinone, (S^-) anionic form of nitroalkane, ($S^{\bullet}$) radical form of nitroalkane, (P_1 and P_2) organic product of the reaction and nitrite.

With nitronates as substrate (Scheme 2), formation of the enzyme-substrate complex (**1**) is followed by the transfer of a single electron from the organic substrate to the enzyme bound flavin (**2**), yielding an anionic flavosemiquinone species (E-FMN$_{sq}$-S$^{\bullet}$). Molecular oxygen then reacts with the E-FMN$_{sq}$-S$^{\bullet}$ complex to oxidize the flavosemiquinone (**3**), resulting in the formation of the product of the reaction, which is subsequently released from the enzyme (**4**). Catalysis with nitroalkane substrates (Scheme 3) is initiated by an enzyme-catalyzed proton abstraction from the substrate α-carbon (**2**) to yield an enzyme-bound alkyl nitronate. This species is then oxidized through the same pathway described above. In the present study, solvent viscosity, pH, and deuterium kinetic isotope effects with neutral and anionic nitroethane (ethylnitronate) as substrate have been used to gain further insights into the mechanism of nitroalkane oxidation catalyzed by 2-nitropropane dioxygenase and the kinetic steps that limit enzymatic turnover with neutral and anionic substrates. A non-oxidative tautomerization pathway, in which the enzyme converts the substrate from its anionic to neutral forms, is proposed based on measurements of α-secondary kinetic isotope effects at saturating oxygen concentrations.
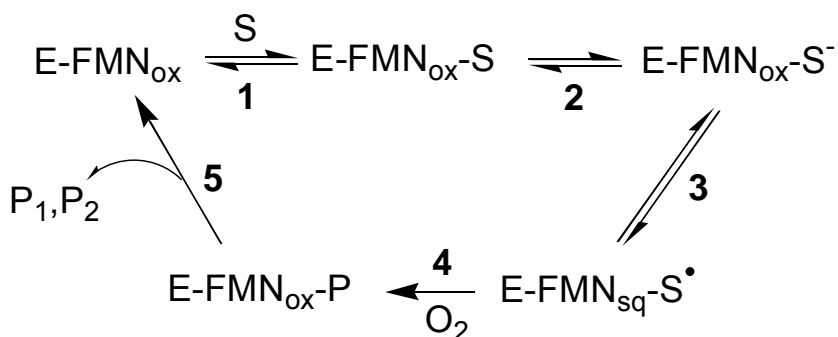
Scheme 4.3 Minimal steady-state kinetic mechanism with nitroalkanes as substrate.
(E) Enzyme, (FMN$_{ox}$) oxidized flavin, (FMN$_{sq}$) flavin semiquinone, (S) neutral form of nitroalkane (S^{-}) anionic form of nitroalkane, (S$^{\bullet}$) radical form of nitroalkane, (P$_1$ and P$_2$) organic product of the reaction and nitrite.

4.3   Materials and Methods

Materials. 2-Nitropropane dioxygenase was obtained through the expression and purification protocols described previously (*1*). Nitroethane, 1,1-[^{2}H$_2$]-nitroethane, and *m*-nitrobenzoic acid, were from Sigma-Aldrich. All other reagents were of the highest purity commercially available.

Methods. Enzyme activity was measured with the method of initial rates (*17*) in air-saturated buffer containing 1% ethanol, by monitoring the rate of oxygen consumption with a computer interfaced Oxy-32 oxygen monitoring system (Hansatech Instrument Ltd.), equipped with a water bath thermostated at 30 ^{o}C. Enzyme concentration was expressed per enzyme bound FMN content, using an ε_{444nm} value of 11,850 M^{-1}cm^{-1} (*1*), and ranged from 0.02 to 3.9 μM. Stock solutions of nitroethane were prepared in 100% ethanol. The nitronate form of substrate was prepared through a reaction of the nitroalkane with a 1.2 molar excess of potassium hydroxide for 24 h at room temperature. In order to minimize changes in the ionization state of the nitroalkane, enzymatic assays were initiated by the addition of substrate to the assay reaction mixture[2]. When both the organic substrate and oxygen were varied, the assay mixtures were equilibrated with the appropriate O$_2$/N$_2$ gas mixture by bubbling the gas for at least 10 min, before the reaction was started with the addition of the enzyme and the organic substrate. Substrate concentrations ranged from 0.5 to 10 mM. When the pH was varied, 50 mM sodium pyrophosphate was used as a buffer between pH 5.5 and 10. Deuterium

---

[2] The second-order rate constant for deprotonation of nitroethane has a value of 6 M^{-1}s^{-1} (*23*), ensuring that in assays initiated with the neutral nitroalkane a negligible amount of anionic substrate is present during the time required to determine initial rates (typically ~30 s). Similarly, the second-order rate constant for protonation of ethylnitronate is 15 M^{-1}s^{-1} (*31*), ensuring a negligible amount of neutral substrate in assays initiated with fully unprotonated alkyl nitronates.

substrate kinetic isotope effects were determined using 1,1-[^{2}H$_2$]-nitroethane in air-saturated buffers or 1-[^{2}H]-ethylnitronate at varying concentrations of both organic substrate and oxygen. Activity assays were carried out by alternating substrate isoptomers, and $^D(k_{cat}/K_m)$ values were calculated from the ratio of the kinetic parameter obtained with unlabeled substrate to that with labeled substrate. The effect of solvent viscosity on the kinetic parameters of the enzyme was determined in 50 mM sodium pyrophosphate at pH 10 with nitroethane, and at pH 6.5 with ethylnitronate using glycerol as viscosigen. The relative viscosities at 30 ^{o}C were calculated from the values at 20 ^{o}C reported by Lide (*18*).

The reductive half reaction of 2-nitropropane dioxygenase with ethylnitronate as substrate was monitored using a Hi-Tech SF-61 stopped-flow spectrophotometer thermostated at 30 ^{o}C. The rate of flavin reduction was measured by monitoring the increase in absorbance at 370 nm that results from anaerobic mixing of the enzyme with substrate at pH 8.5. A ~28 μM solution of 2-nitropropane dioxygenase was loaded into a tonometer and was made anaerobic by a 25-cycle treatment of vacuuming and flushing with oxygen-free argon (pre-treated with an oxygen scrubbing cartridge, Agilent, Palo Alto, Ca). The anaerobic enzyme solution was then mounted onto the stopped-flow instrument, which had been pre-treated with an oxygen scrubbing system composed of 5 mM glucose and 450 units of glucose oxidase. Ethylnitronate was prepared in water and was made anaerobic by flushing with oxygen-free argon for at least 20 min before mounting onto the stopped-flow. 2-Nitropropane dioxygenase was mixed anaerobically with an equal volume of substrate to give a reaction mixture containing ~14 μM enzyme

and 2 to 50 mM ethylnitronate. For each concentration of substrate traces were recorded in triplicate and the average value is reported (measurements typically differed by $\leq 5\%$).

Data Analysis. Steady state kinetic data were fit with KaleidaGraph software (Synergy Software, Reading, PA) or Enzfitter software (Biosoft, Cambridge, UK). Kinetic parameters determined under atmospheric oxygen were obtained by fitting the data to the Michaelis-Menten equation for one substrate. When saturation of 2-nitropropane dioxygenase with organic substrate was not attained the data were fit with eq 1, where k_{cat}/K_a is the second order rate constant for the reaction with the organic substrate, *A* is the concentration of organic substrate and *e* is the concentration of enzyme. When initial rates were determined by varying the concentrations of both the nitroalkane substrate and oxygen the kinetic data were fit to eq 2, which describes a sequential steady state kinetic mechanism. The dissociation constant (K_{is}) for the inhibition of 2-nitropropane dioxygenase by *m*-nitrobenzoate with respect to ethylnitronate as substrate was determined by fitting the data with eq 3, which describes a competitive inhibition pattern, where *I* is the concentration of inhibitor. The pH dependence of the steady state kinetic parameters was determined by fitting initial rate data to eq 4, which describes a bell-shaped curve with a slope of $+1$ at low pH and a slope of -1 at high pH, where *C* is the pH independent value of the kinetic parameter of interest. The pH dependence of the $^D(k_{cat}/K_m)$ values were determined by fitting the data with eq 5, which describes a curve with plateau regions at both high and low pH. Y_L and Y_H are the limiting values at low and high pH, respectively, and K_a is the dissociation constant for the ionizable groups. The pH dependence of *m*-nitrobenzoate inhibition with respect to ethylnitronate as substrate was determined by fitting the data with eq 6, which describes a

curve with a slope of −1 and a plateau region at low pH. The viscosity effects on the kinetic parameters of the enzyme with nitroethane or ethylnitronate as substrate were fit to eq 7, where $(k)_o$ and $(k)_\eta$ are the kinetic parameters of interest determined in the absence and presence of viscosigen, respectively, S is the degree of viscosity dependence and η_{rel} is the relative viscosity. Stopped-flow traces were fit with eq 8, which describes a single exponential process where k_{obs} is the first order rate constant for flavin reduction, t is time, A_t is the absorbance at time t, and A is the final absorbance. Pre-steady state kinetic parameters were determined using eq 9, where k_{obs} is the observed rate of flavin reduction, k_{red} is the limiting rate of flavin reduction at saturating substrate concentrations, K_d is the dissociation constant and S is the concentration of substrate.

$$\frac{v}{e} = \frac{k_{cat}}{K_a} A \tag{1}$$

$$\frac{v}{e} = \frac{k_{cat} A B}{K_a B + K_b A + AB + K_{ia} K_b} \tag{2}$$

$$\frac{v}{e} = \frac{k_{cat} A}{K_a \left[1 + \left(\dfrac{I}{K_{is}} \right) \right] + A} \tag{3}$$

$$logY = log \left(\frac{C}{1 + \dfrac{10^{-pH}}{10^{-pK_{a1}}} + \dfrac{10^{-pK_{a2}}}{10^{-pH}}} \right) \tag{4}$$

$$logY = log \frac{Y_L + Y_H \left(\dfrac{10^{-pK_a}}{10^{-pH}} \right)}{1 + \left(\dfrac{10^{-pK_a}}{10^{-pH}} \right)} \tag{5}$$

$$logY = log\left(\frac{C}{1+\frac{10^{-pKa}}{10^{-pH}}}\right) \tag{6}$$

$$\frac{k_o}{k_\eta} = S(\eta_{rel} - 1) + 1 \tag{7}$$

$$A_{total} = A_t e^{-k_{obs}t} + A \tag{8}$$

$$k_{obs} = \frac{k_{red}S}{K_d + S} \tag{9}$$

4.4   Results

Reductive Half Reaction with Ethylnitronate as Substrate for 2-Nitropropane Dioxygenase. An anionic flavosemiquinone was previously observed during both static mixing and turnover reactions of 2-nitropropane dioxygenase with either ethylnitronate or nitroethane as substrate and was proposed to react with oxygen to generate superoxide (*1*). An alternative possibility is that the flavosemiquinone and the resulting substrate radical react to generate a flavin N(5) adduct, similar to that seen in nitroalkane oxidase (*19*). To test for this possibility the reductive half reaction of 2-nitropropane dioxygenase with ethylnitronate as substrate was monitored at pH 8.5 and 30 $^\circ$C, since a flavin N(5) adduct with typical absorbance in the 320 to 360 nm region of the absorbance spectrum would be formed in the absence of oxygen. As shown in Figure 1A, anaerobic mixing of the enzyme with substrate rapidly generated an anionic flavosemiquinone with peaks centered at 370 and 473 nm. A plot of k_{obs} versus substrate concentration showed hyperbolic behavior with a limiting rate of flavin reduction (k_{red}) of ~380 s^{-1} and a K_d for ethylnitronate binding of ~40 mM. Under the same conditions the k_{cat} value with

ethylnitronate was ~70 s^{-1}, establishing the transient anionic flavosemiquinone as a catalytically relevant species. As shown in Figure 1B, the flavosemiquinone was slowly reduced to the hydroquinone form over >900 s, clearly indicating that this reaction does not occur in the normal catalytic pathway for ethylnitronate oxidation[3]. Thus, the oxidation of nitroalkanes catalyzed by 2-nitropropane dioxygenase occurs with a mechanism that is unique from that of nitroalkane oxidase.
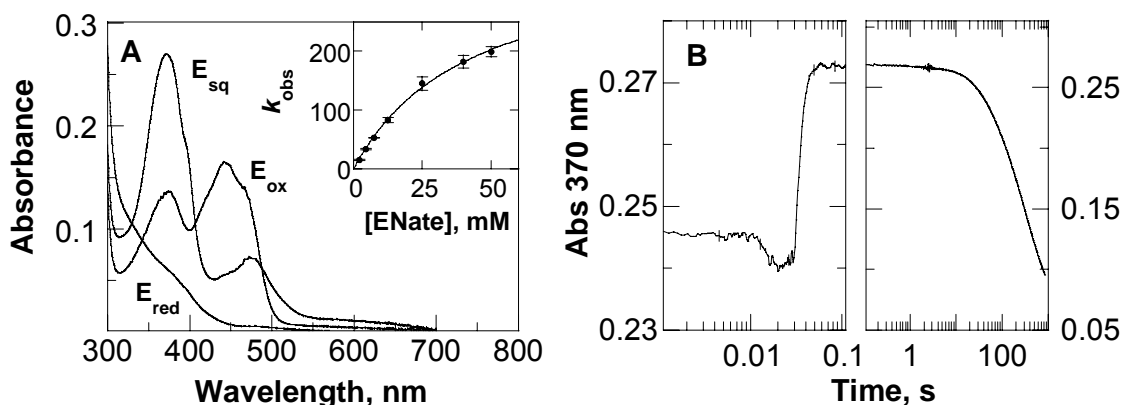
Figure 4.1 Reductive half reaction of 2-nitropropane dioxygenase with ethylnitronate as substrate.
Panel A: UV-visible absorbance spectra of 2-nitropropane dioxygenase in its oxidized, semiquinone, and hydroquinone forms, observed in the stopped-flow spectrophotometer. An anaerobic solution of 2-nitropropane dioxygenase was mixed with either 50 mM sodium pyrophosphate (E_{ox}) or 100 mM ethylnitronate to give a final concentration of enzyme of ~14 μM and a substrate concentration of 50 mM. Spectra were recorded 1 s (E_{sq}) and 78 min (E_{red}) after mixing at pH 8.5 and 30 ^{o}C. Inset: The rate of flavin reduction *versus* concentration of ethylnitronate. 2-Nitropropane dioxygenase (14 μM) was mixed anaerobically with 4 to 100 mM ethylnitronate in 50 mM sodium pyrophosphate, pH 8.5 at 30 ^{o}C, and the absorbance changes at 370 nm were recorded over time. Data were fit with eq 9. Panel B: representative trace showing the absorbance at 370 nm *versus* time obtained with 50 mM ethylnitronate. Note the log scale on the time axis, and the difference scales on the absorbance axis in the two panels.

---

[3] The turnover number of 2-nitropropane dioxygenase with ethylnitronate as substrate at pH 8.5 and 30 ^{o}C is 70 s^{-1}. In order for the hydroquinone to be a catalytically relevant species it would have to form at least 63,000 times in 900 s, clearly establishing that the flavin hydroquinone species, or a flavin N(5) adduct with similar spectroscopic properties, is not formed during the reductive half reaction of 2-nitropropane dioxygenase.

K_m *Values for Oxygen at pH 6 and 9.* Recent steady state kinetic studies of 2-nitropropane dioxygenase showed that the enzyme reacts with oxygen before the release of the organic product of the reaction, with K_m values for oxygen below 5 µM with either nitroethane or ethylnitronate at pH 8 and 30 °C (*1*). As a first step toward the investigation of the pH effects on the $^D(k_{cat}/K_m)$ values with nitroethane and ethylnitronate, the K_m values for oxygen with these substrates were determined here at pH 6 and 9, by measuring initial rates of reaction at varying concentrations of both oxygen and organic substrate. As summarized in Table 1, at both these pH values the K_m values for oxygen determined with nitroethane were at or below 10 µM, allowing for fairly good approximations of the k_{cat}/K_m and k_{cat} values with the neutral substrate to be obtained under atmospheric conditions in the pH range from 6 to 9[4]. In contrast, when ethylnitronate was used as substrate, a K_m value for oxygen of ~45 µM was determined at pH 9 (Table 1). Consequently, while the $^D(k_{cat}/K_m)$ values with nitroethane could be determined at atmospheric oxygen, those with ethylnitronate had to be determined at varying concentrations of both organic substrate and oxygen to avoid artifactual contributions arising from lack of oxygen saturation on the enzyme.

---

[4] The solubility of oxygen in aqueous solution at 30 °C is ~230 µM, a value which is 23-times larger than the upper limiting value of 10 µM experimentally determined for the K_m value for oxygen with nitroethane as substrate for the enzyme between pH 6 and 9. This ensures that in atmospheric oxygen 2-nitropropane dioxygenase is at least 96% saturated with oxygen when nitroethane is used as substrate.

Table 4.1 Steady State Kinetic Parameters for 2-Nitropropane Dioxygenase at pH 6, 8 and 9

pH	k_{cat}, s^{-1}	K_a^b, mM	k_{cat}/K_m, $M^{-1}s^{-1}$	K_{O2}^b, μM	k_{cat}/K_{O2}, $μM^{-1}s^{-1}$	K_{ia}, mM	R^2
			Ethylnitronate				
6	130 ± 3	5.1 ± 0.2	$25,400 \pm 1,400$	20 ± 2	6.2 ± 0.6	0.8 ± 0.4	0.990
8[c]	57 ± 1	3.4 ± 0.1	$16,900 \pm 30$	≤ 5	≥ 11	19 ± 1	0.998
9	25 ± 1	9.5 ± 0.3	$2,500 \pm 100$	45 ± 2	5.3 ± 0.2	9.4 ± 0.6	0.988
			Nitroethane				
6	nd^d	nd^d	40 ± 3	10 ± 3	3.2 ± 0.9	50 ± 20	0.998
8[c]	11 ± 1	19 ± 1	560 ± 10	≤ 5	≥ 2	11 ± 1	0.998
9	4.9 ± 0.1	13 ± 1	375 ± 40	≤ 5	≥ 1	40 ± 5	0.988

[a]Enzyme activity was measured at varying concentrations of both organic substrate and oxygen in 50 mM Tris-Cl, at 30 °C. Data were fit to eq 1. [b]K_a is the Michaelis constant for the organic substrate; K_{O2} is the Michaelis constant for oxygen. [c]From reference 1. [d]Not determined because saturation of the enzyme was not achieved.
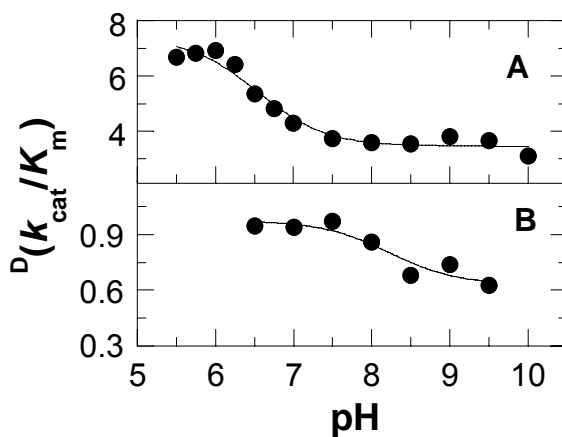
Figure 4.2 pH dependence of the kinetic isotope effects on k_{cat}/K_{NE} and k_{cat}/K_{ENate}. Panel A: pH dependence on the overall kinetic isotope effect with 1,1-[$^2H_2$]-nitroethane as substrate. Panel B: pH dependence of the α-secondary kinetic isotope effect with 1-[^2H]-ethylnitronate as substrate. Kinetic isotope effects were calculated by taking the ratio of k_{cat}/K_m obtained for unlabeled substrate to that of labeled substrate at 30 °C. The data were fit with eq 5.

pH Dependence of the $^D(k_{cat}/K_m)$ Value with 1,1-[$^2H_2$]-Nitroethane. The effect of

pH on the $^D(k_{cat}/K_{NE})$ value[5] with 1,1-[$^2H_2$]-nitroethane as substrate for 2-nitropropane

dioxygenase was determined in air-saturated buffer in the pH range from 5.5 to 10 at 30

^oC. As shown in Figure 2A, the $^D(k_{cat}/K_{NE})$ value decreased from an upper limiting value

of 7.4 ± 0.3 at low pH to a lower limiting value of 3.5 ± 0.1 at high pH, consistent with

the isotope sensitive step in which the neutral organic substrate is enzymatically

deprotonated being partially masked by other kinetic steps belonging to the second-order

rate constant k_{cat}/K_m (*20*). Consistent with previous results showing the requirement for

both an unprotonated and a protonated amino acid residue in the oxidation of neutral
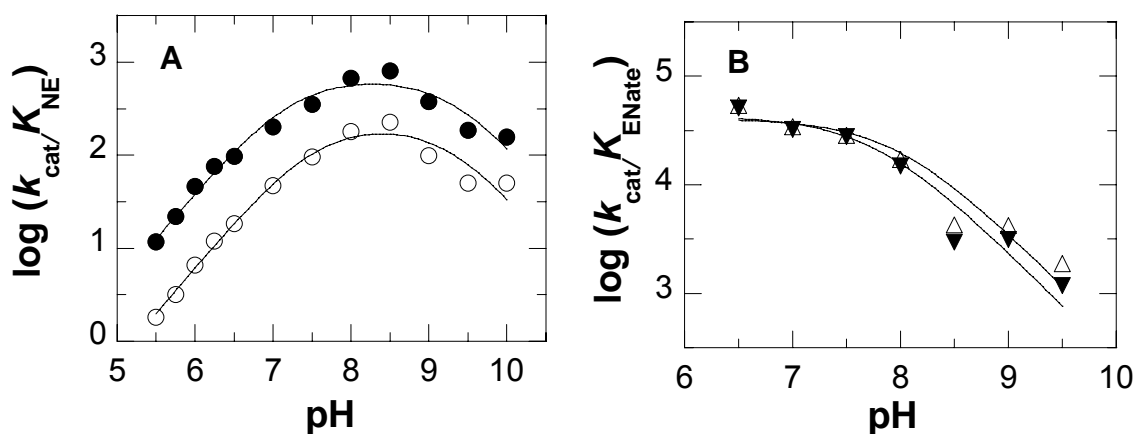
Figure 4.3 pH dependence of k_{cat}/K_m with either nitroethane or ethylnitronate as substrate. Panel A: pH dependence of k_{cat}/K_{NE} with either nitroethane or 1,1-[$^2H_2$]-nitroethane as substrate. Enzymatic activity was measured in air-saturated 50 mM sodium pyrophosphate in the pH range 5.75-10 at varying concentrations of either nitroethane (•) or 1,1-[$^2H_2$]-nitroethane (o) at 30 ^oC. Panel B: pH dependence of k_{cat}/K_{ENate} with either ethylnitronate (▼) or 1-[^2H]-ethylnitronate (Δ) as substrate. Enzymatic activity was measured at varying concentrations of both ethylnitronate and oxygen in 50 mM sodium pyrophosphate in the pH range of 6.5-9.5 at 30 ^oC. Data were fit with eqs 4 and 6 for nitroethane and ethylnitronate, respectively.

---

[5] Saturation of 2-nitropropane dioxygenase with nitroethane, 1,1-[$^2H_2$]-nitroethane, ethylnitronate, or 1-[^2H]-ethylnitronate as substrate was not attained across the entire pH range tested. Consequently, the pH dependence of the $^Dk_{cat, NE}$ and $^Dk_{cat, ENate}$ values could not be determined.

substrates catalyzed by 2-nitropropane dioxygenase (*1*), the pH profiles of the k_{cat}/K_{NE} values were bell-shaped with both the light and heavy substrates (Figure 3A). The pK_a values for the unprotonated and protonated groups required for catalysis were 7.2 ± 0.1 and ≥9.3[6] with nitroethane and 7.5 ± 0.1 and ≥9.3 with 1,1-[^{2}H$_2$]-nitroethane, respectively.

pH Dependence of the $^D(k_{cat}/K_m)$ Value with 1-[^{2}H]-Ethylnitronate. In a recent mechanistic study at atmospheric oxygen, a $^D(k_{cat}/K_{ENate})$ value of ~0.76 was determined with 1-[^{2}H]-ethylnitronate as substrate for 2-nitropropane dioxygenase at pH 8 and 30 ^{o}C

pH Dependence of the $^D(k_{cat}/K_m)$ Value with 1-[^{2}H]-Ethylnitronate. In a recent mechanistic study at atmospheric oxygen, a $^D(k_{cat}/K_{ENate})$ value of ~0.76 was determined with 1-[^{2}H]-ethylnitronate as substrate for 2-nitropropane dioxygenase at pH 8 and 30 ^{o}C (*1*). Such an inverse kinetic isotope effect was assigned to the kinetic step in which superoxide reacts with the nitroalkane radical in the enzyme active site to form peroxynitroethane. In the present study, we have expanded that initial observation by measuring kinetic isotope effects at varying concentrations of both 1-[^{2}H]-ethylnitronate and oxygen as substrates for 2-nitropropane dioxygenase in the pH range from 6.5 to 9.5 at 30 ^{o}C. As shown in Figure 2B, the $^D(k_{cat}/K_{ENate})$ values with 1-[^{2}H]-ethylnitronate as substrate decreased from an upper limiting value of 0.97 ± 0.04 at low pH to a lower limiting value of 0.63 ± 0.06 at high pH[6]. The pK_a values seen in the pH profiles of k_{cat}/K_{ENate} with ethylnitronate and 1-[^{2}H]-ethylnitronate were 7.8 ± 0.2 and 8.0 ± 0.2,

---

[6] Instability of the enzyme at pH values above 10 prevented an accurate determination of the kinetic parameters at high pH. While the available kinetic data clearly indicate the presence of a group that needs to be unprotonated for catalysis with nitroethane and 1,1-[^{2}H$_2$]-nitroethane as substrate, with pK_a value of 9.3 or higher, the lack of kinetic data above pH 10 did not allow for an accurate determination of the pK_a value for the group that must be protonated for catalysis.

respectively, for an amino acid group that needs to be protonated for catalysis (Figure 3B).

Table 4.2 Solvent Viscosity Effects on the Kinetic Parameters of 2-Nitropropane Dioxygenase

kinetic parameter	substrate	viscosity effect (%)[b]	standard error (%)
k_{cat}	nitroethane	0.0	0.3
k_{cat}/K_m	nitroethane	0.1	0.6
k_{cat}	ethylnitronate	2.3	0.4
k_{cat}/K_m	ethylnitronate	-0.4	0.2

[a]Enzymatic activity was measured in 50 mM sodium pyrophosphate in the absence and presence of glycerol at pH 10 (nitroethane) or pH 6.5 (ethylnitronate) at 30 °C. [b]Percent increase of the kinetic parameter in the absence of viscosigen per increase in relative viscosity. The data were fit with eq 7

Solvent Viscosity Effects. The effects of solvent viscosity on the kinetic parameters of 2-nitropropane dioxygenase with nitroethane as substrate were determined at pH 10, in order to establish whether the decreased $^D(k_{cat}/K_{NE})$ value at this pH was the result of slow substrate binding. As shown in Figure 4, increasing the viscosity of the reaction mixture had no effect on the kinetic parameters with nitroethane. Similarly no effects of solvent viscosity were observed on the normalized k_{cat}/K_m and k_{cat} values with ethylnitronate at pH 6.5 (Figure 4), at which $^D(k_{cat}/K_{ENate})$ values near unity were observed with this substrate. Table 2 summarizes the effects of *so*lvent viscosity on the kinetic parameters of the enzyme.
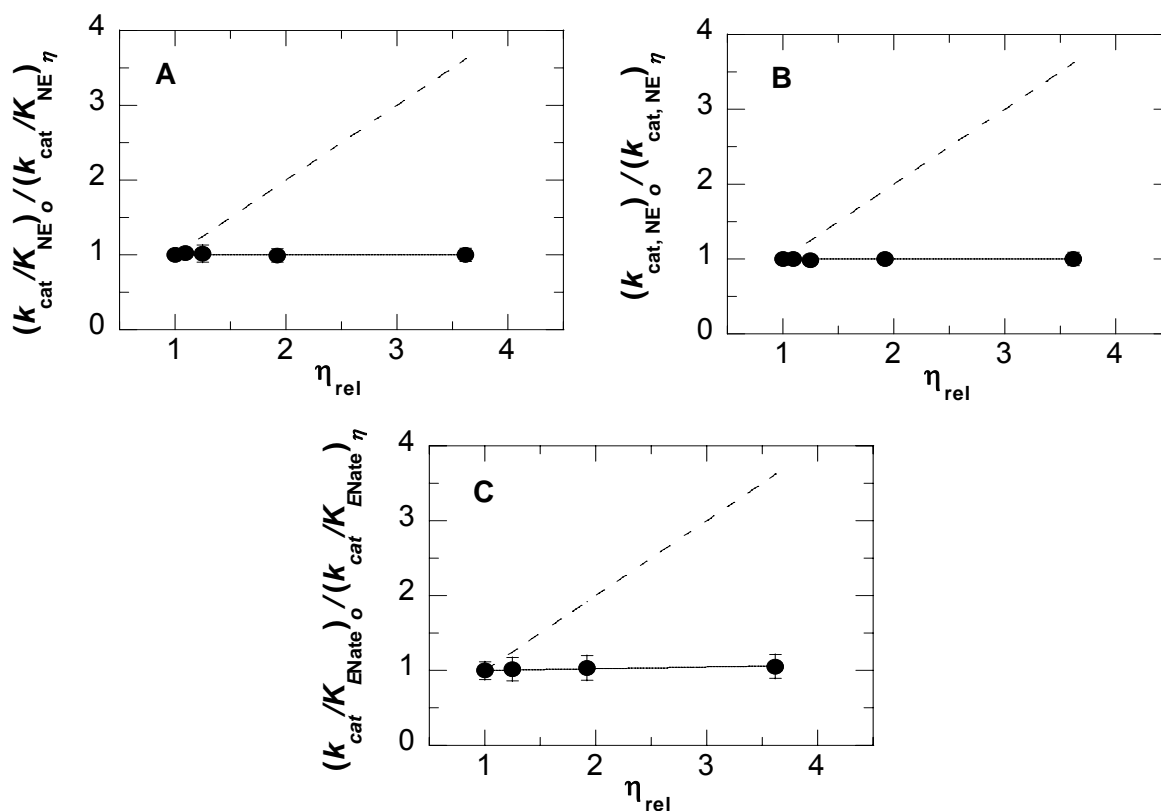
Figure 4.4 Solvent viscosity effects on the kinetic parameters of 2-nitropropane. dioxygenase. Panel A: Effect on k_{cat}/K_{NE} with nitroethane as substrate at pH 10. Panel B: Effect on $k_{cat,\,NE}$ with nitroethane as substrate at pH 10. Panel C: Effect on k_{cat}/K_{ENate} with ethylnitronate as substrate at pH 6.5. Panel D: Effect on $k_{cat,\,ENate}$ with ethylnitronate as substrate at pH 6.5. The solid lines are fits of experimental data with eq 7. The dashed lines represent a case in which the reaction is diffusion controlled. The values of the relative viscosity at 30 °C were calculated from the values at 20 °C reported by Lide (*18*). Enzymatic activity was measured in 50 mM sodium pyrophosphate at 30 °C.

pH Dependence of m-Nitrobenzoate Inhibition. A survey of a number of compounds established that *m*-nitrobenzoate was a competitive inhibitor with respect to ethylnitronate as substrate for 2-nitropropane dioxygenase (Figure 5A), with a K_{is} value of 9 ± 1 mM at pH 7.4 and 30 °C. In order to establish a thermodynamic pK_a for a group within the active site of the enzyme (*20*), the pH dependence of the inhibition by *m*-nitrobenzoate was determined at atmospheric oxygen with ethylnitronate at 30 °C. As shown in Figure 5B, a plot of K_{is} versus pH revealed a pK_a of 7.6 ± 0.1 for a group that needs to be protonated for inhibition.
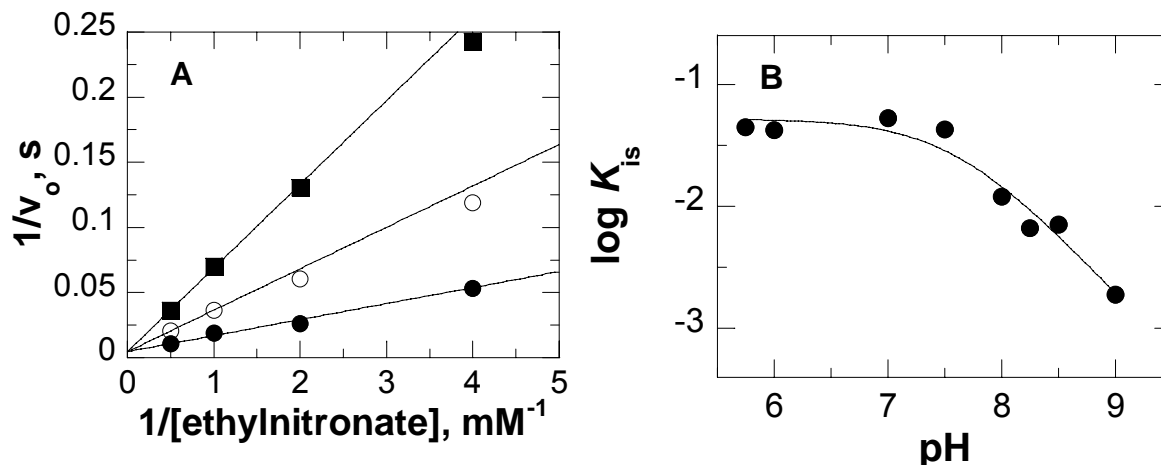
Figure 4.5 Inhibition of 2-nitropropane dioxygenase by *m*-nitrobenzoate with respect to ethylnitronate as substrate.
Panel A: Enzymatic activity was measured in air saturated 50 mM potassium phosphate pH 6 at 30 °C by varying concentrations of ethylnitronate in the presence of 0 mM (•); 38 mM (o) and 100 mM (■) *m*-nitrobenzoate. The data were fit with eq 3. Panel B: pH Dependence of *m*-nitrobenzoate inhibition. The data were fit to eq 6.

4.5   Discussion

The mechanistic data presented in this study, along with the results of a recent kinetic investigation (*1*), are consistent with 2-nitropropane dioxygenase being a catalyst for both the oxidative denitrification of nitroalkanes and nitronates to the corresponding carbonyl compounds, and for the non-oxidative tautomerization between their anionic and neutral forms. In the oxidative denitrification pathway with nitroethane as substrate (Scheme 4), after formation of an oxidized enzyme-nitroalkane complex (k_1), catalysis is initiated by the removal of a proton from the substrate α-carbon by an active site base (k_3), which is likely His196 based on the crystal structure of the enzyme from *P. aeruginosa (16)*, yielding an enzyme-bound alkyl nitronate. After partial reduction of the enzyme-bound flavin through a single electron transfer from the alkyl nitronate (k_5), the resulting anionic flavosemiquinone reacts with molecular oxygen to form superoxide

anion. The resulting superoxide anion then reacts with the nitro radical to yield a nitroperoxide anion species, which will simultaneously, or perhaps subsequently, be protonated in an acid-catalyzed reaction (k_9). The resulting peroxynitroethane is then released from the active site of the enzyme (k_{11}) and undergoes a nucleophilic attack, presumably in a non-enzymatic fashion, yielding nitrite and acetaldehyde. The oxidative pathway with ethylnitronate as substrate proceeds in a similar fashion as that with nitroethane except that the initial proton abstraction step is excluded. In the non-oxidative tautomerization pathway with ethylnitronate, after the formation of the enzyme substrate complex (k_{13}), the enzyme-bound anionic substrate is protonated in the active site of the enzyme to form nitroethane (k_4), which is then released to the solvent (k_2). A similar nitro-aci tautomerization probably occurs with nitroethane, in which after formation of the oxidized enzyme-nitroethane Michaelis complex (k_1) and the subsequent deprotonation of the neutral substrate (k_3), the resulting ethylnitronate dissociates from the active site of the enzyme (k_{14}) completing the catalytic cycle[7]. In the branched mechanisms of Scheme 4, the k_{cat}/K_m values for nitroethane and ethylnitronate when the enzyme is saturated with oxygen are given by eqs 10 and 11, respectively.

$$\frac{k_{cat}}{K_{NE}} = \frac{k_1 k_3 k_5}{k_2(k_4 + k_{14})} \tag{10}$$

$$\frac{k_{cat}}{K_{ENate}} = \frac{k_5 k_{13}}{k_4 + k_{14}} \tag{11}$$
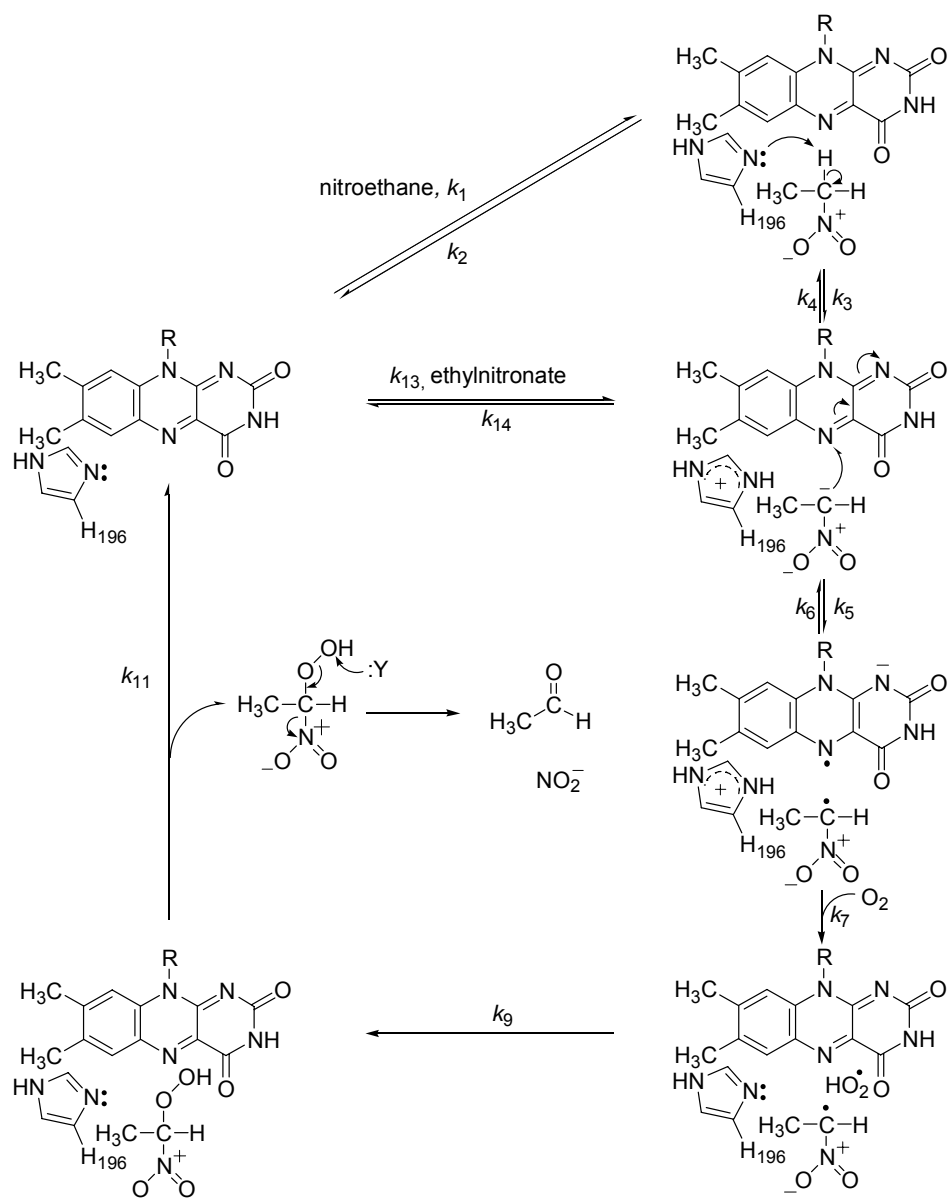
Scheme 4.4 Catalytic mechanism of 2-nitropropane dioxygenase with either nitroethane or ethylnitronate as substrate.

Evidence supporting the oxidative denitrification pathways with nitroethane and ethylnitronate was reported previously under conditions of *atmospheric concentration of oxygen* (*1*), and is substantiated by the results presented in this study at saturating concentration of oxygen. Briefly, an enzymic catalytic base with pK_a of ~7.5 was observed in the pH profiles of the k_{cat}/K_m and k_{cat} values with nitroethane and nitrobutane,

but not in the pH profiles with their corresponding alkyl nitrates (*1*). Formation of an anionic flavosemiquinone that subsequently reacts with oxygen was suggested by enzyme-monitored turnover experiments with ethylnitronate and static anaerobic reductions of the enzyme with nitroethane or ethylnitronate (*1*). This conclusion is further supported by the stopped-flow data on the reductive half-reaction with ethylnitronate presented in this study, showing that the anionic flavosemiquinone forms during catalysis upon a single electron transfer from the enzyme-bound anionic nitronate. The participation of a protonated group in the formation of superoxide anion was suggested by pH profiles of the k_{cat}/K_m and k_{cat} values *at sub-saturating concentrations of oxygen* with nitroethane, nitrobutane, ethylnitronate, and butyl-1-nitronate, showing the requirement for a protonated group for catalysis (*1*). Formation of superoxide was suggested by the effect of superoxide dismutase on the rate of oxygen consumption when propyl nitronates were used as substrate[8] (*1*). Finally, the radical recombination between the superoxide and nitroalkane radicals to form peroxynitroethane was suggested by an inverse α-secondary kinetic isotope effect of ~0.76 on the k_{cat}/K_m value with 1-[^{2}H]-ethylnitronate as substrate determined at pH 8 and *atmospheric oxygen*, which was interpreted as resulting from the change in the hybridization of the α-carbon of the nitroalkane radical from sp^2 to sp^3 (*1*).

Evidence supporting the tautomerization pathway with ethylnitronate comes from the results presented in this study, showing an inverse α-secondary kinetic isotope effect on the k_{cat}/K_m value with 1-[^{2}H]-ethylnitronate at high pH and, most importantly, at *saturating concentration of oxygen*. The latter condition results in the kinetic step k_5 being irreversible, since the radical pair formed by the flavosemiquinone and the

nitroalkane radical does not accumulate at saturating oxygen. Consequently, the subsequent formation of peroxynitroethane cannot contribute to the k_{cat}/K_m value (*21*) when the enzyme is saturated with oxygen, ruling out the assignment of the inverse α-secondary kinetic isotope effect on k_{cat}/K_m to this step. In the oxidative pathway with ethylnitronate there are no other kinetic steps involving a change in the hybridization of the substrate α-carbon from sp^2 to sp^3, suggesting that the observed inverse α-secondary kinetic isotope effect must arise from the conversion of ethylnitronate to nitroethane within the active site of the enzyme. In this respect, 2-nitropropane dioxygenase is similar to another FMN-dependent enzyme, old yellow enzyme, which was previously shown to catalyze a non-oxidative tautomerization of nitroalkanes in the NADPH-linked reduction of nitro-olefins (*22*).

In the reactions catalyzed by 2-nitropropane dioxygenase, substrate binding and product release occur in rapid equilibrium, as suggested by the lack of solvent viscosity effects on the kinetic parameters with nitroethane or ethylnitronate as substrate. Indeed, the lack of viscosity effects on the k_{cat}/K_{NE} and k_{cat}/K_{ENate} values suggests that dissociation of the substrate from the oxidized enzyme-substrate complex is significantly faster than the rate of chemical steps occurring within enzyme-substrate complexes belonging to k_{cat}/K_m, i.e., that k_2 and k_{14} are significantly larger than k_3 and k_5 with nitroethane and ethylnitronate, respectively. This establishes these substrates as non-sticky (*20*), with the important mechanistic implication that any observed decrease in the primary and α-secondary kinetic isotope effects on the k_{cat}/K_m values with nitroethane and ethylnitronate must necessarily be ascribed to some chemical steps occurring within enzyme-substrate complexes that contribute to k_{cat}/K_m rather than to substrate binding (*vide infra*).

Similarly, the lack of solvent viscosity effects on the k_{cat} values with nitroethane and ethylnitronate establishes the products of the reactions of oxidation and tautomerization with these substrates as non-sticky (*20*).

Removal of the proton from the α-carbon of nitroethane (k_3) is fully rate limiting for catalysis at low pH, but it is kinetically masked at high pH by the reverse commitment to catalysis ($C_{r(3)}$), which reflects the net flux of the enzyme-bound intermediates through the reverse of the kinetic step k_3. Evidence supporting this conclusion comes from the pH dependence of the $^D(k_{cat}/K_{NE})$ value with 1,1-[$^2H_2$]-nitroethane as substrate, which decreases between limiting values with increasing pH. The magnitude of the limiting $^D(k_{cat}/K_{NE})$ value at low pH, with a value of ~7.4 that agrees fairly well with the reported value of ~8.5 for the kinetic isotope effect for deprotonation of nitroethane in solution (*23*), is consistent with cleavage of the CH bond of nitroethane being fully rate limiting for catalysis at low pH. The limiting $^D(k_{cat}/K_{NE})$ value of ~3.5 seen at high pH implies that some kinetic steps belonging to k_{cat}/K_{NE} other than CH bond cleavage become partially rate limiting with increasing pH (*20*). Lack of solvent viscosity effects on the k_{cat}/K_{NE} value with nitroethane at pH 10 suggests that nitroethane binding occurs in rapid equilibrium, i.e., with $k_2 \gg k_3$. Similarly, lack of solvent viscosity effects on the $k_{cat, NE}$ value is consistent with release of the ethylnitronate possibly formed in the tautomerization reaction of nitroethane occurring in rapid equilibrium, i.e., with $k_{14} \gg k_3$. These data immediately rule out an external forward commitment to catalysis due to substrate binding[7], which with nitroethane is given by $k_3/(k_2+k_{14})$, as being responsible for the decreased $^D(k_{cat}/K_{NE})$ value (*20*). This, in turn, will abate any internal forward commitment to catalysis possibly arising from $k_5 \gg k_4$. Thus, as illustrated in eq 12, the

decrease in the $^D(k_{cat}/K_{NE})$ value at high pH must necessarily arise from an increase in the $C_{r(3)}$ value. Consistent with this conclusion, a ~0.3 pH units increase of the apparent pK_a value was seen in the k_{cat}/K_{NE} pH-profiles for the group that acts as a base upon substituting nitroethane with $1,1-[^2H_2]$-nitroethane. This is the expected result since substitution of nitroethane with a slower substrate such as $1,1-[^2H_2]$-nitroethane, for which CD bond cleavage is ~7.5-times slower than CH bond cleavage, will (at least partially) abate the perturbation of the kinetic pK_a value for the base seen in the k_{cat}/K_{NE} pH-profiles, as illustrated in eq 13 (20).

$$^D\left(\frac{k_{cat}}{K_{NE}}\right) = \frac{^Dk_3 + {}^DEqC_{r(3)}}{1 + C_{r(3)}} \tag{12}$$

$$\Delta pK_a = log(1 + C_{r(3)}) \tag{13}$$

Formation of the anionic flavosemiquinone (k_5) is facilitated by a protonated group in the active site of the enzyme with a pK_a value of ~7.6 that acts as an electrostatic catalyst, as suggested by the pH profiles of the k_{cat}/K_{ENate} values and of m-nitrobenzoate inhibition. Since pK_a values determined with competitive inhibitors reflect true equilibrium dissociation constants (20), the observation that the pK_a value of ~7.8 seen in the k_{cat}/K_{ENate} pH-profile is not significantly different from the pK_a value of ~7.6 observed with the competitive inhibitor m-nitrobenzoate establishes the latter value as the thermodynamic pK_a value for the active site group that needs to be protonated for catalysis. The recent elucidation of the three-dimensional structure of 2-nitropropane dioxygenase from *P. aeruginosa* shows that the only ionizable group in the active site of the enzyme is a histidine residue (16), corresponding to His196 of the enzyme from *N. crassa*. Thus, it is likely that the pK_a value seen in the pH profiles is that of His196.

With ethylnitronate, the non-oxidative tautomerization of the anionic substrate to nitroethane (via the steps k_{13}, k_4, and k_2) is fully rate limiting at high pH, but it is kinetically masked by the oxidative pathway at low pH. This conclusion is supported by the pH dependence of the α-secondary kinetic isotope effects on the k_{cat}/K_m value with 1-[^{2}H]-ethylnitronate as substrate, which is assigned to the non-oxidative conversion of ethylnitronate to nitroethane (k_4) when the enzyme is saturated with oxygen (*see above*). The inverse kinetic isotope effect with a limiting value of ~0.6 at high pH is consistent with the kinetic step in which the α-carbon of ethylnitronate is converted from sp^2 to sp^3 being slower than other kinetic steps belonging to the oxidative pathway with ethylnitronate. This is the expected result because at high pH the effective concentration of the active site group acting as an acid for protonation of ethylnitronate is low, yielding a significant decrease in the net flux of intermediates through the kinetic step k_4. As the pH progressively decreases, the $^D(k_{cat}/K_{ENate})$ becomes fully masked by some other kinetic step(s) belonging to the oxidative pathway that are included in the k_{cat}/K_m value. According to eq 11, k_{cat}/K_{ENate} includes substrate binding (k_{13}), flavin reduction (k_5) and both the tautomerization (k_4) and release (k_{14}) of ethylnitronate. The lack of solvent viscosity effects with ethylnitronate as substrate at low pH immediately rules out substrate binding and release as being slow, suggesting that the non-oxidative conversion of ethylnitronate to nitroethane is masked by the kinetic step in which an electron is transferred from the enzyme-bound ethylnitronate to the flavin (k_5).

Multiple catalytic strategies exist for the oxidation of nitroalkanes by flavin dependent enzymes as can be seen from a comparison of 2-nitropropane dioxygenase with the well characterized nitroalkane oxidase (for a review see (*24*)). The crystal

structures of both enzymes have been recently solved (*16, 25*) and a wealth of mechanistic data is now available (*1, 19*). Both enzymes initiate the oxidation of neutral nitroalkanes through a base catalyzed proton abstraction from the α-carbon of the substrate. Crystallographic data of 2-nitropropane dioxygenase from *P. aeruginosa* suggest that a hisidine, corresponding to His196 in the enzyme from *N. crassa*, is the catalytic base (*16*). Consistent with this proposed role, upon replacing His196 with alanine the enzyme completely loses the ability of oxidizing nitroethane but not ethylnitronate (Merid Belaineh and Giovanni Gadda; unpublished observations). The corresponding residue in nitroalkane oxidase is an aspartate residue, which has been shown to serve as the catalytic base in crystallographic and mutagenesis studies (*25-27*). Upon generation of the anionic form of substrate the catalytic strategies employed by the two enzymes diverge. As shown in this and previous studies (*1*), the flavin of 2-nitropropane dioxygenase reacts with the anionic substrate to generate an anionic flavosemiquinone. On the other hand, nitroalkane oxidase does not generate an observable flavosemiquinone, but instead forms a flavin N(5) adduct as evident from trapping experiments with cyanide (*28*). Prior to flavin reduction in 2-nitropropane dioxygenase a ternary complex forms between the enzyme, the substrate radical and oxygen. Oxygen then reacts with the flavin semiquinone generating a superoxide anion that combines with the substrate radical generating a peroxynitroalkane species that decays to give the product. Nitroalkane oxidase does not form a ternary complex with oxygen as suggested by its ping-pong steady state mechanism (*29*); rather, flavin reduction is followed by expulsion of nitrite to generate a cationic imine that undergoes a nucleophilic attack to ultimately generate the product (*19*). Thus, the major difference

between 2-nitropropane dioxygenase and nitroalkane oxidase is the formation of an observable flavosemiquinone versus a flavin N(5) adduct.

In conclusion, the results of the steady state investigation with solvent, pH, and substrate kinetic isotope effects presented herein have provided further mechanistic insights on the chemical mechanism for the oxidation of nitroethane and ethylnitronate catalyzed by 2-nitropropane dioxygenase. The enzyme catalyzes both the oxidative denitrification of nitroalkanes and nitronates to the corresponding carbonyl compounds and the non-oxidative tautomerization between their anionic and neutral forms. During enzymatic turnover with neutral substrates, the rate of oxidative denitrification of nitroalkanes is limited by the cleavage of the substrate CH bond at low pH and by the formation of flavosemiquinone at high pH. With anionic substrates, the non-oxidative protonation of nitronates to yield the corresponding nitroalkanes limits enzymatic turnover at high pH. These results provide a firm groundwork for future mechanistic studies aimed at the elucidation of the contribution of quantum mechanical tunneling in the cleavage of the CH bond of nitroethane and of the mechanism of oxygen activation to form superoxide.

4.6   Acknowledgments

4.7 Supporting Information

1. k_{cat}/K_m Expression with Nitroethane as Substrate With Branched Pathways

(Both Oxidative Denitrification and Non-Oxidative Tautomerization)

Applying the method of King and Altman [Altman C. (1956) *J. Phys. Chem.* 60, 1375-1378] to the branched mechanism of Scheme 4 when *oxygen is saturating* gives the initial rate equation of:

$$\frac{v_o}{e} = \frac{AO_2 k_1 k_3 k_5 k_7 k_9 k_{11}}{\begin{aligned}&A(k_1 k_3 k_5 k_9 k_{11} + k_1 k_3 k_6 k_9 k_{11} + k_1 k_4 k_6 k_9 k_{11} + k_1 k_6 k_9 k_{11} k_{14}) + O_2(k_2 k_4 k_7 k_9 k_{11}\\&+ k_2 k_5 k_7 k_9 k_{11} + k_2 k_7 k_9 k_{11} k_{14} + k_3 k_5 k_7 k_9 k_{11} + k_3 k_7 k_9 k_{11} k_{14}) + AO_2(k_1 k_3 k_5 k_7 k_{11}\\&+ k_1 k_3 k_7 k_9 k_{11} + k_1 k_4 k_7 k_9 k_{11} + k_1 k_5 k_7 k_9 k_{11} + k_1 k_7 k_9 k_{11} k_{14}) + k_2 k_4 k_6 k_9 k_{11} + k_2 k_6 k_9 k_{11} k_{14}\\&k_3 k_6 k_9 k_{11} k_{14}\end{aligned}}$$

Where A = [Nitroethane].

The k_{cat}/K_{NE} value for nitroethane is therefore given by:

$$\frac{k_{cat}}{K_{NE}} = \frac{k_1 k_3 k_5 k_7 k_9 k_{11}}{k_2 k_4 k_7 k_9 k_{11} + k_2 k_5 k_7 k_9 k_{11} + k_2 k_7 k_9 k_{11} k_{14} + k_3 k_5 k_7 k_9 k_{11} + k_3 k_7 k_9 k_{11} k_{14}}$$

or,

$$\frac{k_{cat}}{K_{NE}} = \frac{k_1 k_3 k_5}{k_2 k_4 + k_2 k_5 + k_2 k_{14} + k_3 k_5 + k_3 k_{14}}$$

Grouping k_5 and k_{14} in the denominator gives:

$$\frac{k_{cat}}{K_{NE}} = \frac{k_1 k_3 k_5}{k_2 k_4 + k_2(k_5 + k_{14}) + k_3(k_5 + k_{14})}$$

Since based on solvent viscosity effects $k_{14} \gg k_5$ then:

$$\frac{k_{cat}}{K_{NE}} = \frac{k_1 k_3 k_5}{k_2 k_4 + k_2 k_{14} + k_3 k_{14}}$$

Grouping k_2 and k_3 in the denominator gives:

$$\frac{k_{cat}}{K_{NE}} = \frac{k_1 k_3 k_5}{k_2 k_4 + k_{14}(k_2 + k_3)}$$

Since based on solvent viscosity effects $k_2 \gg k_3$ then:

$$\frac{k_{cat}}{K_{NE}} = \frac{k_1 k_3 k_5}{k_2 k_4 + k_2 k_{14}}$$

or, as described in the text:

$$\frac{k_{cat}}{K_{NE}} = \frac{k_1 k_3 k_5}{k_2 (k_4 + k_{14})}$$

2. k_{cat}/K_m Expression with Ethylnitronate as Substrate With Branched Pathways (Both Oxidative Denitrification and Non-Oxidative Tautomerization)

For the branched mechanism of Scheme 4 at *saturating [oxygen]*, the initial rate equation is:

$$\frac{v_o}{e} = \frac{AO_2 k_2 k_5 k_7 k_9 k_{11} k_{13} + AO_2 k_3 k_5 k_7 k_9 k_{11} k_{13}}{\begin{array}{l} A(k_2 k_5 k_9 k_{11} k_{13} + k_2 k_6 k_9 k_{11} k_{13} + k_3 k_5 k_9 k_{11} k_{13} + k_3 k_6 k_9 k_{11} k_{13} + k_6 k_9 k_{11} k_{13} k_{14}) \\ + O_2(k_2 k_4 k_7 k_9 k_{11} + k_2 k_5 k_7 k_9 k_{11} + k_2 k_7 k_9 k_{11} k_{14} + k_3 k_5 k_7 k_9 k_{11} + k_3 k_7 k_9 k_{11} k_{14}) \\ + AO_2(k_2 k_5 k_7 k_9 k_{13} + k_2 k_5 k_7 k_{11} k_{13} + k_2 k_7 k_9 k_{11} k_{13} + k_3 k_5 k_7 k_9 k_{13} + k_3 k_5 k_7 k_{11} k_{13} \\ k_3 k_7 k_9 k_{11} k_{13} + k_7 k_9 k_{11} k_{13} k_{14}) + k_2 k_4 k_5 k_9 k_{11} + k_2 k_6 k_9 k_{11} k_{14} + k_3 k_6 k_9 k_{11} k_{14}) \end{array}}$$

where A = [Ethylnitronate].

The k_{cat}/K_{ENate} value for ethylnitronate is therefore given by:

$$\frac{k_{cat}}{K_{ENate}} = \frac{k_2 k_5 k_7 k_9 k_{11} k_{13} + k_3 k_5 k_7 k_9 k_{11} k_{13}}{k_2 k_4 k_7 k_9 k_{11} + k_2 k_5 k_7 k_9 k_{11} + k_3 k_5 k_7 k_9 k_{11} + k_2 k_7 k_9 k_{11} k_{14} + k_3 k_7 k_9 k_{11} k_{14}}$$

or:

$$\frac{k_{cat}}{K_{ENate}} = \frac{k_2 k_5 k_{13} + k_3 k_5 k_{13}}{k_2 k_4 + k_2 k_5 + k_3 k_5 + k_2 k_{14} + k_3 k_{14}}$$

Grouping k_2 and k_3 in the numerator and denominator gives:

$$\frac{k_{cat}}{K_{ENate}} = \frac{k_5 k_{13}(k_2 + k_3)}{k_2 k_4 + k_5(k_2 + k_3) + k_{14}(k_2 + k_3)}$$

Since based on solvent viscosity effects $k_2 \gg k_3$ then:

$$\frac{k_{cat}}{K_{ENate}} = \frac{k_2 k_5 k_{13}}{k_2 k_4 + k_2 k_5 + k_2 k_{14}}$$

Grouping k_5 and k_{14} in the denominator gives:

$$\frac{k_{cat}}{K_{ENate}} = \frac{k_2 k_5 k_{13}}{k_2 k_4 + k_2(k_5 + k_{14})}$$

Since based on solvent viscosity effects $k_{14} \gg k_5$ then:

$$\frac{k_{cat}}{K_{ENate}} = \frac{k_2 k_5 k_{13}}{k_2 k_4 + k_2 k_{14}}$$

or, as described in the text:

$$\frac{k_{cat}}{K_{ENate}} = \frac{k_5 k_{13}}{k_4 + k_{14}}$$

4.8   References

(1)   Francis, K., Russell, B., and Gadda, G. (2005) Involvement of a flavosemiquinone in the enzymatic oxidation of nitroalkanes catalyzed by 2-nitropropane dioxygenase. *J. Biol. Chem. 280*, 5195-204.

(2)   Porter, D. J., Voet, J. G., and Bright, H. J. (1973) Direct evidence for carbanions and covalent N 5 -flavin-carbanion adducts as catalytic intermediates in the oxidation of nitroethane by D-amino acid oxidase. *J. Biol. Chem. 248*, 4400-16.

(3)   Porter, D. J., and Bright, H. J. (1983) The mechanism of oxidation of nitroalkanes by horseradish peroxidase. *J. Biol. Chem. 258*, 9913-24.

(4)   Porter, D. J., and Bright, H. J. (1977) Mechanism of oxidation of nitroethane by glucose oxidase. *J. Biol. Chem. 252*, 4361-70.

(5)   Porter, D. J., and Bright, H. J. (1987) Propionate-3-nitronate oxidase from *Penicillium atrovenetum* is a flavoprotein which initiates the autoxidation of its substrate by O_2. *J. Biol. Chem. 262*, 14428-34.

(6)   Gadda, G., and Fitzpatrick, P. F. (1999) Substrate specificity of a nitroalkane-oxidizing enzyme. *Arch. Biochem. Biophys. 363*, 309-13.

(7)   Gorlatova, N., Tchorzewski, M., Kurihara, T., Soda, K., and Esaki, N. (1998) Purification, characterization, and mechanism of a flavin mononucleotide-dependent 2-nitropropane dioxygenase from *Neurospora crassa. Appl. Environ. Microbiol. 64*, 1029-33.

(8)   Hanessian, S., and Pham, V. (2000) Catalytic asymmetric conjugate addition of nitroalkanes to cycloalkenones. *Org. Lett. 2*, 2975-8.

(9)   Ballini, R., Barboni, L., and Giarlo, G. (2003) Nitroalkanes in aqueous medium as an efficient and eco-friendly source for the one-pot synthesis of 1,4-diketones, 1,4-diols, delta-nitroalkanols, and hydroxytetrahydrofurans. *J. Org. Chem. 68*, 9173-6.

(10)   Fiala, E. S., Czerniak, R., Castonguay, A., Conaway, C. C., and Rivenson, A. (1987) Assay of 1-nitropropane, 2-nitropropane, 1-azoxypropane and 2-azoxypropane for carcinogenicity by gavage in Sprague-Dawley rats. *Carcinogenesis 8*, 1947-9.

(11)   Conaway, C. C., Nie, G., Hussain, N. S., and Fiala, E. S. (1991) Comparison of oxidative damage to rat liver DNA and RNA by primary nitroalkanes, secondary nitroalkanes, cyclopentanone oxime, and related compounds. *Cancer Res. 51*, 3143-7.

(12)   Dayal, R., Gescher, A., Harpur, E. S., Pratt, I., and Chipman, J. K. (1989) Comparison of the hepatotoxicity in mice and the mutagenicity of three nitroalkanes. *Fundam. Appl. Toxicol. 13*, 341-8.

(13)   Lewis, T. R., Ulrich, C. E., and Busey, W. M. (1979) Subchronic inhalation toxicity of nitromethane and 2-nitropropane. *J. Environ. Pathol. Toxicol. 2*, 233-49.

(14)   Haas-Jobelius, M., Coulston, F., and Korte, F. (1992) Effects of short-term inhalation exposure to 1-nitropropane and 2-nitropropane on rat liver enzymes. *Ecotoxicol. Environ. Saf. 23*, 253-9.

(15)   Sakano, K., Oikawa, S., Murata, M., Hiraku, Y., Kojima, N., and Kawanishi, S. (2001) Mechanism of metal-mediated DNA damage induced by metabolites of carcinogenic 2-nitropropane. *Mutat. Res. 479*, 101-11.

(16)   Ha, J. Y., Min, J. Y., Lee, S. K., Kim, H. S., Kim do, J., Kim, K. H., Lee, H. H., Kim, H. K., Yoon, H. J., and Suh, S. W. (2006) Crystal structure of 2-nitropropane dioxygenase complexed with FMN and substrate. Identification of the catalytic base. *J. Biol. Chem. 281*, 18660-7.

(17)   Allison, R. D., and Purich, D. L. (1979) Practical considerations in the design of initial velocity enzyme rate assays. *Methods Enzymol. 63*, 3-22.

(18)   Lide, D. R. (2000) *Handbook of Chemistry and Physics*, Vol. 2000-2001 ed, 6 ed., CRC Press, Boca Raton, Fl.

(19)   Gadda, G., and Fitzpatrick, P. F. (2000) Mechanism of nitroalkane oxidase: 2. pH and kinetic isotope effects. *Biochemistry 39*, 1406-10.

(20)   Cleland, W. W. (1982) The use of pH studies to determine chemical mechanisms of enzyme-catalyzed reactions. *Methods Enzymol. 87*, 390-405.

(21)   Cleland, W. W. (1975) Partition analysis and the concept of net rate constants as tools in enzyme kinetics. *Biochemistry 14*, 3220-4.

(22)   Meah, Y., and Massey, V. (2000) Old yellow enzyme: stepwise reduction of nitro-olefins and catalysis of aci-nitro tautomerization. *Proc. Natl. Acad. Sci. U. S. A. 97*, 10733-8.

(23)   Gadda, G., Choe, D. Y., and Fitzpatrick, P. F. (2000) Use of pH and kinetic isotope effects to dissect the effects of substrate size on binding and catalysis by nitroalkane oxidase. *Arch. Biochem. Biophys. 382*, 138-44.

(24)   Fitzpatrick, P. F., Orville, A. M., Nagpal, A., and Valley, M. P. (2005) Nitroalkane oxidase, a carbanion-forming flavoprotein homologous to acyl-CoA dehydrogenase. *Arch. Biochem. Biophys. 433*, 157-65.

(25)   Nagpal, A., Valley, M. P., Fitzpatrick, P. F., and Orville, A. M. (2006) Crystal structures of nitroalkane oxidase: insights into the reaction mechanism from a covalent complex of the flavoenzyme trapped during turnover. *Biochemistry 45*, 1138-50.

(26)   Valley, M. P., and Fitzpatrick, P. F. (2003) Inactivation of nitroalkane oxidase upon mutation of the active site base and rescue with a deprotonated substrate. *J. Am. Chem. Soc. 125*, 8738-9.

(27)   Valley, M. P., and Fitzpatrick, P. F. (2003) Reductive half-reaction of nitroalkane oxidase: effect of mutation of the active site aspartate to glutamate. *Biochemistry 42*, 5850-6.

(28)   Valley, M. P., Tichy, S. E., and Fitzpatrick, P. F. (2005) Establishing the kinetic competency of the cationic imine intermediate in nitroalkane oxidase. *J. Am. Chem. Soc. 127*, 2062-6.

(29)   Gadda, G., and Fitzpatrick, P. F. (2000) Iso-mechanism of nitroalkane oxidase: 1. Inhibition studies and activation by imidazole. *Biochemistry 39*, 1400-5.

(30)   Valley, M. P., and Fitzpatrick, P. F. (2004) Comparison of enzymatic and non-enzymatic nitroethane anion formation: thermodynamics and contribution of tunneling. *J. Am. Chem. Soc. 126*, 6244-5.

(31)   Nielsen, A. T. (1969) Nitronic acids and esters, in *The Chemistry of the nitro and nitroso groups* (Feuer, H., Ed.) pp 349-486, Interscience Publishers, New York.

5   CHAPTER V

**THE   NON-OXIDATIVE   CONVERSION   OF   NITROETHANE   TO
ETHYLNITRONATE   IN   NEUROSPORA   CRASSA   2-NITROPROPANE
DIOXYGENASE IS CATALYZED BY HIS-196**

5.1   Abstract

The deprotonation of nitroethane catalyzed by *Neurospora crassa* 2-nitropropane dioxygenase was investigated by measuring the formation and release of ethylnitronate formed in turnover as a function of pH and through mutagenesis studies. Progress curves for the enzymatic reaction obtained by following the increase in absorbance at 228 nm over time were visibly non-linear, requiring a logarithmic approximation of the initial reaction rates for the determination of the kinetic parameters of the enzyme. The pH dependence of the second order rate constant k_{cat}/K_m with nitroethane as substrate implicates the presence of a group with a pK_a of 8.1 ± 0.1 that must be unprotonated for nitronate formation. Mutagenesis studies suggest that this group is histidine 196 as evident from the inability of a H196N variant form of the enzyme to catalyze the formation of ethylnitronate from nitroethane. Replacement of histidine 196 with asparagine resulted in a ~15 fold increase in the k_{cat}/K_m with ethylnitronate as compared to the wild-type, which results from the inability of the mutant enzyme to undergo non-oxidative turnover. The results presented herein are consistent with a branched catalytic mechanism for the enzyme in which the ethylnitronate intermediate formed from the

H196-catalyzed deprotonation of nitroethane partitions between release from the active site and oxidative denitrification to yield acetaldehyde and nitrite.

5.2   Introduction

A variety of enzymes have been shown to catalyze the oxidative denitrification of either (neutral) nitroalkanes or (anionic) nitronates to their corresponding aldehyde compounds and nitrite (*1-14*). These include 2-nitropropane dioxygenase (*1-6*) and nitroalkane oxidase (*8, 9*), both of which physiologically catalyze the reaction, as well as D-amino acid oxidase (*10*), glucose oxidase (*11*), propionate-3-nitronate oxidase (*12*), and horseradish peroxidase (*13*), all of which can utilize nitroalkanes in non-physiological reactions. While the catalytic mechanisms of these enzymes are diverse, they all involve the oxidation of an enzyme-bound form of nitronate during turnover. For nitroalkane oxidase and *Neurospora crassa* 2-nitropropane dioxygenase, which are the only two enzymes capable of effectively utilizing the neutral from of substrate in catalysis (*2, 3, 8, 9*), this oxidation reaction requires the generation of an enzyme-bound nitronate through the initial abstraction of a proton from the α-carbon of the nitroalkane substrate. The proton abstraction step in the nitroalkane oxidase reaction has been extensively characterized (*14-16*), where it has been shown through both mutagenesis and crystallographic studies to be catalyzed by an aspartate residue in the active site of the enzyme (i.e., Asp-402). The identity of the catalytic base in *N. crassa* 2-nitropropane dioxygenase has yet to be elucidated, although a conserved histidine residue has been proposed to be suitably positioned to deprotonate nitroalkanes in the x-ray crystallographic structure of the enzyme from *Pseudomonas aeruginosa* (*17*).

N. crassa 2-nitropropane dioxygenase is the only flavin-dependent enzyme reported to date with the ability to effectively utilize either neutral nitroalkanes or anionic nitronates as substrate in an oxidative denitrification reaction (*2, 3*). An anionic flavosemiquinone is transiently formed in both reactions from a single electron transfer reaction involving the enzyme-bound nitronate, either directly after the anionic substrate binds in the active site of the enzyme or upon deprotonation of the neutral substrate by a catalytic base in the active site of the enzyme (*2, 3*). Studies of the secondary kinetic isotope effects using 1-^{2}H-ethylnitronate as substrate have suggested that at pH ≤7.5 a significant fraction of the enzyme-bound anionic substrate is protonated in the active site of the enzyme to form nitroethane, which is then released to the solvent rather than undergoing oxidative denitrification (Scheme 1) (*3*). Based on the structural similarities between ethylnitronate and nitroethane, a similar partitioning has also been proposed for the ethylnitronate intermediate formed during the enzymatic turnover with nitroethane (*3*), although no direct evidence is available in support of such a hypothesis.
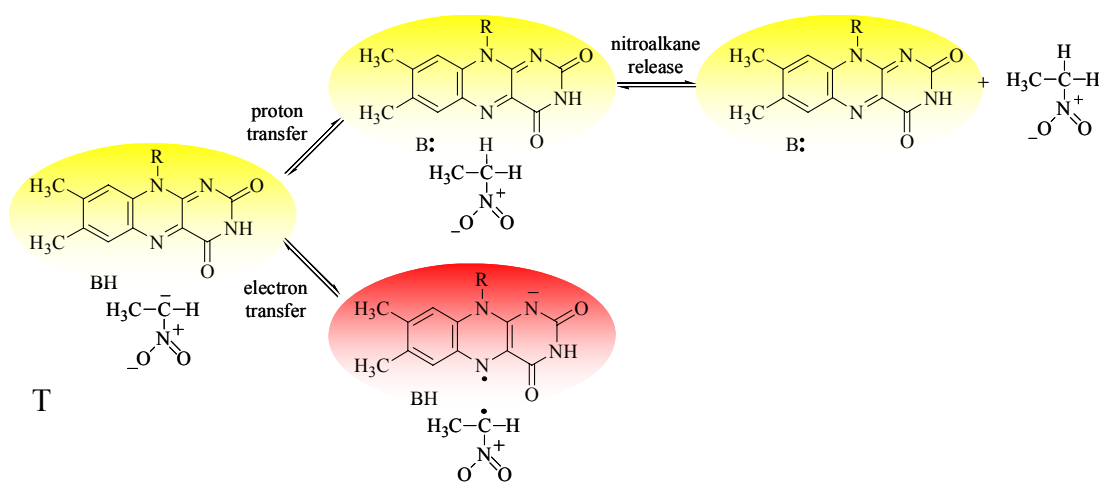
Scheme 5.1 Branching of the Michaelis complex formed during turnover of *N. crassa* 2-nitropropane dioxygenase with ethylnitronate as substrate.
Note that under initial velocity conditions in the absence of exogenous nitroethane the kinetic step of nitroalkane release is practically irreversible. For clarity, further conversion of the anionic flavosemiquinone enzyme through the oxidative denitrification pathway is not shown.

he current study was conducted with the dual purpose of testing the proposed role of the conserved histidine (i.e., His-196) in the deprotonation reaction of nitroethane catalyzed by *N. crassa* 2-nitropropane dioxygenase, and of evaluating whether a fraction of the resulting ethylnitronate is released from the active site of the enzyme rather than proceeding through oxidative catalysis. Towards these aims, a kinetic assay to monitor the time-dependent formation of ethylnitronate from nitroethane was developed for the wild-type *N. crassa* 2-nitropropane dioxygenase and was used to determine the effects of the replacement of histidine 196 with asparagine in the active site of the enzyme. The kinetic data presented herein are consistent with histidine 196 acting as a base in the deprotonation of nitroethane catalyzed by *N. crassa* 2-nitropropane dioxygenase, and with the (partial) release of the ethylnitronate that is formed enzymatically from nitroethane from the active site of the enzyme before oxidation of this intermediate occurs during turnover.

5.3   Experimental Procedures

Materials. Escherichia coli strain Rosetta(DE3)pLysS was from Novagen (Madison, WI). The QIAprep Spin Miniprep kit was from Qiagen (Valencia, CA) and the QuikChange Site-Directed Mutagenesis kit was from Stratagene (La Jolla, CA). Oligonucleotides used for site-directed mutagenesis and for sequencing of the mutant gene were from Sigma Genosys (The Woodlands, TX). Luria-Bertani agar and broth, ampicillin, phenylmethysulfonylfluoride (PMSF), lysozyme and nitroethane were from Sigma-Aldrich (St. Louis, MO). Isopropyl-*β*-D-thiogalactopyranoside (IPTG) was from Promega (Madison, WI). Ammonium sulfate and magnesium chloride were from ICN Biomedicals (Irvine, CA). EDTA was from Fisher Scientific, whereas DNase I and

RNase A were from Roche Biomedicals (Indianapolis, IN). The Hi-Prep 16/10 Octyl Fast

Flow column and the DEAE-Sepharose used in packing the DEAE column were from GE

Healthcare (Barrington, IL). All other reagents were of the highest purity commercially

available.

Expression and Purification of N. crassa 2-Nitropropane Dioxygenase. The

enzyme was obtained utilizing the protocol described previously (*2*) with the following

modifications. *E. coli* strain BL21(DE3) cells harboring plasmid pET/2NPDnc were used

to inoculate 6 x 1.25 L of Luria-Bertani broth containing 50 μg/mL ampicillin and the

cultures were incubated at 37 ^{o}C until an OD_{600} of 0.6 to 0.8 was reached, at which point

IPTG was added to a final concentration of 0.1 mM. After 6 h of induction at 37 ^{o}C, the

cells were harvested and treated in the same manner described previously (*2*).

Purification of *N. crassa* 2-nitropropane dioxygenase was achieved through a simplified

protocol involving a 70% ammonium sulfate fractionation step and a single anion

exchange chromatographic step as described previously (*2*), but at pH 7 to facilitate the

binding of the enzyme to the column. Fractions of the highest purity were pooled,

dialyzed against 50 mM potassium phosphate, pH 7.4, and stored at -20 ^{o}C until use. The

simplified procedure resulted in the obtainment of highly purified enzyme (>95%) as

judged by SDS-PAGE.

Preparation and Purification of N. crassa 2-Nitropropane Dioxygenase H196N.

A QuikChange kit was used to prepare a mutant form of *N. crassa* 2-nitropropane

dioxygenase in which histidine 196 was replaced with asparagine. The method used was

according to the manufacturer's instructions, using a pET/2NPDnc plasmid (*2*) as a

template, and the oligonucleotides For.H196N

(5'GGATCGATGCGGGAGGG<u>AAT</u>CAGCTTGCTACAGGG3') and Rev.H196N (5'CTCCCTGTAGCAAGCTG<u>ATT</u>CCCTCCCGCATCGATCCC3') as forward and reverse primers (underlined letters indicate the site of mutation). The DNA was then sequenced at the DNA Core Facility at Georgia State University using an Applied Biosystems Big Dye Kit on an Applied Biosystems model ABI 377 DNA Sequencer, which confirmed the presence of the mutant gene in the correct orientation. *E. coli* strain Rosetta(DE3)pLysS competent cells were transformed with plasmid pET/2NPDnc-H196N by electroporation and were stored at -80 ^{o}C as a 7% DMSO suspension.

 E. coli strain Rosetta(DE3)pLysS cells harboring plasmid pET/2NPDnc-H196N were used to inoculate 5 x 1.25 L of Luria-Bertani broth containing 50 μg/mL ampicillin plus 34 μg/mL chloramphenicol and the cultures were incubated at 37 ^{o}C until an OD_{600} of 0.6 to 0.8 was reached. The mutant enzyme was then expressed through induction with IPTG at a final concentration of 0.2 mM at 37 ^{o}C for 6 h. The cells were harvested by centrifugation and were suspended at pH 8 with four volumes of 1 mM EDTA, 100 mM NaCl, 1 mM PMSF, 0.2 mg/mL lysozyme, 20 μg/mL DNase I, 20 μg/mL RNase A and 10 mM $MgCl_2$, in 50 mM Tris-Cl and were incubated on ice for 30 min. After sonication and collection of the cell free extract by centrifugation for 20 min at 4 ^{o}C, the sample was brought to 60% ammonium sulfate saturation and was incubated on ice for 20 min. The supernatant collected after centrifugation was then loaded directly onto an Octyl Fast Flow column (3.5 x 20 cm) equilibrated with 2.75 M ammonium sulfate in 50 mM potassium phosphate containing 10% glycerol, pH 7.4, connected to an Åkta*prime* Amersham Biotech system (Barrington, IL). Protein elution was carried out with a linear gradient from 2.75 to 0 M ammonium sulfate over 500 mL at a flow rate of 2 mL/min.

Fractions of the highest purity were pooled, dialyzed against 5 mM potassium phosphate containing 10% glycerol, pH 7.4, and were loaded onto a DEAE Fast Flow column (4 x 30 cm) equilibrated with the same buffer. The column was eluted with a linear gradient from 0 to 500 mM ammonium sulfate developed over 1 L at a flow rate of 2 mL/min. Fractions of the highest purity were pooled, concentrated using polyethylene glycol 10,000, and dialyzed against 50 mM potassium phosphate at pH 7.4. The purified enzyme was stored at -20 $^{\circ}$C until use.

Spectrophotometric Studies. Stock solutions of nitroethane (100 mM) were prepared in water and were diluted to concentrations ranging from 0.1 to 1 mM. Absorbance spectra in the 200 to 300 nm region were recorded for each concentration of nitroethane at 30 $^{\circ}$C using a cuvette with a 1 cm path length on an Agilent Technologies diode-array spectrophotometer model HP 8453 (Santa Clara, CA). The molar extinction coefficient was determined from a plot of the absorbance at 202 nm versus concentration of nitroethane using the Lambert-Beer equation. The determination of the molar extinction coefficient of ethylnitronate at 228 nm was carried out in a similar manner using concentrations ranging from 10 to 100 μM. Ethylnitronate was prepared in water upon incubating a solution of nitroethane with a 1.2 molar excess of potassium hydroxide for at least 24 h at room temperature.

The UV-visible absorbance spectra recorded during the reductive half reaction of the wild-type and H196N variant forms of *N. crassa* 2-nitropropane dioxygenase with ethylnitronate as substrate were obtained using a TgK Scientific SF-61 stopped-flow spectrophotometer equipped with a photo-diode array detector. Spectra were recorded in 50 mM sodium pyrophosphate at pH 7 and 30 $^{\circ}$C after anaerobically mixing the enzyme

with ethylnitronate with final concentration of 10 µM and 0.5 mM, respectively. Anaerobic mixing of the enzyme with substrate was achieved using the method described previously (*3*).

Kinetic Studies. The kinetic parameters for the non-oxidative reaction catalyzed by *N. crassa* 2-nitropropane dioxygenase with nitroethane as substrate were determined by monitoring the increase in absorbance at 228 nm resulting from mixing the enzyme at a concentration of 1.07 µM in air-saturated 50 mM sodium pyrophosphate with substrate (in the concentration range from 1 to 3 mM). The pH dependence of the kinetic parameters was determined in the range from 6 to 10. The enzyme concentration used in the assays was expressed per enzyme-bound FMN content[1] using an $\varepsilon_{444\ nm}$ value of 11850 $M^{-1}cm^{-1}$ (*2*). The results reported are the averages of three independent measurements, which typically differed by ≤3%. Steady-state turnover of *N. crassa* 2-nitropropane dioxygenase (1.07 µM) with 3 mM nitroethane was also determined by monitoring oxygen consumption using a computer interfaced Oxy-32 oxygen monitoring system (Hansatech Instrument Ltd.), equipped with a thermostated water bath. Assays were carried out at pH 6, 8 and 10, and were allowed to proceed for at least 120 s after mixing the enzyme with substrate. The enzymatic activity of the H196N variant of 2-nitropropane dioxygenase with nitroethane or ethylnitronate as substrate was measured by monitoring oxygen consumption after mixing 2.17 µM enzyme with 1 mM substrate

---

[1] The choice of defining the enzymatic activity of *N. crassa* 2-nitropropane dioxygenase as a function of the FMN content of the protein stems from the observation that the non-oxidative turnover in which ethylnitronate is formed from nitroethane occurs only with the holoenzyme (Kevin Francis and Giovanni Gadda; unpublished observation). Expressing the enzymatic activity in terms of FMN content also corrects for any variation that may exist in the flavin to protein stoichiometry between different preparations of the wild-type and mutant enzymes.

in air-saturated 50 mM sodium pyrophosphate at pH 10. The kinetic parameters for the oxidative reactions of *N. crassa* 2-nitropropane dioxygenase and the H196N variant form the enzyme with ethylnitronate as substrate were determined in 50 mM sodium pyrophosphate containing 1% ethanol at pH 9.5 and 30 $^{\mathrm{o}}$C as previously described in (*3*). Substrate concentrations ranged from 1 to 50 mM, whereas enzyme concentrations were $\leq$110 nM.

Data Analysis. Kinetic data were fit using KaleidaGraph (Synergy Software, Reading, PA) or Enzfitter (Biosoft, Cambridge, UK) software. Initial rates for the non-enzymatic formation of ethylnitronate from nitroethane were determined from fits of the stopped-flow traces with eq 1, where A_{o} is the initial absorbance at 228 nm, k_{obs} is the pseudo-first order rate constant for the change in absorbance at 228 nm and t is time. The k_{obs} values were then converted into rates of product formation using the experimentally determined $\Delta\varepsilon_{228\ \mathrm{nm}}$ of 8,520 M^{-1}cm^{-1}, which corresponds to the difference between the extinction coefficients for ethylnitronate ($\varepsilon_{228\ \mathrm{nm}}$ value of 8625 M^{-1}cm^{-1}; this study) and nitroethane ($\varepsilon_{228\ \mathrm{nm}}$ value of 105 M^{-1}cm^{-1}; this study). Initial rates for the enzymatic formation of ethylnitronate from nitroethane were determined by fitting the non-linear reaction progress curves to the empirical equation developed by Fei and Lu (*18*) (eq 2). A_{o} is the initial absorbance at 228 nm, b is defined as a shape parameter, t is time and x is the scale of the logarithmic curve. The initial rate is given by the slope of a tangent line to the curve that intersects through the origin and is found by taking the derivative of y with respect to t when the latter is set equal to zero. The resulting value is converted to initial rates of product formation using the experimentally determined $\Delta\varepsilon_{228\ \mathrm{nm}}$ value and after correcting for the 1 cm path length used (l) (eq 3). Initial rates determined in this fashion

reflect the overall rate of ethylnitronate formation and are converted to enzymatic reaction rates by subtraction of the non-enzymatic component of the reaction determined in parallel under the same conditions. The resulting data were fit with eq 4, where k_{cat}/K_m is the second order rate constant for the enzymatic reaction and S is the concentration of nitroethane. The pH dependence of the k_{cat}/K_m values was determined by fitting the initial rate data to eq 5, which describes a curve with a slope of +1 and a plateau region at high pH. C is the pH independent value of the k_{cat}/K_m value. When initial rates were determined by measuring oxygen consumption the data were fit eq 6, where K_a and K_b represent the Michaelis constants for the nitronate substrate (A) and oxygen (B), and k_{cat} is the turnover number of the enzyme (e).

$$v_0 = A_o + k_{obs}t \tag{1}$$

$$y = A_o + b\ln\left(1+\frac{t}{x}\right) \tag{2}$$

$$v_0 = \left(\frac{b}{x}\right)\left(\frac{1}{\Delta\varepsilon_{228nm}l}\right) \tag{3}$$

$$\frac{v_o}{e} = \frac{k_{cat}}{K_m}S \tag{4}$$

$$\log Y = \log\left(\frac{C}{1+\dfrac{10^{-pH}}{10^{-pK_a}}}\right) \tag{5}$$

$$\frac{v}{e} = \frac{k_{cat}AB}{K_aB + K_bA + AB + K_{ia}K_b} \tag{6}$$

5.4   Results

Assay for the Formation of Ethylnitronate from Nitroethane. As a prerequisite for studies of the deprotonation of nitroethane catalyzed by *N. crassa* 2-nitropropane dioxygenase, the UV absorbance properties of the neutral and anionic forms of the substrate were studied at 30 $^{\circ}$C. The UV absorbance spectra of nitroethane and ethylnitronate exhibit absorbance maxima at 202 and 228 nm, respectively (SI, Figure S1). Molar extinction coefficients for nitroethane of 1240 ± 10 $M^{-1}cm^{-1}$ and 105 ± 2 $M^{-1}cm^{-1}$ were determined at 202 and 228 nm using the Lambert-Beer law. Similarly, a molar extinction coefficient of 8625 ± 335 $M^{-1}cm^{-1}$ was determined for ethylnitronate at 228 nm. These results establish that the formation of ethylnitronate from nitroethane could be

monitored directly by measuring the increase in absorbance at 228 nm over time, as illustrated in Figure 1 for a non-enzymatic reaction mixture consisting of 50 mM sodium pyrophosphate and 0.15 mM nitroethane at pH 8 and 30 $^{\circ}$C. In a similar fashion, ethylnitronate accumulated over time upon incubating *N. crassa* 2-nitropropane dioxygenase with 0.15 mM nitroethane in 50 mM sodium pyrophosphate at pH 8 and 30 $^{\circ}$C could be monitored using the assay (data not shown).
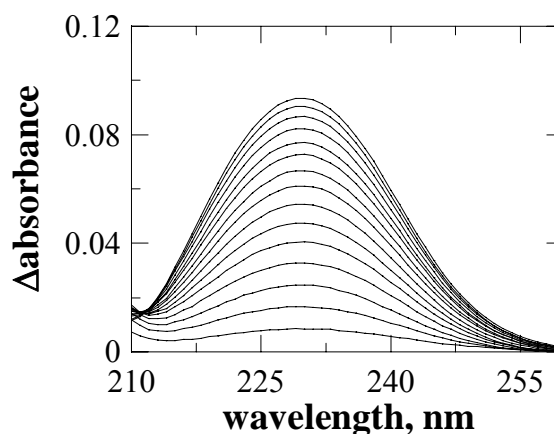
Figure 5.1 Non-enzymatic formation of ethylnitronate from nitroethane at pH 8 and 30 $^{\circ}$C .
A solution of 50 mM sodium pyrophosphate was mixed with 0.15 mM nitroethane. The UV absorbance spectrum of the reaction mixture was recorded 20 s after mixing and additional spectra were recorded over 15 min at 1 min intervals. Difference spectra were constructed by subtracting the spectrum recorded 20 s after mixing from those recorded at later times and are shown in order of increasing incubation time from the bottom to the top spectrum.
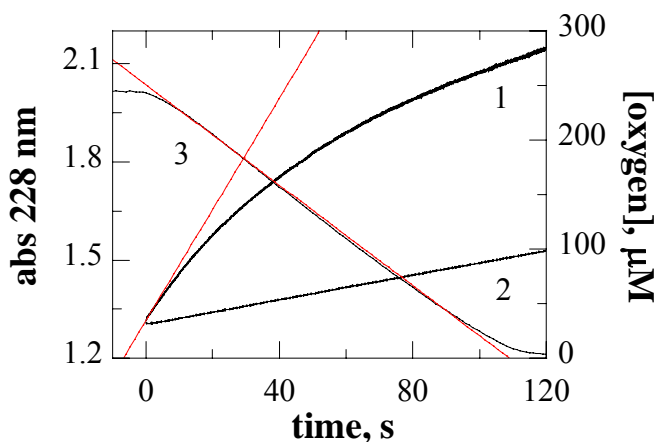
Figure 5.2 Reaction progress curves for the enzymatic and non-enzymatic formation of ethylnitronate from nitroethane.
A 3 mM solution of nitroethane in water was mixed with either 1.07 µM *N. crassa* 2-nitropropane dioxygenase in 50 mM sodium pyrophosphate (trace 1) or with 50 mM sodium pyrophosphate alone (trace 2) at pH 8 and 30 °C and the absorbance at 228 nm was monitored over 120 s. For clarity, the starting absorbance of the non-enzymatic reaction was arbitrarily increased to match that of the enzymatic reaction. Trace 3 shows a control experiment in which the progress curve for the enzymatic reaction carried out under the same conditions was followed by monitoring the concentration of oxygen over time using a Clark oxygen electrode. The red lines represent linear fits of traces 1 and 3 as tangents to the reaction progress curves at the initial stages of the reaction.

Enzymatic Formation of Ethylnitronate from Nitroethane. The reaction progress curves for the formation of ethylnitronate from nitroethane were measured upon mixing 3 mM nitroethane with 50 mM sodium pyrophosphate in either the absence or presence of 1.07 µM *N. crassa* 2-nitropropane dioxygenase at pH 8 and 30 °C to determine if the enzyme catalyzes the deprotonation reaction. As shown in Figure 2, the rate of absorbance increase at 228 nm over time was higher for the

reaction containing the enzyme than that containing only sodium pyrophosphate, consistent with *N. crassa* 2-nitropropane dioxygenase catalyzing the formation and release of ethylnitronate with nitroethane as substrate. Moreover, while the non-enzymatic reaction yielded linear progress curves, those for the enzymatic reaction were visibly non-linear across the pH range from 6 to 10, as illustrated in Figure 2 for the case of pH 8, suggesting a role of the enzyme in the formation of ethylnitronate from nitroethane. The non-linear reaction progress curves indicate that the concentration of

enzyme turning over with the substrate progressively decreases over the time course of the assay. In principle, a progressive, time-dependent decrease in the concentration of enzyme turning over (e.g., ES complex) can be due to a decrease in the concentration of either the enzyme or the substrate. The curvature of the time courses being the result of a decrease in the enzyme concentration, either due to enzyme instability or inhibition, could be ruled out based on the observation that the rate of oxygen consumption during turnover of the enzyme with nitroethane under the same conditions maintained linearity for at least 90 s (Figure 2). Instead, the progressive decrease in the amount of enzyme turning over with the substrate could be readily explained with the time-dependent, enzymatic depletion of nitroethane when the reaction occurs at sub-saturating concentrations of substrate, i.e., with [S] « K_m. In support of this rationale, only the second order rate constants k_{cat}/K_m for the enzymatic formation and release of ethylnitronate from nitroethane could be estimated in this study (*vide infra*), but not turnover numbers (k_{cat}) and Michaelis constants (K_m) for the reaction. Similar results demonstrating that the overall rates of ethylnitronate formation are higher in the presence of the enzyme as compared to the corresponding non-enzymatic reactions, were obtained at each pH tested in the range from 6 to 10 (data not shown). As for the case of pH 8, enzyme instability or inhibition could be ruled out as a possible cause for the curved time courses at pH 6 and pH 10 based on the linear reaction progress curves obtained by monitoring oxygen consumption over prolonged times (SI; Figure S2).

Determination of Initial Rates for the Enzymatic Formation of Ethylnitronate from Nitroethane. The curvature observed in the time courses for the enzymatic production of ethylnitronate from nitroethane (Figure 2) indicates that the concentration

of the enzyme undergoing turnover is not constant over time, thereby preventing the use of linear regression analysis to determine the initial rates of the reaction. Consequently, an alternative method based on a logarithmic approximation of the initial rates (eqs 2 and 3) that was originally developed by Fei and Lu (*18*) was used to determine initial rates of ethylnitronate release from the enzyme. A value of 1.6 ± 0.1 µM s^{-1} was determined with 3 mM nitroethane at pH 8 and 30 °C using this method, irrespective of whether the progress curves were acquired for time intervals comprised between 60 and 180 s (data not shown). For comparison, the rate of the non-enzymatic reaction determined under the same conditions from linear reaction progress curves by using eq 1 (Figure 2) was found to be significantly lower, with a value of 0.27 ± 0.02 µM s^{-1}. Consequently, a value of ~1.3 µM s^{-1} was determined for the enzymatic formation of ethylnitronate under these conditions (e.g., 1.07 µM enzyme, 50 mM sodium pyrophosphate, pH 8 and 30 °C), by subtracting the rate of the non-enzymatic reaction from the overall reaction rate that
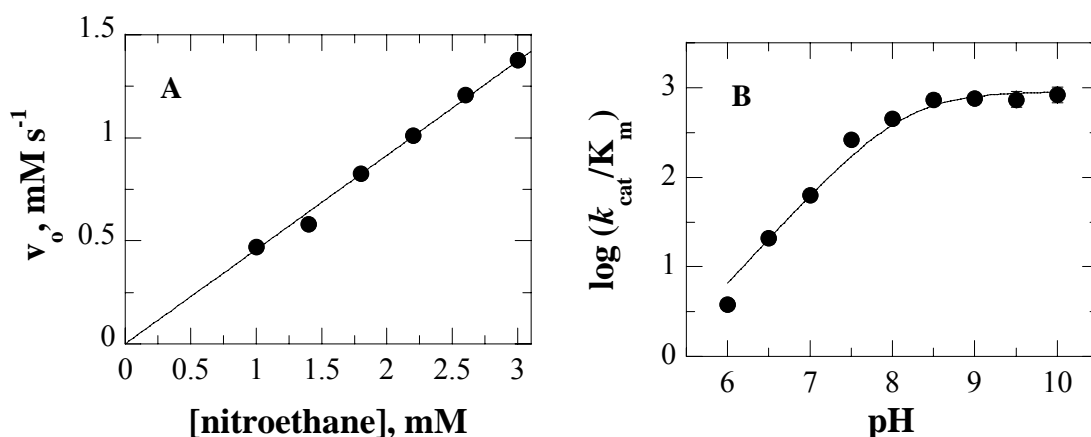
Figure 5.3 pH Dependence of k_{cat}/K_m with nitroethane as substrate for *N. crassa* 2-nitropropane dioxygenase.
Panel A: Nitroethane (1 to 3 mM) was mixed with 1.07 µM enzyme in 50 mM sodium pyrophosphate in a stopped flow spectrophotometer at pH 8 and 30 °C and absorbance changes at 228 nm were observed over 120 s. Reaction rates determined through fits of the traces with eq 2 were plotted as a function of nitroethane concentration. Each data point is the average of three independent measurements and is the enzymatic reaction rate subtracted by the non-enzymatic reaction rate determined under the same conditions in parallel experiments. Panel B: The pH dependence of k_{cat}/K_m was determined in the range from 6 to 10 at 30 °C by measuring rates of nitronate formation at varying concentrations of nitroethane. The data were fit with eq 5 ($R^2 = 0.981$).

includes both the enzymatic and non-enzymatic components.

pH Dependence of the k_{cat}/K_m Values with Nitroethane as Determined by Monitoring Ethylnitronate Formation. The deprotonation of nitroethane to yield ethylnitronate catalyzed by *N. crassa* 2-nitropropane dioxygenase was further examined by determining the second order rate constants k_{cat}/K_m for the non-oxidative reaction as a function of pH. The k_{cat}/K_m values were determined by measuring reaction rates using the method described above at varying concentrations of nitroethane. As shown in Figure 3A, the rate of the reaction increased linearly with the concentration of nitroethane in the range from 1 to 3 mM, allowing for the determination of a k_{cat}/K_m value of 450 ± 10 M^{-1}s^{-1} for the enzymatic reaction at pH 8 and 30 ^{o}C. Since concentrations of nitroethane >3 mM could not be used due to the high absorbance in the UV region of the resulting reaction mixtures, neither k_{cat} nor K_m values could be determined using this approach. As shown in Figure 3B, the k_{cat}/K_m values for the enzymatic reaction increased with increasing pH and reached a plateau at high pH. A pH independent upper limiting value for k_{cat}/K_m of 900 ± 150 M^{-1}s^{-1} and a pK_a of 8.1 ± 0.1 were determined from the fit of the curve in Figure 3B to eq 5, suggesting that an unprotonated group is required for the catalytic formation of ethylnitronate from nitroethane.

Identification of the Catalytic Base of N. crassa 2-Nitropropane Dioxygenase. Histidine 196 in *N. crassa* 2-nitropropane dioxygenase was replaced was replaced with asparagine through site directed mutagenesis to evaluate whether this residue acts as the catalytic base that abstracts the proton from the α-carbon of nitroethane during turnover. The role of His-196 in the deprotonation of nitroethane was tested by monitoring the formation of of ethylnitronate upon mixing the H196N variant form *N. crassa* 2-

nitropropane dioxygenase with the neutral nitroalkane using the assay developed in this study. The assays were carried out at pH 10 to ensure that the catalytic base, if present in the mutant, is in the correct ionization state to react with nitroethane. In contrast to the wild-type enzyme (*see above*), the rate of ethylnitronate formation from nitroethane upon mixing the mutant form of *N. crassa* 2-nitropropane dioxygenase with nitroethane was not significantly different from that of the buffer-catalyzed reaction, with a value of ~0.04 min^{-1} at pH 10 and 30 ^{o}C as compared to ~0.05 min^{-1} for a control reaction ran under the same conditions in the absence of enzyme. This suggests that the H196N variant is incapable of catalyzing the deprotonation of nitroethane to ethylnitronate. The activity of the mutant enzyme with nitroethane as substrate was further investigated by testing the ability of the H196N variant to consume oxygen in the presence of the nitroalkane. As
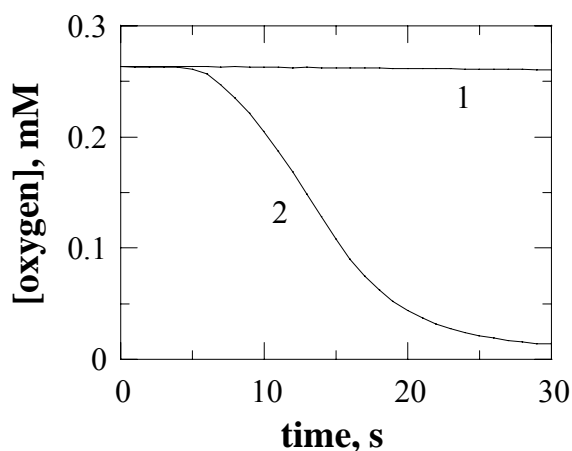
Figure 5.4 Identification of the catalytic base of *N. crassa* 2-nitropropane dioxygenase. Time courses measuring the concentration of oxygen after mixing the H196N variant form of the enzyme (2.17 μM) with 1 mM of either nitroethane (trace 1) or ethylnitronate (trace 2) at pH 10 and 30 ^{o}C were followed using a Clark oxygen electrode.

shown in Figure 4, oxygen consumption was not observed upon mixing the mutant enzyme with 1 mM nitroethane at pH 10 and 30 ^{o}C. In contrast, mixing of the H196N variant with ethylnitronate under the same conditions resulted in the complete depletion of oxygen from the assay reaction mixture within 30 s after initiating the reaction. These data suggest that the mutant enzyme is properly folded and capable of undergoing catalytic turnover with anionic substrates for

which a catalytic base is not required in the wild-type (*2, 3*). The lack of rate enhancement for the formation of ethylnitronate as compared to the non-enzymatic reaction and the lack of oxygen consumption observed upon mixing the H196N enzyme with neutral substrates unequivocally establish that *N. crassa* 2-nitropropane dioxygenase loses the ability to deprotonate nitroethane when histidine 196 is replaced with asparagine.

Table 5.1 Steady State Kinetic Parameters of Wild-type and H196N *N. crassa* 2-Nitropropane Dioxygenase with Ethylnitronate as Substrate

enzyme	k_{cat} (s^{-1})	K_a^b (mM)	k_{cat}/K_a $(M^{-1}s^{-1})$	K_{O2}^b (μM)	k_{cat}/K_{O2} ($\mu M^{-1}s^{-1}$)	K_{ia} (mM)	R^2
			ethylnitronate				
wt	16.2 ± 0.1	15.9 ± 0.3	1020 ± 20	≤ 5	≥ 1	100 ± 10	0.993
H196N	185 ± 1	11.0 ± 0.1	16800 ± 100	34 ± 1	5.5 ± 0.1	1.2 ± 0.2	0.998
			1-^{2}H-ethylnitronate				
wt	16.5 ± 0.2	10.6 ± 0.4	1560 ± 50	≤ 5	≥ 1	140 ± 20	0.994
H196N	195 ± 5	11.5 ± 1.1	16900 ± 1600	35 ± 4	5.6 ± 0.6	2.3 ± 1.8	0.995

[a]Enzyme activity was measured at varying concentrations of both organic substrate and oxygen in 50 mM sodium pyrophosphate at pH 9.5 and 30 ^{o}C. Data were fit to eq 6. [b]K_a refers to the Michaelis constant for the organic substrate; K_{O2} refers to the Michaelis constant for oxygen.

Effect of Replacing His-196 with Asparagine on Enzyme Activity with Ethylnitronate as Substrate. The steady-state kinetic parameters with ethylnitronate as substrate for the mutant form of *N. crassa* 2-nitropropane dioxygenase were determined at pH 9.5 and 30 ^{o}C to investigate the role of histidine 196 in turnover of the enzyme with anionic substrates. As shown in Table 1, the H196N enzyme showed a ~15 fold increase in the k_{cat}/K_m value and a ~10 fold increase in the k_{cat} value when rates of oxygen consumption were measured. A $^D(k_{cat}/K_m)$ value with 1-^{2}H-ethylnitronate of 0.99 ± 0.09 was also determined. In contrast, the $^D(k_{cat}/K_m)$ value for the wild-type enzyme was 0.65 ± 0.02, in good agreement with the value of 0.63 previously reported (*3*). The data demonstrate that the H196N variant is a better catalyst than the wild-type enzyme for oxidative turnover with ethylnitronate.
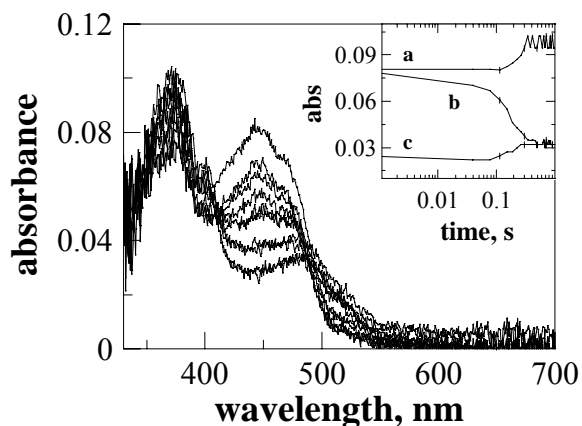
Figure 5.5 Anionic flavosemiquinone formation in the reductive half reaction of H196N *N. crassa* 2-nitropropane dioxygenase.
The mutant enzyme (~10 μM final concentration) was mixed anaerobically with ethylnitronate (0.5 mM final concentration) at pH 7 and 30 °C, and UV-visible absorbance spectra were recorded using a stopped-flow spectrophotometer equipped with a photo-diode array detector. The spectra shown were collected from 0.75 ms to 1 s after the end of flow. *Inset*, time courses for the UV-visible absorbance of the FMN cofactor of the H196N variant at 371 (a) 442 (b) and 495 (c) nm. The time indicated is after the end of flow (2.2 ms).

Effect of Replacing His-196 with Asparagine on Flavin Reduction with Ethylnitronate as Substrate. Previous studies have demonstrated that an anionic flavosemiquinone forms during catalytic turnover of *N. crassa* 2-nitropropane dioxygenase with ethylnitronate as substrate (*2, 3*). The requirement for His-196 in the formation of the flavosemiquinone was investigated in the current study by monitoring flavin visible absorbance spectra during the reductive half reaction of the H196N variant with ethylnitronate as substrate at pH 7 and 30 °C. As shown in Figure 5, anaerobic mixing of the H196N variant with ethylnitronate resulted in the formation of an anionic flavosemiquinone as indicated by the peaks in the visible absorbance spectra at 371 and 496 nm that developed during the course of flavin reduction. Thus, replacing histidine 196 with asparagine has no affect on the mechanism of electron transfer in the reductive half reaction of the enzyme nor does it alter the ionization state of the catalytically relevant flavosemiquinone.

5.5   Discussion

Previous studies of the *N. crassa* 2-nitropropane dioxygenase reaction with nitroethane are consistent with the formation of an enzyme-ethylnitronate complex during turnover (*2, 3*), which is produced in the enzyme-catalyzed deprotonation of the substrate by the action of an active site catalytic group acting as a base. In this study, a continuous spectrophotometric assay was developed to evaluate whether the ethylnitronate that is produced from the enzymatic deprotonation of nitroethane is released to the solvent. A logarithmic approximation of the initial rates of the enzymatic reaction was then used to assess the kinetic parameters for the non-oxidative deprotonation of nitroethane catalyzed by *N. crassa* 2-nitropropane dioxygenase and a mutant variant of the enzyme in which the conserved histidine 196 was replaced with asparagine.

Ethylnitronate is released to the solvent during enzymatic turnover of *N. crassa* 2-nitropropane dioxygenase with nitroethane, as indicated by the progressive, non-linear increase in absorbance at 228 nm after mixing the enzyme with nitroethane. Initial rates of reaction for the formation and release of ethylnitronate from the active site of the enzyme could be approximated despite the non-linearity of the reaction progress curves. This was achieved using the method originally developed by Fei and Lu (*18*), which involves fitting the entire reaction progress curve to a logarithmic function. The slope of a tangent line to the curve that intersects through the origin is analogous to that found using traditional methods to determine initial rates of enzymatic reactions that rely on a steady-state accumulation or depletion of a reaction species (*19*). Both methods measure changes in the concentration of either a substrate or product with respect to time during the initial stages of the reaction. The logarithmic approximation is generally applicable to

any enzymatic reaction resulting in non-linear progress curves due to the concentration of substrate being significantly smaller than the K_m value, provided that the curvature is not the result of enzyme instability or inhibition.
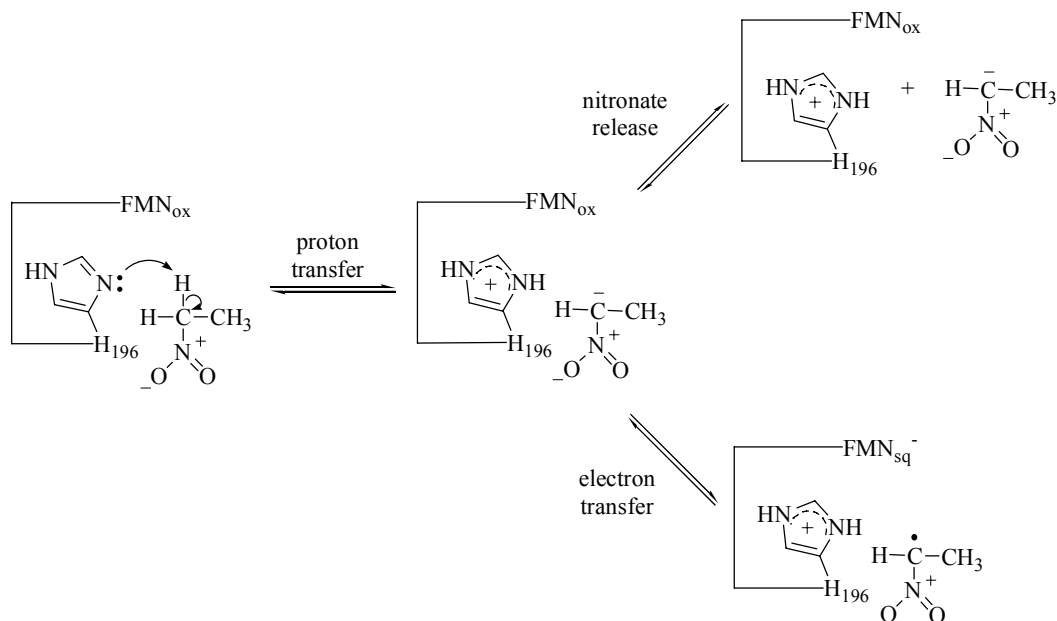
Scheme 5.2 Branching of the enzyme-ethylnitronate complex during turnover of *N. crassa* 2-nitropropane dioxygenase with nitroethane as substrate.
Note that under initial velocity conditions in the absence of exogenous ethylnitronate the kinetic step of nitronate release is practically irreversible. For clarity, further conversion of the anionic flavosemiquinone enzyme through the oxidative denitrification pathway is not shown.

The kinetic studies of the formation and release of ethylnitronate from *N. crassa* 2-nitropropane dioxygenase in turnover with nitroethane along with previous results on the flavin-dependent oxidative denitrification of nitroethane catalyzed by the enzyme (*2, 3*) demonstrate a branched catalytic mechanism for the enzyme with the nitroalkane as substrate (Scheme 2). The catalytic cycle is initiated by the base-catalyzed deprotonation of nitroethane to yield ethylnitronate. This enzyme-bound nitronate is then either released to the solvent or is oxidized through the transfer of a single electron transfer to the flavin cofactor of *N. crassa* 2-nitropropane dioxygenase. The time-dependent increase in the UV absorbance at 228 nm seen upon mixing the enzyme with nitroethane is consistent

with the accumulation of ethylnitronate in solution during the course of the assay. While the non-enzymatic deprotonation of nitroethane to ethylnitronate is known to occur in solution (*20, 21*), the initial rates of the reaction determined in this study were higher in the presence of the enzyme than those obtained in buffer alone, clearly establishing that *N. crassa* 2-nitropropane dioxygenase catalyzes the reaction. Nitronate release during turnover of the enzyme with nitroethane as substrate thus occurs in addition to the previously described oxidative denitrification of ethylnitronate that occurs during catalysis (*2, 3*). The partitioning of the enzyme-ethylnitronate complex results in a branched catalytic mechanism of the type seen for the cytochrome p450 class of enzymes (*22-24*), the aromatic amino acid hydroxylases (*25*) and the hemoprotein-lipoxygenase fusion protein (*26*).

The catalytic base involved in the deprotonation of nitroethane in the reaction catalyzed by the *N. crassa* 2-nitropropane dioxygenase is histidine 196. Evidence supporting this conclusion comes from the lack of rate enhancement for ethylnitronate formation by a reaction mixture containing the H196N enzyme compared to control reactions carried out in buffer alone. The lack of enzymatic activity is not due to a deleterious effect of the mutation on the general properties of the enzyme because oxygen consumption is observed when ethylnitronate is used as a substrate for the mutant enzyme. Turnover of the mutant enzyme with ethylnitronate is expected to occur based on previous studies demonstrating that catalysis with the nitronate does not require an unprotonated group (*2, 3, 21*). The kinetic data implicating the role of His 196 as the catalytic base in the reaction of the enzyme with nitroethane are consistent with crystallographic studies of *P. aeruginosa* 2-nitropropane dioxygenase in complex with 2-

nitropropane (*17*), which shows the conserved histidine next to the α-proton of the substrate.

Replacement of histidine 196 with asparagine in *N. crassa* 2-nitropropane dioxygenase results in a better catalyst for the oxidative denitrification of ethylnitronate, as suggested by the ~15-fold increase in the k_{cat}/K_m value observed with the H196N variant as compared to the wild-type enzyme. This is likely due to the inability of the mutant enzyme to catalyze the non-oxidative conversion of ethylnitronate to nitroethane, as suggested by the lack of an α-secondary kinetic isotope on the k_{cat}/K_m value with 1-^{2}H-ethylnitronate. Indeed this conversion is associated with a change in the hybridization of the α-carbon of the substrate, which would result in an inverse $^D(k_{cat}/K_m)$ value as observed in the wild-type enzyme (this study and ref. *3*). In the H196N enzyme all of the productive complexes between the enzyme and the anionic substrate that form during turnover are therefore destined for oxidative denitrification, rather than branching through oxidative and non-oxidative catalysis as in the wild-type enzyme.

Histidine 196 is not required for the formation of the obligatory, anionic flavosemiquinone that is transiently formed during the reductive half-reaction in which ethylnitronate is oxidized by the wild-type enzyme (*2, 3*). Evidence supporting this conclusion comes from anaerobic stopped-flow measurements in which the H196N enzyme was mixed with ethylnitronate, showing the formation of the anionic flavosemiquinone. This, in turn, suggests that the reaction pathway for oxidative denitrification of ethylnitronate in *N. crassa* 2-nitropropane dioxygenase is unaltered upon replacing His-196 with asparagine.

In conclusion, a kinetic assay was developed to demonstrate that *N. crassa* 2-nitropropane dioxygenase utilizes a branched catalytic mechanism with nitroethane as substrate. The branch point occurs at the enzyme-ethylnitronate complex and involves either the release of the nitronate or an oxidative denitrification reaction. The partitioning of the enzyme-nitronate complex results in the formation of multiple products from independent catalytic pathways with nitroethane as substrate for the enzyme. In the non-oxidative pathway, nitroethane is deprotonated by histidine 196 to generate ethylnitronate which is subsequently released from the enzyme as a reaction product. The oxidative denitrification pathway was established in previous studies of the enzyme (*2, 3*) and involves the oxidation of ethylnitronate by the enzyme bound flavin to generate acetaldehyde and nitrite as product. The mechanistic factors that determine the partitioning of the enzyme-ethylnitronate complex between oxidation and release from the enzyme active site are the focus of a current investigation of the enzyme.

5.6 Acknowledgements

5.7   Supporting Information

Table 5.2 shows the fits of the reaction progress curves for the reaction of *N. crassa* 2-nitropropane dioxygenase with nitroethane at pH 8 and 30 $^{\circ}$C.

Table 5.3 shows the fits of the progress curves for the non-enzymatic reaction of 50 mM sodium pyrophosphate with nitroethane at pH 8 and 30 $^{\circ}$C.

Table 5.4 summarizes the kinetic parameters of the enzymatic and non-enzymatic deprotonation of nitroethane as a function of pH.

Figure 5.6 shows the concentration dependence of the UV absorbance spectra of nitroethane and ethylnitronate.

Figure 5.7 shows time courses of oxygen consumption during the enzymatic reaction of *N. crassa* 2-nitropropane dioxygenase in 50 mM sodium pyrophosphate with nitroethane at pH 6 and 10 at 30 $^{\circ}$C.

Table 5.2 *N. crassa* 2-Nitropropane Dioxygenase Catalyzed Deprotonation of Nitroethane

[nitroethane], mM	abs_o [b]	b [b]	x [b]	$abs_{228\,nm}$/time[c], s^{-1}	v_o[d], $\mu M\ s^{-1}$	R^2
3.0	1.44 ± 0.01	0.45 ± 0.01	30 ± 1	0.015 ± 0.001	1.75 ± 0.06	0.999
3.0	1.31 ± 0.01	0.51 ± 0.01	36 ± 1	0.014 ± 0.001	1.63 ± 0.04	0.999
3.0	1.39 ± 0.01	0.47 ± 0.01	35 ± 1	0.014 ± 0.001	1.56 ± 0.05	0.999
2.6	1.05 ± 0.01	0.45 ± 0.01	40 ± 1	0.011 ± 0.001	1.30 ± 0.03	0.999
2.6	1.01 ± 0.01	0.46 ± 0.01	30 ± 1	0.015 ± 0.001	1.76 ± 0.06	0.999
2.6	1.04 ± 0.01	0.46 ± 0.01	40 ± 1	0.012 ± 0.001	1.33 ± 0.03	0.999
2.2	0.85 ± 0.01	0.37 ± 0.01	34 ± 1	0.011 ± 0.001	1.28 ± 0.04	0.999
2.2	0.83 ± 0.01	0.37 ± 0.01	37 ± 1	0.010 ± 0.001	1.16 ± 0.03	0.999
2.2	0.84 ± 0.01	0.37 ± 0.01	33 ± 1	0.011 ± 0.001	1.29 ± 0.04	0.999
1.8	0.67 ± 0.01	0.27 ± 0.01	30 ± 1	0.0091 ± 0.0001	1.06 ± 0.04	0.999
1.8	0.68 ± 0.01	0.27 ± 0.01	32 ± 1	0.0086 ± 0.0002	0.99 ± 0.03	0.999
1.8	0.67 ± 0.01	0.28 ± 0.01	34 ± 1	0.0083 ± 0.0002	0.96 ± 0.03	0.999
1.4	0.54 ± 0.01	0.18 ± 0.01	20 ± 1	0.0090 ± 0.0001	1.04 ± 0.01	0.999
1.4	0.54 ± 0.01	0.18 ± 0.01	25 ± 1	0.0074 ± 0.0003	0.85 ± 0.04	0.999
1.4	0.53 ± 0.01	0.19 ± 0.01	38 ± 1	0.0050 ± 0.0001	0.58 ± 0.02	0.999
1.0	0.47 ± 0.01	0.14 ± 0.01	39 ± 1	0.0036 ± 0.0001	0.42 ± 0.01	0.999
1.0	0.47 ± 0.01	0.15 ± 0.01	41 ± 1	0.0036 ± 0.0001	0.41 ± 0.01	0.999
1.0	0.47 ± 0.01	0.14 ± 0.01	21 ± 1	0.0067 ± 0.0003	0.78 ± 0.04	0.999

[a] In 50 mM sodium pyrophosphate at pH 8 and 30 °C. [b] From a fit of a time course monitoring ethylnitronate formation to $y = abs_o + b\ln(1+t/x)$, where abs_o is the initial absorbance of the reaction mixture at 228 nm, b is a shape parameter and x is the scale of the logarithmic curve. [c] Initial rate found from the slope of a tangent line to the curve that intersects through the origin and is found by taking the derivative of *y* with respect to *t* when the latter is set equal to zero, (b/x). [d] Initial rate calculated by converting the absorbance change at 228 nm to ethylnitronate concentration using the experimentally determined molar extinction coefficient for the nitronate.

Table 5.3 Deprotonation of Nitroethane in 50 mM Sodium Pyrophosphate

[nitroethane][a], mM	abs_o[b]	$abs_{228}/time$[b], s^{-1}	v_o[c], $\mu M\ s^{-1}$	R^2
3.0	1.15 ± 0.01	0.0024 ± 0.0001	0.27 ± 0.01	0.999
3.0	1.13 ± 0.01	0.0025 ± 0.0001	0.28 ± 0.01	0.999
3.0	1.18 ± 0.01	0.0024 ± 0.0001	0.27 ± 0.01	0.999
2.6	0.99 ± 0.01	0.0023 ± 0.0001	0.25 ± 0.01	0.999
2.6	1.00 ± 0.01	0.0022 ± 0.0001	0.25 ± 0.01	0.999
2.6	1.01 ± 0.01	0.0022 ± 0.0001	0.25 ± 0.01	0.999
2.2	0.83 ± 0.01	0.0018 ± 0.0001	0.20 ± 0.01	0.999
2.2	0.82 ± 0.01	0.0018 ± 0.0001	0.20 ± 0.01	0.999
2.2	0.82 ± 0.01	0.0019 ± 0.0001	0.20 ± 0.01	0.999
1.8	0.68 ± 0.01	0.0015 ± 0.0001	0.17 ± 0.01	0.999
1.8	0.69 ± 0.01	0.0016 ± 0.0001	0.17 ± 0.01	0.999
1.8	0.69 ± 0.01	0.0016 ± 0.0001	0.18 ± 0.01	0.999
1.4	0.51 ± 0.01	0.0012 ± 0.0001	0.13 ± 0.01	0.999
1.4	0.51 ± 0.01	0.0011 ± 0.0001	0.13 ± 0.01	0.999
1.4	0.51 ± 0.01	0.0012 ± 0.0001	0.13 ± 0.01	0.999
1.0	0.35 ± 0.01	0.00080 ± 0.00001	0.089 ± 0.001	0.996
1.0	0.35 ± 0.01	0.00082 ± 0.00001	0.092 ± 0.001	0.997
1.0	0.33 ± 0.01	0.00080 ± 0.00001	0.089 ± 0.001	0.998

[a]At pH 8 and 30 °C. [b]From a fit of a time course monitoring ethylnitronate formation to y = mx + b, where abs_o is the initial absorbance of the reaction mixture at 228 nm. The rate of the reaction is found from the slope of the line. [c]Initial rate calculated by converting the absorbance change at 228 nm to ethylnitronate concentration using the experimentally determined molar extinction coefficient for the nitronate.

Table 5.4 pH Dependence of the Knetic Parameters for the Deprotonation of Nitroethane

pH	k_{obs}[b], h^{-1}	k_{cat}/K_m[c], $M^{-1}s^{-1}$
6.0	0.035 ± 0.001	3.8 ± 0.1
6.5	0.044 ± 0.001	20 ± 1
7.0	0.085 ± 0.001	60 ± 5
7.5	0.21 ± 0.01	270 ± 10
8.0	0.32 ± 0.01	450 ± 10
8.5	0.59 ± 0.01	730 ± 20
9.0	0.90 ± 0.01	760 ± 10
9.5	1.55 ± 0.02	740 ± 20
10.0	3.00 ± 0.03	830 ± 25

[a]Nitroethane (1 to 3 mM) was mixed with 1.07 μM 2-nitropropane dioxygenase in 50 mM sodium pyrophosphate or 50 mM sodium pyrophosphate alone in a stopped-flow spectrophotometer at 30 °C and the absorbance at 228 nm was observed over time. [b]Pseudo first order rate constant for the non-enzymatic deprotonation of nitroethane in 50 mM sodium pyrophosphate. [d]k_{cat}/K_m value with nitroethane as substrate for *N. crassa* 2-nitropropane dioxygenase.
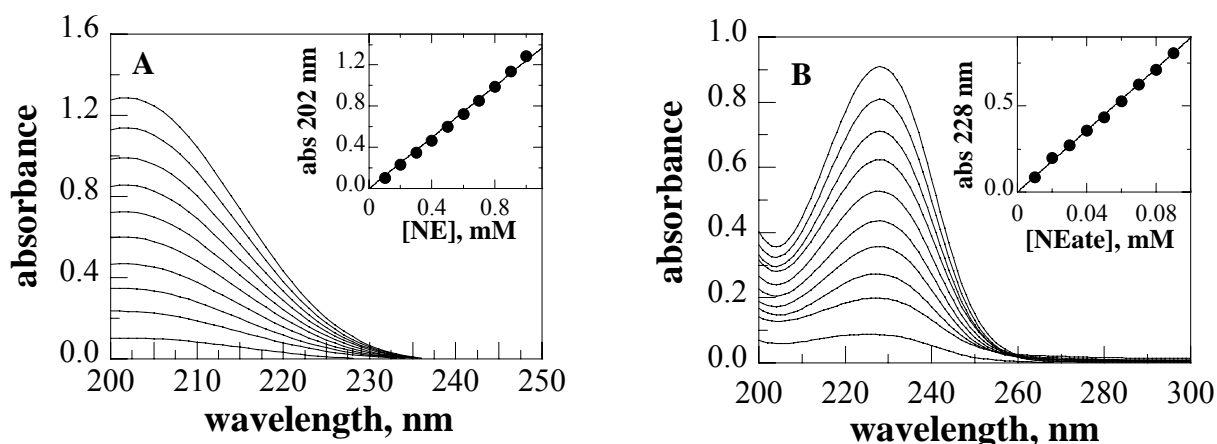
Figure 5.7 UV absorbance properties of nitroethane and ethylnitronate.
Panel A: Determination of the molar extinction coefficient of nitroethane at 202 nm. The UV absorbance spectrum of nitroethane was recorded at concentrations ranging from 0.1 (bottom) to 1 mM (top) at 0.1 mM increments. *Inset*: the absorbance at 202 nm versus nitroethane concentration. The data were fit to y = εcl (R^2 = 0.996). Panel B: Determination of the molar extinction coefficient of ethylnitronate at 228 nm. A 100 μM solution of ethylnitronate was prepared by incubating nitroethane with a 1.2 molar excess of potassium hydroxide in water for at least 24 hours. The UV absorbance spectrum of ethylnitronate was recorded at concentrations ranging from 10 (bottom) to 100 μM (top) at 10 μM increments. *Inset*: the absorbance at 228 nm versus ethylnitronate concentration. The data were fit to y = εcl (R^2 = 0.999). All spectra were recorded at 30 °C using a cuvette with a 1 cm path length.
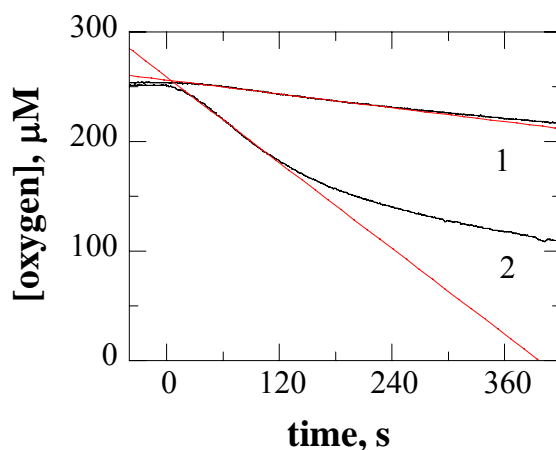
Figure 5.6 Time courses monitoring changes in oxygen concentration during turnover of *N. crassa* 2-nitropropane with nitroethane.
Reactions were carried out at 30 °C using 3 mM nitroethane in 50 mM sodium pyrophosphate at pH 6 (trace 1) or 10 (trace 2). The red lines are tangent curves to the traces at the initial stages of the reactions.

5.8   References

1.   Little, H. N. (1951) Oxidation of Nitroethane By Extracts From *Neurospora*. *J. Biol. Chem. 193*, 347-358.

2.   Francis, K., Russell, B., and Gadda, G. (2005) Involvement of a flavosemiquinone in the enzymatic oxidation of nitroalkanes catalyzed by 2-nitropropane dioxygenase. *J. Biol. Chem. 280*, 5195-5204.

3.   Francis, K., and Gadda, G. (2006) Probing the chemical steps of nitroalkane oxidation catalyzed by 2-nitropropane dioxygenase with solvent viscosity, pH, and substrate kinetic isotope effects. *Biochemistry 45*, 13889-13898.

4.   Kido, T., Soda, K., Suzuki, T., and Asada, K. (1976) A new oxygenase, 2-nitropropane dioxygenase of *Hansenula mrakii*. Enzymologic and spectrophotometric properties. *J. Biol. Chem. 251*, 6994-7000.

5.   Kido, T., and Soda, K. (1978) Properties of 2-nitropropane dioxygenase of *Hansenula mrakii*. Formation and participation of superoxide. *J. Biol. Chem. 253*, 226-232.

6.   Gorlatova, N., Tchorzewski, M., Kurihara, T., Soda, K., and Esaki, N. (1998) Purification, characterization, and mechanism of a flavin mononucleotide-dependent 2-nitropropane dioxygenase from *Neurospora crassa. Appl. Environ. Microbiol. 64*, 1029-1033.

7.   Mijatovic, S., and Gadda, G. (2008) Oxidation of alkyl nitronates catalyzed by 2-nitropropane dioxygenase from *Hansenula mrakii. Arch. Biochem. Biophys. 473,* 61-68.

8.   Heasley, C. J., and Fitzpatrick, P. F. (1996) Kinetic mechanism and substrate specificity of nitroalkane oxidase. *Biochem. Biophys. Res. Commun. 225*, 6-10.

9.   Gadda, G., and Fitzpatrick, P. F. (1999) Substrate specificity of a nitroalkane-oxidizing enzyme. *Arch. Biochem. Biophys. 363*, 309-313.

10.   Porter, D. J., Voet, J. G., and Bright, H. J. (1973) Direct evidence for carbanions and covalent N 5 -flavin-carbanion adducts as catalytic intermediates in the oxidation of nitroethane by D-amino acid oxidase. *J. Biol. Chem. 248*, 4400-4416.

11.   Porter, D. J., and Bright, H. J. (1977) Mechanism of oxidation of nitroethane by glucose oxidase. *J. Biol. Chem. 252*, 4361-4370.

12.   Porter, D. J., and Bright, H. J. (1987) Propionate-3-nitronate oxidase from *Penicillium atrovenetum* is a flavoprotein which initiates the autoxidation of its substrate by O_2. *J. Biol. Chem. 262*, 14428-14434.

13.   Porter, D. J., and Bright, H. J. (1983) The mechanism of oxidation of nitroalkanes by horseradish peroxidase. *J. Biol. Chem. 258*, 9913-9924.

14.   Valley, M. P., and Fitzpatrick, P. F. (2003) Inactivation of nitroalkane oxidase upon mutation of the active site base and rescue with a deprotonated substrate. *J. Am. Chem. Soc. 125*, 8738-8739.

15.   Valley, M. P., and Fitzpatrick, P. F. (2003) Reductive half-reaction of nitroalkane oxidase: effect of mutation of the active site aspartate to glutamate. *Biochemistry 42*, 5850-5856.

16.   Fitzpatrick, P. F., Bozinovski, D. M., Heroux, A., Shaw, P. G., Valley, M. P., and Orville, A. M. (2007) Mechanistic and Structural Analyses of the Roles of Arg409 and Asp402 in the Reaction of the Flavoprotein Nitroalkane Oxidase. *Biochemistry 46*, 13800-13808.

17.   Ha, J. Y., Min, J. Y., Lee, S. K., Kim, H. S., Kim do, J., Kim, K. H., Lee, H. H., Kim, H. K., Yoon, H. J., and Suh, S. W. (2006) Crystal structure of 2-nitropropane dioxygenase

complexed with FMN and substrate. Identification of the catalytic base. *J. Biol. Chem. 281*, 18660-18667.

18.   Lu, W. P., and Fei, L. (2003) A logarithmic approximation to initial rates of enzyme reactions. *Anal. Biochem. 316*, 58-65.

19.   Allison, R. D., and Purich, D. L. (1979) Practical considerations in the design of initial velocity enzyme rate assays. *Methods Enzymol. 63*, 3-22.

20.   Gao, J., Wong, K. Y., and Major, D. T. (2007) Combined QM/MM and path integral simulations of kinetic isotope effects in the proton transfer reaction between nitroethane and acetate ion in water. *J. Comput. Chem. 29*, 514-522.

21.   Valley, M. P., and Fitzpatrick, P. F. (2004) Comparison of enzymatic and non-enzymatic nitroethane anion formation: thermodynamics and contribution of tunneling. *J. Am. Chem. Soc. 126*, 6244-6245.

22.   Austin, R. N., Deng, D., Jiang, Y., Luddy, K., van Beilen, J. B., Ortiz de Montellano, P. R., and Groves, J. T. (2006) The diagnostic substrate bicyclohexane reveals a radical mechanism for bacterial cytochrome P450 in whole cells. *Angew. Chem. Int. Ed. Engl. 45*, 8192-8194.

23.   Makino, M., Sugimoto, H., Shiro, Y., Asamizu, S., Onaka, H., and Nagano, S. (2007) Crystal structures and catalytic mechanism of cytochrome P450 StaP that produces the indolocarbazole skeleton. *Proc. Natl. Acad. Sci. U. S. A. 104*, 11591-11596.

24.   Jiang, Y., He, X., and Ortiz de Montellano, P. R. (2006) Radical intermediates in the catalytic oxidation of hydrocarbons by bacterial and human cytochrome P450 enzymes. *Biochemistry 45*, 533-542.

25.   Fitzpatrick, P. F. (2003) Mechanism of aromatic amino acid hydroxylation. *Biochemistry*
       42, 14083-14091.

26.   Schneider, C., Niisuke, K., Boeglin, W. E., Voehler, M., Stec, D. F., Porter, N. A., and
       Brash, A. R. (2007) Enzymatic synthesis of a bicyclobutane fatty acid by a hemoprotein
       lipoxygenase fusion protein from the cyanobacterium *Anabaena* PCC 7120. *Proc. Natl.*
       Acad. Sci. U. S. A. 104, 18941-18945.

6   CHAPTER VI

INFLATED KINETIC ISOTOPE EFFECTS IN THE BRANCHED MECHANISM OF

NEUROSPORA CRASSA 2-NITROPROPANE DIOXYGENASE

6.1   Abstract

Catalytic turnover of *Neurospora crassa* 2-nitropropane dioxygenase with nitroethane as substrate occurs through both nonoxidative and oxidative pathways. The pH dependence of the kinetic isotope effects with $[1,1-^2H_2]$nitroethane as substrate was measured in the current study by monitoring the formation of the nitronate product in the nonoxidative pathway. The kinetic isotope effect on the second-order rate constant for nitronate formation, k_{cat}/K_m, decreased from an upper limiting value of 23 ± 1 at low pH to a lower limiting value of 11 ± 1 at high pH. These kinetic isotope effects are 3 times larger than those determined previously through measurements of oxygen consumption that occurs in the oxidative pathway of the enzyme [*Biochemistry* **2006, 45,** (46), 13889]. Analytical expressions for the k_{cat}/K_m values determined in each study show that the difference in the kinetic isotope effects arise from the branching of an enzyme-ethylnitronate reaction intermediate through oxidative and nonoxidative turnover. This branching is isotope sensitive due to a kinetic isotope effect on nitronate release rather than on flavin reduction as indicated by the pH independent $^D k_{red}$ value of 0.99 ± 0.06 with ethylnitronate as substrate. The kinetic isotope effect on ethylnitronate release likely arises from the deprotonation of histidine-196, which provides electrostatic interactions with the nitronate to keep it bound in the active site for oxidation. The isotope effect on branching results in an inflation of the kinetic isotope observed for the nonoxidative pathway to values that are larger than the intrinsic values associated with CH bond cleavage.

6.2   Introduction

The use of kinetic isotope effects as mechanistic probes of enzymes with branched kinetic mechanisms is often complicated by isotope effects that are expressed on the partitioning of reaction intermediates formed during turnover. This has been best documented in the case of the cytochrome p450 class of enzymes (*1-3*) and the aromatic amino acid hydroxylases (*4-7*). The presence of branch points in a kinetic mechanism of an enzyme tends to reduce the observed kinetic isotope effect from the intrinsic values on bond cleavage as evident from the small kinetic isotope effects generally seen for these enzymes (*3, 8, 9*). The use of intramolecular isotope effects, to which extensive theory has been developed (*10-12*), has been successfully used in the cytrochrome p450 class of enzymes to unmask the effects of branching on the kinetic isotope effect for the reaction. In the case of the aromatic amino acid hydroxylases, the masking effects arising from branching have been overcome by uncoupling the reaction through site-directed mutagenesis (*13, 14)*. This approach has been successfully employed with tyrosine hydroxylase (*13*) and recently with phenylalanine hydroxylase (*14*) to allow the intrinsic value for the kinetic isotope effect on CH bond cleavage to be observed in the reactions. In contrast to enzymatic reactions, branching of reaction intermediates to produce multiple products is a much more widely documented process for nonenzymatic reactions, where it has been demonstrated that it can result in an inflation or deflation of the observed kinetic isotope effects from the intrinsic value (*15-17*).
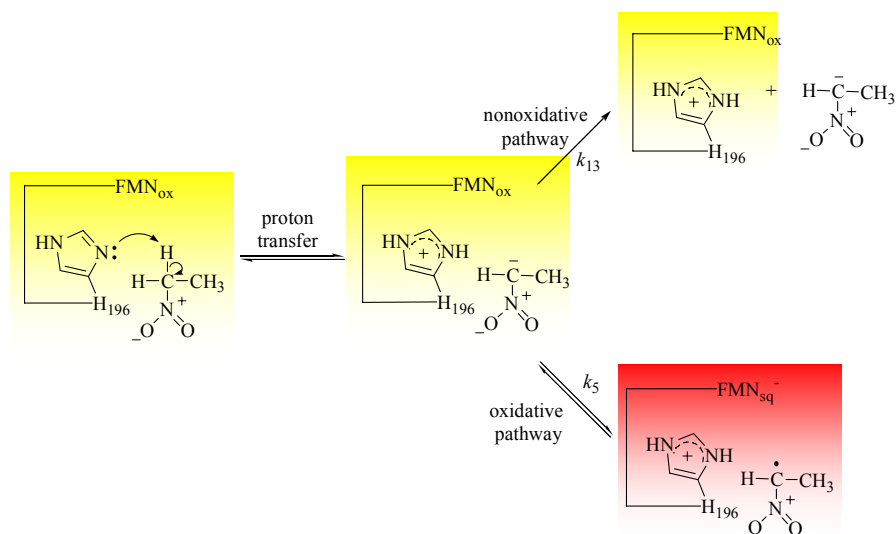
Scheme 6.1 Proposed branch point in the steady-state kinetic mechanism of N. crassa 2-NPD with nitroethane as substrate.
The enzyme-ethylnitrate complex partitions through an oxidative catalytic pathway (via k_5) and a nonoxidative catalytic pathway (via k_{13}) at the branch point. Note that the kinetic step for the release of ethylnitronate (k_{13}) from the active site of the enzyme surface is shown as being irreversible because initial rates were measured in the absence of this species. For clarity, further kinetic steps occurring along the oxidative pathway are not shown.

Recently, an FMN dependent enzyme 2-nitropropane dioxygenase (2-NPD) from *Neurospora crassa* was demonstrated to utilize a branched catalytic cycle with either the neutral or anionic (nitronate) form of nitroethane as substrate (*18, 19*). The enzyme catalyzes the oxidative denitrification of nitroalkanes to the corresponding aldehyde compounds and nitrite through the formation of an anionic flavosemiquinone intermediate (*18-20*). As illustrated in Scheme 1, the branch point with nitroethane as substrate occurs after an isotope sensitive step involving a proton abstraction reaction from the α-carbon of neutral nitroalkane catalyzed by histidine 196 (*19*). Branching occurs as a result of the partitioning of an enzyme-ethylnitronate transient intermediate formed with nitroethane as substrate through a nitronate dissociation step (k_{13} in Scheme 1) in a nonoxidative pathway and an electron transfer reaction with the flavin in an oxidative pathway (k_5 in Scheme 1). Reoxidation of the flavin in the oxidative pathway results in the formation of superoxide, which subsequently reacts with the enzyme-bound nitronate

radical to form a peroxynitroethane intermediate. This intermediate is then likely released from the active site, where it decays to give the acetaldehyde and nitrite products of the oxidative pathway. *N. crassa* 2-NPD can also utilize the deprotonated form of nitroethane as substrate, where a similar branching mechanism occurs as was demonstrated through measurements of the pH dependence of the secondary kinetic isotope effects with [1-^{2}H] ethylnitronate as substrate (*18*).

In the present study, the pH dependence of the kinetic isotope effects with nitroethane as substrate for the enzyme was determined by following the formation of the nitronate product formed during the nonoxidative pathway. The results were then compared with previous studies of the kinetic isotope effects with nitroethane as substrate measured by following oxygen consumption occurring during the oxidative pathway of the enzyme (*18*). The data indicate that the branching of reaction intermediates through multiple catalytic pathways results in an inflation of the observed kinetic isotope effects for the nonoxidative catalytic pathway as compared to that for nitroethane oxidation. This study represents the first instance in which an observed kinetic isotope effect in an enzymatic reaction is inflated above the intrinsic value associated with CH bond cleavage due to branch points occurring during catalytic turnover.

6.3   Experimental Procedures

Materials. N. crassa 2-NPD was obtained using the expression and purification protocols described previously (*19*). Nitroethane and [1,1-^{2}H$_2$]nitroethane were from Sigma-Aldrich (St. Louis, MO). All other reagents were of the highest purity commercially available.

Methods. The kinetic parameters for the formation of ethylnitronate when nitroethane is used as substrate for *N. crassa* 2-NPD were determined by monitoring the increase in absorbance at 228 nm resulting from mixing the enzyme (1.07 μM final concentration) in air-saturated 50

mM sodium pyrophosphate with substrate (in the range from 1 to 3 mM final concentrations). The non-linear time courses for the enzymatic reaction required the use of a logarithmic approach to determine initial rates, which was carried out as described previously (*19*). This approach was necessary to prevent an underestimation of the true initial rates for the reaction, which would result from arbitrarily considering only a portion of the reaction progress curve that might appear linear to the observer. Deuterium kinetic isotope effects were determined in assays carried out by alternating substrate isotopomers, and were calculated from the ratio of the k_{cat}/K_m value obtained with unlabeled substrate to that with labeled substrate. The limited solubility of nitroethane prevented an accurate determination of the turnover numbers (k_{cat}), Michaelis constants (K_m) and the corresponding kinetic isotope effects for the enzyme with this substrate. The pH dependence of the $^D(k_{cat}/K_m)_{nox}$ values with [1,1-^{2}H$_2$]nitroethane as substrate was determined in air-saturated 50 mM sodium pyrophosphate in the pH range from 6.0 to 10.0 at 30 $^\circ$C. Rates for the reductive half reaction of the enzyme with ethylnitronate as substrate were determined at 30 $^\circ$C using a TgK Scientific SF-61 stopped-flow spectrophotometer as previously described (*18*). The pH dependence of the reductive half reaction was determined in the pH range from 6.0 to 10.1, by monitoring either the increase in absorbance at 370 nm (pH 7.0-10.1) or the decrease in absorbance at 444 nm (pH 6.0-6.5)[1] that results from the anaerobic mixing of the enzyme with the substrate. Nitronate solutions (100 mM) were prepared in water through incubation of the corresponding nitroalkane with a 1.2 M excess of potassium hydroxide for at least 24 hours.

---

[1] The reductive half reaction was monitored at 440 nm at pH values ≤6.5 because a species that absorbs light at 380 nm was observed upon mixing ethylnitronate with sodium pyrophosphate in the absence of enzyme (Francis and Gadda; unpublished observations). This species is likely a nitroethane dimer based on previous studies by Porter and Bright [*J. Biol. Chem.* (1977), 252, 4261-4370], but was not identified in this study because its formation is clearly non-enzymatic.

Data Analysis. Kinetic data were fit with KaleidaGraph software (Synergy Software, Reading, PA). For the nonenzymatic deprotonation of either nitroethane or [1,1-^{2}H$_2$]nitroethane, stopped-flow traces were fit with eq 1, which is a simplified expression for a pseudo first-order reaction evaluated at initial rates (*i.e.*, t = 0). A$_o$ is the initial absorbance at 228 nm, k_{obs} is the observed rate constant for the increase in absorbance at 228 nm and t is time. The rate of product formation was determined from the k_{obs} value using the experimentally determined $\Delta\varepsilon_{228\ nm}$ value of 8,520 M^{-1}cm^{-1}, which is the $\varepsilon_{228\ nm}$ value for ethylnitronate corrected by the absorbance of nitroethane at that wavelength (*19*). Reaction progress curves with either nitroethane or [1,1-^{2}H$_2$]nitroethane as substrate for the enzyme were fit with eq 2, where A$_o$ is the initial absorbance at 228 nm, b is defined as a shape parameter, t is time and x is the scale of the logarithmic curve. Initial rates were determined from the slope of a tangent line to the progress curve that intersects through the origin. This is found by taking the derivative of y in eq 2 with respect to t when the latter is set equal to zero (eq 3) and is converted to rates of nitronate formation using the experimentally determined $\Delta\varepsilon_{228\ nm}$ value[2] and correcting by the 1 cm path length (l) used as explained previously (*19*). The overall rate of product formation determined in this fashion was converted to enzymatic reaction rates by subtraction of the nonenzymatic component determined under the same conditions. Second-order rate constants, $(k_{cat}/K_m)_{nox}$, for the enzymatic reaction of ethylnitronate formation and release were determined by fitting initial rate data to eq 4, where S is the concentration of substrate. The pH dependence of $(k_{cat}/K_m)_{nox}$ was determined by fitting the initial rate data to eq 5, which describes a curve with a slope of +1 and a plateau region at high pH. *C* is the pH independent value of $(k_{cat}/K_m)_{nox}$ and K_a is the dissociation constant for the ionizable group. The pH dependence of both the $^D(k_{cat}/K_m)_{nox}$ value and the UV-visible

---

[2] The acetaldehyde and nitrite products of the oxidative pathway of the enzyme do not significantly absorb light at 228 nm as compared with ethylnitronate and were thus not taken into account when calculating rates of nitronate formation.

absorbance spectrum of the enzyme were determined by fitting the data with eq 6, which describes a curve with plateau regions at both high and low pH. Y_L and Y_H are the limiting values at low and high pH, respectively, and K_a is the dissociation constant for the ionizable groups. Stopped-flow traces monitoring the reductive half reaction of the enzyme were fit to eq 7, which describes a single exponential process where k_{obs} is the observed rate constant for flavin reduction, A_t is the absorbance at time t, and A is the final absorbance. Pre-steady state kinetic parameters were determined using eq 8, where k_{obs} is the observed rate of flavin reduction, k_{red} is the limiting rate constant for flavin reduction at saturating substrate concentrations, K_d is the dissociation constant for substrate binding and S is the concentration of substrate. The pH dependence of the reductive half reaction was determined by fitting the data with eq 9, which describes a curve that decreases from an upper limiting value at low pH to a lower limiting plateau at an intermediate pH range and then with a slope of -1 at high pH. Y_L and Y_I are the limiting values at low and intermediate pH, respectively, and K_a is the dissociation constant for the ionizable groups.

$$v_0 = A_o + k_{obs}t \qquad (1)$$

$$A_{228} = A_o + b\ln\left(1+\frac{t}{x}\right) \qquad (2)$$

$$v_0 = \left(\frac{b}{x}\right)\left(\frac{1}{\Delta\varepsilon_{228nm}l}\right) \qquad (3)$$

$$\frac{v_o}{e} = \left(\frac{k_{cat}}{K_m}\right)_{nox} S \qquad (4)$$

$$\log\left(\frac{k_{cat}}{K_m}\right)_{nox} = \log\left(\frac{C}{1+\dfrac{10^{-\text{pH}}}{10^{-\text{p}K_a}}}\right) \tag{5}$$

$$\log Y = \log\frac{Y_L + Y_H\left(\dfrac{10^{-pK_a}}{10^{-pH}}\right)}{1+\left(\dfrac{10^{-pK_a}}{10^{-pH}}\right)} \tag{6}$$

$$A_{total} = A_t e^{-k_{obs}t} + A \tag{7}$$

$$k_{obs} = \frac{k_{red}S}{K_d + S} \tag{8}$$

$$\log k_{red} = \log\left(\frac{Y_L}{1+\dfrac{10^{-pKa_1}}{10^{-pH}}} + \frac{Y_I}{1+\dfrac{10^{-pKa_2}}{10^{-pH}}}\right) \tag{9}$$

6.4 Results

Effects of pH on the $^D(k_{cat}/K_m)_{nox}$ Values with Nitroethane as Substrate for the Nonoxidative Catalytic Pathway. The pH dependence of the kinetic isotope effect on the k_{cat}/K_m value of *N. crassa* 2-NPD with [1,1-^{2}H$_2$]nitroethane as substrate was determined in air-saturated 50 mM sodium pyrophosphate in the pH range from 6.0 to 10.0 at 30 $^\circ$C by following nitronate formation during turnover. The kinetic isotope effect on the k_{cat}/K_m, denoted as $^D(k_{cat}/K_m)_{nox}$[3], decreased from an upper limiting value of 23 ± 1 at low pH to a lower limiting value at high pH

---

[3] For clarity, subscripts are placed next to the kinetic parameters described in this report to denote the method in which they were determined. Thus, $(k_{cat}/K_m)_{ox}$ refers to the kinetic parameter determined through measurements of oxygen consumption and $(k_{cat}/K_m)_{nox}$ refers to that obtained by following nitronate formation. The corresponding kinetic isotope effects on these values are expressed using the familiar superscript and are written as $^D(k_{cat}/K_m)_{ox}$ or $^D(k_{cat}/K_m)_{nox}$.

of 11 ± 1 (Figure 1A). For comparison, the pH profile of the $^{D}(k_{cat}/K_m)_{ox}$ values previously

determined by measuring rates of oxygen consumption with [1,1-^{2}H$_2$]nitroethane as substrate

yielded a similar pH-dependent behavior with limiting values of 7.4 ± 0.3 at low pH and 3.5 ±

0.1 at high pH (Figure 1A) (*18*). Those limiting values are 3.1 ± 0.2 and 3.1 ± 0.3 times lower

than those determined here for $^{D}(k_{cat}/K_m)_{nox}$ at low and high pH, respectively. In agreement with

previous studies on the pH profile of the $(k_{cat}/K_m)_{ox}$ values for the oxidative pathway (*19*), the pH

profiles for the $(k_{cat}/K_m)_{nox}$ values with both nitroethane and [1,1-^{2}H$_2$]nitroethane as substrate

showed the requirement for an unprotonated group for nitronate formation (Figure 1B). This is

the expected pattern given that deprotonation of nitroethane occurs in a kinetic step that is

common to both the nonoxidative and the oxidative catalytic pathways (Scheme 1). The kinetic

parameters obtained by measuring nitronate formation and oxygen consumption are summarized

in Table 1.
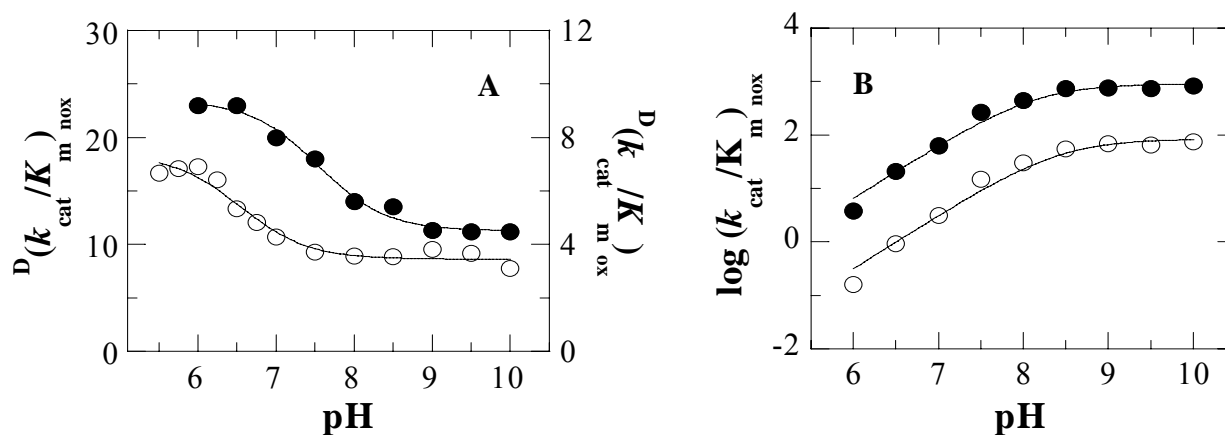
Figure 6.1 pH Dependence of $^{D}(k_{cat}/K_m)_{nox}$ and $^{D}(k_{cat}/K_m)_{ox}$ with [1,1-^{2}H]nitroethane as substrate for *N. crassa* 2-NPD.
Panel A: The $^{D}(k_{cat}/K_m)$ values were calculated from ratio of k_{cat}/K_m with nitroethane as substrate for the enzyme to that with [1,1-^{2}H]nitroethane measured by following nitronate formation (•) or oxygen consumption (o) during turnover. The data for $^{D}(k_{cat}/K_m)_{ox}$ are taken from ref 18. Each curve is a fit of the data to eq 6. Panel B: The $(k_{cat}/K_m)_{nox}$ values were determined by monitoring the increase in absorbance at 228 nm that results from mixing enzyme with either nitroethane (•) or 1,1-^{2}H$_2$-nitroethane (o) as a function of pH at 30 °C. Data were fit with eq 5. The data for the $(k_{cat}/K_m)_{nox}$ pH profile are from ref 19.

Table 6.1 pH Dependence of the $(k_{cat}/K_m)_{nox}$ and $(k_{cat}/K_m)_{ox}$ Values of *N. crassa* 2-NPD with Either Nitroethane or [1,1-^{2}H]Nitroethane as Substrate

pH	$(k_{cat}/K_{NE})_{nox}$ [b,c] $\text{M}^{-1}\text{s}^{-1}$	$(k_{cat}/K_{DNE})_{nox}$ [d] $\text{M}^{-1}\text{s}^{-1}$	$(k_{cat}/K_{NE})_{ox}$ [b,e] $\text{M}^{-1}\text{s}^{-1}$	$(k_{cat}/K_{DNE})_{ox}$ [d,e] $\text{M}^{-1}\text{s}^{-1}$	$^D(k_{cat}/K_m)_{nox}$	$^D(k_{cat}/K_m)_{ox}$
6.0	4 ± 1	0.162 ± 0.004	50 ± 1	7 ± 1	23 ± 1	6.9 ± 0.1
6.5	20 ± 1	0.925 ± 0.045	100 ± 4	20 ± 1	23 ± 1	5.0 ± 0.3
7.0	60 ± 2	3.11 ± 0.05	200 ± 10	50 ± 2	20 ± 1	4.3 ± 0.1
7.5	265 ± 4	14.7 ± 0.2	350 ± 5	95 ± 5	18 ± 1	3.7 ± 0.2
8.0	450 ± 10	30 ± 2	675 ± 20	180 ± 5	14 ± 1	3.6 ± 0.2
8.5	730 ± 16	54 ± 2	800 ± 25	225 ± 15	13 ± 1	3.6 ± 0.1
9.0	760 ± 10	68 ± 1	375 ± 20	100 ± 10	11 ± 1	3.7 ± 0.4
9.5	740 ± 23	66 ± 3	185 ± 10	50 ± 3	11 ± 1	3.7 ± 0.3
10.0	830 ± 25	74 ± 3	155 ± 10	50 ± 4	11 ± 1	3.1 ± 0.3

[a] All assays were carried out in 50 mM sodium pyrophosphate at 30 °C. [b] With nitroethane as substrate. [c] From ref 19. [d] With [1,1-^{2}H]nitroethane as substrate. [e] From ref 18.

Effects of pH on the $^D(k_{red})$ Values with Ethylnitronate as Substrate for the Oxidative Catalytic Pathway. Previous studies have shown that the ethylnitronate product of the nonoxidative pathway of *N. crassa* 2-NPD is also an effective substrate for oxidative turnover of the enzyme (*18-20*). The pH dependence of the kinetic isotope effect on flavin reduction in the oxidative pathway of *N. crassa* 2-NPD with [1-^{2}H]ethylnitronate as substrate was determined in 50 mM sodium pyrophosphate in the pH range from 6.0 to 10.1 at 30 °C. Consistent with previous studies on the reductive half reaction of the enzyme (*18, 19*), anaerobic mixing of *N. crassa* 2-NPD with ethylnitronate resulted in the formation of an anionic flavosemiquinone with absorbance bands in the ~370 and ~470 nm regions (Figure 2A). As shown in Figure 2B for the example at pH 8.0, at any pH tested the rate of flavin reduction increased hyperbolically with substrate concentration and was the same irrespective of whether ethylnitronate or [1-^{2}H]ethylnitronate was used as substrate. Indeed, the kinetic isotope effect on the limiting rates of flavin reduction ($^D k_{red}$) was pH independent in the range from 6.0 to 10.1 with an average value of 0.99 ± 0.06 (Table 2). This is an expected result since the single electron transfer reaction from an enzyme-bound ethylnitronate to the flavin does not involve hybridization changes of the
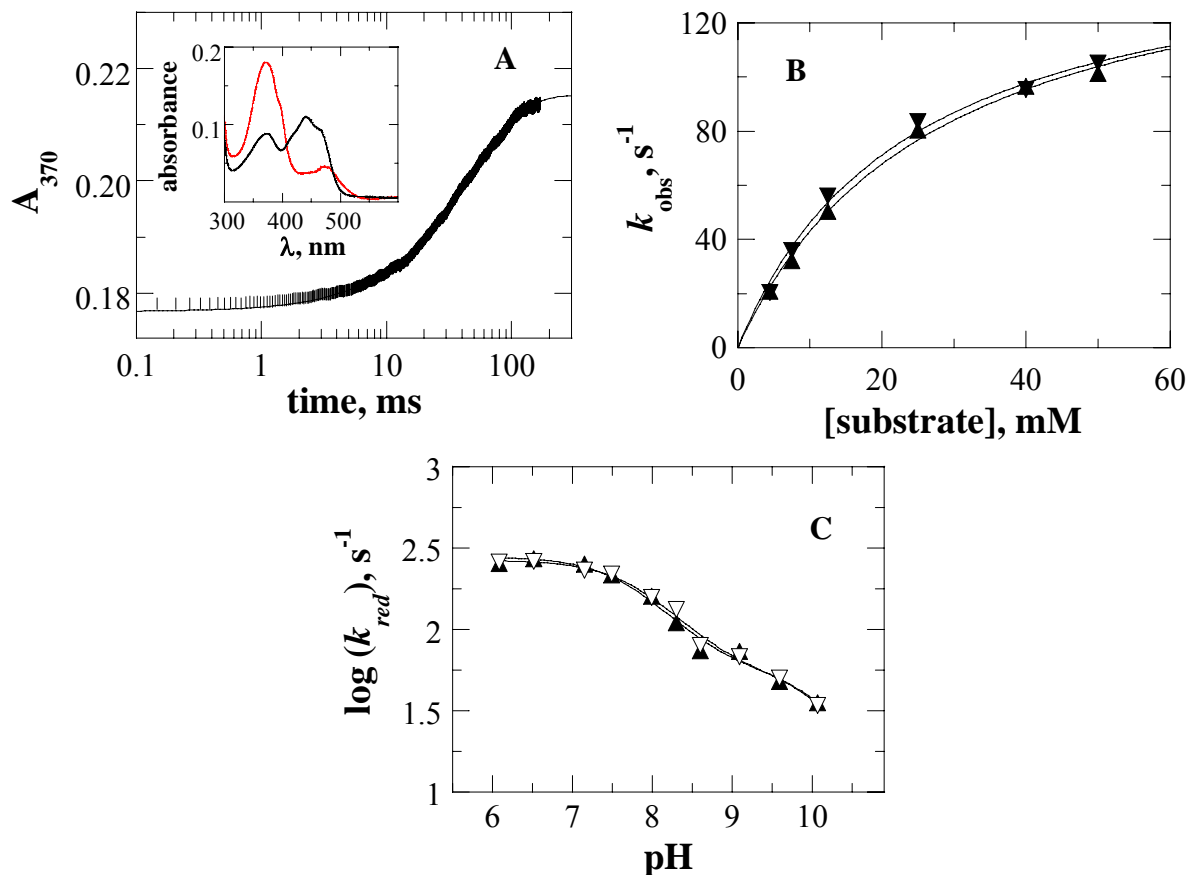
Figure 6.2 pH Dependence of the $^D k_{red}$ value with [1-^{2}H]ethylnitronate as substrate for *N. crassa* 2-NPD.

Panel A: The absorbance at 370 nm was monitored over time after anaerobic mixing of *N. crassa* 2-NPD with ethylnitronate at pH 8.0 and 30 °C to give final concentrations of 15 μM enzyme and 4.5 mM substrate. The time indicated is after the end of flow (2.2 ms). *Inset.* Flavin absorbance spectra before (black) and ~30 s after (red) anaerobic mixing of the enzyme with ethylnitronate. Panel B: Rates of flavin reduction determined from fits of stopped-flow traces to eq 7 were plotted as function of either ethylnitronate (▲) or [1-^{2}H]ethylnitronate (▼) concentration and were fit with eq 8 to obtain limiting rates of flavin reduction (k_{red}). Panel C: The pH profile of k_{red} with ethylnitronate (▲) or [1-^{2}H]ethylnitronate (∇) in the pH range from 6.0-10.1. The data were fit with eq 9.

Table 6.2 pH Dependence of the Reductive Half Reaction of *N. crassa* 2-NPD with Either Ethylnitronate or [1-²H]Ethylnitronate as Substrate

pH	$k_{red(H)}$ [b], s^{-1}	$k_{red(D)}$ [c], s^{-1}	$^D k_{red}$	$K_{d(H)}$ [b], mM	$K_{d(D)}$ [c], mM
6.1	255 ± 30	260 ± 70	1.0 ± 0.3	15 ± 2	15 ± 5
6.5	270 ± 90	260 ± 90	1.0 ± 0.5	25 ± 10	30 ± 10
7.15	250 ± 10	230 ± 10	1.1 ± 0.1	30 ± 3	25 ± 2
7.5	220 ± 10	220 ± 10	1.1 ± 0.1	25 ± 2	30 ± 3
8.0	160 ± 10	160 ± 10	1.1 ± 0.1	30 ± 3	25 ± 4
8.3	110 ± 3	125 ± 5	0.9 ± 0.1	10 ± 1	10 ± 1
8.6	75 ± 10	80 ± 10	0.9 ± 0.1	35 ± 6	40 ± 7
9.1	70 ± 5	70 ± 5	1.0 ± 0.1	25 ± 5	20 ± 3
9.6	50 ± 4	50 ± 5	1.0 ± 0.1	40 ± 5	40 ± 10
10.1	35 ± 2	35 ± 3	1.0 ± 0.1	20 ± 5	20 ± 5

[a] *N. crassa* 2-NPD was anaerobically mixed with substrate in 50 mM sodium pyrophosphate at 30 °C in a stopped-flow spectrophotometer and the absorbance changes at 370 or 440 nm were monitored over time. [b] With ethylnitronate as substrate. [c] With [1-²H]ethylnitronate as substrate.
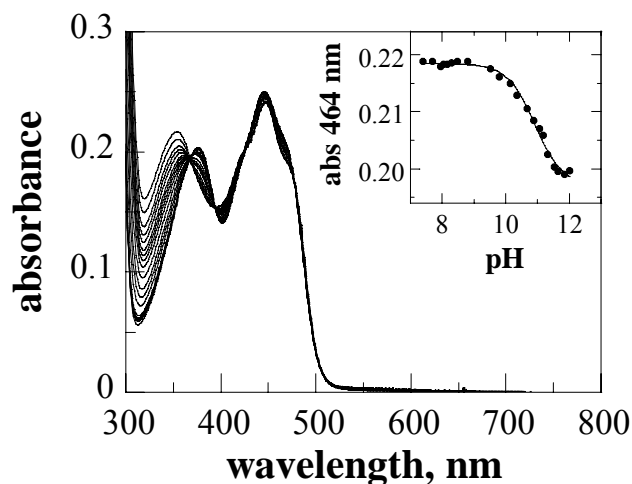
Figure 6.3 pH Dependence of the UV-visible absorbance properties of *N. crassa* 2-NPD. UV-Visible absorbance spectra of the enzyme (21 μM) were recorded in 50 mM sodium phosphate at 10 °C in the pH range from 7.4-12.0 *Inset.* UV-visible absorbance values at 464 nm as a function of pH. The data were fit with eq 6.

α-carbon of the substrate. The limiting rates of flavin reduction (k_{red}) with both isotopomers decreased from a limiting value of ~220 s^{-1} at low pH to lower values with increasing pH, showing the presence of two pK_a values for groups that need to be protonated for catalysis (Figure 2C). The lower pK_a values of 7.8 ± 0.1 and 8.0 ± 0.1 seen with ethylnitronate and [1-²H]ethylnitronate, respectively, are consistent with previous results obtained on the steady-state kinetics for the oxidative pathway suggesting the involvement of electrostatic

catalysis in the formation of the anionic flavosemiquinone[4] (18). The requirement of a second

protonated group with a pK_a value of ≥ 10.3 was also observed in the pH profiles of the k_{red}

values (Figure 2C). This pK_a is possibly due to the deprotonation of the N(3) atom of the

enzyme-bound FMN, which was independently shown in a pH titration of the UV-visible

absorbance spectrum of the enzyme to have a pK_a of 10.9 ± 0.2 (Figure 3). The negative charge

formed upon ionization of the N(3) atom of the flavin at high pH would prevent the single

electron transfer reaction from the nitronate and would give rise to the pH dependence observed

for the reductive half reaction of the enzyme (Figure 2C).

6.5   Discussion

Partitioning of reaction intermediates during turnover of an enzyme utilizing a branched

kinetic mechanism can result in an inflation of the observed kinetic isotope effect well above the

intrinsic value associated with bond cleavage as illustrated in the results of the current study.

Branching during turnover of *N. crassa* 2-NPD with nitroethane as substrate occurs after the

nitroalkane is deprotonated by histidine 196 (k_3) and involves the partitioning of the resulting

enzyme-ethylnitronate complex through nonoxidative and oxidative pathways (Scheme 2) (*19*).

Ethylnitronate is released as a reaction product during nonoxidative turnover (k_{13}), but is retained

in the active site in the oxidative pathway that results from a single electron transfer reaction

with the enzyme-bound flavin cofactor (k_5). The formation of the ethylnitronate product during

nonoxidative turnover can be mointered spectrophotometrically to determine recation rates as

---

[4] The pH profile of the k_{cat}/K_m value with ethylnitronate as substrate was previously fit to an equation describing the requirement of a single protonated group for catalysis [*Biochemistry* **2006,** 45, (46), 13889]. The fit resulted in an apparent outlier at pH 8.5 which, despite repeated measurements, showed a k_{cat}/K_m value lower than expected from the curve. The increased precision provided by the stopped-flow measurements reported here showed that the pH profile of the k_{red} value shows a plateau region in the pH range from ~8.5-9.0. This plateau is likely displayed in the k_{cat}/K_m pH profile, but was not defined due to the less precise measurements of enzyme activity reported in that study [*Biochemistry* **2006,** 45, (46), 13889].
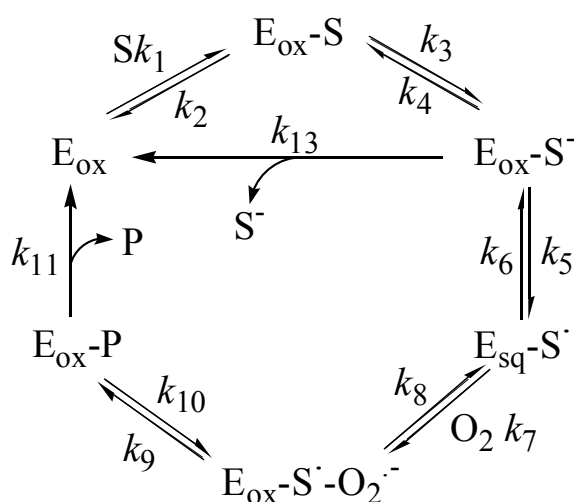
Scheme 6.4 Proposed steady-state kinetic mechanism of *N. crassa* 2-NPD with nitroethane as substrate.
E_{ox} is the oxidized form of enzyme; E_{sq} is the flavosemiquinone form of enzyme; S is nitroethane; S^- is ethylnitronate, $S^{\cdot}$ and P is a radical intermediate and the product of the oxidative pathway of the enzyme, respectively. Note that the kinetic steps for the release of ethylnitronate (S^-) and the oxidative product (P) are shown as being irreversible because initial rates were measured in the absence of these species.

carried out in this and a previous study of the enzyme (*19*). Alternatively, rates of oxygen consumption during oxidative catalysis can be measured to determine enzymatic activity as described previously (*18*). Both methods have been used to measure the second-order rate constant, k_{cat}/K_m, for the reaction of *N. crassa* 2-NPD with nitroethane as substrate (*18, 19*). The k_{cat}/K_m values determined from these methods are fundamentally different kinetic parameters for the enzyme as evident from the differences in the magnitude, pH dependence and extent to which a kinetic isotope effect is expressed when each assay is used to measure activity (*18, 19*).

The differences in the kinetic parameters determined by following either nitronate formation or oxygen consumption are readily explained by considering the branched nature of the catalytic cycle of the enzyme. The general definition of the k_{cat}/K_m value for an enzymatic reaction states that the kinetic parameter is a reflection of the rate of substrate capture into productive enzyme complexes destined to form products at some later time (*21, 22*). Branching during turnover of *N. crassa* 2-NPD with nitroethane as substrate results in multiple destinations for the enzyme-nitronate complex, which gives rise to the different k_{cat}/K_m values. Following the reaction by monitoring nitronate formation gives a $(k_{cat}/K_m)_{nox}$ value that reflects the rate of

capture of nitroethane into productive complexes destined to form ethylnitronate at some later time (Scheme 2). When oxygen consumption is measured, the resulting $(k_{cat}/K_m)_{ox}$ value reflects capture rates for productive complexes destined to form the products of the oxidative catalytic pathway of the enzyme (Scheme 2).

Branching of the enzyme-ethylnitronate intermediate formed with nitroethane as substrate for *N. crassa* 2-NPD affects the k_{cat}/K_m values for the reaction because all of the kinetic steps leading to its formation are reversible (Scheme 2). In general, an analytical expression for the k_{cat}/K_m value of an enzymatic reaction includes rate constants for all kinetic steps from substrate binding up to and including the first irreversible step of the mechanism (*23*). As shown in Scheme 2, the branch point in the kinetic mechanism of *N. crassa* 2-NPD occurs after the reversible steps of substrate binding (k_1, k_2) and the proton abstraction with histidine 196 (k_3, k_4). Substrate binding is reversible at the low concentrations of nitroethane used when k_{cat}/K_m is measured. The subsequent proton transfer reaction is also reversible as evident from previous studies demonstrating that the enzyme utilizes a sequential steady state kinetic mechanism with nitroethane as substrate (*18, 20*). The reversibility of the steps leading to the branch point expands the expression for k_{cat}/K_m to include all of the rate constants leading to the first irreversible steps of each catalytic pathway of the enzyme. In the nonoxidative pathway this includes only the nitronate release step (k_{13}), which is irreversible because initial rates were measured in the absence of ethylnitronate. At saturating concentrations of oxygen, the net flux of the enzyme-nitronate intermediate through the flavin reduction step (k_5, k_6) in the oxidative pathway becomes practically irreversible (*23*). This is because the bimolecular oxidation of the flavosemiquinone becomes significantly faster than its formation (i.e. $O_2k_7 \gg k_5$) when oxygen is saturating, thereby depleting the steady-state concentration of the reduced enzyme-nitronate

radical complex (E_{sq}-S$^{.}$ in Scheme 2) that would be required needed for the reverse electron transfer reaction (k_6). The k_{cat}/K_m values for the *N. crassa* 2-NPD reaction therefore includes only the kinetic steps for the formation and break down of the enzyme-nitroethane Michaelis complex (k_1, k_2), the reversible proton abstraction from the nitroalkane (k_3, k_4) and the partitioning of the enzyme-nitronate complex through the release of ethylnitronate as a product (k_{13}) and flavin reduction (k_5). Expressions for both $(k_{cat}/K_m)_{nox}$ and $(k_{cat}/K_m)_{ox}$ were derived using the method of King and Altman (*24*) to give eqs 10 and 11:[5]

$$\left(\frac{k_{cat}}{K_m}\right)_{nox} = k_{13}\left(\frac{k_1 k_3}{k_2 (k_4 + k_5 + k_{13})}\right)$$

(10)

$$\left(\frac{k_{cat}}{K_m}\right)_{ox} = k_5\left(\frac{k_1 k_3}{k_2 (k_4 + k_5 + k_{13})}\right)$$

(11)

A comparison of the k_{cat}/K_m values with nitroethane as substrate for *N. crassa* 2-NPD reveals how the enzyme-ethylnitronate complex formed during turnover partitions through the nonoxidative and oxidative catalytic pathways. Each value describes identical productive complexes that form as a result of nitroethane binding to the enzyme (k_1) and the deprotonation of the nitroalkane by the active site residue histidine 196 (k_3) (*19*). Since the same productive complexes are described by each expression, the kinetic steps leading to their steady-state formation and breakdown must also be the same. This is reflected in the parenthesis of the expressions for k_{cat}/K_m shown in eqs 10 and 11. Taking the ratio of these k_{cat}/K_m values cancels

---

[5] The simplified expressions for k_{cat}/K_m are based on experimental data made in a previous report [*Biochemistry* **2006,** 45, (46), 13889] showing that the enzyme is saturated with oxygen under atmospheric conditions across the pH range tested and that the kinetic step $k_2 \gg k_3$. This was shown through measurements of the K_m for oxygen and from the lack of solvent viscosity effects on the $(k_{cat}/K_m)_{ox}$ value with nitroethane as substrate for the enzyme, respectively. The previous derivation of $(k_{cat}/K_m)_{ox}$ assumed that $k_{13} \gg k_5$ based on the lack of solvent viscosity effects on k_{cat}/K_m with ethylnitronate as substrate [*Biochemistry* **2006,** 45, (46), 13889]. This assumption was not applied in the current study with nitroethane as substrate because the observation of both oxygen consumption and nitronate release during turnover clearly demonstrates that k_{13} is comparable to k_5.

the terms in the parenthesis to provide a direct measure of how the enzyme-ethylnitronate complex partitions between nitronate release (k_{13}) and flavin reduction (k_5) as shown in eq 12. The partition ratios (P) of the *N. crassa* 2-NPD reaction with either nitroethane or [1,1-^{2}H]nitroethane calculated from eq 12 are shown in Table 3.

$$P = \frac{\left(k_{cat}/K_m\right)_{nox}}{\left(k_{cat}/K_m\right)_{ox}} = \frac{k_{13}}{k_5} \tag{12}$$

A partition isotope effect is expressed on the *N. crassa* 2-NPD reaction as the result of a kinetic isotope effect on the release of the nitronate formed with either nitroethane or [1,1-^{2}H]nitroethane as substrate. Evidence supporting this conclusion comes from the differences in the partition ratios calculated with nitroethane and [1,1-^{2}H]nitroethane (Table 3) and the lack of a kinetic isotope effect on the reductive half reaction of the enzyme. Partition ratios for the reaction catalyzed by *N. crassa* 2-NPD reflect the relative rates of nitronate release (k_{13}) and flavin reduction (k_5) (eq 12). Since the limiting rate constant for flavin reduction with

Table 6.3 Partition Ratios with Nitroethane or
[1,1-^{2}H]Nitroethane as Substrate for *N. crassa* 2-NPD

pH	P_H[b]	P_D[b]	P_H/P_D
6.0	0.08 ± 0.02	0.023 ± 0.003	3.5 ± 1.0
6.5	0.20 ± 0.01	0.046 ± 0.003	4.3 ± 0.4
7.0	0.30 ± 0.02	0.062 ± 0.003	4.8 ± 0.4
7.5	0.76 ± 0.02	0.16 ± 0.01	4.8 ± 0.3
8.0	0.67 ± 0.03	0.17 ± 0.01	3.9 ± 0.3
8.5	0.91 ± 0.04	0.24 ± 0.02	3.8 ± 0.3
9.0	2.0 ± 0.1	0.68 ± 0.07	2.9 ± 0.3
9.5	4.0 ± 0.3	1.3 ± 0.1	3.1 ± 0.3
10.0	5.4 ± 0.4	1.5 ± 0.1	3.6 ± 0.4

[a] In 50 mM sodium pyrophosphate at 30 °C. [b] Partition ratios with nitroethane (P_H) or [1,1-^{2}H]nitroethane (P_D) obtained by dividing the k_{cat}/K_m value measured by monitoring rates of nitronate formation to that determined by measuring rates of oxygen consumption.

ethylnitronate is not isotope sensitive, the partition isotope effect must arise from different rates of nitronate release with nitroethane or $[1,1\text{-}^2\text{H}]$nitroethane as substrate for the enzyme. The kinetic isotope effect on nitronate release likely arises from the deprotonation of histidine 196, which was previously shown to be the catalytic base for the reaction of the enzyme with nitroethane as substrate (*19*). The positive charge formed on the imidazolium side chain of histidine 196 as a result of the proton transfer reaction with nitroethane likely establishes electrostatic interactions with the anionic nitronate intermediate to keep it bound in the active site for oxidation. Deprotonation of histidine 196 would disrupt these interactions to promote nitronate release and would be isotope sensitive since it involves the transfer of a deuteron instead of a proton when $[1,1\text{-}^2\text{H}]$nitroethane is the substrate. The role of histidine 196 for nitronate release is supported by both the partition ratios for the reaction, which increase with increasing pH, and the magnitude of the partition isotope effects of the reaction (Table 3), which are within the range of between 3 and 4 previously reported for the kinetic isotope effect on the deprotonation of imidazolium (*26, 27*).

The partition isotope effect expressed on nonoxidative turnover of *N. crassa* 2-NPD with nitroethane as substrate inflates the observed limiting $^D(k_{cat}/K_m)_{nox}$ above the intrinsic value associated with the deprotonation of the nitroalkane. The increase in the limiting value of the $^D(k_{cat}/K_m)_{nox}$ at low pH from that previously determined for $^D(k_{cat}/K_m)_{ox}$ (*i*.e. 23 versus 7.4 at low pH) (*18*) corresponds well with the partition isotope effect of ~3 that can be calculated from the P_H and P_D values shown in Table 3. Only the limiting values of $^D(k_{cat}/K_m)$ can be compared in this analysis because pH effects alter the kinetic isotope effects measured with each assay (eqs 13 and 14; derivations are shown in SI). As the pH is raised above the pK_a of histidine 196, the rate of nitronate release (k_{13}) increases, while the rates of nitronate oxidation (k_5) and protonation

(k_4) decrease to a limiting value and zero, respectively. Thus, the partition ratio increases from a lower limiting value at low pH to an upper limiting value at high pH, while the reverse commitment to catalysis decreases from an upper limiting value at low pH to zero. As shown in eqs 13 and 14, the increase in the partition ratio with increasing pH results in a decrease in the $^D(k_{cat}/K_m)$ values for the reaction. Since the isotope effect on the partition ratio arises from different rates of nitronate release (k_{13}) during nonoxidative turnover of the enzyme with nitroethane as substrate and not from different rates of electron transfer (k_5) it is only expressed on $^D(k_{cat}/K_m)_{nox}$ (eq 14). As shown in eq 14, the overall $^D(k_{cat}/K_m)_{nox}$ value of *N. crassa* 2-NPD is therefore given by both a primary isotope effect arising from CH bond cleavage ($^D(k_{cat}/K_m)_{ox}$) and a partition isotope effect resulting from different rates of nitronate release with nitroethane and [1,1-^{2}H]nitroethane as substrate ($^Dk_{13}$). Thus, the limiting $^D(k_{cat}/K_m)_{nox}$ of ~23 is inflated from the intrinsic value ~8 to 9, which was previously measured for the deprotonation of nitroethane in solution (*28, 29*).

$$
^D\left(\frac{k_{cat}}{K_m}\right)_{ox} = \frac{^Dk_3 + {}^Dk_3\left(\dfrac{1}{^Dk_{13}}P\right) + {}^DK_{eq3}C_r}{1 + C_r + P}
\tag{13}
$$

where $P = \dfrac{k_{13}}{k_5}$, $C_r = \dfrac{k_4}{k_5}$ and $^DK_{eq3} = \dfrac{^Dk_3}{^Dk_4}$

$$
^D\left(\frac{k_{cat}}{K_m}\right)_{nox} = {}^Dk_{13} \; {}^D\left(\frac{k_{cat}}{K_m}\right)_{ox}
\tag{14}
$$

The present investigation of the *N. crassa* 2-NPD reaction represents the first instance of an enzymatic reaction where the observed kinetic isotope effect is inflated well above the intrinsic value that is associated with CH bond cleavage because of the branching of a reaction intermediate. This study therefore complements previous works on other enzymes showing that

branching of reaction intermediates can inflate observed kinetic isotope effects observed for one pathway to their intrinsic values (*7, 13*) or, as is more commonly observed, decrease the magnitude of the observed kinetic isotope effect (*1-5, 30*). A rate-limiting step involving bond cleavage may therefore give rise to a kinetic isotope effect that is inflated from the intrinsic value or is completely abated due to the presence of branching in the kinetic mechanism of an enzyme.

6.6 Acknowledgements

6.7 Supporting Information

Derivation of (k_{cat}/K_m)$_{nox}$. The initial rate equation for the branched mechanism of Scheme 2 that applies when the reaction is followed by monitoring nitronate release during enzymatic turnover with nitroethane is given by:

$$\frac{v_o}{e} = \left[ES^-\right] k_{13} \tag{1}$$

Where ES$^-$ is the enzyme-ethylnitronate complex.

The [ES$^-$] can be converted into kinetic rate constants by applying the method of King and Altman [King, E.L. and Altman, C. (1956) *J. Phys. Chem. 60*, 1375-1378] to express the initial rate equation as:

$$\frac{v_o}{e} = \frac{AO_2 k_1 k_3 k_7 k_9 k_{11} k_{13} + A k_1 k_3 k_6 k_9 k_{11} k_{13}}{A(k_1 k_3 k_5 k_9 k_{11} \ldots + k_1 k_6 k_9 k_{11} k_{13}) + O_2(k_2 k_4 k_7 k_9 k_{11} \ldots + k_3 k_7 k_9 k_{11} k_{13})}$$
$$+ AO_2(k_1 k_3 k_5 k_7 k_9 \ldots + k_1 k_7 k_9 k_{11} k_{13}) + k_2 k_4 k_6 k_9 k_{11} \ldots + k_3 k_6 k_9 k_{11} k_{13}$$

(2)

Where A = [Nitroethane].

Since O_2 is saturating under the atmospheric conditions used [Francis, K. and Gadda, (2006) *Biochemistry 45*, 13889-13898] the net flux of the enzyme enzyme-nitronate intermediate through the flavin reduction step becomes practically irreversible. The expression for $(k_{cat}/K_m)_{nox}$ after canceling common terms in both the numerator and denominator is therefore given by:

$$\left(\frac{k_{cat}}{K_m}\right)_{nox} = \frac{k_1 k_3 k_{13}}{k_3 k_5 + k_2 k_5 + k_2 k_4 + k_2 k_{13} + k_3 k_{13}}$$

(3)

Based on the lack of solvent viscosity effects previously measured for $(k_{cat}/K_m)_{ox}$ $k_2 \gg k_3$ [Francis, K. and Gadda, (2006) *Biochemistry 45*, 13889-13898]. Grouping these terms in the denominator and canceling k_3 gives:

$$\left(\frac{k_{cat}}{K_m}\right)_{nox} = \frac{k_1 k_3 k_{13}}{k_2 k_5 + k_2 k_{13} + k_2 k_4}$$

(4)

Or as described in the text:

$$\left(\frac{k_{cat}}{K_{NE}}\right)_{nox} = k_{13}\left(\frac{k_1 k_3}{k_2(k_4 + k_5 + k_{13})}\right)$$

(5)

Derivation of $(k_{cat}/K_m)_{ox}$. The initial rate equation for the branched mechanism of Scheme 2 that applies when the reaction is followed by monitoring oxygen consumption during enzymatic turnover with nitroethane is given by:

$$\frac{v_o}{e} = [EP]k_{11} \tag{6}$$

Where EP is the enzyme-peroxynitroethane complex.

The [EP] can be converted into kinetic rate constants by applying the method of King and Altman [King, E.L. and Altman, C. (1956) *J. Phys. Chem. 60*, 1375-1378] to express the initial rate equation as:

$$\frac{v_o}{e} = \frac{AO_2 k_1 k_3 k_5 k_7 k_9 k_{11}}{A(k_1 k_3 k_5 k_9 k_{11} \ldots + k_1 k_6 k_9 k_{11} k_{13}) + O_2(k_2 k_4 k_7 k_9 k_{11} \ldots + k_3 k_7 k_9 k_{11} k_{13})} \\ + AO_2(k_1 k_3 k_5 k_7 k_9 \ldots + k_1 k_7 k_9 k_{11} k_{13}) + k_2 k_4 k_6 k_9 k_{11} \ldots + k_3 k_6 k_9 k_{11} k_{13} \tag{7}$$

Where $A = $ [Nitroethane].

The expression for $(k_{cat}/K_m)_{ox}$ after canceling common terms in both the numerator and denominator is therefore given by:

$$\left(\frac{k_{cat}}{K_m}\right)_{ox} = \frac{k_1 k_3 k_5}{k_2 k_4 + k_2 k_5 + k_2 k_{13} + k_3 k_5 + k_3 k_{13}} \tag{8}$$

Based on the lack of solvent viscosity effects previously measured for $(k_{cat}/K_m)_{ox}$ $k_2 \gg k_3$ [Francis, K. and Gadda, (2006) *Biochemistry 45*, 13889-13898]. Grouping these terms in the denominator and canceling k_3 gives:

$$\left(\frac{k_{cat}}{K_m}\right)_{ox} = \frac{k_1 k_3 k_5}{k_2 k_4 + k_2 k_5 + k_2 k_{13}} \tag{9}$$

Or as described in the text:

$$\left(\frac{k_{cat}}{K_{NE}}\right)_{ox} = k_5 \left(\frac{k_1 k_3}{k_2(k_4 + k_5 + k_{13})}\right) \tag{10}$$

Derivation of $^D(k_{cat}/K_m)_{ox}$. In the mechanism of Scheme 2, the kinetic steps k_3, k_4 and k_{13} are isotope sensitive. Taking the ratio of $(k_{cat}/K_m)_{ox}$ with nitroethane and $[1,1-{}^2H_2]$nitroethane therefore gives:

$$^D\left(\frac{k_{cat}}{K_m}\right)_{ox} = \frac{k_1 k_3 k_5}{k_2 k_4 + k_2 k_5 + k_2 k_{13}} \times \frac{k_2 k_{4D} + k_2 k_5 + k_2 k_{13D}}{k_1 k_{3D} k_5} = \frac{k_3 k_{4D} + k_3 k_5 + k_3 k_{13D}}{k_{3D} k_4 + k_{3D} k_5 + k_{3D} k_{13}} \qquad (11)$$

Or:

$$^D\left(\frac{k_{cat}}{K_m}\right)_{ox} = {}^D k_3 \left(\frac{k_{4D} + k_5 + k_{13D}}{k_4 + k_5 + k_{13}}\right) \qquad (12)$$

Where the subscript D denotes the rate of the kinetic step with $[1,1-{}^2H_2]$nitroethane as substrate.

Dividing each term in the parenthesis by k_4 gives:

$$^D\left(\frac{k_{cat}}{K_m}\right)_{ox} = {}^D k_3 \left(\frac{\dfrac{k_{4D}}{k_4} + \dfrac{k_5}{k_4} + \dfrac{k_{13D}}{k_4}}{1 + \dfrac{k_5}{k_4} + \dfrac{k_{13}}{k_4}}\right) \qquad (13)$$

Or:

$$^D\left(\frac{k_{cat}}{K_m}\right)_{ox} = \frac{{}^D K_{eq3} + {}^D k_3 \left(\dfrac{k_5}{k_4}\right) + {}^D k_3 \left(\dfrac{k_{13D}}{k_4}\right)}{1 + \dfrac{k_5}{k_4} + \dfrac{k_{13}}{k_4}} \qquad (14)$$

Where $^D K_{eq3} = \dfrac{{}^D k_3}{{}^D k_4}$

Dividing each term by $\dfrac{k_5}{k_4}$ gives:

$$D\left(\frac{k_{cat}}{K_m}\right)_{ox} = \frac{{}^D K_{eq3}\left(\frac{k_4}{k_5}\right) + {}^D k_3 + k_{13D}\left(\frac{{}^D k_3}{k_5}\right)}{\frac{k_4}{k_5} + 1 + \frac{k_{13}}{k_5}} \tag{15}$$

Since ${}^D k_{13} = \left(\frac{k_{13}}{k_{13D}}\right)$, ${}^D k_{13}$ can be written as $\frac{k_{13}}{{}^D k_{13}}$. Inserting this expression into (15)

gives:

$$D\left(\frac{k_{cat}}{K_m}\right)_{ox} = \frac{{}^D K_{eq3}\left(\frac{k_4}{k_5}\right) + {}^D k_3 + \frac{{}^D k_3}{{}^D k_{13}}\left(\frac{k_{13}}{k_5}\right)}{\frac{k_4}{k_5} + 1 + \frac{k_{13}}{k_5}} \tag{16}$$

Defining P as $\frac{k_{13}}{k_5}$ and C_r as $\frac{k_4}{k_5}$ gives eq 14 of the main text:

$$D\left(\frac{k_{cat}}{K_m}\right)_{ox} = \frac{{}^D k_3 + {}^D k_3\left(\frac{1}{{}^D k_{13}} P\right) + {}^D K_{eq3} C_r}{1 + C_r + P} \tag{17}$$

Derivation of ${}^D(k_{cat}/K_m)_{nox}$. In the mechanism of Scheme 2, the kinetic steps k_3, k_4 and k_{13} are isotope sensitive. Taking the ratio of $(k_{cat}/K_m)_{nox}$ with nitroethane and $[1,1-{}^2H_2]$nitroethane therefore gives eq 18:

$$D\left(\frac{k_{cat}}{K_m}\right)_{nox} = \frac{k_1 k_3 k_{13}}{k_2 k_5 + k_2 k_{13} + k_2 k_4} \times \frac{k_2 k_5 + k_2 k_{13D} + k_2 k_{4D}}{k_1 k_{3D} k_{13D}} = \frac{k_3 k_{13} k_5 + k_3 k_{13} k_{13D} + k_3 k_{13} k_{4D}}{k_5 k_{3D} k_{13D} + k_{13} k_{3D} k_{13D} + k_4 k_{3D} k_{13D}}$$

Or:

$$D\left(\frac{k_{cat}}{K_m}\right)_{ox} = {}^D k_3\, {}^D k_{13}\left(\frac{k_{4D} + k_5 + k_{13D}}{k_4 + k_5 + k_{13}}\right) \tag{19}$$

Since this expression is eq 13 multiplied by $^{D}k_{13}$, the expression for $(k_{cat}/K_m)_{nox}$ is the that for $(k_{cat}/K_m)_{ox}$ multiplied by $^{D}k_{13}$ as shown in the main text:

$$^{D}\left(\frac{k_{cat}}{K_m}\right)_{nox} = {^{D}k_{13}}\left[\frac{{^{D}k_3} + {^{D}k_3}\left(\frac{1}{{^{D}k_{13}}}P\right) + {^{D}K_{eq3}}C_r}{1 + C_r + P}\right] \quad (20)$$

6.8   References

1.   Austin, R. N., Deng, D., Jiang, Y., Luddy, K., van Beilen, J. B., Ortiz de Montellano, P. R., and Groves, J. T. (2006) The diagnostic substrate bicyclohexane reveals a radical mechanism for bacterial cytochrome P450 in whole cells. *Angew. Chem. Int. Ed. Engl.* *45*, 8192-8194.

2.   Jiang, Y., He, X., and Ortiz de Montellano, P. R. (2006) Radical intermediates in the catalytic oxidation of hydrocarbons by bacterial and human cytochrome P450 enzymes. *Biochemistry 45*, 533-542.

3.   Guengerich, F. P., Miller, G. P., Hanna, I. H., Sato, H., and Martin, M. V. (2002) Oxidation of methoxyphenethylamines by cytochrome P450 2D6. Analysis of rate-limiting steps. *J. Biol. Chem. 277*, 33711-33719.

4.   Pavon, J. A., and Fitzpatrick, P. F. (2005) Intrinsic isotope effects on benzylic hydroxylation by the aromatic amino acid hydroxylases: evidence for hydrogen tunneling, coupled motion, and similar reactivities. *J. Am. Chem. Soc. 127*, 16414-16415.

5.   Hillas, P. J., and Fitzpatrick, P. F. (1996) A mechanism for hydroxylation by tyrosine hydroxylase based on partitioning of substituted phenylalanines. *Biochemistry 35*, 6969-6975.

6.   Fitzpatrick, P. F. (2003) Mechanism of aromatic amino acid hydroxylation. *Biochemistry 42*, 14083-14091.

7.   Fitzpatrick, P. F. (2006) Isotope Effects from Partitioning of Intermediates in Enzyme-Catalyzed Hydroxylation Reactions. in *Isotope Effects in Chemistry and Biology* (Kohen, A. and Limbach, H.H., Ed.) pp 861-873, Taylor and Francis, Boca Raton, Fl.

8.   Korzekwa, K. R., Swinney, D. C., and Trager, W. F. (1989) Isotopically labeled chlorobenzenes as probes for the mechanism of cytochrome P-450 catalyzed aromatic hydroxylation. *Biochemistry 28*, 9019-9027.

9.   Higgins, L., Bennett, G. A., Shimoji, M., and Jones, J. P. (1998) Evaluation of cytochrome P450 mechanism and kinetics using kinetic deuterium isotope effects. *Biochemistry 37*, 7039-7046.

10.   Miwa, G. T., Garland, W. A., Hodshon, B. J., Lu, A. Y., and Northrop, D. B. (1980) Kinetic isotope effects in cytochrome P-450-catalyzed oxidation reactions. Intermolecular and intramolecular deuterium isotope effects during the N-demethylation of N,N-dimethylphentermine. *J. Biol. Chem. 255*, 6049-6054.

11.   Jones, J. P., Korzekwa, K. R., Rettie, A. E., and Trager, W. F. (1986) Isotopically sensitive branching and its effect on the observed intramolecular isotope effects in cytochrome P-450 catalyzed reactions: a new method for the estimation of intrinsic isotope effects. *J. Am. Chem. Soc. 108*, 7074-7078.

12.   Korzekwa, K. R., Trager, W. F., and Gillette, J. R. (1989) Theory for the observed isotope effects from enzymatic systems that form multiple products via branched reaction pathways: cytochrome P-450. *Biochemistry 28*, 9012-9018.

13.   Frantom, P. A., and Fitzpatrick, P. F. (2003) Uncoupled forms of tyrosine hydroxylase unmask kinetic isotope effects on chemical steps. *J. Am. Chem. Soc. 125*, 16190-16191.

14.   Panay, A. J., and Fitzpatrick, P. F. (2008) Kinetic isotope effects on aromatic and benzylic hydroxylation by *Chromobacterium violaceum* phenylalanine hydroxylase as probes of chemical mechanism and reactivity. *Biochemistry 47*, 11118-111124.

15.   Thibblin, A. (1989) Reaction branching and extreme kinetic isotope effects in the study of reaction mechanisms. *Chem. Soc. Rev. 18*, 209-224.

16.   Thibblin, A. (1988) Reaction branching as a mechanistic alternative to tunneling in explaining anomalous temperature dependencies of kinetic isotope effects. *J. Phys. Org. Chem. 1*, 161-167.

17.   Oelwegaard, M., McEwen, I., Thibblin, A., and Ahlberg, P. (1985) Stepwise base-promoted elimination of hydrochloric acid via hydrogen-bonded carbanions studied by reaction branching and extreme deuterium isotope effects. Parallel carbocationic and carbanionic reactions. *J. Am. Chem. Soc. 107*, 7494-7499.

18.   Francis, K., and Gadda, G. (2006) Probing the chemical steps of nitroalkane oxidation catalyzed by 2-nitropropane dioxygenase with solvent viscosity, pH, and substrate kinetic isotope effects. *Biochemistry 45*, 13889-13898.

19.   Francis, K. and Gadda G. (2008) The Nonoxidative Conversion of Nitroethane to Ethylnitronate in *Neurospora crassa* 2-Nitropropane Dioxygenase is Catalyzed by His-196. *Biochemistry 47*, 9136-9144.

20.   Francis, K., Russell, B., and Gadda, G. (2005) Involvement of a flavosemiquinone in the enzymatic oxidation of nitroalkanes catalyzed by 2-nitropropane dioxygenase. *J. Biol. Chem. 280*, 5195-5204.

21.   Northrop, D. B. (1998) On the meaning of Km and V/K in enzyme kinetics. *J. Chem. Ed. 75*, 1153-1157.

22.   Northrop, D. B. (1999) So what exactly is V/K, anyway? *Biomed. and Health Res. 27*, 250-263.

23.   Cleland, W. W. (1975) Partition analysis and the concept of net rate constants as tools in enzyme kinetics. *Biochemistry 14*, 3220-3224.

24.   King, E. L., and Altman, C. (1956) A Schematic Method of Deriving the Rate Laws for Enzyme-Catalyzed Reactions. *J. Phys. Chem. 60*, 1375-1378.

26.   Jencks, W. P., and Carriuolo, J. (1959) Imidazole catalysis. III. General base catalysis and the reactions of acetyl imidazole with thiols and amines. *J. Biol. Chem. 234*, 1280-1285.

27.   Jencks, W. P., and Carriuolo, J. (1961) General Base Catalysis of Ester Hydrolysis. *J. Am. Chem. Soc. 83*, 1743-1749.

28.   Gadda, G., Choe, D. Y., and Fitzpatrick, P. F. (2000) Use of pH and kinetic isotope effects to dissect the effects of substrate size on binding and catalysis by nitroalkane oxidase. *Arch. Biochem. Biophys. 382*, 138-144.

29.   Valley, M. P., and Fitzpatrick, P. F. (2004) Comparison of enzymatic and non-enzymatic nitroethane anion formation: thermodynamics and contribution of tunneling. *J. Am. Chem. Soc. 126*, 6244-6245.

30.   Guengerich, F. P. (1991) Reactions and significance of cytochrome P-450 enzymes. *J. Biol. Chem. 266*, 10019-10022.

7   CHAPTER VII

KINETIC EVIDENCE FOR AN ANION BINDING POCKET IN THE ACTIVE SITE OF

NITRONATE MONOOXYGENASE

(This chapter has been published verbatim in Francis, K. and Gadda, G., (2008), *Bioorg. Chem. 5:* 167-172)

7.1   Abstract

A series of monovalent, inorganic anions and aliphatic aldehydes were tested as inhibitors for *Hansenula mrakii* and *Neurospora crassa* nitronate monooxygenase, formerly known as 2-nitropropane dioxygenase, to investigate the structural features that contribute to the binding of the anionic nitronate substrates to the enzymes. A linear correlation between the volumes of the inorganic anions and their effectiveness as competitive inhibitors of the enzymes was observed in a plot of pK_{is} versus the ionic volume of the anion with slopes of 0.041 ± 0.001 mM/ Å^3 and 0.027 ± 0.001 mM/ Å^3 for the *H. mrakii* and *N. crassa* enzymes, respectively. Aliphatic aldehydes were weak competitive inhibitors of the enzymes, with inhibition constants that are independent of their alkyl chain lengths. The reductive half reactions of *H. mrakii* nitronate monooxygenase with primary nitronates containing two to four carbon atoms all showed apparent K_d values of ~5 mM. These results are consistent with the presence of an anion binding pocket in the active site of nitronate monooxygenase that interacts with the nitro group of the substrate, and suggest a minimal contribution of the hydrocarbon chain of the nitronates to the binding of the ligands to the enzyme

7.2   Introduction

Nitronate monooxygenase (E.C. 1.13.11.32; NMO), formerly known as 2-nitropropane dioxygenase [1] is a flavin mononucleotide-dependent (FMN) enzyme that catalyzes the oxidative denitrification of alkyl nitronates to their corresponding aldehyde and keto compounds
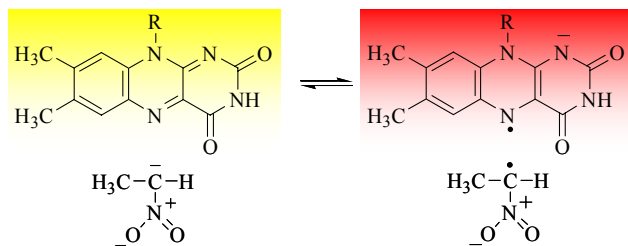
Scheme 7.1 The one-electron oxidation of ethylnitronate catalyzed by 2-nitropropane dioxygenase.

and nitrite [2-3]. The most extensively characterized NMOs studied to date are those from *Neurospora crassa* [2, 4-6] and *Hansenula mrakii* [3, 7], although the x-ray crystallographic structure of the enzyme from *Pseudomonas aeruginosa* has also been reported [8]. Detailed mechanistic studies have been carried out only for *N. crassa* NMO where it was shown that a transient anionic flavosemiquinone is formed during oxidative catalytic turnover of the enzyme through a single electron transfer reaction between an enzyme-bound nitronate and the flavin cofactor (Figure 1) [2, 4]. The formation of an anionic flavosemiquinone intermediate during oxidative catalysis is a characteristic feature of NMO that distinguishes it from the well characterized nitroalkane oxidase [9], which catalyzes a similar oxidation reaction through a different mechanism that involves the formation of a covalent flavin N(5)-adduct [10-13].

Recombinant NMO from *H. mrakii* was recently cloned and expressed in *Escherichia coli* cells and the resulting purified enzyme was characterized in its biochemical and kinetic properties [3]. The enzyme is similar to that from *N. crassa* in that it contains a single non-covalently bound FMN per monomer of enzyme and is devoid of metal cofactors [2-3]. Moreover, an anionic flavosemiquinone was observed upon anaerobic mixing of *H. mrakii* NMO with alkyl nitronates with chain-lengths ranging from two to six carbon atoms [3]. Neither hydrogen peroxide nor superoxide is released during turnover of the enzyme with primary alkyl nitronates as evident from the absence of superoxide dismutase or catalase effects on the rates of

oxygen consumption in activity assays of *H. mrakii* NMO [3], a result that was also obtained with the *N. crassa* enzyme [2].

Both *H. mrakii* and *N. crassa* NMOs are able to effectively oxidize a number of alkyl nitronates into their corresponding carbonyl compounds and nitrite. Such an enzymatic oxidation is of considerable interest given that many alkyl nitronates are known to be toxic or mutagenic [14-17]. Ingestion of propyl-2-nitronate, for example, has been demonstrated to result in the formation of 8-aminodeoxyguanosine and 8-oxodeoxyguanosine through a phenol sulfotransferase-mediated metabolic pathway in both human and rat cell lines [18-19]. Despite their toxicity, alkyl nitronates are widely used in chemical industry because they provide a quick and efficient route for the synthesis of a wide range of commercially useful compounds [20-22]. An investigation of the substrate specificity of NMO can therefore provide the basis for use of the enzyme in bioremediation applications to detoxify waste generated from industrial uses of alkyl nitronates.

In the current study, the contributions of both the nitro and hydrocarbon moieties of the alkyl nitronate substrate of NMO for binding and specificity were investigated through inhibition and rapid kinetics studies. The results are consistent with the presence of an anion binding pocket in both the *H. mrakii* and *N. crassa* enzymes, which interacts with the nitro group of the substrate. These interactions are key determinants for binding and recognition of the substrate by the enzyme, rather than the hydrophobic interactions that could occur between the enzyme and the alkyl moiety of the substrate, as in the case of nitroalkane oxidase [23-24].

7.3 Materials and Methods

Materials. NMOs from *H. mrakii* and *N. crassa* were obtained through the expression and purification protocols described previously [3, 5]. Nitroethane, 1-nitropropane and 1-nitrobutane were from Sigma-Aldrich (St. Louis, MO). All other reagents were of the highest purity commercially available.

Steady state kinetics. Enzymatic activity was measured in 50 mM potassium phosphate at pH 7.4 and 30 ^{o}C with the method of initial rates [25] by monitoring the rate of oxygen consumption with a computer interfaced Oxy-32 oxygen monitoring system (Hansatech Instrument Ltd.). Enzyme concentrations were expressed per bound FMN content using experimentally determined values of 13,100 M^{-1}cm^{-1} (ε_{446nm}) for the *H. mrakii* enzyme [3] and of 11,850 M^{-1}cm^{-1} (ε_{444nm}) for the *N. crassa* enzyme [2]. The final concentration of enzyme used in each assay was between 25 and 65 nM, whereas substrate concentrations ranged from 0.5 to 20 mM. The nitronate form of the substrate was prepared in 100% ethanol by incubating the corresponding nitroalkane with 1.2 molar excess of potassium hydroxide for at least 24 h at room temperature. Since the second-order rate constant for the protonation of ethylnitronate is 15 M^{-1}s^{-1} [26], enzymatic activity assays were initiated by the addition of substrate to the reaction mixture to ensure that a negligible amount of the neutral form of the nitronate is formed during the time required to determine initial rates of reaction (typically ~30 s).

Pre-steady state kinetics. The pre-steady state kinetic parameters of *H. mrakii* NMO were determined in 50 mM potassium phosphate at pH 7.4 and 30 ^{o}C using a TgK Scientific SF-61 stopped-flow spectrophotometer. Rates of flavin reduction were measured by monitoring the increase in absorbance at 372 nm that results from anaerobic mixing of the enzyme with substrate as previously described for *N. crassa* NMO [4]. Nitronate solutions (100 mM) were

prepared in water by incubating the nitroalkane in a 1.2 molar excess of potassium hydroxide for at least 24 hours and were diluted in water prior to use. The final enzyme concentration in each assay was between 9 and 20 μM, whereas the substrate concentrations used ranged from 0.1 to 50 mM, thereby ensuring that the enzymatic reaction follows pseudo first-order kinetics.

UV-visible absorbance spectra of NMO in the presence of sodium nitrite. Changes in the UV-visible absorbance spectrum of NMO upon addition of sodium nitrite were monitored using an Agilent Technologies diode-array spectrophotometer Model HP 8453, thermostated at 15 $^{\circ}$C. Spectra of the *H. mrakii* and *N. crassa* enzymes (at concentrations of ~80 μM) were recorded before and after addition of 1 mM sodium nitrite. Difference spectra were then constructed by subtracting the final absorbance spectrum of the enzyme in the presence of sodium nitrite from that of the free enzyme.

Data analysis. Steady state kinetic data were fit with either Enzfitter (Biosoft, Cambridge, UK) or KaleidaGraph software (Synergy Software, Reading, PA). Stopped-flow traces monitoring the reductive half reaction of *H. mrakii* NMO were fit with equation 1, which describes a single exponential process where k_{obs} is the observed first-order rate for the increase in absorbance at 372 nm, A_t is the absorbance at time t, and A is the final absorbance. Pre-steady state kinetic parameters were determined using equation 2, where k_{obs} is the observed rate of flavin reduction, k_{red} is the limiting rate constant for flavin reduction at saturating substrate concentrations, and K_d is the apparent dissociation constant of the substrate (S). Inhibition data were fit with equation 3, which describes a competitive inhibition pattern where K_{is} is the dissociation constant for the inhibitor (I).

$$A_{total} = A_t e^{-k_{obs}t} + A \tag{1}$$

$$k_{obs} = \frac{k_{red}S}{K_d + S} \tag{2}$$

$$\frac{v_o}{e} = \frac{k_{cat}S}{K_m\left[1+\left(\dfrac{I}{K_{is}}\right)\right]+S}$$

(3)

7.4   Results

Nitrite inhibition of NMO with respect to ethylnitronate as substrate. In order to establish if the nitro group of the akyl nitronate substrates of *H. mrakii* and *N. crassa* NMO contributes to binding and specificity, nitrite was used as a mimic of the substrate to establish whether it inhibits the enzymes in 50 mM potassium phosphate pH 7.4 and 30 °C. As shown in Fig. 1A for the case of the *H. mrakii* enzyme, sodium nitrite behaved as a competitive inhibitor with respect to ethylnitronate as substrate for both enzymes as indicated by the pattern of lines that intersect on the y-axis in double reciprocal plot of the initial rate of oxygen consumption *versus*
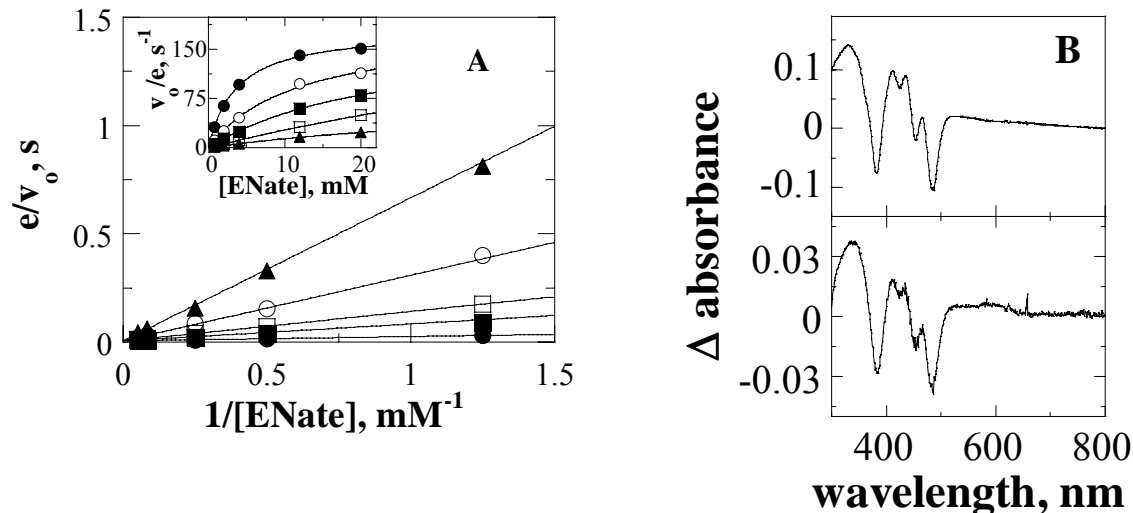
Figure 7.1 Inhibition of *H. mrakii* 2NPD by sodium nitrite with respect to ethylnitronate as substrate.
Enzymatic activity was measured at varying concentrations of ethylnitronate in the presence of 0 mM (●); 5 mM (o); 10 mM (■); 20 mM (□) and 50 mM (▲) sodium nitrite in 50 mM potassium phosphate at pH 7.4 and 30 °C. The lines are from fits of the data to equation 3. *Panel B:* UV-Visible absorbance spectral changes induced upon addition of 1 mM sodium nitrite to *H. mrakii* (top) of *N. crassa* (bottom) 2NPDin 50 mM potassium phosphate pH 7.4 at 15 °C. Difference spectra were constructed by subtracting the final absorbance spectrum of the enzyme in the presence of nitrite from that of the free enzyme.

ethylnitronate concentration at different fixed concentrations of inhibitor[1]. The corresponding

inhibition constants (K_{is}) were 1.7 ± 0.1 mM for the *H. mrakii* enzyme and 9.8 ± 0.6 mM for the

N. crassa enzyme. The effect of the nitrite on the UV-visible absorbance spectra of the FMN

cofactor of the *H. mrakii* and *N. crassa* NMOs was also determined. As shown in Fig. 1B,

binding of sodium nitrite to both enzymes induced spectral changes in the FMN cofactor bound

at the active sites of the enzymes as seen from the increase in the absorbance intensities at 333,

414, 436 and 465 nm along with the concomitant decrease in absorbance intensities at 381 and

485 nm. All taken together, the inhibition and spectroscopic studies are consistent with binding

of nitrite occurring at the active site of the enzyme.

Inorganic anion inhibition of NMO with respect to ethylnitronate as substrate. A series of

monovalent, inorganic anions were tested as inhibitors for NMO in 50 mM potassium phosphate

pH 7.4 and 30 °C to determine if the enzyme contains an anion binding site for recognition of the

nitro group of the substrate. As shown in Table 1, inorganic anions ranging in size from 25 to 64

$Å^3$ were competitive inhibitors for the *H. mrakii* enzyme, with inhibition constants ranging from

~80 mM with potassium fluoride to ~1 mM with potassium iodide. Similar results were obtained

for the *N. crassa* NMO, with inhibition constants ranging from ~125 mM for potassium fluoride

inhibition to ~5 mM for potassium iodide inhibition. Neither enzyme was inhibited by potassium

phosphate at concentrations as high as 100 mM, suggesting that either dianions or anions with an

ionic volume of 90 $Å^3$ [27] are unable to bind at the active site of both the NMOs tested.

A plot of the pK_{is} values as a function of the ionic volume of the inorganic anions tested

as inhibitors in the range from 25 to 64 $Å^3$ (Fig. 2) yielded a straight line with both enzymes,

with the exception of sodium nitrite. The experimentally determined inhibition constants for

---

[1] All of the inhibition data reported in this study were also fit with equations describing noncompetitive and uncompetitive inhibition patterns. Since the data were all best fit with a model describing competitive inhibition, only these fits are shown.

Table 7.1 Inorganic Anion Inhibition of 2NPD with Respect to Ethylnitronate as Substrate

inhibitor	ionic volume, Å^{3} [b]	*H. mrakii* K_{is}, mM [c]	*N. crassa* K_{is}, mM [d]
sodium nitrite	55	1.7 ± 0.1	10 ± 1
potassium fluoride	25	77 ± 2	125 ± 7
potassium chloride	47	11.3 ± 0.3	30 ± 2
potassium bromide	56	4.0 ± 0.3	20 ± 1
sodium nitrate	64	1.9 ± 0.1	12 ± 1
potassium iodide	72	0.95 ± 0.06	6.0 ± 0.4

[a] Enzymatic activity was measured at varying concentrations of ethylnitronate and several fixed concentrations of inhibitor in 50 mM potassium phosphate pH 7.4 at 30 °C. Data were fit with equation 3. [b] From [26]. [c] Average kinetic parameters: $k_{cat} = 180 \pm 15\ \text{s}^{-1}$; $K_m = 3.6 \pm 0.2$; $k_{cat}/K_m = 48{,}500 \pm 6{,}500\ \text{M}^{-1}\text{s}^{-1}$. [c] Average kinetic parameters: $k_{cat} = 68 \pm 1\ \text{s}^{-1}$; $K_m = 1.6 \pm 0.1$; $k_{cat}/K_m = 42{,}700 \pm 3{,}300\ \text{M}^{-1}\text{s}^{-1}$.
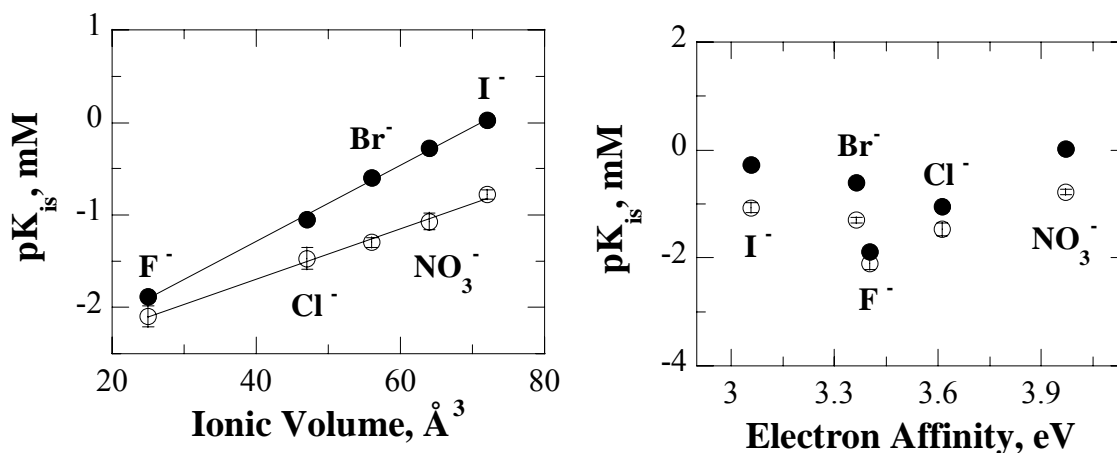
Figure 7.2 Anion inhibition of 2NPDwith respect to ethylnitronate as substrate. The inhibition constants (K_{is}) for a series of mono-valent anions were determined by measuring enzymatic activity of *H. mrakii* (•) or *N. crassa* (○) 2NPD at varying concentrations of ethylnitronate in the presence of several fixed concentrations of inhibitor. All assays were carried out in 50 mM potassium phosphate at pH 7.4 and 30 °C. *Top panel:* plots of pK_{is} versus ionic volume. Values for the ionic volumes of the anions used were taken from [26]. *Bottom panel:* plots of pK_{is} versus electron affinity. Values for the electron affinity were taken from [30].

sodium nitrite (Table 1) were between two- to three-times lower than the values that can be predicted from the size of the inorganic anion by lines of Fig. 2 of 4.7 mM for the *H. mrakii* and 19 mM for the *N. crassa* enzymes. Inhibition of the *H. mrakii* enzyme was more sensitive to the volume of the inorganic anion as indicated by the slope of 0.041 ± 0.001 mM/ Å^{3} in the plot of pK_{is} *versus* ionic volume of the anion used as a competitive inhibitor for the enzyme, as compared to 0.027 ± 0.001 mM/ Å^{3} for the *N. crassa* NMO (Fig. 2). The y-intercepts determined

from the linear fitting of the data as shown in Fig. 2 were similar to one another irrespective of the enzyme used, with a value of ~ -2.8 mM. No correlation between the electron affinities of the inorganic anions tested and the inhibition constants of NMO was found, as illustrated in Fig. 2. The counterions of the inhibitors tested had no effect on the inhibition of either enzyme as indicated by the inhibition constants of sodium nitrate, which conformed to the linear relationship between the ionic volumes of the anions tested using potassium salts with the inhibition constants of the NMO.
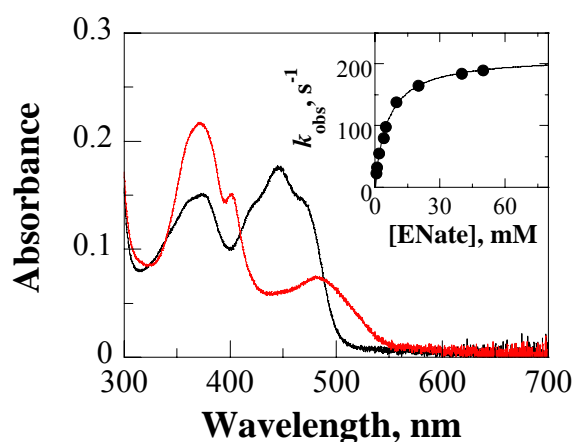
Figure 7.3 Pre-steady state kinetics of *H. mrakii* 2NPDwith ethylnitronate as substrate in 50 mM potassium phosphate pH 7.4 and 30 $^{\circ}$C.
Flavin absorbance at 372 nm was monitored over time after anaerobic mixing of the enzyme with ethylnitronate to give final concentrations of 13µM enzyme and 0.5 mM ethylnitronate. The UV-visible absorbance spectra before (black) and ~30 s after mixing (red) are shown. *Inset*. Rates of flavin reduction determined from the fits of the stopped-flow traces at 372 nm to equation 1 were plotted as function of ethylnitronate concentration (0.5 to 50 mM) and were fit with equation 2.

Contributions of the alkyl chain length to substrate binding in NMO. In order to establish whether the hydrocarbon chain of the alkyl nitronate substrate is a determinant for binding to the active site of the enzymes, the dissociation constants for a number of nitronate substrates and aliphatic aldehydes inhibitors with hydrocarbon chains of various lengths were determined in 50 mM potassium phosphate at pH 7.4 and 30 $^{\circ}$C. As shown in Fig. 3 for the case of ethylnitronate as substrate, stopped-flow measurements demonstrated that the reductive half reaction of the *H. mrakii* NMO involves the formation of an anionic flavosemiquinone as evident from the peaks centered at ~372 and 490 nm in the UV-visible absorbance spectrum obtained after

anaerobic mixing of the enzyme with the substrate. The observed rates of flavin reduction increased hyperbolically with the concentration of nitronate and showed similar apparent K_d values of ~5 mM with ethylnitronate, propyl-1-nitronate and butyl-1-nitronate, suggesting that the length of the alkyl chain of the substrate is not a determinant factor for binding of the substrate to the enzyme. The kinetic parameters for the reductive half reaction of *H. mrakii* NMO are summarized in Table 2.

Table 7.2 Reductive Half Reaction of *H. mrakii* 2NPD at pH 7.4 at 30 °C

substrate	k_{red}, s^{-1}	K_d, mM	R$^{2\,b}$
ethylnitronate	210 ± 5	5.9 ± 0.3	0.997
propyl-1-nitronate	200 ± 5	5.3 ± 0.3	0.999
butyl-1-nitronate	350 ± 5	5.7 ± 0.2	0.999

[a] *H. mrakii* 2NPD was anaerobically mixed with substrate in 50 mM potassium phosphate in a stopped-flow spectrophotometer and the absorbance changes at 372 nm were monitored over time. [b] From a plot of the observed rate of flavin reduction *versus* substrate concentration that was fit with equation 2.

Each aldehyde tested was a competitive inhibitor with respect to ethylnitronate for the *H. mrakii* enzyme with inhibition constants of ~60 mM, which further suggests that the alkyl chain length of the substrate contributes only minimally with respect to the nitro moiety (K_{is} ~2 mM) for binding of the substrate to the enzyme (Table 3). Similar, results were obtained with the *N. crassa* enzyme with propanal, butanal, pentanal or hexanal, in that the inhibition constants for aldehyde inhibition were large (i.e., ≥70 mM), though accurate determinations could not be attained due to limited solubility of the inhibitors in aqueous solution.

Table 7.3 Aldehyde Inhibition of *H. mrakii* 2NPD with Respect to Ethylnitronate as Substrate

Inhibitor	K_{is}, mM^b
propanal	58 ± 3
butanal	60 ± 1
pentanal	58 ± 3
hexanal	60 ± 2

[a] Enzymatic activity was measured at varying concentrations of ethylnitronate and several fixed concentrations of inhibitor in 50 mM potassium phosphate pH 7.4 at 30 °C. [b] Data were fit with equation 3. [c] Average kinetic parameters: $k_{cat} = 185 \pm 3$ s^{-1}; $K_m = 3.3 \pm 0.2$; $k_{cat}/K_m = 55,000 \pm 2,200$ M^{-1}s^{-1}.

7.5   Discussion

Binding of alkyl nitronates to NMO is primarily mediated through interactions of an anion binding pocket within the active site of the enzyme and the nitro moiety of the substrate. Evidence supporting this conclusion comes from inhibition studies of the *H. mrakii* and *N. crassa* enzymes with a series of monovalent, inorganic anions of varying ionic volumes. Binding of the anions likely occurs at the active site of the enzymes as evident from the spectroscopic changes of the FMN cofactor induced upon incubation of the enzyme with nitrite, which resemble those induced by binding of anthranilate to the active site of L-amino acid oxidase [28], and the competitive inhibition pattern observed with respect to ethylnitronate as substrate. The linear correlation between the ionic volumes of the inorganic anions used as inhibitors and the inhibition constants that describe their binding to the enzymes suggests the presence of a discrete binding pocket with a well-defined size, where the interactions at the anion binding site of the two enzymes between the ligand and the enzyme are maximized as the volume of the inorganic anion increases. The lack of inhibition of either enzyme by phosphate suggests that the anion binding pocket can accommodate either monovalent ligands, but not divalent ones, or only those with an ionic volume smaller than 90 $Å^3$ [27] which, by assuming a spherical geometry of the inorganic anion, corresponds to a diameter of the monovalent anion that is smaller than 5.6 Å. In agreement with the estimate of the binding pocket deriving from our kinetic analysis, the available three dimensional structure of NMO from *P. aeruginosa* clearly indicates that an anion binding site is present at the active site of the bacterial enzyme in proximity of the nitro moiety of the substrate [8], as illustrated in Fig. 4. In that enzyme, the anion binding pocket is comprised mainly of the side chain of His_{152}, the peptidyl nitrogen of Gly_{151} and the side chain of Ser_{288}. Although the crystal structures of the enzymes studied in this report are not yet available, the

alignment of the amino acid sequences of the three enzymes show that these residues are conserved in all three NMOs [1]. In the *H. mrakii* enzyme, the amino acid residues corresponding to the anion binding pocket of the bacterial enzyme are His_{197}, Gly_{196} and Ser_{351}. The equivalent residues in the *N. crassa* enzyme are His_{196}, Gly_{195} and Ser_{342} (or Thr_{344}).
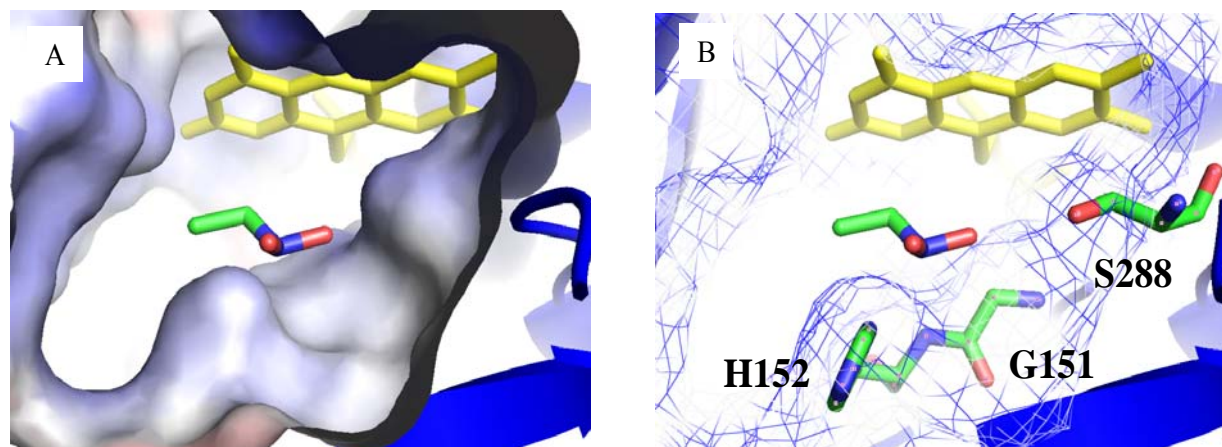
Figure 7.4 Anion Binding site in *P. aeruginosa* 2NPD.
An electrostatic potential map was generated for the x-ray crystallographic structure of *P. aeruginosa* 2NPD in complex with 2-nitropropane (PDB ID: 2GJN) using an Adaptive Poisson-Boltzmann Solver [31] and visualized using Pymol. Panel A: Electrostatic ponetial surface of the active site of *P. aeruginosa* 2NPD. Panel B: Active site amino acid residues that comprise the anion binding site in *P. aeruginosa* 2NPD.

A comparison of the slopes in the plots of pK_{is} *versus* ionic volumes for the inorganic anions acting as inhibitors of the *H. mrakii* and *N. crassa* NMOs is consistent with the anion binding pocket of the *H. mrakii* enzyme being slightly smaller than that of the *N. crassa* enzyme. In this respect, the slopes of the lines that fit the data in the plots of Fig. 2 depend on either the values of the inhibition constants that describe the binding of the inorganic anions to the enzyme, the ionic volumes of the inorganic anions, or both. In principle, the binding of the inorganic anions to the binding pockets in the two enzymes can be affected by a number of factors including geometric, steric, or electrostatic effects. However, the observation that the fits of the data in Fig. 2 yields values for the y-intercepts for the two enzymes that are similar to one another is consistent with the slope effect that is experimentally observed being due primarily to

the volume of the anion binding pockets of each enzyme rather than other factors. The accurate determination of the sizes and geometries of the anion binding pockets at the active sites of the enzymes from *H. mrakii* and *N. crassa* will have to await the elucidation of the x-ray crystallographic structures of the two enzymes, which is currently ongoing in collaboration with Weber's group at Georgia State University.

Substrate recognition by NMO is predominantly determined by the interactions occurring at the active site binding pocket of the enzyme with the nitro group of the alkyl nitronate substrate with minimal, if any, hydrophobic interactions of the enzyme with the alkyl chain of the substrate. Evidence supporting this conclusion comes from the comparison of the K_{is} values for aldehyde inhibition with respect to nitrite inhibition, which shows that the former are at least 10-times smaller than the latter with both the enzymes tested. Lack of interaction of the alkyl chain of the ligand with the enzyme is independently supported by the similar values for the dissociation constants for substrate binding (K_d) determined for the *H. mrakii* enzyme with alkyl nitronates of varying chain lengths of between two and four carbon atoms. Indeed, one would expect a progressive decrease in the K_d values for the substrate with increasing lengths of the alkyl chain of the substrate if hydrophobic interactions played a significant role for substrate binding. The results suggesting that NMO does not discriminate its ligands by exploiting the organic moiety of the substrate are consistent with previous studies of the enzyme from *N. crassa* that established that *m*-nitrobenzoate effectively binds to the enzyme (i.e., K_{is} value of 9.1 mM at pH 7.4), despite its large size and aromatic character [4]. Further in agreement with minimal contribution of the alkyl chain of the substrate to binding are previous studies of the *H. mrakii* and *N. crassa* enzymes showing that the k_{cat}/K_m values for nitronates ranging from two to six carbon atoms are independent of the alkyl chain length of the substrate [2-3]. As illustrated in

Fig. 4, the three dimensional structure of the bacterial enzyme from *P. aeruginosa* with 2-nitropropane bound at the active site shows the presence of a wide cavity in the active site of the enzyme, which is large enough to accommodate substrates of various lengths or different structures [8].

7.6   Conclusions

In conclusion, the results presented herein demonstrate that the active site of yeast NMO contains an anion binding pocket, which participates in the binding of the nitro group of the alkyl nitronate substrates. Thus, the nitro group of the substrate is the key determinant for binding of the substrate at the active site of the enzyme as opposed to the hydrocarbon chain of the nitronate molecule acting as substrate, which plays a minimal role, if any, in binding by the enzyme. These results contrast those previously reported for nitroalkane oxidase, whose ability to bind substrates at the active site increases with increasing lengths of the alkyl chain of the substrate and reaches a maximum value with substrates containing four or more carbon atoms [24]. A study of the pH and kinetic isotope effects on nitroalkane oxidase revealed that each methylene group of the substrate provides approximately 2.6 kcal/mol of binding energy [23], which was recently explained through structural studies of the enzyme that demonstrated a hydrophobic channel leading to the active site of the enzyme [12, 29-30]. Although structural studies have yet to be reported for the *H. mrakii* and *N. crassa* enzymes, the x-ray crystallographic structure of *P. aeruginosa* NMO shows a solvent accessible active site that lacks a hydrophobic channel like that seen in nitroalkane oxidase [8]. The elucidation of binding pockets for anionic ligands in the active site of enzymes through inhibition studies with inorganic anions of various ionic volumes demonstrates a kinetic method that should be generally applicable to any enzyme whose crystallographic structure is not yet available.

7.7 Acknowledgements

7.8   References

1. Marcus, Y., Jenkins, H. D. B., and Glasser, L. (2002) Ion volumes: a comparison, *J. Chem. Soc. Dal. Trans.*, 3795-3798.

2.   Baker, N. A., Sept, D., Joseph, S., Holst, M. J., and McCammon, J. A. (2001) Electrostatics of nanosystems: application to microtubules and the ribosome, *Proc. Natl. Acad. Sci. U. S. A. 98*, 10037-10041.

3.   Gadda, G., and Francis, K. (2009) Nitronate monooxygenase, a model for anionic flavin semiquinone intermediates in oxidative catalysis, *Arch. Biochem. Biophys. 493*, 53-61.

4.   Francis, K., Russell, B., and Gadda, G. (2005) Involvement of a flavosemiquinone in the enzymatic oxidation of nitroalkanes catalyzed by 2-nitropropane dioxygenase, *J. Biol. Chem. 280*, 5195-5204.

5.   Mijatovic, S., and Gadda, G. (2008) Oxidation of alkyl nitronates catalyzed by 2-nitropropane dioxygenase from *Hansenula mrakii*, *Arch. Biochem. Biophys. 473*, 61-68.

6.   Francis, K., and Gadda, G. (2006) Probing the chemical steps of nitroalkane oxidation catalyzed by 2-nitropropane dioxygenase with solvent viscosity, pH, and substrate kinetic isotope effects, *Biochemistry 45*, 13889-13898.

7.   Francis, K., and Gadda, G. (2008) The nonoxidative conversion of nitroethane to ethylnitronate in *Neurospora crassa* 2-nitropropane dioxygenase is catalyzed by histidine 196, *Biochemistry 47*, 9136-9144.

8.   Francis, K., and Gadda, G. (2009) Kinetic evidence for an anion binding pocket in the active site of nitronate monooxygenase, *Bioorg. Chem. 37*, 167-172.

9.   Tchorzewski, M., Kurihara, T., Esaki, N., and Soda, K. (1994) Unique primary structure of 2-nitropropane dioxygenase from Hansenula mrakii, *Eur. J. Biochem. 226*, 841-846.

10. Rienstra-Kiracofe, J. C., Tschumper, G. S., Schaefer, H. F., 3rd, Nandi, S., and Ellison, G. B. (2002) Atomic and molecular electron affinities: photoelectron experiments and theoretical computations, *Chem. Rev. 102*, 231-282.

11. Ha, J. Y., Min, J. Y., Lee, S. K., Kim, H. S., Kim do, J., Kim, K. H., Lee, H. H., Kim, H. K., Yoon, H. J., and Suh, S. W. (2006) Crystal structure of 2-nitropropane dioxygenase complexed with FMN and substrate. Identification of the catalytic base, *J. Biol. Chem. 281*, 18660-18667.

12. Fitzpatrick, P. F., Orville, A. M., Nagpal, A., and Valley, M. P. (2005) Nitroalkane oxidase, a carbanion-forming flavoprotein homologous to acyl-CoA dehydrogenase, *Arch. Biochem. Biophys. 433*, 157-165.

13. Gadda, G., and Fitzpatrick, P. F. (2000) Mechanism of nitroalkane oxidase: 2. pH and kinetic isotope effects, *Biochemistry 39*, 1406-1410.

14. Gadda, G., and Fitzpatrick, P. F. (2000) Iso-mechanism of nitroalkane oxidase: 1. Inhibition studies and activation by imidazole, *Biochemistry 39*, 1400-1405.

15. Nagpal, A., Valley, M. P., Fitzpatrick, P. F., and Orville, A. M. (2006) Crystal structures of nitroalkane oxidase: insights into the reaction mechanism from a covalent complex of the flavoenzyme trapped during turnover, *Biochemistry 45*, 1138-1150.

16. Valley, M. P., Tichy, S. E., and Fitzpatrick, P. F. (2005) Establishing the kinetic competency of the cationic imine intermediate in nitroalkane oxidase, *J. Am. Chem. Soc. 127*, 2062-2066.

17. Hornfeldt, C. S., and Rabe, W. H., 3rd. (1994) Nitroethane poisoning from an artificial fingernail remover, *J. Toxicol. Clin. Toxicol. 32*, 321-324.

18.   Kohl, C., and Gescher, A. (1997) Denitrification of the genotoxicant 2-nitropropane: relationship to its mechanism of toxicity, *Xenobiotica 27*, 843-852.

19.   Kohl, C., Mynett, K., Davies, J. E., Gescher, A., and Chipman, J. K. (1994) Propane 2-nitronate is the major genotoxic form of 2-nitropropane, *Mutat. Res. 321*, 65-72.

20.   Shepherd, G., Grover, J., and Klein-Schwartz, W. (1998) Prolonged formation of methemoglobin following nitroethane ingestion, *J. Toxicol. Clin. Toxicol. 36*, 613-616.

21.   Fiala, E. S., Czerniak, R., Castonguay, A., Conaway, C. C., and Rivenson, A. (1987) Assay of 1-nitropropane, 2-nitropropane, 1-azoxypropane and 2-azoxypropane for carcinogenicity by gavage in Sprague-Dawley rats, *Carcinogenesis 8*, 1947-1949.

22.   Kreis, P., Brandner, S., Coughtrie, M. W., Pabel, U., Meinl, W., Glatt, H., and Andrae, U. (2000) Human phenol sulfotransferases hP-PST and hM-PST activate propane 2-nitronate to a genotoxicant, *Carcinogenesis 21*, 295-299.

23.   Ballini, R., Bosica, G., Fiorini, D., Palmieri, A., and Petrini, M. (2005) Conjugate additions of nitroalkanes to electron-poor alkenes: recent results, *Chem. Rev. 105*, 933-971.

24.   Ballini, R., Palmieri, A., and Barboni, L. (2008) Nitroalkanes as new, ideal precursors for the synthesis of benzene derivatives, *Chem. Commun. (Camb)*, 2975-2985.

25.   Gadda, G., Choe, D. Y., and Fitzpatrick, P. F. (2000) Use of pH and kinetic isotope effects to dissect the effects of substrate size on binding and catalysis by nitroalkane oxidase, *Arch. Biochem. Biophys. 382*, 138-144.

26.   Gadda, G., and Fitzpatrick, P. F. (1999) Substrate specificity of a nitroalkane-oxidizing enzyme, *Arch. Biochem. Biophys. 363*, 309-313.

27.   Allison, R. D., and Purich, D. L. (1979) Practical considerations in the design of initial velocity enzyme rate assays, *Methods Enzymol. 63*, 3-22.

28.   Nielsen, A. T. (1969) Nitronic acids and esters, In *The Chemistry of the nitro and nitroso groups* (Feuer, H., Ed.), pp 349-486, Interscience Publishers, New York.

29.   MacHeroux, P., Seth, O., Bollschweiler, C., Schwarz, M., Kurfurst, M., Au, L. C., and Ghisla, S. (2001) L-amino-acid oxidase from the Malayan pit viper *Calloselasma rhodostoma*. Comparative sequence analysis and characterization of active and inactive forms of the enzyme, *Eur. J. Biochem. 268*, 1679-1686.

30.   Heroux, A., Bozinovski, D. M., Valley, M. P., Fitzpatrick, P. F., and Orville, A. M. (2009) Crystal structures of intermediates in the nitroalkane oxidase reaction, *Biochemistry 48*, 3407-3416.

31.   Nagpal, A., Valley, M. P., Fitzpatrick, P. F., and Orville, A. M. (2004) Crystallization and preliminary analysis of active nitroalkane oxidase in three crystal forms, *Acta Crystallogr. D. Biol. Crystallogr. 60*, 1456-1460.

8   CHAPTER VIII

A NOVEL ACTIVITY FOR FUNGAL NITRONATE MONOOXYGENASE: DETOXIFICATION OF THE METABOLIC INHIBITOR PROPIONATE-3-NITRONATE

8.1   Abstract

Nitronate monooxygenase (NMO; E.C. 1.13.12.16) is an FMN dependent enzyme that oxidizes alkyl nitronates to their corresponding carbonyl compounds and nitrite. While the kinetic and mechanistic properties of NMO from *Neurospora crassa* and *Williopsis saturnus* var. Mrakii have been extensively characterized, the physiological role of the enzyme is still unknown. The current study demonstrates that the enzyme oxidizes propionate-3-nitronate (P3N), the highly toxic conjugate base of the plant metabolite 3-nitropropionate (3NPA), and provides compelling evidence that the physiological role of NMO is in detoxification. The Michaelis constants of both NMOs tested were significantly lower with P3N as substrate than was previously measured with primary alkyl nitronates. The ability of NMO to detoxify P3N *in vivo* was tested by measuring growth curves of recombinant *Escherichia coli* cells containing the gene encoding for the enzyme in either the absence or presence of the nitronate. P3N is toxic to *E. coli* cells lacking NMO, but the toxicity is overcome through either induction of the recombinant gene or through addition of exogenous enzyme to the cultures. The growth of the fungi on 3NPA was also tested to establish that the physiological role of NMO is for detoxification. Both *W. saturnus* and wild-type *N. crassa* were able to grow on up to 20 mM 3NPA, while a knockout mutant of *N. crassa* lacking the gene encoding for NMO could not grow on the toxin at concentrations above 600 μM. The results were confirmed by monitoring the linear growth rate of the wild-type and knockout forms N. *crassa*, which showed no growth

of the mutant above 500 μM of the toxin. From these results, it is proposed that NMO functions to protect the fungi from the environmental occurrence of the toxin 3NPA and its ionic form P3N.

8.2   Introduction

3-Nitropropionate is a highly toxic, nitro aliphatic compound produced by a variety of leguminous plants and several microbial species (8, 9, 37). The toxin was originally isolated from the bark of *Hiptage mandoblota* in the 1920's and was identified as hiptagenic acid (20). In 1949, hiptagenic acid was reclassified as 3-nitropropionate, which represented the first organic nitro compound ever isolated from plants (8, 20). 3-Nitropropionate has subsequently been found in several plants including *Indigofera spicata*, *Coronilla varia*, *Lotus pedunculatus*, *Viola odorata* and a variety of *Astragalus* species (22). The toxin has also been found in many fungal species including *Aspergillus flavus, Aspergillus wenti*, *Arthrinium saccharicola*, *Arthrinium sacchari* and *Penicillium atrovenetum* (22). The concentrations of 3-nitropropionate produced by these organisms are surprisingly high, with the plants producing ~50 μmol per g of fresh weight (24) and the fungal species containing the toxin at concentrations up to 10 mM (7, 9, 41, 46). 3-Nitropropionate likely serves as a means of protection of the organism against herbivory (23) and is involved in nitrification by leguminous plants (24).
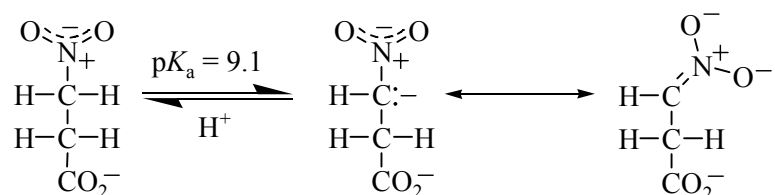
Scheme 8.1 Ionization of 3-nitropropionate (left) to propionate-3-nitronate (right) (7).

The toxicity of 3-nitropropionate arises from its conjugate base, propionate-3-nitronate, which readily forms at physiological pH (i.e. 7.4) as the result of a slow ionization of the α-

carbon (7, 17, 38) (Scheme 8.1). Given the pK_a value of 9.1 for the conversion of propionate-3-nitronate to 3-nitropropionate (7) the effective concentration of the nitronate at pH 7.4 is ~2% of the total amount of the nitro-compound present at equilibrium (i.e. ~200 µM at a total concentration of 10 mM of the nitro compound). Even at these low concentrations propionate-3-nitronate is a potent inhibitor of succinate dehydrogenase (2, 11, 25) and fumarate (42) and is therefore extremely toxic. Propionate-3-nitronate, a structural analogue of succinate, forms an irreversible covalent adduct with a key arginine residue in the active site of succinate dehydrogenase rendering the enzyme completely inactive (2, 11, 25). The nitronate is also a high affinity transition state analogue of fumarate (K_{iss} = 64 no), an enzyme involved in the Krebs cycle (42). The inhibition of essential metabolic enzymes effectively halts energy production in poisoned cells leading to a variety of neurological disorders (5) and, at sufficiently large doses, death (6, 36). Cases of 3-nitropropionate poisoning have been widely documented in both domestic livestock and humans (22, 26, 34, 47). Clinical signs of intoxication in cattle include poor coordination of the limbs, foaming of the mouth and nose and respiratory distress (22). In humans, fatal cases of 3-nitropropionate poisoning have been linked to the ingestion of moldy sugarcane, which spoiled during the transport and storage of the crop (32, 33).

Several propionate-3-nitronate oxidizing enzymes have been isolated from plants and microorganisms that produce 3-nitropropionate. These include enzymes from *P. atrovenetum (43)*, *Hippocrepis comosa (23), Burkholderia phytofirmans* and *Pseudomonas aeruginosa* (39). All of the propionate-3-nitronate oxidizing enzymes described to date contain a flavin cofactor (either FAD or FMN) and are most active, or in most cases exclusively active, on propionate-3-nitronate rather than 3-nitropropionate. The plant enzymes are proposed to be involved in both self-protection against propionate-3-nitronate toxicity (23) and to serve as a means of

nitrification through the release of nitrate and nitrite into the soil (24). The recently discovered bacterial enzymes have been demonstrated to both detoxify the nitronate and use the toxin as a sole source of carbon and nitrogen when grown on minimal media (40).

In recent years, the biochemical and mechanistic properties of another class of flavin-dependent nitronate oxidizing enzymes, the fungal nitronate monooxygenases (NMO; E.C. 1.13.12.16), have been described (18). NMOs from *Williopsis saturnus* var. Mrakii (IFO 0895) and *Neurospora crassa* (ATCC 10337) have been most extensively characterized and can effectively oxidize primary alkyl nitronates with alkyl chain lengths ranging from 2 to 6 carbon atoms (16, 35). These enzymes were first described as 2-nitropropane dioxygenases (19, 31) (E.C. 1.13.11.32), but were recently reclassified as NMOs by the International Union of Biochemistry and Molecular Biology. Despite the numerous studies of the enzyme during the past 60 years since its discovery (13-16, 19, 27, 31, 35), the physiological role of NMO has yet to be elucidated. Indeed, it is unlikely that alkyl nitronates are the physiological substrates of the enzyme since they are not present in cells at concentrations approaching the K_m (~3 mM) of the enzyme (13). In the current study, 3-nitropropionate and propionate-3-nitronate were tested as substrates for NMO and the protective effects of the enzyme against nitronate poisoning *in vivo* was evaluated using recombinant *E. coli* cells.

8.3   Materials and Methods

Materials.   Luria-Bertani (LB) agar and broth, chloramphenicol, phenylmethysulfonylfluoride, superoxide dismutase, catalase, and 3-nitropropionic acid (> 97%) were from Sigma-Aldrich (St. Louis, MO). Ampicillin was from Fisher Scientific (Pittsburgh, PA). 3-Nitropropionic acid (> 96%) used in experiments where bacterial growth curves where measured was from Fluka (St. Louis, MO). The bacterial strains used in this study are listed in

Table 8.1. NMOs from *W. saturnus* (NMO-Ws) and *N. crassa* (NMO-Nc) were expressed and purified as described previously (16, 35). All other reagents were of the highest purity commercially available.

   Enzyme Assays. Enzymatic activity was measured with the method of initial rates (1) in air saturated 50 mM potassium phosphate, pH 7.4 and 30 $^{\circ}$C, by monitoring rates of oxygen consumption with a computer interfaced Oxy-32 oxygen monitoring system (Hansatech Instrument Ltd.). The concentrations of enzyme used in the assays were expressed per content of bound FMN using the experimentally determined extinction coefficients of 13,100 $M^{-1}cm^{-1}$ (446 nm) for the *W. saturnus* enzyme (35) and 11,850 $M^{-1}cm^{-1}$ (444 nm) for the *N. crassa* enzyme (16). Stock solutions of 3-nitropropionic acid were prepared in water. Propionate-3-nitronate was prepared by incubating 3-nitropropionic acid with a 2.2 molar excess of potassium hydroxide for at least 24 h at room temperature. Enzymatic activity assays were initiated by the addition of substrate, in order to minimize changes in the ionization state of the nitroalkane as described previously (16, 35). The release of superoxide anion during turnover of NMO with propionate-3-nitronate or 3-nitropropionate was monitored by measuring the rate of oxygen consumption with 2 mM substrate, in either the presence or absence of 40 or 96 units of superoxide dismutase. Production of hydrogen peroxide during turnover was monitored by measuring the rate of oxygen consumption with 2 mM substrate, in either the presence or absence of 700 units of catalase. The apparent steady state kinetic parameters of NMO with propionate-3-nitronate as substrate were determined using either 6 nM of NMO-Nc or 3 nM of NMO-Ws and between 25-2000 µM of substrate. Oxygen was held constant at atmospheric concentrations (i.e. 230 µM at 30 $^{\circ}$C).

Table 8.1 Strains and Plasmids Used in this Study

Stain	Plasmid	NMO encoded	source
Rosetta(DE3)	pLysS	none	Novagen
Rosetta(DE3)	pLysS-2NPDhm6	*W. saturnus*	prepared in (36)
BL21(DE3)	pLysS	none	Novagen
BL21(DE3)	pLysS-2NPDnc13	*N. crassa*	prepared in (16)

Cell Growth. Overnight cultures of *E. coli* strains (Table 8.1) grown in LB broth containing 50 μg/mL ampicillin and 34 μg/mL choramphenicol were used to inoculate 3 x 70 mL (for *E. coli*-NMO-Ws) or 3 x 100 mL (for *E. coli*-NMO-Nc) of LB broth containing an effective concentration of either 0 or 5 mM propionate-3-nitronate[1] to an optical density at 600 nm of ~0.02. The cultures were then grown in a shaker at 250 rpm and 37 ^{o}C for ~12 h. Isopropyl-β-D-thiogalactopyranoside (IPTG) was added to each culture ~80 min after inoculation to a final concentration of 100 μM. Bacterial growth was monitored by measuring the optical density at 600 nm of the cultures with a Shimadzu UV-3101 PC UV-Vis-NIR Scanning Spectrophotometer. After 6 h, 32 mL of *E. coli*-NMO-Ws grown in the presence of effective concentration of 5 mM propionate-3-nitronate were transferred to an autoclaved flask and purified NMO-Ws was added to a final concentration of 200 nM. Samples (1 to 2 mL) were withdrawn from the cultures after each optical density measurement and the cells were harvested by centrifugation at 14,000 x g. Cell extracts were then prepared by suspending the cells in 50 mM Tris-Cl, 10 mM EDTA, 1 mM phenymethylsulfonylfluoride, 10% glycerol, pH 8.0, before sonication for 4 rounds of 30 sec on ice. Enzymatic activity was measured for selected samples by monitoring the rate of oxygen consumption with 1 mM propionate-3-nitronate in 50 mM

---

[1] The concentration of the nitronate admistered to the culture was 100 mM, but because of the equilibration of the toxin to to its protonted form that occurs during the time course of the experiment the concentration at equilibrium is reported, and indicated as the effective concentration.

potassium phosphate, pH 7.4 and 30 $^{\circ}$C. The amount of protein in each cell extract was determined using the method of Bradford (4). The expression of NMO was visualized by SDS-PAGE for strains of *E. coli* that either contained or lacked the gene encoding for the *N. crassa* enzyme after harvesting 20 mL of each culture and preparing cell extracts as described above. Fungal growth was carried out at room temperature on Vogel's media (*43*) supplemented with either 1.5% sorbose or 1.5% glucose and between 0 to 20 mM 3-nitropropionate. Linear growth of *N. crassa* was measured using 13 mL race tubes at 25 $^{\circ}$C using the method of White (*44*). Each sample was measured in triplicate and the average value is reported.

8.4   Results

Enzymatic Activity of NMO with Either 3-Nitropropionate or Propionate-3-Nitronate as Substrate. 3-Nitropropionate and propionate-3-nitronate were tested as substrates for the purified NMOs from *W. saturnus* and *N. crassa* by monitoring the consumption of oxygen that occurs during catalytic turnover of the enzymes. 3-Nitropropionate is not a substrate for NMO-Ws as evident from the lack of oxygen consumption observed when the enzyme is mixed with the nitro-compound (Fig. 1A). Addition of propionate-3-nitronate to the reaction mixture, however, resulted in the rapid depletion of oxygen, indicating that the nitronate is an effective substrate for the enzyme. In contrast to the *W. saturnus* enzyme, NMO-Nc is able to utilize either 3-nitropropionate or propionate-3-nitronate as substrate (Figs. 1B and 1C). These observations agree with previous results demonstrating that the NMO-Nc can effectively oxidize both nitronates and nitroalkanes, whereas NMO-Ws can only act on the nitronates (16, 35).
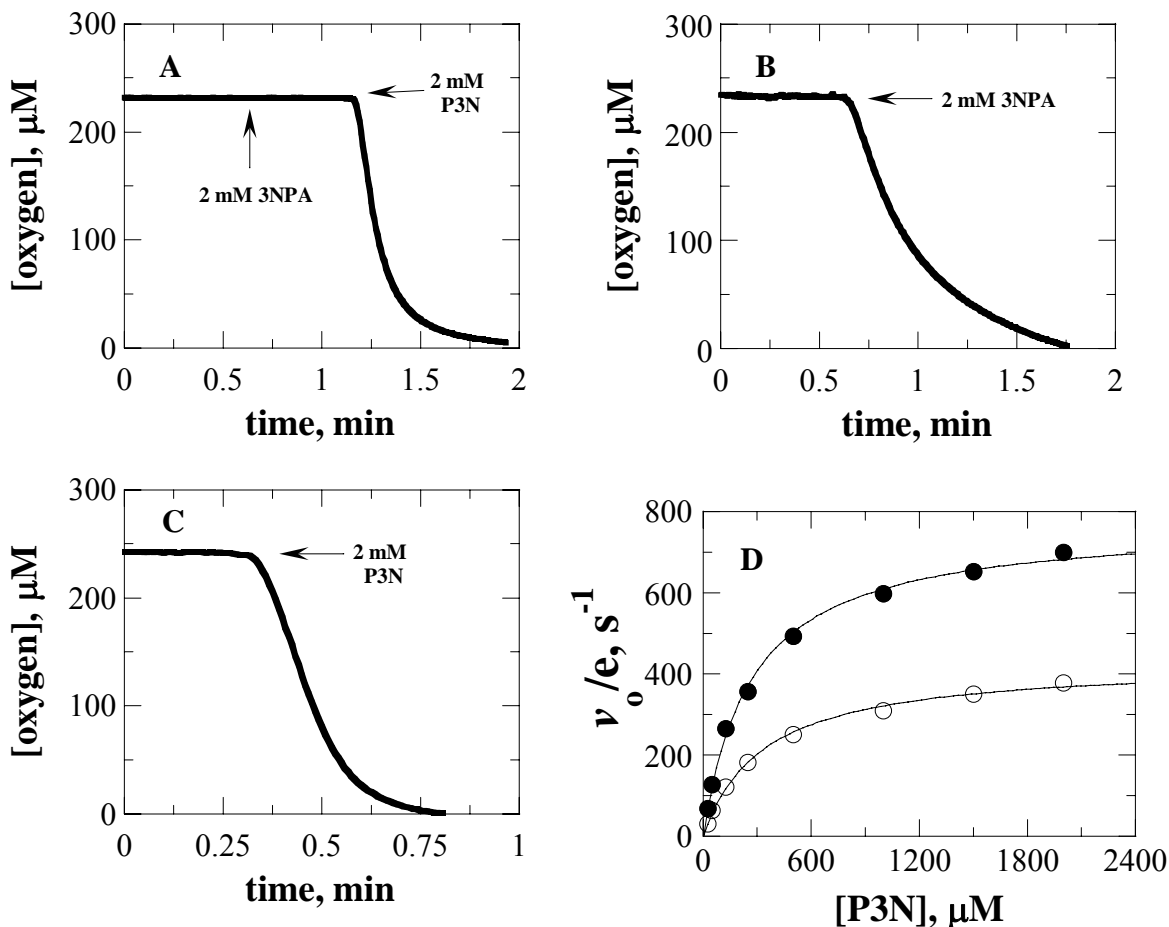
Figure 8.1 Activities of NMO with 3-nitropropionate (3NPA) or propionate-3-nitronate (P3N).
(A) 3-Nitropropionate was added to a reaction mixture containing 40 nM NMO-Ws. After ~30 sec of incubation, propionate-3-nitronate was then added to the reaction mixture. (B) 3-Nitropropionate was added to a reaction mixture containing 1.40 μM NMO-Nc. C) Propionate-3-nitronate was added to a reaction mixture containing 73 nM NMO-Nc. D) Michaelis-Menten plots of NMO-Ws (closed circle) or NMO-Nc (open circle) with propionate-3-nitronate as substrate. All assays were carried out in air-saturated 50 mM potassium phosphate at pH 7.4 and 30 °C by monitoring oxygen consumption with a Clark oxygen electrode.

Effects of superoxide dismutase on the enzymatic activity of NMO with propionate-3-nitronate or 3-nitropropionate as substrate. Given the known reactivity of nitroalkanes with superoxide anion (30) and that many flavin dependent enzymes transiently produce superoxide during turnover (29, 44), it is important to establish whether the oxygen consumption observed when NMO is mixed with propionate-3-nitronate is an enzymatic activity or the result of a non-enzymatic reaction. The effect of superoxide dismutase on the rates of oxygen consumption during turnover of NMO was therefore determined to establish whether superoxide anion is released during catalytic turnover of the enzyme. The rate of oxygen consumption observed when NMO-Ws was mixed with propionate-3-nitronate was unaffected by the presence of superoxide dismutase (Table 8.2). The result establishes that oxygen consumption catalyzed by the *W. saturnus* enzyme with propionate-3-nitronate as substrate is solely due to the enzymatic oxidation of the nitronate. In contrast, the *N. crassa* enzyme showed a significant decrease in the rate of oxygen consumption when assays were carried out in the presence of superoxide dismutase (Table 8.2). Thus, the activity of NMO-Nc toward propionate-3-nitronate or 3-nitropropionate is partially the result of a non-enzymatic reaction of the nitro compounds with superoxide anion. Enzymatic oxidation was also substantial as indicated by oxygen consumption when superoxide dismutase is included in the assay (Table 8.2).

Table 8.2 Effect of Superoxide Dismutase on the Activity of NMO with Propionate-3-Nitronate or 3-Nitropropionate as Substrate

SOD	NMO-Ws, s^{-1}	NMO-Nc, s^{-1}	NMO-Nc, s^{-1}
	propionate-3-nitronate[b]		3-nitropropionate[c]
0 U	700	430	5.49
40 U	700	380	2.12
96 U	700	380	2.10

[a] Enzymatic activity was measured in 50 mM potassium phosphate at pH 7.4 and 30 °C. [b] 2 mM final concentration. [c] 1 mM final concentration.

Effects of Catalase on the Enzymatic Activity of NMO with Propionate-3-Nitronate as Substrate. The effect of catalase on the enzymatic activity of NMO with propionate-3-nitronate or 3-nitropropionate was tested in order to establish whether hydrogen peroxide is produced and released by the enzyme during catalytic turnover. The activity of the *W. saturnus* enzyme was unaffected by the presence of catalase (Table 8.3) suggesting that hydrogen peroxide is not released during turnover of the enzyme with propionate-3-nitronate. In contrast, when catalase was included in assays of the *N. crassa* enzyme with either propionate-3-nitronate or 3-nitropropionate the rate of oxygen consumption decreased significantly (Table 8.3).

Table 8.3 Effect of Catalase on the Activity of NMO with Propionate-3-Nitronate or 3-Nitropropionate as Substrate

catalase	NMO-Ws, s^{-1}	NMO-Nc, s^{-1}	NMO-Nc, s^{-1}
	propionate-3-nitronate[b]		3-nitropropionate[b]
0 U	700	430	6.3
400 U	700	225	3.7
700 U	700	230	3.6

[a] Enzymatic activity was measured in 50 mM potassium phosphate at pH 7.4 and 30 $^{\circ}$C. [b] 2 mM final concentration.

The effect of catalase on the observed rate of oxygen consumption by NMO-Nc with propionate-3-nitronate as substrate was also determined in the presence of superoxide dismutase. When 40 U of superoxide dismutase was included in the reaction mixture the rate of oxygen consumption with 2 mM propionate-3-nitronate was 380 s^{-1} either in the presence or absence of catalase. Similarly, the rate of oxygen consumption with 3-nitropropionate as substrate for the NMO-Nc in the presence of superoxide dismutase was unaffected by the presence of catalase, with a value of 3.4 s^{-1}. These results suggest that the hydrogen peroxide detected in the absence of superoxide dismutase is produced by a non-enzymatic reaction with superoxide anion and not from the NMO catalyzed reaction with the nitro-compound.

Steady-State Kinetic Parameters of NMO with Propionate-3-Nitronate or 3-Nitropropionate as Substrate. The steady state kinetic parameters with either propionate-3-nitronate or 3-nitropropionate as substrate for NMO were determined in air-saturated 50 mM potassium phosphate at pH 7.4 and 30 ^{o}C. Since enzymatic activity was measured under atmospheric oxygen (i.e. 230 μM at 30 ^{o}C) the steady-state kinetic parameters represent apparent values as opposed to the true values that would be obtained by saturating the enzyme with both the organic substrate and oxygen (10). The primary purpose of these experiments, however, was to evaluate the biological activity of the enzyme with the nitro-substrates, which requires that the oxygen concentration be at physiological (sub-saturating) levels. The initial rates of the reaction of the NMO-Ws were hyperbolically dependent on the concentration of propionate-3-nitronate, allowing for the determination of the kinetic parameters of the enzyme through a fit of the data to the Michaelis-Menten equation with one substrate (Figure 8.1D). Initial rates of the reaction of NMO-Nc were determined in the presence of superoxide dismutase to prevent the non-enzymatic oxidation of the nitro-compounds and were also hyperbolically dependent on the substrate concentration. The kinetic parameters determined for each enzyme are summarized in Table 8.4. The results indicate that propionate-3-nitronate is effectively oxidized by the *N. crassa* and *W. saturnus* enzymes.

Table 8.4 Apparent Steady State Kinetic Parameters of NMO

source	substrate	$^{app}(K_m)$, mM	$^{app}(k_{cat})$, s^{-1}	$^{app}(k_{cat}/K_m)$, M^{-1}s^{-1}
W. saturnus	propionate-3-nitronate	0.27 ± 0.02	775 ± 15	$(2.8 \pm 0.2) \times 10^6$
N. crassa[b]	propionate-3-nitronate	0.34 ± 0.02	430 ± 10	$(1.3 \pm 0.1) \times 10^6$
N. crassa[b]	3-nitropropionate	0.58 ± 0.05	4.4 ± 0.2	$(7.6 \pm 0.7) \times 10^3$

[a] Enzymatic activity was measured in 50 mM potassium phosphate at pH 7.4 and 30 ^{o}C. [b] Measured in the presence of 40 U superoxide dismutase.
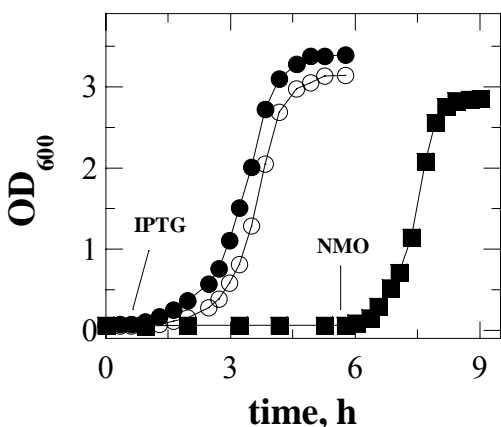
Figure 8.2 Protective Effects of NMO-Ws against propionate-3-nitronate poisoning in *E. coli.*
Bacterial growth was monitored by measuring the optical density at 600 nm after incubating each culture at 37 °C and 250 rpm. Closed Circles: *E. coli* Rosetta(DE3)pLysS lacking the gene encoding for NMO-Ws grown in the absence of propionate-3-nitronate. Open circles: Rosetta(DE3)pLysS-2NPDhm6 (36) grown in the presence of an effective concentration of 5 mM propionate-3-nitronate. Closed Squares: *E. coli* Rosetta(DE3)pLysS incubated in the presence of an effective concentration 5 mM propionate-3-nitronate. IPTG and purified NMO were added at the times indicated on the plot.

Protection of E. coli From Propionate-3-Nitronate Toxicity by NMO-Ws. The ability of NMO-Ws to detoxify propionate-3-nitronate was tested by measuring growth of *E. coli*-NMO-Ws in the presence of the toxin compared with growth of a control strain lacking the NMO gene. Antibiotics were not included in the culture media in order to reveal whether the expression of NMO could provide a selective pressure for the bacterium to retain the plasmid containing the gene encoding for the enzyme. An effective concentration of 5 mM propionate-3-nitronate prevented the growth of *E. coli* (Figure 8.2). Inducing the expression of NMO-Ws with IPTG allowed *E. coli* to overcome the bacteriostatic effects of propionate-3-nitronate and grow as effectively as the control culture that did not contain the nitronate.

Addition of exogenous NMO-Ws to the culture also allowed the bacteria to grow in the presence of the nitronate (squares in Figure 8.2). The results demonstrate that the expression of NMO-Ws *in vivo* or the addition of purified enzyme to the culture, can protect bacteria against the toxicity of propionate-3-nitronate.
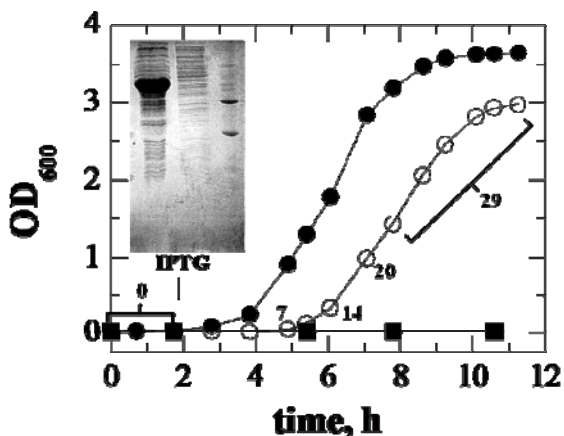
Figure 8.3 Protective Effects of NMO-Nc against propionate-3-nitronate poisoning in *E. coli*.
Each culture was grown at 37 °C and 250 rpm in the presence of 50 μg/mL ampicillin and 34 μg/mL chloramphenicol at 37 °C and 250 rpm. Bacterial growth was monitored by measuring the optical density at 600 nm. Closed circles: *E. coli* BL21(DE3)pLysS lacking the gene encoding for NMO-Nc grown in the absence of propionate-3-nitronate. Open circles: *E. coli* BL21(DE3)pLysS-2NPDnc13 (15) grown in the presence of an effective concentration of 5 mM propionate-3-nitronate. Closed Squares: *E. coli* BL21(DE3)pLysS incubated in the presence of an effective concentration of 5 mM propionate-3-nitronate. The numbers correspond to the specific activities of cell free extracts determined as described in the materials and methods. *Inset*: *SDS*-PAGE: Lane 1: Cell free extract obtained from *E. coli* BL21(DE3)pLysS-2NPDnc13; Lane 2: Cell free extract obtained from *E. coli* BL21(DE3)pLysS; Lane 3: Sigma S8445 Marker proteins. IPTG and purified NMO were added at the times indicated on the plot.

Protection of E. coli from Propionate-3-Nitronate Toxicity by NMO-Nc. Results similar to those described above for NMO-Ws were obtained with NMO-Nc in that propionate-3-nitronate prevented the growth of the bacteria except when the expression of NMO was induced (Figure 8.3). The increase in the optical density at 600 nm (Figure 8.3) correlated well with an increase in specific activity of NMO. SDS-PAGE analysis of extracts prepared from stationary phase cultures revealed a predominant band corresponding to the molecular mass of NMO-Nc only in extracts that contained NMO activity and not in the control sample. The results clearly demonstrate that the bacterostatic effects of propionate-3-nitronate were overcome due to the expression of NMO by *E. coli*.

Effects of 3-Nitropropionate on the Growth of N. crassa and W. saturnus. N. crassa strains that either contain or lack the gene encoding for NMO were grown in the presence of 3-nitropropionate to establish if the expression of the enzyme would allow the fungus to overcome the toxicity of the compound. As shown in Table 8.5, the wild-type strain of *N. crassa* can grow

in up to 20 mM 3-nitropropionate, which was the highest concentration tested, whereas a knockout mutant lacking the NMO, gene was unable to grow at concentrations higher than 0.6 mM. *W. saturnus*, which contains the NMO gene encoding for the enzyme, was also able to grow in media containing 3-nitropropionate at concentrations as high as 20 mM.

Table 8.5 Fungal Growth in Either the Absence or Presence of 3-Nitropropionate

[3NPA][b], mM	*N. crassa* wild-type	*N. crassa* mutant	*W. saturnus*
0	+	+	+
0.25	+	+	+
0.5	+	+	+
0.6	+	-	+
1	+	-	+
10	+	-	+
20	+	-	+

[a] + indicates growth, - indicates no growth; [b] 3NPA is 3-nitropropionate

Linear Growth Rate of N. crassa Wild-Type and Knock-out Mutant in the Absence or Presence of 3-Nitropropionate. The effects of 3-nitropropionate on the growth rate of *N. crassa* was determined by monitoring mycelial growth of the fungus in race tubes containing increasing concentrations of the toxin. As shown in Table 8.6, 3-nitropropionate slowed the growth of wild-type *N. crassa* but the fungus was still able to grow at up to 8 mM of the toxin. Different results were obtained with the knock-out mutant, which showed no growth above 0.5 mM of the toxin.

Table 8.6 Linear Growth of *N. crassa* in Either the Absence or Presence of 3-NPA

[3NPA][b], mM	Wild-type, cm/h	Knockout, cm/h
0	0.312 ± 0.002	0.233 ± 0.001
0.5	0.308 ± 0.001	0.156 ± 0.001
1	0.164 ± 0.005	no growth
2	0.287 ± 0.002	no growth
4	0.267 ± 0.005	no growth
8	0.109 ± 0.008	no growth

[a] Growth of *N. crassa* was measured in 13 mL race tubes at 25 °C. The results are an average of triplicate measurements. [b] 3NPA is 3-nitropropionate.

8.5   Discussion

The Michaelis constants of NMO for propionate-3-nitronate determined under atmospheric oxygen ($^{app}K_m$) indicate that the nitro-compound is the physiological substrate for the enzyme. The $^{app}K_m$ values for both the *N. crassa* and *W. saturnus* enzymes are in the μM

range, which is at least five times lower than those determined previously for primary alkyl nitronates as substrate for NMO (16, 35). More importantly, the Michaelis constants with propionate-3-nitronate as substrate for the *W. saturnus* and *N. crassa* enzymes are within the physiological range of propionate-3-nitronate concentrations found in legumes and fungi (46). *Arthrinium* species, for example, accumulates up to 15 mM 3-nitropropionate (calculated from the reported value of 1716 μg/mL of culture) when the fungus is grown in sugarcane juice (46). Given the pK_a value of 9.1 for the ionization of 3-nitropropionate to yield propionate-3-nitronate (7) a concentration of 15 mM corresponds to an effective concentration of 300 μM nitronate at the physiological pH of 7.4. The correlation of the $^{app}K_m$ values of NMO with propionate-3-nitronate as substrate with the concentrations of the nitronate found in natural environments strongly implicates the toxin as the physiological substrate for the enzyme. Furthermore, the $^{app}(k_{cat}/K_m)$ values of NMO with propionate-3-nitronate of ~10^6 M^{-1}s^{-1} are typical for physiological substrates for enzymes.

Of all of the substrates tested to date, propionate-3-nitronate is most effectively oxidized by NMO as evident from the apparent steady state kinetic parameters measured in this study. Previous investigations of the *W. saturnus* and *N. crassa* enzymes established that primary alkyl nitronates are substrates for NMO and that the kinetic parameters are not dependent on the alkyl chain length of substrates ranging from 2 to 6 carbon atoms (16, 35). The turnover numbers, $^{app}k_{cat}$, and the rates of substrate capture[2], $^{app}(k_{cat}/K_m)$, under atmospheric oxygen are at least 4

---

[2] The definition of Northrop (42) for the k_{cat}/K_m value of an enzymatic reaction is used here instead of the more conventional definition that describes the kinetic parameter as the specificity constant. This was chosen based on previous results of NMO-Nc with nitroethane as substrate, which showed that branching of a reaction intermediate during catalysis results in different values of k_{cat}/K_m with nitroethane as substrate depending on whether the rates of oxygen consumption or nitronate release are measured (12). Since both values for k_{cat}/K_m describe the reaction of NMO-Nc with nitroethane as substrate, defining the kinetic parameter as a specificity constant of the enzyme for the nitroalkane is inadequate. Instead, the kinetic parameter describes the rate of substrate capture into productive enzyme complexes destined to form products at a later time as eloquently defined by Northrop (42).

and 30 times larger with propionate-3-nitronate than with ethylnitronate as substrate for NMO, respectively. The activity of NMO with propionate-3-nitronate is in accordance with a previous kinetic investigation of the enzyme, which demonstrated that substrate recognition is predominantly achieved through the interaction of an active site anion binding pocket with the nitro group of the substrate (13). The crystal structure of NMO from *P. aeruginosa* in complex with 2-nitropropane also shows a large solvent accessible cavity that could accommodate the carboxylate of propionate-3-nitronate (21). An asparagine residue located at the end of the cavity could act as a hydrogen bond donor to provide extra interactions with propionate-3-nitronate, which may explain the lower K_m value of the enzyme for this substrate (Figure 8.4).
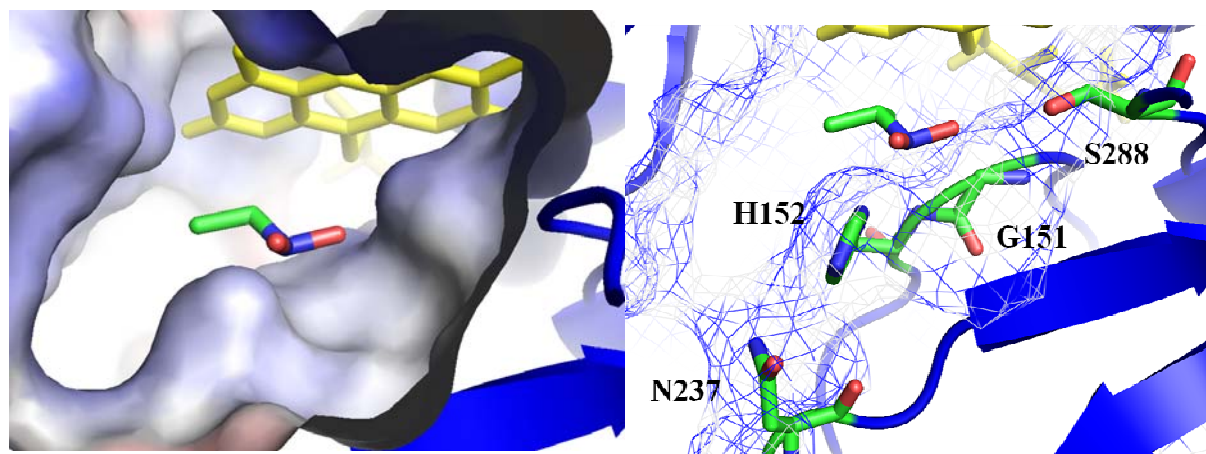
Figure 8.4 Active site structure of NMO from *P. aeurogionsa* (NMO-Pa).
The reported crystal structure of NMO-Pa (22) was used to generate an electrostatic potential map of the active site with an Adaptive Poisson-Boltzmann Solver (3), which was visualized using Pymol. Left Panel: Electrostatic potential surface of the active site of NMO-Pa. Right Panel: Active site amino acid residues that comprise the anion binding site in NMO-Pa.

The fact that catalase has no effect on the observed rates of oxygen consumption by NMO-Ws with either propionate-3-nitronate or 3-nitropropionate as substrate indicates that hydrogen peroxide is not released during catalytic turnover of the enzyme with propionate-3-nitronate as substrate. In contrast, hydrogen peroxide is detected in activity assays with NMO-Nc. during The formation of hydrogen peroxide is most likely not due to the NMO catalyzed

reaction, but rather a non-enzymatic, free radical reaction of the nitronate substrate and the superoxide anion. Such a reaction between nitronates and superoxide has been previously established and shown to terminate with the production of hydrogen peroxide (30). The conclusion that hydrogen peroxide is not produced by MNO-Nc is supported by the fact that catalase has no effect on oxygen consumption by the enzyme when superoxide is scavenged during turnover with propionate-3-nitronate by the addition of superoxide dismutase.

Although propionate-3-nitronate nitronate has long been recognized as a toxic metabolite of plants and fungi (2, 37) to our knowledge this study represents the first demonstration that the nitronate is toxic to *E. coli*. The effect of propionate-3-nitronate likely arises from the inhibition of key metabolic enzymes given that the compound has been shown to be a potent inhibitor of both succinate dehydrogenase (2, 11, 25) and fumarase (42). Studies of the inhibition of succinate dehydrogenase and fumarase have established that it is the propionate-3-nitronate form of the toxin, and not 3-nitropropionate that inhibits the enzymes *in vitro*. The majority of studies on the toxicity and biological occurrence of the toxin have focused on 3-nitropropionate, which has been shown to accumulate up to millimolar concentrations in plants and fungal cell cultures (7, 9, 46). 3-Nitropropionate is likely produced to such high levels because the equilibrium between the nitro-compound and propionate-3-nitronate favors the non-toxic form at physiological pH. The production of millimolar concentration of 3-nitropropionate would ensure that a sufficient amount of the compound ionizes to the toxic nitronate, which can provide a means of defense to the fungus.

The *in vivo* expression of NMO protects microorganisms against the toxicity of propionate-3-nitronate. Evidence supporting this conclusion comes from the observation that induction of the expression of recombinant NMO or exogenous addition of the enzyme to

cultures of *E. coli* was required for growth in the presence of propionate-3-nitronate. The presence of ITPG or antibiotics as the cause for growth of recombinant *E. coli* can be ruled out since each compound was present in the cultures that did not grow and lacked the gene encoding for NMO. In addition, a correlation between expression of NMO and growth of the bacterium was established through measurements of the specific activities of the enzyme with propionate-3-nitronate as substrate and visualization of the NMO by SDS-PAGE. The plasmid containing the gene encoding for *W. saturnus* NMO is retained even when the bacterium is grown in the absence of antibiotics. This further suggests that NMO is essential for the survival of the bacterium in the presence of propionate-3-nitronate, since the plasmid would not be retained without the selective pressure of detoxification of the nitronate by the enzyme. Taken together the results indicate that the enzyme can detoxify propionate-3-nitronate *in vivo*.

The results presented here demonstrate that propionate-3-nitronate is an effective and likely physiological substrate for the NMOs from *W. saturnus* and *N. crassa*. Expression of the enzymes in *E. coli* confers resistance to propionate-3-nitronate toxicity, which may be the physiological function of NMO in the fungal species. The demonstration of propionate-3-nitronate oxidizing activity in the fungal NMOs along with the recent detection of NMOs in *P. aeruginosa*, *Cupriavidus* JS190, and *B. phytofirmans* that detoxify the nitronate (40) suggest that the enzyme is widespread in nature. There are currently over 1800 genes annotated as 2-nitropropane dioxygenase in GenBank (http://www.ncbi.nlm.nih.gov/sites/entrez), the majority of which have yet to be experimentally characterized. The demonstration of propionate-3-nitronate oxidizing enzymes in microorganisms in this and a recent study (40) suggests that many of the putative 2-nitropropane dioxygenases may be actually NMOs. Current studies are underway to test this hypothesis.

8.6 References

1. Allison, R. D., and D. L. Purich. (1979) Practical considerations in the design of initial velocity enzyme rate assays. *Methods Enzymol. 63*, 3-22.

2. Alston, T. A., L. Mela, and H. J. Bright. (1977) 3-Nitropropionate, the toxic substance of *Indigofera*, is a suicide inactivator of succinate dehydrogenase. *Proc. Natl. Acad. Sci. U. S. A. 74,* 3767-3771.

3. Baker, N. A., D. Sept, S. Joseph, M. J. Holst, and J. A. McCammon. (2001) Electrostatics of nanosystems: application to microtubules and the ribosome. *Proc. Natl. Acad. Sci. U. S. A. 98,* 10037-10041.

4. Bradford, M. M. (1976) A rapid and sensitive method for the quantitation of microgram quantities of protein utilizing the principle of protein-dye binding. *Anal. Biochem. 72,* 248-254.

5. Brouillet, E., C. Jacquard, N. Bizat, and D. Blum. (2005) 3-Nitropropionic acid: a mitochondrial toxin to uncover physiopathological mechanisms underlying striatal degeneration in Huntington's disease. *J. Neurochem. 95,* 1521-1540.

6. Burdock, G. A., I. G. Carabin, and M. G. Soni. (2001) Safety assessment of b-nitropropionic acid: a monograph in support of an acceptable daily intake in humans. *Food Chemistry 75,* 1-27.

7. Bush, M. T., O. Touster, and J. E. Brockman. (1951) The production of beta-nitropropionic acid by a strain of *Aspergillus flavus*. *J. Biol. Chem. 188*, 685-693.

8. Carter, C. L., and C. W. Mc. (1949) Hiptagenic acid identified as beta-nitropropionic acid. *Nature 164,* 575.

9.   Chomcheon, P., S. Wiyakrutta, N. Sriubolmas, N. Ngamrojanavanich, D. Isarangkul, and P. Kittakoop. (2005) 3-Nitropropionic acid (3-NPA), a potent antimycobacterial agent from endophytic fungi: is 3-NPA in some plants produced by endophytes? *J. Nat. Prod. 68,* 1103-1105.

10.   Cleland, W. W. (1975) Partition analysis and the concept of net rate constants as tools in enzyme kinetics. *Biochemistry 14,* 3220-3224.

11.   Coles, C. J., D. E. Edmondson, and T. P. Singer. 1979. Inactivation of succinate dehydrogenase by 3-nitropropionate. *J. Biol. Chem. 254*, 5161-5167.

12.   Ding-Ling Wei, S.-C. C., Shu-Chien Lin, Ming-Luen Doong, and Shung-Chang Jong. (1994) Production of 3-Nitropropionic acid by *Arthrinium* Species. *Curr. Microbiol. 28*, 1-5.

13.   Francis, K., and G. Gadda. (2009) Kinetic evidence for an anion binding pocket in the active site of nitronate monooxygenase. *Bioorg. Chem. 37*, 167-72.

14.   Francis, K., and G. Gadda. (2008) The nonoxidative conversion of nitroethane to ethylnitronate in Neurospora crassa 2-nitropropane dioxygenase is catalyzed by histidine 196. *Biochemistry 47,* 9136-9144.

15.   Francis, K., and G. Gadda. 2006. Probing the chemical steps of nitroalkane oxidation catalyzed by 2-nitropropane dioxygenase with solvent viscosity, pH, and substrate kinetic isotope effects. *Biochemistry* 45, 13889-13998.

16.   Francis, K., B. Russell, and G. Gadda. 2005. Involvement of a flavosemiquinone in the enzymatic oxidation of nitroalkanes catalyzed by 2-nitropropane dioxygenase. *J. Biol. Chem*. 280, 5195-204.

17. Gadda, G., D. Y. Choe, and P. F. Fitzpatrick. (2000) Use of pH and kinetic isotope effects to dissect the effects of substrate size on binding and catalysis by nitroalkane oxidase. *Arch. Biochem. Biophys. 382,* 138-144.

18. Gadda, G., and K. Francis. (2009) Nitronate monooxygenase, a model for anionic flavin semiquinone intermediates in oxidative catalysis. *Arch Biochem Biophys.*

19. Gorlatova, N., M. Tchorzewski, T. Kurihara, K. Soda, and N. Esaki. (1998) Purification, characterization, and mechanism of a flavin mononucleotide-dependent 2-nitropropane dioxygenase from *Neurospora crassa*. *Appl. Environ. Microbiol. 64*, 1029-1033.

20. Gorter, K. (1920) L'Hiptagine, Glucoside Nouveau Retire De L'Hiptage Madablota Gaertin, vol. 2. Archipel Brukkerij, Builenzora, Indonesia.

21. Ha, J. Y., J. Y. Min, S. K. Lee, H. S. Kim, J. Kim do, K. H. Kim, H. H. Lee, H. K. Kim, H. J. Yoon, and S. W. Suh. (2006) Crystal structure of 2-nitropropane dioxygenase complexed with FMN and substrate. Identification of the catalytic base. *J. Biol. Chem. 281*, 18660-18667.

22. Hamilton, B. F., D. H. Gould, and D. L. Gustine. (1999) History of 3-Nitropropionic acid. *In* P. R. Sanberg, H. Nishino, and C. V. Borlongan (ed.), Mitchrondrial Inhibitors and Neurodegenerative Disorders. Humana Press, Totowa, NJ.

23. Hipkin, C. R., M. A. Salem, D. Simpson, and S. J. Wainwright. (1999) 3-nitropropionic acid oxidase from horseshoe vetch (*Hippocrepis comosa*): a novel plant enzyme. *Biochem. J. 340* (Pt 2), 491-495.

24. Hipkin, C. R., D. J. Simpson, S. J. Wainwright, and M. A. Salem. (2004) Nitrification by plants that also fix nitrogen. *Nature 430*, 98-101.

25.   Huang, L. S., G. Sun, D. Cobessi, A. C. Wang, J. T. Shen, E. Y. Tung, V. E. Anderson, and E. A. Berry. (2006) 3-nitropropionic acid is a suicide inhibitor of mitochondrial respiration that, upon oxidation by complex II, forms a covalent adduct with a catalytic base arginine in the active site of the enzyme. *J. Biol. Chem. 281*, 5965-5972.

26.   James, L. F., W. J. Hartley, and K. R. Van Kampen. (1981) Syndromes of astragalus poisoning in livestock. *J. Am. Vet. Med. Assoc. 178*, 146-150.

27.   Kido, T., K. Soda, T. Suzuki, and K. Asada. (1976) A new oxygenase, 2-nitropropane dioxygenase of *Hansenula mrakii*. Enzymologic and spectrophotometric properties. *J. Biol. Chem. 251,* 6994-7000.

28.   Kido, T., T. Yamamoto, and K. Soda. (1976) Purification and properties of nitroalkane-oxidizing enzyme from *Hansenula mrakii*. *J. Bacteriol. 126*, 1261-1265.

29.   Klinman, J. P. (2001) Life as aerobes: are there simple rules for activation of dioxygen by enzymes? *J. Biol. Inorg. Chem. 6*, 1-13.

30.   Kuo, C. F., and I. Fridovich. (1986) Free-radical chain oxidation of 2-nitropropane initiated and propagated by superoxide. *Biochem. J. 237,* 505-510.

31.   Little, H. N. (1951) Oxidation of nitroethane by extracts from *Neurospora*. *J. Biol. Chem. 193*, 347-358.

32.   Liu, X., Luo, X., and Hu, W. (1992) Studies on the epidemiology and etiology of moldy sugar can poisoning in China, *Biomed. Enviro. Sci.*, 161-177.

33.   Ludolph, A. C., F. He, P. S. Spencer, J. Hammerstad, and M. Sabri. (1991) 3-Nitropropionic acid-exogenous animal neurotoxin and possible human striatal toxin. *Can. J. Neurol. Sci. 18,* 492-498.

34.   Mathews, F. P. (1940) Poisioning in sheep and goats by sacahuiste (*Nolina texana*) buds and blooms, *J. Am. Vet. Med. Assoc. 97*, 125-134.

35.   Mijatovic, S., and G. Gadda. 2008. Oxidation of alkyl nitronates catalyzed by 2-nitropropane dioxygenase from *Hansenula mrakii*. *Arch. Biochem. Biophys. 473,* 61-68.

36.   Ming, L. (1995) Moldy sugarcane poisoning--a case report with a brief review. *J Toxicol Clin Toxicol 33,* 363-367.

37.   Morris, M. P., C. Pagan, and H. E. Warmke. (1954) Hiptagenic Acid, a Toxic Component of *Indigofera endecaphylla*. *Science 119,* 322-323.

38.   Nielsen, A. T. (1969) Nitronic acids and esters, p. 349-486. *In* H. Feuer (ed.), The Chemistry of the nitro and nitroso groups, vol. 1. Interscience Publishers, New York.

39.   Nishino, S. F., K. A. Shin, R. B. Payne, and J. C. Spain. (2010) Growth of bacteria on 3-nitropropionic acid as a sole source of carbon, nitrogen, and energy. *Appl. Environ. Microbiol. 76,* 3590-3598.

40.   Orth, R. (1977) Mycotoxins of *Aspergillus oryzae* Strains for Use in the Food Industry as Starters and Enzyme Producing Molds. *Ann. Nutr. Alim. 31,* 617-624.

41.   Porter, D. J., and H. J. Bright. (1980) 3-Carbanionic substrate analogues bind very tightly to fumarase and aspartase. *J. Biol. Chem. 255*, 4772-4480.

42.   Porter, D. J., and H. J. Bright. (1987) Propionate-3-nitronate oxidase from *Penicillium atrovenetum* is a flavoprotein which initiates the autoxidation of its substrate by O_2. *J. Biol. Chem. 262,* 14428-14434.

43.   Roth, J. P., and J. P. Klinman. (2003) Catalysis of electron transfer during activation of O_2 by the flavoprotein glucose oxidase. *Proc. Natl. Acad. Sci. U. S. A. 100,* 62-67.

44.   Shenk, J. S., P. J. Wangsness, R. M. Leach, D. L. Gustine, J. L. Gobble, and R. F. Barnes. (1976) Relationship between beta-nitropropionic acid content of crownvetch and toxicity in nonruminant animals. *J. Anim. Sci. 42,* 616-621.

45.   Wei, D.-L., S.-C. Chang, M.-L. Lin, Doong, and S.-C. Jong. (1994) Production of 3-Nitropropionic Acid by *Arthrinium* Species. *Curr. Microbiol. 28*, 1-5.

46.   Williams, M. C., L. F. James, and B. O. Bond. (1979) Emory milkvetch (Astragalus emoryanus var emoryanus) poisoning in chicks, sheep, and cattle. *Am. J. Vet. Res. 40*, 403-406.

9   CHAPTER IX

EXPRESSION,   PURIFICATION   AND   PRELIMINAREY   BIOCHEMICAL CHARACTERIZATION   OF   PROPIONATE-3-NITRONATE   MONOOXYGENASE FROM PSEUDOMONAS SP. JS189

9.1   Abstract

A propionate-3-nitrate oxidizing enzyme from *Pseudomonas* Sp. JS189 was recently identified and shown to allow the bacterium to grow on the toxin as a sole source of nitrogen, carbon and energy. The plasmid containing the gene encoding for the enzyme was used to transform *Escherichia coli* Rosetta(DE3)pLysS and the enzyme was expressed and purified to a high degree. The cofactor of the enzyme was identified as FMN through a fluorescence analysis of the flavin extracted from the enzyme before and after treatment with phosphodiesterase. A molar extinction coefficient of 13.6 ± 0.7 M^{-1}cm^{-1} (λ_{446} at pH 7.4) was also determined for the FMN cofactor of the enzyme. Enzymatic activity with propionate-3-nitrate was unaffected by the presence of either superoxide dismutase or catalase in the assay reaction mixture, suggesting the turnover of the enzyme occurs without the production and release of superoxide anion or hydrogen peroxide, respectively. A sequential steady state kinetic mechanism was established for the enzyme by measuring initial rates at varying concentrations of both the nitrate and oxygen. The pH dependence of the intrinsic steady state kinetic parameters of NMO was also determined in a pH range from 4 to 11.0. The turnover number of the enzyme decreased from an upper limiting value at low pH to a lower limiting value at high pH and showed a pK_a value of 9.3 ± 0.1 for a group that must be protonated for catalysis. The pH profile for the k_{cat}/K_m value with propionate-3-nitrate was bell shaped implicated a group that must be protonated and a group that must be unprotonated for substrate capture, while the k_{cat}/K_m value for oxygen was pH

independent. The preliminary data presented in this Chapter will be discussed along with a proposal of the experiments that should be preformed to complete the study and their expected outcomes.

9.2   Introduction

Propionate-3-nitronate is a highly toxic nitro compound that is widely distributed in legumes and fungi (*1-8*). The nitronate is an irreversible inhibitor of mitochondrial succinate dehydrogenase (*2, 9, 10*), that upon ingestion leads to a variety of neurological disorders (*11-13*) and, at sufficiently high concentrations, death (*14-18*). Plants that produce the toxin also express propionate-3-nitronate oxidizing enzymes that convert the toxin into malonate semialdehyde, nitrate, nitrite and hydrogen peroxide (*8, 19*). The enzymatic activities of these enzymes are thought to serve as a means of protection against the self-poisoning of the plant by the toxin (*8, 19*) and to play a role in the nitrogen cycle by releasing inorganic nitrogen derived from the nitronate into the soil (*8*).

$$3 \quad {}^{-}\!O\!-\!\!\!\overset{O}{\underset{}{\big\|}}\!\!\!\sim\!\!NO_2 \quad + \; 3\,O_2 \longrightarrow 3 \quad {}^{-}\!O\!-\!\!\!\overset{O\quad O}{\underset{}{\big\|\;\big\|}}\!\!\!H \quad + \quad NO_2^- \; + \; 3\,NO_3^- \; + \; H_2O_2$$

3-nitropropionate   malonic semialdehyde
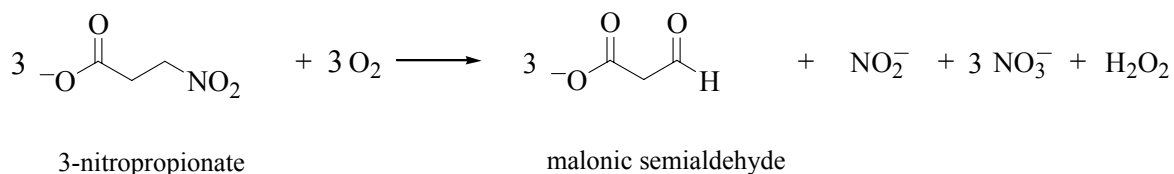
Scheme 9.1 Oxidation of propionate-3-nitronate to yield malonic semialdehyde in bacteria.

Bacteria that are able to grow on and utilize the toxin as a sole source of carbon, nitrogen and energy were recently isolated from soil and the enzymes involved in the degradation of 3-nitropropionate were identified (*20*). A propionate-3-nitronate oxidizing enzyme was found to transform the toxin into malonate semialdehyde, nitrite, nitrate and hydrogen peroxide according to Scheme 9.1 (*20*). The malonate semialdehyde that is produced by the enzyme is then

decarboxylated by a malonate semialdehyde oxidative decarboxylase to yield acetyl CoA, which then enters central metabolic pathways (*20*). While the physiological roles of the recently discovered bacterial propionate-3-nitronate oxidizing enzymes have been established, little is known about their biochemical or mechanistic properties.

The current Chapter describes the expression and purification of a bacterial propionate-3-nitronate monooxygenase from *Pseudomonas* sp. JS189. A preliminary biochemical investigation of the enzyme is presented along with studies of the pH dependence of the kinetic parameters with propionate-3-nitronate as substrate. The data collected to date will be discussed in the context of the well characterized fungal nitronate monooxygenases (*21-27*) and experiments needed to complete the study will be proposed along with their expected outcomes.

9.3 Materials and Methods

Materials. The expression strain of *Escherichia coli* BL21Star(DE3)/pET21a:*pno*A (*1*) containing the gene encoding for propionate-3-nitronate monooxygenase from *Pseudomonas* Sp. JS189 was a kind gift from Dr. Jim Spain at the Georgia Institute of Technology, Atlanta, Georgia. The plasmid extraction kit used to extract the plasmid containing the *pno*A gene from *E. coli* BL21Star(DE3)/pET21a:*pno*A was from Qiagen. DNase I, and RNase A were from Roche Biomedicals. Luria-Bertani agar and broth, chloramphenicol, FMN, FAD, phenylmethysulfonylfluoride (PMSF), superoxide dismutase, lysozyme and 3-nitropropionic acid were from Sigma-Aldrich. Ammonium sulfate and $MgCl_2$ were from ICN Biomedicals. EDTA and ampicillin was from Fisher Scientific. The expression strain *E. coli* Rosetta(DE3)pLysS was from Novagen. The Hi-Prep 16/10 Octyl Fast Flow column and the DEAE-Sepharose matrix used in packing the DEAE Fast Flow column were from Amersham Pharmacia Biotech. All other reagents were of the highest purity commercially available.

Instruments. UV-visible absorbance spectra were recorded using an Agilent Technologies diode-array spectrophotometer Model HP 8453, equipped with a thermostated water bath. Fluorescence emission spectra were recorded with a Shimadzu Spectrofluorometer Model RF-5301 PC, thermostated at 15 ^{o}C. Enzymatic activity was measured by monitoring the rate of oxygen consumption with a computer interfaced Oxy-32 oxygen monitoring system (Hansatech Instrument Ltd.).

Expression and Purification of Propionate-3-Nitronate Monooxygenase. The plasmid pET21a:*pno*A containing the gene encoding for propionate-3-nitronate monooxygenase was extracted according to the manufacturer's instructions and used to transform *E. coli* strain Rosetta(DE3)pLysS by heat shock (*2*). Overnight cultures of the resulting strain were used to inoculate 6 x 1 liter of Luria-Bertani broth containing 50 μg/ml ampicillin and 34 μg/ml chloramphenicol at 37 ^{o}C. After the cultures reached an optical density at 600 nm of ~0.6 the temperature was lowered to 22 ^{o}C and isopropyl-β-D-thiogalactopyranoside (IPTG) was added at a final concentration of 0.1 mM. After incubation for 20 h, cells were harvested by centrifugation and were suspended with four volumes of 1 mM EDTA, 100 mM NaCl, 0.1 mM PMSF, 0.2 mg/mL lysozyme, 5 μg/mL DNase I and 10 mM $MgCl_2$, in 50 mM potassium phosphate, 20% glycerol at pH 8, before sonication and collection of the cell extract by centrifugation at 12,000 *g* for 20 min. The extract was brought to 30% ammonium sulfate saturation and the suprenant was collected after centrifugation. After a 65% ammonium sulfate saturation and centrifugation, the resultant pellet was dialyzed against 50 mM potassium phosphate, 10% glycerol, pH 7.4, and was loaded onto a DEAE Fast Flow column (20 mL bed volume) connected to an Åkta*prime* Amersham Biotech system equilibrated with the same buffer. The column was eluted with a linear gradient from 0 to 500 mM NaCl developed over 500 mL at a flow rate of 2 mL/min.

Catalytically active fractions were pooled, concentrated by 65 % ammonium sulfate saturation and dialyzed against 50 mM potassium phosphate, 10% glycerol, pH 7.4. The partially purified enzyme solution was adjusted to a final concentration of 1 M ammonium sulfate before loading onto a Hi-Prep 16/10 Octyl Fast Flow column (5 mL bed volume) equilibrated with 1M ammonium sulfate in 50 mM potassium phosphate, 10% glycerol pH 7.4. Protein elution was carried out with a linear gradient from 1 to 0 M ammonium sulfate over 100 mL at a flow rate of 0.5 mL/min. Fractions of the highest purity were pooled, dialyzed against 50 mM potassium phosphate, 10% glycerol, 100 mM NaCl, pH 7.4, and stored at -20 $^{\circ}$C until use.

Biochemical Methods. The concentration of propionate-3-nitronate monooxygenase was determined with the method of Bradford (*3*), using the Bio-Rad protein assay kit with bovine serum albumin as standard. The flavin to protein stoichiometry was determined by incubating the enzyme at 100 $^{\circ}$C for 30 min, followed by removal of precipitated protein by centrifugation. The flavin content per monomer of enzyme was calculated from the ratio of the concentration of flavin released from the enzyme, using an ε_{455nm} value of 12,500 $M^{-1}cm^{-1}$ (*4*), to the concentration of protein determined by the Bradford assay. Identification of the flavin cofactor of was determined by monitoring the changes in the fluorescence emission of the extracted flavin after treatment with phosphodiesterase using the method of Forti (*5*). The molar extinction coefficient of the flavin cofactor was determined by following the change in UV-visible absorbance at 446 nm of the enzyme at pH 7.4.

Enzyme Kinetics. Enzymatic activity was measured in 50 mM potassium phosphate, pH 7.4, at 30 $^{\circ}$C with the method of initial rates (*6*) in air saturated buffer by monitoring the rate of oxygen consumption. Enzyme concentration was expressed per enzyme bound FMN content, using the experimentally determined ε_{446nm} value of 13.6 $M^{-1}cm^{-1}$ (this study). Propionate-3-

nitronate was prepared in water by incubating 3-nitropropionate with a 2.2 molar excess of potassium hydroxide for at least 24 h at room temperature. Enzymatic activity assays were initiated by the addition of substrate, in order to minimize changes in the ionization state of the propionate-3-nitronate. When both the organic substrate and oxygen were varied, the assay mixtures were equilibrated with the appropriate O_2/N_2 gas mixture by bubbling the gas for at least 10 min before the reaction was started with the addition of the enzyme and the organic substrate. When the pH was varied, 50 mM piperzine was used as a buffer between 4.0 and 5.8, and sodium pyrophosphate was between pH 6.0 and 11.0. The release of superoxide during turnover of the enzyme with propionate-3-nitronate was monitored by measuring the rate of oxygen consumption at a fixed concentration of substrate, in either the presence or absence of 125 units of superoxide dismutase, in air saturated 50 mM potassium phosphate, pH 7.4, at 30 °C. Production and release of hydrogen peroxide during turnover was monitored by measuring the rate of oxygen consumption at a fixed concentration of substrate, in either the presence or absence of 75 units of catalase.

Data Analysis. Kinetic data were fit using KaleidaGraph (Synergy Software, Reading, PA) or Enzfitter (Biosoft, Cambridge, UK) software. Kinetic parameters determined in atmospheric oxygen were obtained by fitting the data to the Michaelis-Menten equation for one substrate. When initial rates were determined by varying the concentrations of both propionate-3-nitronate and oxygen, the data were fit to equations 1 and 2, which describe a sequential and ping-pong steady state kinetic mechanism, respectively. K_a and K_b represent the Michaelis constants for the propionate-3-nitronate (A) and oxygen (B), respectively, k_{cat} is the turnover number of the enzyme (e) and K_{ia} is the dissociation constant of substrate A from the ternary complex. The pH dependence of the steady state kinetic parameters was determined through fits

of the data to equations 3 and 4, which describe a bell shaped curve with a slope of +1 at low pH and a slope of −1 at high pH, and a curve that decreases from an upper limiting value at low pH to a lower limiting plateau at an intermediate pH range and then with a slope of -1 at high pH, respectively.

$$\frac{v}{e} = \frac{k_{cat}AB}{K_a B + K_b A + AB + K_{ia}K_b} \tag{1}$$

$$\frac{v}{e} = \frac{k_{cat}AB}{K_a B + K_b A + AB} \tag{2}$$

$$\log Y = \log\left(\frac{C}{1 + \dfrac{10^{-pH}}{10^{-pKa1}} + \dfrac{10^{-pKa2}}{10^{-pH}}}\right) \tag{3}$$

$$\log Y = \log\left(\frac{Y_L}{1 + \dfrac{10^{-pKa_1}}{10^{-pH}}} + \frac{Y_I}{1 + \dfrac{10^{-pKa_2}}{10^{-pH}}}\right) \tag{4}$$

9.4   Results

Expression and Purification of Propionate-3-Nitronate. The expression and purification protocols developed in this study allowed for the attainment of soluble and highly pure propionate-3-nitronate monooxygenase as judged by SDS-PAGE analysis (*data not shown*). As shown in Table 9.1, 30 mg of recombinant propionate-3-nitronate monooxygenase could be obtained from 6 L of bacterial cell culture using two chromatographic steps involving a DEAE-Sepharose and an Octyl-Sepharose column.

Table 9.1 Purification of Proprionate-3-Nitronate Monooxygenase

Step	total protein, mg	total activity[b], $\mu mol\ O_2\ min^{-1}$	specific activity, $\mu mol\ O_2\ min^{-1} mg^{-1}$
Cell extract	6,780	226,400	1
30% $(NH_4)_2SO_4$ saturation	2350	204,500	2.6
65% $(NH_4)_2SO_4$ saturation	2135	192,200	2.7
DEAE-Sepharose FF	1345	119,300	2.7
Octyl-Sepharose FF	30	36,900	39

[a]Starting from 40 g of wet cell paste; [b]Enzyme activity was determined with 1 mM propionate-3-nitronate in air-saturated 50 mM potassium phosphate pH 7.4 and 30 °C.
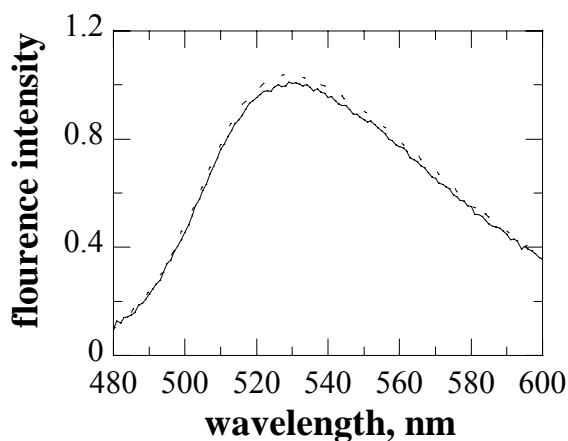
Figure 9.1 Identification of the flavin cofactor of propionate-3-nitronate monooxygenase.
Flavin fluorescence was measured before and after treatment of the extracted cofactor by 30 mU of phopshodiesterase at in 50 mM potassium phosphate pH 7.4 and 20 °C.

Identification of the Flavin Cofactor, Stoichiometry and Extinction Coefficient of Propionate-3-Nitronate Monooxygenase. The flavin content of propionate-3-nitronate monooxygenase was determined by monitoring the fluorescence emission of the extracted cofactor before and after treatment with phosphodiesterase. If the enzyme contains FAD, phosphodiesterase treatment would result in an increase in the flavin fluorescence since it would remove the quenching that arises from the adenine dinucleotide moiety of the cofactor. As shown in Figure 9.1, treatment of the flavin extracted from the enzyme did not result in changes in the fluorescence intensity, which demonstrates that propionate-3-nitronate monooxygenase contains FMN as cofactor. An extinction coefficient of 13.6 ± 0.7 $M^{-1}cm^{-1}$ (λ_{446} at pH 7.4) was determined for the enzyme-

bound FMN from the average ratio of the absorbance of bound to free FMN extracted by heat treatment of the enzyme in three independent measurements. A flavin to protein stoichiometry of 0.31 was determined from the ratio of the concentration of flavin released after heat treatment of the enzyme to the concentration of enzyme determined by the Bradford assay.

Effect of Superoxide Dismutase and Catalase on the Enzymatic Activity of Propionate-3-Nitronate Monooxygenase. The rates of oxygen consumption by propionate-3-nitronate oxidase were unaffected by the presence of either superoxide dismutase or catalase and had an average value of 710 ± 2 s^{-1} with 0.5 mM substrate at pH 7.4 and 30 ^{o}C. Thus, the observed rates of oxygen consumption measured with propionate-3-nitronate as substrate do not arise from a non-enzymatic reaction of the nitronate with superoxide and do not occur with the production of hydrogen peroxide.
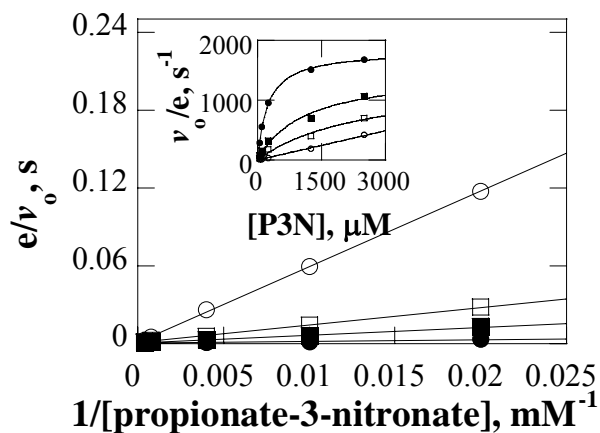
Figure 9.2 Double reciprocal plot of the reaction catalyzed by propionate-3-nitronate monooxygenase with propionate-3-nitronate as substrate.
Enzyme activity was measured at varying concentrations of both the organic substarte and oxygen in 50 mM potassium phosphate, pH 7.4 and 30 ^{o}C. The concentrations of oxygen used were: 20 μM (o); 35 μM (□); 250 μM (■) and 300 μM (•). *Panel B,* The lines are fits of the data to equation 1. *Inset.* Michaelis-Menton plots of the data.

Steady State Kinetic Mechanism of Propionate-3-Nitronate Monooxygenase. The steady state kinetic mechanism of the enzyme with propionate-3-nitronate as substrate was determined in 50 mM potassium phosphate at pH 7.4 and 30 ^{o}C. As shown in Figure 9.2, the enzyme utilizes a sequential steady state kinetic mechanism as evident from the pattern of intersecting lines seen in a double reciprocal plot of the initial rate of oxygen consumption as a function of substrate concentration. Furthermore, the data were best fit with equation

1, which describes a sequential steady state kinetic mechanism. The kinetic parameters determined at pH 7.4 and 30 °C are shown in Table 9.2.

Table 9.2 Steady-State Kinetic Parameters of Propionate-3-Nitronate Monooxygenase

k_{cat}	1600 ± 100 s^{-1}
$K_a{}^b$	0.11 ± 0.02 mM
k_{cat}/K_m,	$(1.5 \pm 0.2) \times 10^7$ M^{-1}s^{-1}
$K_b{}^c$	135 ± 20 μM
k_{cat}/K_b	$(1.2 \pm 0.2) \times 10^7$ M^{-1}s^{-1}
K_{ia}	0.14 ± 0.02 mM
R^2	0.997

[a]Enzyme activity was measured at varying concentrations of both the organic substrate and oxygen in 50 mM potassium phosphate, pH 7.4 and 30 °C. Data were fit with equation 1. [b]K_a is the Michaelis constant for propionate-3-nitronate; [c]K_b is the Michaelis constant for oxygen.

pH Dependence of the Steady-State Kinetic Parameters of Propionate-3-Nitronate Monooxygenase. The pH dependences of the kinetic parameters of propionate-3-nitronate monooxygenase were determined in the pH range from 4.5 to 11.0 by varying the concentrations of both the organic substrate and oxygen. The turnover number of the enzyme decreases from an upper limiting value of 2135 ± 5 s^{-1} at low pH to a lower limiting value of 275 ± 2 s^{-1} at high pH (Figure 9.3A). As shown in Figure 9.3B, the k_{cat}/K_m values with propionate-3-nitronate as substrate yielded a bell-shaped pH profile, consistent with the involvement of two ionizable groups that must be protonated and unprotonated for the oxidation of the nitronate. The k_{cat}/K_m value for oxygen as substrate for the enzyme is pH independent with an average value of $(1.2 \pm 0.1) \times 10^7$ M^{-1}s^{-1}(Figure 9.3C). The pK_a values determined in this study are summarized in Table 9.2.

Table 9.3 Kinetic pK_a Values Determined with Propionate-3-Nitronate as Substrate for Propionate-3-Nitronate Monooxygenase

kinetic parameter	pK_1	pK_2	eq.
k_{cat}		9.3 ± 0.1	4
k_{cat}/K_m	5.7 ± 0.1	8.9 ± 0.1	3

Enzyme activity was measured at varying concentrations of both the organic substrate and oxygen in 50 mM buffer in the pH range from 4.5 to 11.0 at 30 °C.

Table 9.4 pH Depnedence of the Steady State Kinetic Paramaters of Propionate-3-Monooxygenase with Propionate-3-Nitronate as Substrate

pH	k_{cat}, s^{-1}	K_a, µM	K_b, µM	k_{cat}/K_a, M^{-1}s^{-1}	k_{cat}/K_b, M^{-1}s^{-1}	K_{ia}, µM	R^2
4.0	2,300 ± 1	8,750 ± 1	150 ± 1	(2.6 ± 0.1) x 10^5	(1.5 ± 0.1) x 10^7	20 ± 1	0.996
4.5	2,200 ± 2	2,250 ± 10	70 ± 1	(9.7 ± 0.1) x 10^5	(3.2 ± 0.1) x 10^7	1,380 ± 40	0.989
5.0	2,200 ± 10	630 ± 10	400 ± 5	(3.4 ± 0.1) x 10^6	(5.9 ± 0.1) x 10^7	80 ± 10	0.996
5.5	2,000 ± 10	80 ± 1	110 ± 5	(2.4 ± 0.1) x 10^7	(2.0 ± 0.1) x 10^6	140 ± 30	0.985
6.0	2,100 ± 30	250 ± 10	450 ± 10	(1.1 ± 0.1) x 10^7	(5.7 ± 0.1) x 10^7	40 ± 5	0.999
6.5	1940 ± 100	500 ±70	190 ± 20	(4.0 ± 0.6) x 10^6	(1.0 ± 0.1) x 10^7	380 ± 100	0.997
7.0	2,200 ± 1	120 ± 1	110 ± 1	(1.8 ± 0.1) x 10^6	(2.0 ± 0.1) x 10^7	1,250 ± 10	0.996
7.4	1,600 ± 100	110 ± 20	140 ± 20	(1.2 ± 0.2) x 10^7	(1.2 ± 0.2) x 10^7	80 ± 20	0.997
8.5	1,650 ± 60	75 ± 20	120 ± 30	(2.1 ± 0.5) x 10^7	(1.3 ± 0.3) x 10^7	830 ± 250	0.996
9.0	1,380 ± 10	140 ± 5	120 ± 2	(1.0 ± 0.1) x 10^7	(1.1 ± 0.1) x 10^7	120 ± 5	0.999
9.5	630 ± 50	160 ± 30	50 ± 10	(4.0 ± 0.8) x 10^6	(1.3 ± 0.4) x 10^7	400 ± 180	0.994
10.0	400 ± 2	890 ± 10	20 ± 1	(4.7 ± 0.1) x 10^5	(1.7 ± 0.1) x 10^7	300 ± 20	0.995
10.5	360 ± 10	770 ± 60	30 ± 2	(4.7 ± 0.5) x 10^5	(1.3 ± 0.1) x 10^7	140 ± 70	0.995
11.0	300 ± 1	3,960 ± 20	30 ± 1	(7.5 ± 0.1) x 10^4	(8.5 ± 0.1) x 10^6	20 ± 1	0.992

Enzyme activity was measured at varying concentrations of both the organic substrate and oxygen in 50 mM buffer in the pH range from 4.5 to 11.0 at 30 °C.
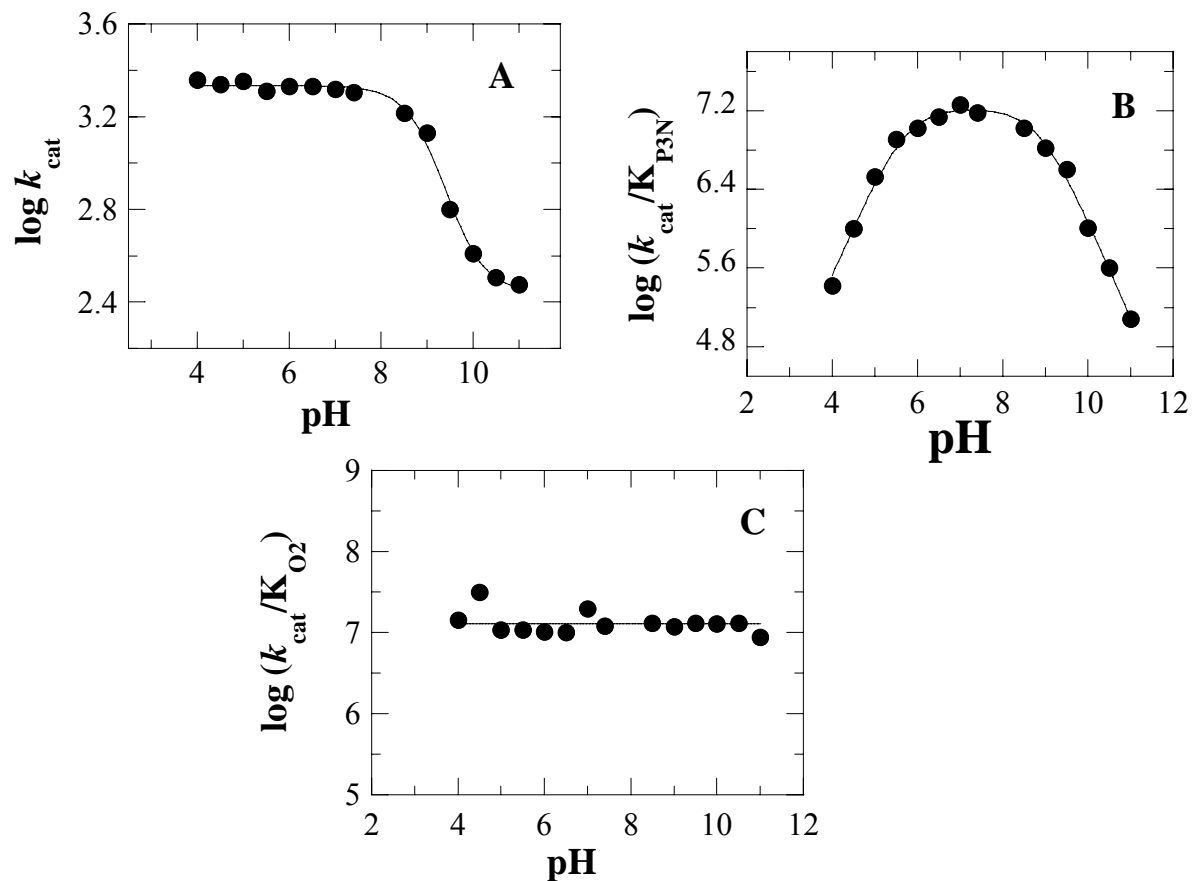
Figure 9.3 pH dependence of the steady state kinetic parameters of propionate-3-nitronate monooxygenase.
Initial rates were measured in air saturated, 50 mM buffer at 30 $^{\circ}$C, in the pH range from 4.5 to 11.0. Panel A, pH profile of the k_{cat} value. The data was fit with equation 4; Panel B, pH profile of the k_{cat}/K_m value with propionate-3-nitronate as substrate. The data was fit with equation 3; Panel C, k_{cat}/K_m values with oxygen as substrate.

9.5 Discussion

The propionate-3-nitronate oxidizing enzyme from *Pseudomonas* sp JS189 has been expressed and purified to high levels. The enzyme appears to be similar to the nitronate monooxygenases from *N. crassa* (24) and *W. saturnus* (*27*) in that it contains a single FMN cofactor per monomer. While detailed mechanistic studies to establish if the bacterial enzyme also stabilizes an anionic flavosemiquinone during the reductive half reaction have yet to be carried out, the evidence collected to date suggests a similar catalytic mechanism as that of the fungal nitronate monooxygenases. Evidence suggesting a similar catalytic mechanism for the bacterial enzyme comes from the lack of superoxide dismutase or catalase effects on the observed rates of oxygen consumption with propionate-3-nitronate as substrate as is the case for the fungal nitronate monooxygenases (see Chapter 8). Further results to suggest that the bacterial propionate-3-nitronate monooxygenase is similar to the fungal enzymes comes from the pattern of intersecting lines observed in the double reciprocal plots of the initial rates of the reaction versus substrate concentration, which demonstrates a sequential steady state kinetic mechanism. The discussion of the pH profiles of the kinetic parameters will assume that the fungal and bacterial enzymes utilize similar mechanisms and further experiments to confirm this hypothesis will be presented.

A minimal steady-state kinetic mechanism for propionate-3-nitronate monooxygenase from *Pseudomonas* Sp. JS189 is shown in Scheme 9.2.

Scheme 9.2 Minimal steady-state kinetic mecahanism for propionate-3-nitronate monooxygenase from *Pseudonomas* Sp. JS189.
E_{ox} is the oxidized enzyme; E_{sq} is the anionic flavosemiquinone enzyme intermediate; S^- is propionate-3-nitronate; $S^{\cdot}$ and S' are a radical intermediate and peroxpropionate-3-nitronate intermediate formed during turnover. P_1 and P_2 are malonate semialdehyde and nitrite, respectively.

After binding the nitronate a single electron transfer between the enzyme bound substrate and the flavin cofactor would occur to generate an anionic flavosemiquinone intermediate form of the enzyme and a substrate radical. Molecular oxygen would then reoxidize the flavin and generate a radical intermediate that would combine with superoxide anion in the active site to generate a peroxypropionate-3-nitronate intermediate. This intermediate would then be released from the active site and undergo a non-enzymatic reaction to yield malonate semialdehyde and nitrite as suggested for the fungal nitronate monooxygenases (*21, 26*). Expressions for the kinetic parameters measured at saturating concentrations of oxygen for the mechanism of Scheme 9.2 were derived using the method of King and Altman (*33*) and are shown in equations 5 through 7.

$$k_{cat} = \frac{k_3 k_7 k_9}{k_3 k_7 + k_3 k_8 + k_3 k_9 + k_7 k_9} \qquad (5)$$

$$\left(\frac{k_{cat}}{K_a}\right) = \frac{k_1 k_3}{k_2 + k_3} \qquad (6)$$

$$\left(\frac{k_{cat}}{K_B}\right) = O_2 k_5 \qquad (7)$$

The pH profile of the k_{cat} value with propionate-3-nitronate as substrate for the bacterial enzyme demonstrates the presence of a group that must be protonated for efficient turnover of the enzyme. Previous studies of2w *N. crassa* nitronate monooxygenase demonstrated that the formation of the anionic flavosemiquinone intermediate during turnover is facilitated by the protonated form of histidine 196 that serves as an electrostatic catalyst to stabilize the negative charge that forms after flavin reduction (*21, 34*). If the bacterial enzyme oxidizes propionate-3-nitronate through the formation of an anionic flavosemiquinone (k3 in Scheme 9.2) a positively charged residue would catalyze the reaction in a manner similar to that established for the fungal

nitronate monooxygenases (*24, 27*) and would account for the higher turnover numbers at low pH values.

propyl-1-nitronate

propionate-3-nitronate
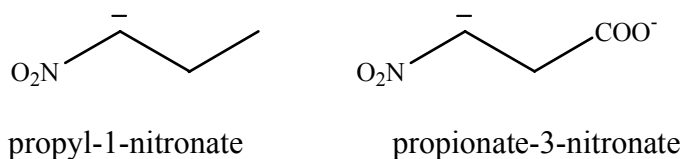
Figure 9.4 The chemical structures of propyl-1-nitronate and propionate-3-nitronate.

As shown in Scheme 9.2, the kinetic step of flavin reduction (k_3) is common to both the k_{cat} and the k_{cat}/K_m values of the enzyme with propionate-3-nitronate as substrate. Thus, the decrease in the k_{cat}/K_m value observed at high pH is likely also due to a decrease in the rate of flavin reduction. However, the pH profile of the k_{cat}/K_m value also shows a group that must be unprotonated for catalysis. This behavior was not observed with ethylnitronate or butyl-1-nitronate as substrates for *N. crassa* nitronate monooxygenase (*24*) and thus could be assigned to the carboxylate of propionate-3-nitronate, which is absent in the primary alkyl nitronates (Figure 9.4). A previous study of fungal nitronate monooxygenase established that substrate recognition is achieved through the interaction of the nitro moiety of the alkyl nitronate substrate with an active site anion binding pocket (*23*). The carboxylate group of propionate-3-nitronate might serve a similar function in the bacterial enzyme by providing an electrostatic attraction to keep the substrate properly oriented for efficient catalysis. This hypothesis will be tested by determining the pH profile of the enzyme with propyl-1-nitronate as substrate, which has similar chemical structure, but lacks the carboxylate functional group that is present in propionate-3-nitronate. If the acidic limb observed in the pH profile with propionate-3-nitronate as substrate is due to the protonation of the carboxylate, then a decrease in the k_{cat}/K_m value at low pH with propyl-1-nitronate would not be seen since the primary alkyl nitronate lacks the carboxylate group.

Future studies will also have to be carried out to establish that an anionic flavosemiquinone is formed upon anaerobic reduction of the enzyme with propionate-3-nitronate. In addition, the protocol to obtain pure enzyme will have to be optimized to avoid the loss of the FMN cofactor during purification.

In conclusion the studies presented in this Chapter have set the framework for detailed mechanistic studies of the enzyme to be carried out. An efficient expression protocol has been developed allowing for the rapid attainment of enzyme. The enzyme contains an FMN cofactor, utilizes a sequential steady state kinetic mechanism and does not release reactive oxygen species during catalytic turnover. Thus, the enzyme appears to be similar to the fungal nitronate monooxygenase in all aspects tested.

9.6   References

1.   Abramovitz, A. S., and Massey, V. (1976) Purification of intact old yellow enzyme using an affinity matrix for the sole chromatographic step, *J. Biol. Chem. 251*, 5321-5326.

2.   Alston, T. A., Mela, L., and Bright, H. J. (1977) 3-Nitropropionate, the toxic substance of *Indigofera*, is a suicide inactivator of succinate dehydrogenase, *Proc. Natl. Acad. Sci. U. S. A. 74*, 3767-3771.

3.   Bush, M. T., Touster, O., and Brockman, J. E. (1951) The production of beta-nitropropionic acid by a strain of *Aspergillus flavus*, *J. Biol. Chem. 188*, 685-693.

4.   Candish, E., La Croix, L. J., and Unran, A. M. (1969) The Biosynthesis of 3-Nitropropionic Acid in Creeping Indigo (*Indigofera spicata*), *Biochemistry 8*, 182-186.

5.   Carter, C. L., and Mc, C. W. (1949) Hiptagenic acid identified as beta-nitropropionic acid, *Nature 164*, 575.

6.   Chomcheon, P., Wiyakrutta, S., Sriubolmas, N., Ngamrojanavanich, N., Isarangkul, D., and Kittakoop, P. (2005) 3-Nitropropionic acid (3-NPA), a potent antimycobacterial agent from endophytic fungi: is 3-NPA in some plants produced by endophytes?, *J. Nat. Prod. 68*, 1103-1105.

7.   Ding-Ling Wei, S.-C. C., Shu-Chien Lin, Ming-Luen Doong, and Shung-Chang Jong. (1994) Production of 3-Nitropropionic acid by *Arthrinium* Species, *Curr. Microbiol. 28*, 1-5.

8.   Hipkin, C. R., Simpson, D. J., Wainwright, S. J., and Salem, M. A. (2004) Nitrification by plants that also fix nitrogen, *Nature 430*, 98-101.

9.   Coles, C. J., Edmondson, D. E., and Singer, T. P. (1979) Inactivation of succinate dehydrogenase by 3-nitropropionate, *J. Biol. Chem. 254*, 5161-5167.

10. Huang, L. S., Sun, G., Cobessi, D., Wang, A. C., Shen, J. T., Tung, E. Y., Anderson, V. E., and Berry, E. A. (2006) 3-nitropropionic acid is a suicide inhibitor of mitochondrial respiration that, upon oxidation by complex II, forms a covalent adduct with a catalytic base arginine in the active site of the enzyme, *J. Biol. Chem. 281*, 5965-5972.

11. Brouillet, E., Jacquard, C., Bizat, N., and Blum, D. (2005) 3-Nitropropionic acid: a mitochondrial toxin to uncover physiopathological mechanisms underlying striatal degeneration in Huntington's disease, *J. Neurochem. 95*, 1521-1540.

12. Burdock, G. A., Carabin, I. G., and Soni, M. G. (2001) Safety assessment of b-nitropropionic acid: a monograph in support of an acceptable daily intake in humans, *Food Chemistry 75*, 1-27.

13. He, F., Zhang, S., Qian, F., and Zhang, C. (1995) Delayed dystonia with striatal CT lucencies induced by a mycotoxin (3-nitropropionic acid), *Neurology 45*, 2178-2183.

14. Hamilton, B. F., Gould, D. H., and Gustine, D. L. (1999) History of 3-Nitropropionic acid, In *Mitrochrondrial Inhibitors and Neurodegenerative Disorders* (Sanberg, P. R., Nishino, H., and Borlongan, C. V., Eds.), Humana Press, Totowa, NJ.

15. James, L. F., Hartley, W. J., and Van Kampen, K. R. (1981) Syndromes of astragalus poisoning in livestock, *J. Am. Vet. Med. Assoc. 178*, 146-150.

16. James, L. F., Hartley, W. J., Williams, M. C., and Van Kampen, K. R. (1980) Field and experimental studies in cattle and sheep poisoned by nitro-bearing *Astragalus* or their toxins, *Am. J. Vet. Res. 41*, 377-382.

17. Williams, M. C., James, L. F., and Bond, B. O. (1979) Emory milkvetch (Astragalus emoryanus var emoryanus) poisoning in chicks, sheep, and cattle, *Am. J. Vet. Res. 40*, 403-406.

18. Williams, M. C., van Kampen, K. R., and Norris, F. A. (1969) Timber milkvetch poisoning in chickens, rabbits, and cattle, *Am. J. Vet. Res. 30*, 2185-2190.

19. Hipkin, C. R., Salem, M. A., Simpson, D., and Wainwright, S. J. (1999) 3-nitropropionic acid oxidase from horseshoe vetch (Hippocrepis comosa): a novel plant enzyme, *Biochem. J. 340 (Pt 2)*, 491-495.

20. Nishino, S. F., Shin, K. A., Payne, R. B., and Spain, J. C. (2010) Growth of bacteria on 3-nitropropionic acid as a sole source of carbon, nitrogen, and energy, *Appl. Environ. Microbiol. 76*, 3590-3598.

21. Francis, K., and Gadda, G. (2006) Probing the chemical steps of nitroalkane oxidation catalyzed by 2-nitropropane dioxygenase with solvent viscosity, pH, and substrate kinetic isotope effects, *Biochemistry 45*, 13889-13898.

22. Francis, K., and Gadda, G. (2008) The nonoxidative conversion of nitroethane to ethylnitronate in Neurospora crassa 2-nitropropane dioxygenase is catalyzed by histidine 196, *Biochemistry 47*, 9136-9144.

23. Francis, K., and Gadda, G. (2009) Kinetic evidence for an anion binding pocket in the active site of nitronate monooxygenase, *Bioorg. Chem. 37*, 167-172.

24. Francis, K., Russell, B., and Gadda, G. (2005) Involvement of a flavosemiquinone in the enzymatic oxidation of nitroalkanes catalyzed by 2-nitropropane dioxygenase, *J. Biol. Chem. 280*, 5195-5204.

25. Gadda, G., and Fitzpatrick, P. F. (2000) Iso-mechanism of nitroalkane oxidase: 1. Inhibition studies and activation by imidazole, *Biochemistry 39*, 1400-1405.

26. Gadda, G., and Francis, K. (2009) Nitronate monooxygenase, a model for anionic flavin semiquinone intermediates in oxidative catalysis, *Arch. Biochem. Biophys. 493*, 53-61.

27. Mijatovic, S., and Gadda, G. (2008) Oxidation of alkyl nitronates catalyzed by 2-nitropropane dioxygenase from *Hansenula mrakii*, *Arch. Biochem. Biophys. 473*, 61-68.

28. Inoue, H., Nojima, H., and Okayama, H. (1990) *Gene 96*, 23-28.

29. Bradford, M. M. (1976) *Anal. Biochem. 72*, 248-254.

30. Whitby, L. G. (1953) A new method for preparing flavin-adenine dinucleotide, *Biochem. J. 54*, 437-442.

31. Forti, G., and Sturani, E. (1968) On the Structure and function of reduced nicatinamide adenine dinucleotide phosphate-cytochrome f of reductase of spinach chloroplasts, *Eur. J. Biochem. 3*, 461-472.

32. Allison, R. D., and Purich, D. L. (1979) Practical considerations in the design of initial velocity enzyme rate assays, *Methods Enzymol. 63*, 3-22.

33. King, E. L., and Altman, C. . (1956) A Schematic Method of Deriving the Rate Laws for Enzyme-Catalyzed Reactions, *J. Phys. Chem. 60*, 1375-1378.

34. Gadda, G., and Francis, K. (2009) Inflated kinetic isotope effects in the branched mechanism of N. crassa 2-nitropropane dioxygenase, *Biochemistry*.

10   **Chapter X**

CONCLUSIONS AND GENERAL DISSCUSSION

10.1 Closing Remarks

A wealth of information on the biochemical, mechanistic and physiological role of nitronate monooxygenase has been gained from the doctoral research presented in this dissertation. At the onset of the research project described here the nitroalkane oxidizing enzyme from *Neurospora crassa* was classified as a 2-nitropropane dioxygenase and its physiological role was a mystery. Investigations of the substrate specificity and catalytic mechanism revealed that the enzyme is significantly more active with primary alkyl nitronates over secondary nitroalkanes such as 2-nitropropane. In recognition of the work presented in Chapters 3 through 6 of the dissertation, the International Union of Biochemistry and Molecular Biology officially reclassified the enzyme as a nitronate monooxygenase on January 1, 2010.

While the enzyme does indeed oxidize nitronates through a monooxygenase catalytic mechanism, the primary alkyl nitronates, such ethylnitronate, used in the majority of the studies presented in the dissertation are most likely not the physiological substrates for the enzyme. Instead, the evidence presented in Chapter 8 strongly implicates that the enzyme is involved in the detoxification of the plant and fungal metabolite propionate-3-nitronate. As reviewed in Chapter 2, propionate-3-nitronate is the highly toxic, anionic form of 3-nitropropionate, which has been implicated in the poisoning of both humans and domestic livestock (*1-4*). The toxicity of propionate-3-nitronate arises from the irreversible inhibition of the key metabolic enzyme succinate dehydrogenase (*5-7*). Oxidation of the nitronate to malonic semialdehyde by nitronate monooxygenase (*8*) likely serves a vital role in the survival of *N. crassa* against the environmental occurrence of the toxin. The recent identification of propionate-3-nitronate

oxidizing enzymes in the soil bacteria *Pseudomonas aeruginosa* and *Burkholderia phytofirmans* (*8*), along with the fact that there are over 2,100 annotated 2-nitropropane dioxygenases in the GenBank (http://www.ncbi.nlm.nih.gov/COG/grace/wiew.cgi?COG2070), suggests that nitronate monooxygenases are widespread in nature and are not just confined to the plants that produce the toxin as might be concluded from the a survey of the literature on this topic (*9, 10*).

Prior to the recent study establishing the physiological role of nitronate monooxygenase, the enzyme was a less appreciated version of old yellow enzyme (*11-15*) in that it held the answers to many pressing questions in both flavoprotein chemistry and enzyme catalysis in general, despite the fact that researchers were puzzled by its purpose in nature. The studies carried out using the non-physiological substrate, ethylnitronate, allowed for a detailed characterization of anionic flavosemiquinones in catalysis by flavin dependent enzymes, which was previously inaccessible due to the transient nature of the intermediate in most systems. These studies established that a positive charge, which is provided by histidine 196 in *N. crassa* nitronate monooxygenase (*16*) is essential to provide an electrostatic catalysis for the reaction (*17*). While the detection of a catalytically relevant anionic flavosemiquinone in enzyme catalysis is rare, the studies of the intermediate in nitronate monooxygenase have since been used by other researchers in the field to further understand their systems (*18-20*).

The branched steady-state kinetic mechanism of nitronate monooxygenase, described in Chapters 4 through 6 (*16, 21, 22*), has revealed important lessons concerning both the true meaning of the Michaelis-Menten parameter, k_{cat}/K_m, and the interpretation of kinetic isotope effects as a probe of enzyme mechanism. Branching occurs after the formation of an enzyme-ethylnitronate intermediate and involves either the release of the nitronate in a non-oxidative turnover of the enzyme or flavin reduction that occurs during oxidative catalysis (*23*). The

release of ethylnitronate can be experimentally detected by monitoring the increase in the UV absorbance at 228 nm that occurs after mixing the enzyme with nitroethane (*16*). Alternatively, enzymatic activity can be followed by monitoring rates of oxygen consumption that results from the oxidation of the anionic flavosemiquinone intermediate formed during oxidative turnover of nitronate monooxygenase (*17, 21*). Comparing both the kinetic parameters and substrate kinetic isotope effects measured using the two methods under identical experimental conditions reveals a curious aspect of the kinetic complexities that arise from the release of reaction intermediates in enzyme catalyzed reactions. These concepts are not entirely novel since they have been theoretically discussed in review articles on enzyme kinetics (*24, 25*) and have long been realized in the physical organic chemistry community (*26-28*). However, the studies on nitronate monooxygenase do provide one of the first examples of the kinetic consequences of branching in enzyme catalyzed reactions. Since a detailed account of the experiments that demonstrate these effects are provided in Chapter 6, only a further elaboration will be provided below.

$$E + S \underset{k_2}{\overset{k_1}{\rightleftharpoons}} ES \xrightarrow{k_3} E + P \qquad k_{cat}/K_m = (k_1 k_3)/(k_2 + k_3)$$

Scheme 10.1 The k_{cat}/K_m value for a single substrate enzymatic reaction.

The k_{cat}/K_m value for an enzymatic reaction is typically described in textbooks as a measure of the specificity of an enzyme for a given substrate. This vague definition is usually accompanied by the scheme for a single substrate enzymatic reaction and a mathematical description of the kinetic parameter (Scheme 1). Emphasis is typically placed on the other two kinetic parameters in the Michaelis-Menten model, namely the turnover number (k_{cat}) and the Michaelis-Menten constant (K_m), which gives the impression that the k_{cat}/K_m value has little mechanistic value, but is more useful for comparing multiple compounds as substrates for a

given enzyme. As first pointed out by Northrop (*24, 25*), the k_{cat}/K_m value reveals a great deal of information on the catalytic mechanism of an enzyme and should not be thought of as merely a measure of the specificity of an enzyme for a given substrate or a complex set of rate constants.

The use of the k_{cat}/K_m value as a measure of specificity is clearly not always valid as evident from the kinetic studies of nitronate monooxygenase with nitroethane as substrate (*16, 21, 23*). The k_{cat}/K_m value obtained with nitroethane as substrate differs when activity is measured by either monitoring oxygen consumption or nitronate release (*16, 21, 23*). At least in the case of nitronate monooxygenase, the kinetic parameter clearly cannot be a measure of specificity, since different values are obtained with the same substrate depending on which signal is used to detect activity. Rather as eloquently defined by Northrop (*24, 25*), the k_{cat}/K_m value is "the rate of substrate capture into productive enzyme complexes destined to form products at some later time". In the case of nitronate monooxygenase, the two values reflect rates of capture of nitroethane into productive complexes destined to form either ethylnitronate or acetaldehyde at a later time.

Branching also effects the observed kinetic isotope effects for the reaction of nitronate monooxygenase with nitroethane as substrate in a manner similar to organic reactions that give rise to multiple products (*27-29*). In the case of nitronate monooxygenase, the release of ethylnitronate is accompanied by a kinetic isotope effect on the deprotonation of the imadazolium side chain of histidine 196 (*23*). The overall kinetic isotope effect measured is thus a combination of the deprotonation of the nitroalkane and the ionization of an active site residue. Kinetic isotope effects as high as 23 are therefore observed for the nitronate monooxygenase catalyzed reaction (*23*), which are well above the semi-classical limit of ~7-8 for primary deuterium kinetic isotope effects. Thus, the studies on nitronate monooxygenase represent an

additional consideration that must be applied when ascribing the magnitude of an observed kinetic isotope effect to the physical nature of the reaction catalyzed.

In conclusion, the studies on nitronate monooxygenase reveal how many lessons can be learned from an enzyme whose biological role is undefined. The once poorly understood enzyme now serves as a model to understand the reactivity of flavosemiquinones in enzymatic catalysis (*30*), the kinetic implication of branching of reaction intermediates (*23*) and more recently the ways in which microorganism cope with environmental toxins (*8*).

10.2 References

1.	Hamilton, B. F., Gould, D. H., and Gustine, D. L. (1999) History of 3-Nitropropionic acid, In *Mitrochrondrial Inhibitors and Neurodegenerative Disorders* (Sanberg, P. R., Nishino, H., and Borlongan, C. V., Eds.), Humana Press, Totowa, NJ.

2.	Ming, L. (1995) Moldy sugarcane poisoning-a case report with a brief review, *J. Toxicol. Clin. Toxicol. 33*, 363-367.

3.	Williams, M. C., James, L. F., and Bond, B. O. (1979) Emory milkvetch (*Astragalus emoryanus* var emoryanus) poisoning in chicks, sheep, and cattle, *Am. J. Vet. Res. 40*, 403-406.

4.	Williams, M. C., van Kampen, K. R., and Norris, F. A. (1969) Timber milkvetch poisoning in chickens, rabbits, and cattle, *Am. J. Vet. Res. 30*, 2185-2190.

5.	Alston, T. A., Mela, L., and Bright, H. J. (1977) 3-Nitropropionate, the toxic substance of *Indigofera*, is a suicide inactivator of succinate dehydrogenase, *Proc. Natl. Acad. Sci. U. S. A. 74*, 3767-3771.

6.	Coles, C. J., Edmondson, D. E., and Singer, T. P. (1979) Inactivation of succinate dehydrogenase by 3-nitropropionate, *J. Biol. Chem. 254*, 5161-5167.

7.	Huang, L. S., Sun, G., Cobessi, D., Wang, A. C., Shen, J. T., Tung, E. Y., Anderson, V. E., and Berry, E. A. (2006) 3-nitropropionic acid is a suicide inhibitor of mitochondrial respiration that, upon oxidation by complex II, forms a covalent adduct with a catalytic base arginine in the active site of the enzyme, *J. Biol. Chem. 281*, 5965-5972.

8.	Nishino, S. F., Shin, K. A., Payne, R. B., and Spain, J. C. (2010) Growth of bacteria on 3-nitropropionic acid as a sole source of carbon, nitrogen, and energy, *Appl. Environ. Microbiol. 76*, 3590-3598.

9. Hipkin, C. R., Salem, M. A., Simpson, D., and Wainwright, S. J. (1999) 3-nitropropionic acid oxidase from horseshoe vetch (*Hippocrepis comosa*): a novel plant enzyme, *Biochem. J. 340 (Pt 2)*, 491-495.

10. Hipkin, C. R., Simpson, D. J., Wainwright, S. J., and Salem, M. A. (2004) Nitrification by plants that also fix nitrogen, *Nature 430*, 98-101.

11. Massey, V., and Schopfer, L. M. (1986) Reactivity of old yellow enzyme with alpha-NADPH and other pyridine nucleotide derivatives, *J. Biol. Chem. 261*, 1215-1222.

12. Stewart, R. C., and Massey, V. (1985) Potentiometric studies of native and flavin-substituted Old Yellow Enzyme, *J. Biol. Chem. 260*, 13639-13647.

13. Abramovitz, A. S., and Massey, V. (1976) Purification of intact old yellow enzyme using an affinity matrix for the sole chromatographic step, *J. Biol. Chem. 251*, 5321-5326.

14. Matthews, R. G., Massey, V., and Sweeley, C. C. (1975) Identification of p-hydroxybenzaldehyde as the ligand in the green form of old yellow enzyme, *J. Biol. Chem. 250*, 9294-9298.

15. Matthews, R. G., and Massey, V. (1969) Isolation of old yellow enzyme in free and complexed forms, *J. Biol. Chem. 244*, 1779-1786.

16. Francis, K., and Gadda, G. (2008) The nonoxidative conversion of nitroethane to ethylnitronate in Neurospora crassa 2-nitropropane dioxygenase is catalyzed by histidine 196, *Biochemistry 47*, 9136-9144.

17. Francis, K., Russell, B., and Gadda, G. (2005) Involvement of a flavosemiquinone in the enzymatic oxidation of nitroalkanes catalyzed by 2-nitropropane dioxygenase, *J. Biol. Chem. 280*, 5195-5204.

18. Toogood, H. S., Fryszkowska, A., Hare, V., Fisher, K., Roujeinikova, A., Leys, D., Gardiner, J. M., Stephens, G. M., and Scrutton, N. S. (2008) Structure-Based Insight into the Asymmetric Bioreduction of the C=C Double Bond of alpha,beta-Unsaturated Nitroalkenes by Pentaerythritol Tetranitrate Reductase, *Adv. Synth. Catal. 350*, 2789-2803.

19. Manoj, K. M., Gade, S. K., and Mathew, L. (2010) Cytochrome P450 reductase: a harbinger of diffusible reduced oxygen species, *PLoS. One 5*, e13272.

20. Durchschein, K., Silva, B. F. D., Wallner, S., Macheroux, P., Kroutil, W., Glueck, S. M., and Faber, K. (2010) The flavoprotein-catalyzed reduaction of aliphatic nitro-compnds represents a biocatlytic equivelent to the Nef-reaction, *Green Chem. 12*, 616-619.

21. Francis, K., and Gadda, G. (2006) Probing the chemical steps of nitroalkane oxidation catalyzed by 2-nitropropane dioxygenase with solvent viscosity, pH, and substrate kinetic isotope effects, *Biochemistry 45*, 13889-13898.

22. Francis, K., and Gadda, G. (2009) Kinetic evidence for an anion binding pocket in the active site of nitronate monooxygenase, *Bioorg. Chem. 37*, 167-172.

23. Francis, K., and Francis, K. (2009) Inflated kinetic isotope effects in the branched mechanism of N. crassa 2-nitropropane dioxygenase, *Biochemistry. 48*, 2403-2410.

24. Northrop, D. B. (1998) On the meaning of K_m and V/K in enzyme kinetics., *J. Chem. Ed. 75*, 1153-1157.

25. Northrop, D. B. (1999) So what exactly is V/K, anyway?, *Biomed. and Health Res. 27*, 250-263.

26. Murthy, Y., and Massey, V. (1996) 19F NMR studies with 2'-F-2'-deoxyarabinoflavoproteins, *J. Biol. Chem. 271*, 19915-19921.

27. Oelwegaard, M., McEwen, I., Thibblin, A., and Ahlberg, P. (1985) Stepwise base-promoted elimination of hydrochloric acid via hydrogen-bonded carbanions studied by reaction branching and extreme deuterium isotope effects. Parallel carbocationic and carbanionic reactions., *J. Am. Chem. Soc. 107*, 7494-7499.

28. Thibblin, A. (1988) Reaction branching as a mechanistic alternative to tunneling in explaining anomalous temperature dependencies of kinetic isotope effects., *J. Phys. Org. Chem. 1*, 161-167.

29. Watt, C. I. F. (2010) Primary kinetic hydrogen isotope effects in deprotonations of carbon acids, *J. Phys. Org. Chem. 23,* 561-571.

30. Gadda, G., and Francis, K. (2009) Nitronate monooxygenase, a model for anionic flavin semiquinone intermediates in oxidative catalysis, *Arch Biochem Biophys. 493*, 53-61.